Development of a cost effective process for biodiesel production through model guided high cell density cultivation of *Chlorella* sp. FC2 IITG

A Thesis

Submitted for the Degree of

DOCTOR OF PHILOSOPHY

by

BASAVARAJ PALABHANVI
(11610605)

Under supervision of

Dr. Debasish Das

September 2016

Department of Biosciences & Bioengineering
Indian Institute of Technology Guwahati
Guwahati 781 039, Assam, India

INDIAN INSTITUTE OF TECHNOLOGY GUWAHATI

Department of Biosciences & Bioengineering

STATEMENT

I do hereby declare that the content embodied in this thesis is the result of investigations carried out by me in the Department of Biosciences & Bioengineering, Indian Institute of Technology Guwahati, Guwahati, Assam, India under the supervision of Dr. Debasish Das.

In keeping with the general practice of reporting scientific observations, due acknowledgements have been made wherever the work described is based on the findings of other investigators.

Date: **September 2016** **Basavaraj Palabhanvi**

INDIAN INSTITUTE OF TECHNOLOGY GUWAHATI

Department of Biosciences & Bioengineering

CERTIFICATE

It is certified that the work described in this thesis entitled "**Development of a cost effective process for biodiesel production through model guided high cell density cultivation of *Chlorella* sp. FC2 IITG**" by Mr. Basavaraj Palabhanvi for the award of degree of Doctor of Philosophy is an authentic record of the results obtained from the research work carried out under my supervision in the Department of Biosciences & Bioengineering, Indian Institute of Technology Guwahati, Guwahati, India. The work embodied in this thesis has not been submitted elsewhere for a degree.

Dr. Debasish Das
Associate Professor
(Thesis Supervisor)
Department of Biosciences & Bioengineering
Indian Institute of Technology Guwahati
Guwahati 781 039, India

Acknowledgements

I would like to express my deepest gratitude to my thesis supervisor, ***Dr. Debasish Das,*** Department of Biosciences and Bioengineering, for giving me the opportunity to pursue this research work, for his continuous care, valuable advice, guidance, encouragement, and supervision of the research. I must acknowledge the freedom to think, plan, execute and express, that was given to me at every step of my research work, while keeping faith and confidence in my capabilities.

I am indebted to my doctoral committee members, ***Dr. Arun Goyal, Dr. Aiyagari Ramesh*** and ***Dr. Soumen Kumar Maiti*** who guided me through all these years. Their constructive criticism and suggestions helped me to improve my work pertaining to Ph.D. thesis. I would also like to thank ***Dr. G.K. Suraishkumar, Dr. Senthilkumar*** and ***Dr. Dipankar Bandyopadhyay*** for their valuable suggestions and evaluating my thesis. I am extremely grateful to ***Dr. Venkata Dasu Veeranki, Dr. K. Pakshirajan, Dr. Lingaraj Sahoo*** and ***Dr. Aloke K Ghoshal*** for their timely advice and encouragement during my research work at IIT Guwahati.

I owe my thanks to the ***Department of Biosciences and Bioengineering***, ***Centre for Energy***, and ***Central Instrumentation Facility***, IIT Guwahati for providing the necessary research facilities to accomplish my Ph.D. thesis objectives. I would also like to thank ***Dr. Akhilesh Kumar Maurya***, Department of Civil Engineering for allowing me to use his laboratory instruments and ***Mr. Mrinal Sarmah***, Technical Staff, for providing procedural support.

My heartfelt thanks are due to *lab in charges* ***Mr. Nurul***, ***Mrs. Anita, Mrs. Prarthana, Mr. Dipankar, Mr. Chandan, Mr. Raghuveer P. Yadav and Mr. Niranajan***, and *office staff* ***Mr. Bidyut Gogoi, Mr. Dipangkar Sharma*** and ***Mr. Pankaj Bhuyan*** during the course of my research.

I would like to gratefully acknowledge ***IIT Guwahati*** for providing financial assistance, ***MHRD*** and ***DST*** for funding my Ph.D. project, which made this study possible.

It was a pleasure to work with ***Muthusivaramapandian, Vikram, Saumya, Mayurketan, Baskar, Kumaran, Bidhu, Deepesh, Naveen, Mehak, Sumanth, Meenakshi, Reeshav, Bikas, Anwesha, Gargi, Suraj, and Shamik***. I would like to thank them for their valuable suggestions, for the sleepless nights we were working, sticking together in tough times, celebrating successes, and making my Ph. D an unforgettable experience.

I would like thank to my *friends in the institute especially* ***Mohan, Yoganand, Deepika, Himanshu, Arun, Santhosh, Thiyagarajan, Somaiah, Sunil, Nitin, Anuma, Srikanth, Dhamodharan, Payel, Rupak, Mrinal, Ashish, Bapi*** for being supportive and providing a welcome diversion from the difficult situations during my Ph.D., whenever I needed. I greatly value their friendship and appreciate their unconditional love, encouragement and support.

My special thanks and appreciation goes to ***my parents***, as well as my ***family members*** for their blessings, love, patience, support and understanding throughout my studies and most of all to the ***Almighty God*** who made everything possible.

Date: September 2016 **Basavaraj Palabhanvi**

Abstract

Around two percent of the world's total fossil reserves are getting depleted every year and are in need for replacement by alternate renewable fuels. India being a rapidly developing nation and a fore runner on the world stages has significant energy requirements but contributes less towards the global production of biofuel. Suiting such a requirement to overcome the shortage in the long chain of supply and demand, it is considered for an independent research outlook towards alternate energy generation. Aligned to such an initiative is the development of microalgae based biodiesel which can be attributed to its inherent ability of high growth rate and accumulation of intracellular neutral lipid. However, there still exist certain bottlenecks that are a hindrance towards the development of an industrially feasible and economically sustainable process strategy for biodiesel production. Such impending bottlenecks can serve as motivations towards development of a rationale for strain improvement or novel process strategy design; that will accentuate research towards industrialization of microalgal biodiesel.

The present study aims to realize and resolve the above mentioned bottlenecks through high cell density-lipid rich cultivation of a novel microalgal strain *Chlorella* sp. FC2 IITG under heterotrophic growth condition. This objective was achieved via combined approach of (i) identification of growth promoting and/or lipid inducing substrates; (ii) optimization of the key limiting nutrients for growth and lipid accumulation; (iii) design of model guided nutrient feeding recipe coupled with substrate driven pH control for high biomass titer and lipid enrichment via addition of selected lipid inducer in fed-batch operation; (iv) model based optimization of control variables e.g. feed

stream concentrations and dilution rate for continuous production of lipid rich algal biomass with high productivity in chemostat; and (v) Flux balance analysis (FBA) to understand the complex interplay between energy metabolism, carbon fixation, and assimilation pathways.

The strain was initially characterized under different pH and temperature conditions which showcased the robustness of the strain as it was able to grow in a wide range of pH from 4 to 10 with a temperature ranging between 20-44°C. Glucose and sodium acetate when used as sole carbon source and lipid elicitor respectively yielded enhanced biomass and lipid content. Growth media was optimized with two different objective functions for maximization of specific growth rate and biomass titer. Optimization of media for specific growth rate resulted in a highest growth rate of 2.115 day^{-1} whereas 7.81 g L^{-1} cell density was achieved in case of maximization of biomass titer. Optimized supplementation of 24 g L^{-1} sodium acetate resulted in maximum of ~66% w/w, DCW neutral lipid accumulation.

The multi-nutrient mechanistic model developed on the basis of segregation of intracellular nutrients into structural form of nutrient (SFN), readily utilizable intracellular stored nutrients (RUN), non-readily utilizable intracellular nutrients (Non-RUN) and their sequential consumption during starvation. Hypothesis developed on the preferential and sequential utilization of extra cellular nutrients (ECN) under nutrient sufficient condition followed by RUN and Non-RUN under starvation was established by an *in-silico* model and experimentally validated. The model exhibited in this study showed better predictability than existing models such as Monod kinetics and Droop cell quota model. The model formed the basis of developing a feeding strategy for high cell density cultivation. To that end, a biphasic fed batch approach was followed wherein, firstly, a high cell density cultivation was obtained through model guided optimized feeding

strategy and nutrient driven pH control; secondly, intracellular lipid enrichment was attained via addition of sodium acetate. This strategy resulted in biomass titer of 90.15 g L^{-1} with biomass and lipid productivity 19.75 g L^{-1} day^{-1} and 7.7 g L^{-1} day^{-1} respectively.

Subsequently, a two-step chemostat cultivation methodology was designed where two separate bioreactors were connected in series. The first reactor resorted to the high cell density cultivation via model optimized substrate feeding parameters and predicted dilution rate to ensure a high biomass productivity whereas the second reactor was solely dedicated to lipid induction; both the reactors operating in tandem for the efficient design of a process strategy. The strategy yielded the biomass and lipid productivity of 92.7 g L^{-1} day^{-1} and 9.76 g L^{-1} day^{-1} respectively, which was significantly high amongst similarly reported literatures.

Understanding of lipid biosynthesis pathway with respect to energetics and carbon flux distribution is a prerequisite for efficient utilization of microalgae as cell factory for biodiesel production. In this study, metabolic model was developed to study the flux map and energetics during starvation and sodium acetate supplemented conditions in comparison to nutrient sufficient condition. During nutrient starvation, an enhanced lipid accumulation in biomass was observed with concomitant 6 fold increase in non-growth associated (NGA) maintenance energy to combat stress. In case of sodium acetate supplementation, lipid induction in biomass was found to be higher than starvation with no significant increase in NGA maintenance energy. Hence sodium acetate was found to be a better option for lipid induction in biomass towards cost effective bioprocess development for biodiesel production. The biodiesel obtained from microalga FC2 grown under heterotrophic condition can be used for commercial applications as it satisfied American and European standards. Therefore the process strategy developed in present study opens up scope for further economic feasibility analysis and scale up for commercial production.

Contents

भारतीय प्रौद्योगिकी संस्थान गुवाहाटी
Indian Institute of Technology Guwahati

List of figures

List of tables

CHAPTER 1

Introduction

1.1. Background and motivation

Demographic expansion in association with economic improvement has led to the extensive extraction of conventional fossil fuel reserves, accentuating the search for alternative, sustainable and renewable energy resources (Mirsiaghi and Reardon, 2015). In pursuit of meeting the ever increasing global energy demand, oleaginous microalgae based biodiesel production is the most promising alternative (Griffiths and Harrison, 2009). This is attributed to its intrinsic properties like faster growth rate in comparison to plants and ability to grow in marginal areas, saline, brackish and waste water (Becker, 1994). Even though microalgae are unicellular photosynthetic organism, some can grow heterotrophically at higher growth rate and lipid content than photoautotrophic condition (Shen et al., 2010). They are known to produce wide range of byproducts such as therapeutic proteins, lipids, polysaccharides, biopolymers, vitamins and pigments (Borowitzka, 2013) and hence microalgae have potential applications in many industries.

Currently, microalgae based biodiesel production suffers from economical infeasibility (Chisti, 2013) and low marginal net energy ratio (NER) of biomass production (Slade and Bauen, 2013) even by use of proven technologies. NER is defined as the ratio of total energy required for cultivation, harvesting and drying, to the energy content of dry biomass. This is attributed to low biomass titer and associated higher harvesting cost, increased chances of contamination, lower light penetration, fluctuating climatic conditions and self-shading effect of cells in the photoautotrophic open race way pond systems which are largely used for commercial scale cultivation of microalgae (Chae et al., 2006; Chinnasamy et al., 2010; Shen et al., 2010). Interestingly, heterotrophic

cultivation in a closed bioreactor can offer consistent biomass productivity, improved cell density with less chances of cross species contamination and ease of controlling process parameters (Shen et al., 2010). Nevertheless, the cost of organic carbon sources utilized in heterotrophic condition remains an unsolved issue in view of economic feasibility. A possible solution can be exploitation of alternate lignocellulosic biomass and other cheaper carbon sources for the growth of microalgal systems (Turon et al., 2015). Another alternative way to achieve feasibility is through process development for high cell density cultivation and improved lipid productivity along with commercialization of residual components of biomass after lipid extraction (Tabernero et al., 2012).

Feasible process development includes series of progressive steps towards desired goal from basic characterization of microalgae to novel strategy for process engineering (Xiong et al., 2008) coupled with metabolic modeling to understand the regulation of lipid biosynthesis. This can be carried out in two separate modular work packages; one is upstream process engineering study to enhance the lipid productivity through lipid rich-high cell density cultivation with the help of kinetic and metabolic models. Another segment of work (downstream processing) is cost-effective conversion of intracellular lipid into biodiesel and commercialization of remaining components of cell. The upstream study needs to commence with detailed physico-chemical characterization and media optimization in order to provide growth favorable conditions for microalgae. Further, high cell density can be achieved in fed-batch via feeding of limiting substrates in the course of fermentation (Doucha and Lívanský, 2012). Similarly, superior biomass productivity can be achieved in continuous cultivation of organism in optimal operational conditions (Chen and Johns, 1996; Stanbury et al., 2003). The momentary exhaustion or over concentration of substrates affects the growth rate of organism and eventually the productivity. Hence, optimal substrate feeding recipe can be designed with the help of suitable mathematical

models as they are effective tools for growth kinetics (Alagesan et al., 2013). This optimized nourishment is expected to offer high growth rate and shortened fermentation time leading to reduced operational cost of fermentation. However, this may hinder the accumulation of intracellular lipid in cells due to mutually exclusive nature of growth and lipid content (Rodolfi et al., 2009). To that end, two-stage cultivation can be developed to enhance both biomass titer and lipid content where first stage is used to generate high biomass followed by induction of intracellular lipid in second stage (Rodolfi et al., 2009). Second stage of cultivation needs the understanding of regulation and metabolism of organism towards lipid accumulation in cell.

However, microalgal lipid biosynthesis pathway is a complicated network which is not yet clearly understood. To that end, quantification of carbon flux distribution in the metabolic network can be done via metabolic modeling like flux balance analysis (FBA). It can be an effective tool to understand energy metabolism, carbon assimilation and lipid biosynthesis of the organism. Therefore, identification of regulation and rate limiting step of lipid biosynthesis pathway can be the potential targets for either genetic engineering or process engineering. For instance, metabolic modeling strategy was employed to better understand lipid metabolism, its regulation and controls (Montagud et al., 2010) which defines the ways to channelize metabolic fluxes towards lipid biosynthesis via genetic manipulation or usage of lipid elicitors. The above mentioned strategies guided by metabolic modeling may result in improvement of lipid productivity which is a prerequisite of biodiesel production. Thus, high cell density cultivation with enhanced lipid productivity still requires focus on the development of innovative process engineering strategies and detailed understanding of lipid biosynthetic pathway through metabolic modeling (Hu et al., 2008). In view of this the following objectives were framed to develop a feasible algal biodiesel process under heterotrophic condition.

1.2. Objectives of the present study

- *Characterization of Chlorella sp. FC2 IITG under wide ranges of pH, temperature, carbon and nitrogen sources.*
- *Optimization of nutrients concentration for maximization of growth and lipid content of FC2 in batch cultivation*
- *Development of multi-nutrient mechanistic model to predict heterotrophic growth kinetics of Chlorella sp. FC2 IITG under both nutrient sufficient and nutrient depleted conditions.*
- *Process development for high cell density-lipid rich cultivation in fed-batch operation via model guided feeding recipe and substrate driven pH control.*
- *Process development for high biomass and lipid productivity in continuous mode of cultivation via model based optimization of control variables.*
- *Flux balance analysis to understand the regulations of carbon partitioning and lipid metabolism of Chlorella sp. FC2 IITG at different nutritional condition under heterotrophic cultivation.*

1.3. Approach

Chlorella sp. FC2 IITG (hereafter referred as FC2), a novel indigenous strain isolated in our laboratory from the North-East region, was used as the model organism in this study. Combined bioprocess development and metabolic modeling approaches were employed to characterize the strain in detail and to achieve high cell density and improved neutral lipid productivity which is the desired characteristic while choosing a feedstock for microalgae based biodiesel production (Fig. 1.1).

Process development commenced with preliminary characterization of the strain under different physico-chemical parameters e.g. temperature and initial pH of the medium to find out their respective values which support optimal growth. The initial

characterization also includes a detailed characterization of the strain on wide range of carbon and nitrogen sources in order to screen the nutrient which could be growth supportive or lipid inductive or both, followed by optimization of these key nutrients via statistical optimization method. Further, a multi-nutrient mechanistic model was developed to predict growth kinetics of the organism under different nutritional conditions which differ in terms of the type of nutrient limitation and their concentration. Model could predict growth kinetics both in nutrient sufficient and starvation condition as it was based on preferential utilization of extracellular and different forms of intracellular stored nutrients.

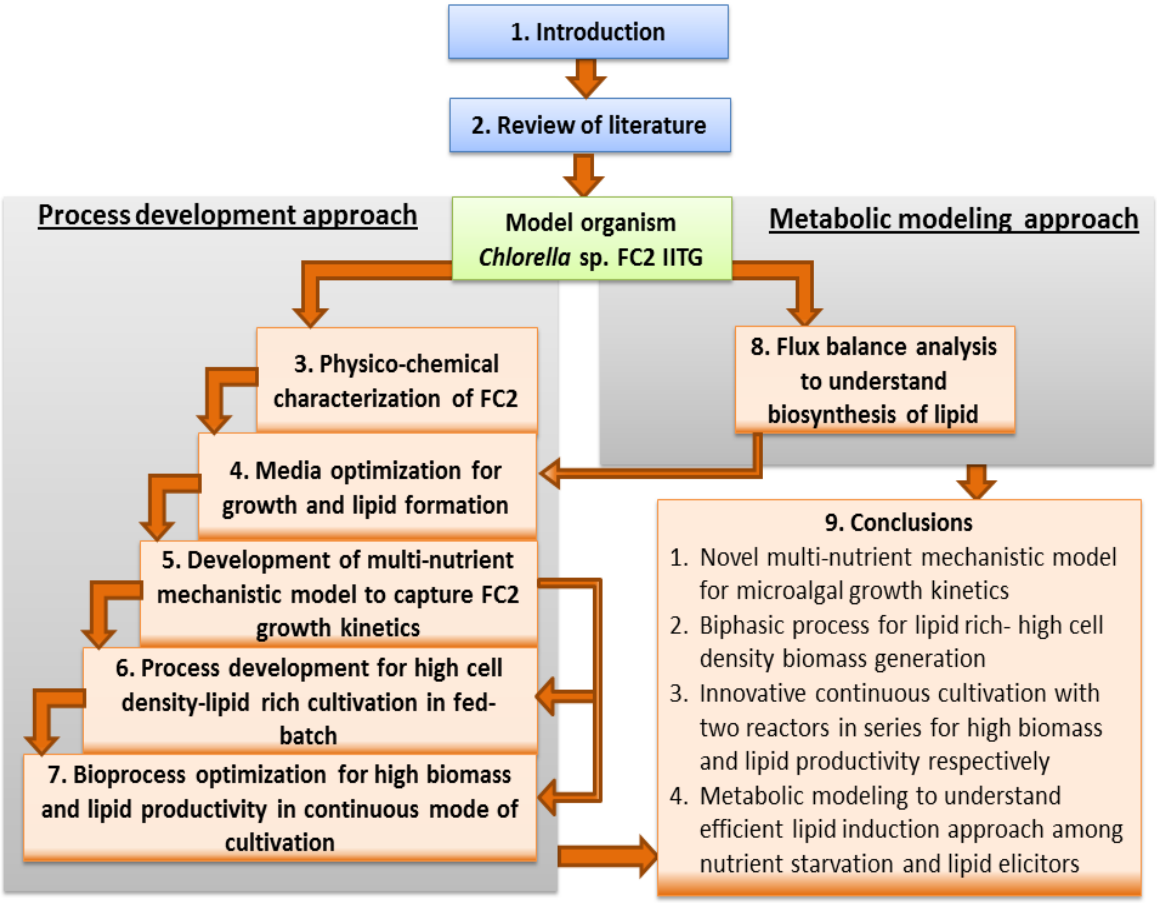

Fig. 1.1 Bioprocess development and metabolic modeling approaches employed to achieve high cell density and improved lipid productivity towards biodiesel production and to understand the regulations involved in lipid biosynthesis for a novel indigenous microalgal strain *Chlorella* sp. FC2 IITG

Finally, the developed model was used to design the substrate feeding recipe for high cell density fed-batch cultivation. While in case of continuous mode of operation it was employed to optimize the control variables such as dilution rate and feed stream substrates concentrations for high biomass productivity. Lipid was enriched in biomass by supplementation of lipid inducers in biphasic fed-batch cultivation and serially connected two-stage chemostat operation after generation of high cell density or high productivity biomass. Intracellular lipid was transesterified and analyzed in gas chromatography (GC) to determine the quality of biodiesel.

The metabolic modeling approach involved FBA which was carried out for nutrient starvation condition and lipid inducer supplemented condition with respect to nutrient sufficient condition to understand the complex carbon partitioning mechanism involved in the microalgal system. Carbon flux distribution towards lipid biosynthetic pathway, other biosynthetic pathways and non-growth associated maintenance energy was captured for all the conditions. Efficient condition for lipid induction was evaluated through energetics and flux maps obtained from FBA analysis. In the broader context, current study was focused to develop a cost effective generation of lipid-rich microalgal feed-stock for biodiesel production by reducing fermentation time, enhanced lipid content in biomass and increased cell concentration in broth.

1.4. Organization of the thesis

The thesis consists of 9 Chapters. Chapter 1 deals with general background, motivation, objectives of present study and approaches to resolve existing hurdles. Chapter 2 includes a detailed literature survey on algal biotechnology, research advancements towards algal biodiesel and the existing bottlenecks associated with the current state of art technologies. Chapter 3 describes the characterization of strain under wide ranges of pH, temperature for growth followed by screening of growth supportive and lipid inducing

carbon and nitrogen sources as well as evaluation of their effect on biodiesel properties. Chapter 4 focuses on media optimization for growth in term of specific growth rate and cell density, evaluation of trace and micro elements effect on growth and finally determination of optimal concentration of lipid inducer for enhanced lipid enrichment. Chapter 5 details the development of a multi-nutrient mechanistic model for capturing the heterotrophic growth kinetics of *Chlorella* sp. FC2 IITG under both nutrient sufficient and nutrient depleted conditions. Chapter 6 deals with strategic process development for high cell density-lipid rich cultivation in fed-batch operation. This strategy involves a combined approach of model guided intermittent feeding of the limiting nutrients, substrate based pH control and decoupling of growth and lipid induction phase. Chapter 7 targets the further improvement of biomass and lipid productivity in serially connected two-stage chemostat operation at model guided optimal condition. Chapter 8 describes the flux balance analysis (FBA) under nutrient starvation condition and lipid inducer supplemented condition with respect to nutrient sufficient condition in order to understand the regulations and controls involved in the lipid biosynthesis pathway. Chapter 9 summarizes key research highlights obtained from the present study with way out for future prospects.

1.5. References

1. Alagesan S., Gaudana S.B., Krishnakumar S., Wangikar P.P., 2013. Model based optimization of high cell density cultivation of nitrogen-fixing cyanobacteria. Bioresource Technology. 148, 228–233.
2. Becker E.W., 1994. Microalgae: biotechnology and microbiology. Cambridge University Press, Cambridge, New York.
3. Borowitzka M.A., 2013. High-value products from microalgae—their development and commercialisation. Journal of Applied Phycology. 25, 743–756.

4. Chae S.R., Hwang E.J., Shin H.S., 2006. Single cell protein production of *Euglena gracilis* and carbon dioxide fixation in an innovative photo-bioreactor. Bioresource Technology. 97, 322–329.

5. Chen F., Johns M.R., 1996. Heterotrophic growth of *Chlamydomonas reinhardtii* on acetate in chemostat culture. Process Biochemistry. 31, 601–604.

6. Chinnasamy S., Bhatnagar A., Claxton R., Das K.C., 2010. Biomass and bioenergy production potential of microalgae consortium in open and closed bioreactors using untreated carpet industry effluent as growth medium. Bioresource Technology. 101, 6751–6760.

7. Chisti Y., 2013. Constraints to commercialization of algal fuels. Journal of Biotechnology. 167, 201–214.

8. Doucha J., Lívanský K., 2012. Production of high-density *Chlorella* culture grown in fermenters. Journal of applied phycology. 24, 35–43.

9. Griffiths M.J., Harrison S.T., 2009. Lipid productivity as a key characteristic for choosing algal species for biodiesel production. Journal of Applied Phycology. 21, 493–507.

10. Hu Q., Sommerfeld M., Jarvis E., Ghirardi M., Posewitz M., Seibert M., Darzins A., 2008. Microalgal triacylglycerols as feedstocks for biofuel production: perspectives and advances. The Plant Journal. 54, 621–639.

11. Mirsiaghi M., Reardon K.F., 2015. Conversion of lipid-extracted *Nannochloropsis salina* biomass into fermentable sugars. Algal Research. 8, 145–152.

12. Montagud A., Navarro E., de Córdoba P.F., Urchueguía J.F., Patil K.R., 2010. Reconstruction and analysis of genome-scale metabolic model of a photosynthetic bacterium. BMC System Biology. 4, 156.

13. Rodolfi L., Chini Zittelli G., Bassi N., Padovani G., Biondi N., Bonini G., Tredici M.R., 2009. Microalgae for oil: Strain selection, induction of lipid synthesis and outdoor mass cultivation in a low-cost photobioreactor. Biotechnology and Bioengineering. 102, 100–112.

14. Shen Y., Yuan W., Pei Z., Mao E., 2010. Heterotrophic culture of *Chlorella protothecoides* in various nitrogen sources for lipid production. Applied Biochemistry and Biotechnology. 160, 1674–1684.

15. Slade R., Bauen A., 2013. Micro-algae cultivation for biofuels: cost, energy balance, environmental impacts and future prospects. Biomass and Bioenergy. 53, 29–38.

16. Stanbury P.F., Whitaker A., Hall S.J., 2003. Principles of fermentation technology. 2nd ed. Butterworth-Heinemann, Oxford, UK.

17. Tabernero A., del Valle E.M.M., Galán M.A., 2012. Evaluating the industrial potential of biodiesel from a microalgae heterotrophic culture: scale-up and economics. Biochemical Engineering Journal. 63, 104–115.

18. Turon V., Trably E., Fayet A., Fouilland E., Steyer J.-P., 2015. Raw dark fermentation effluent to support heterotrophic microalgae growth: microalgae successfully outcompete bacteria for acetate. Algal Research. 12, 119–125.

19. Xiong W., Li X., Xiang J., Wu Q., 2008. High-density fermentation of microalga *Chlorella protothecoides* in bioreactor for microbio-diesel production. Applied Microbiology and Biotechnology. 78, 29–36.

CHAPTER 2

Review of literature

2.1. Energy demand, crisis and alternatives

Population expansion, increased industrialization and economic improvement are resulting into huge requirement of energy which is 5.43×10^{20} Joules $year^{-1}$ as per present demand (British Petroleum, 2015). This is satisfied by petroleum oil, natural gas, coal, nuclear energy and renewable energy in share of 32.6, 23.7, 30, 4.4 and 9.25% respectively. Being a developing country, India shares 5% of the total energy consumption with maximum usage of coal (56.5%) followed by oil (28.3%). Recent statistics states that the majority of the demand is fulfilled by fossil fuels and hence they are anticipated to be exhausted within 50 years. As carbon was naturally sequestrated in fossil fuels, their extensive utilization has led to global warming due to release of carbon dioxide and other anthropogenic greenhouse gases to the environment. The 40% increment in average concentration of carbon dioxide was observed from pre-industrial era (1870) to present time which was mainly attributed to the release of 1.465×10^{12} tonnes of CO_2 to the environment through burning of fossil fuels (Le Quéré et al., 2015). In this period, the CO_2 emission was found to increase exponentially from 0.54 Gt $year^{-1}$ to 35.9 Gt $year^{-1}$ (Fig. 2.1) which is an alarming condition with the practice of burning fossil fuels. Further ~1800 Gt CO_2 could be released to the environment on complete consumption of fossil fuels which may result in climatic changes with increase in more than 2°C average global temperature (British Petroleum, 2015; Le Quéré et al., 2015; Met Office, 2015). In conclusion, disturbed carbon cycle may cause adverse effect on the sustenance of mankind and other living beings. Huge variation in anthropogenic greenhouse gases, espeacially CO_2 is not beneficial towards existing biotic environment as earth's temperature would be

risen or frozen with differences in their concentrations. As maintenance of normal concentration of CO_2 is essential, technology for generation of carbon neutral alternative fuels must be developed.

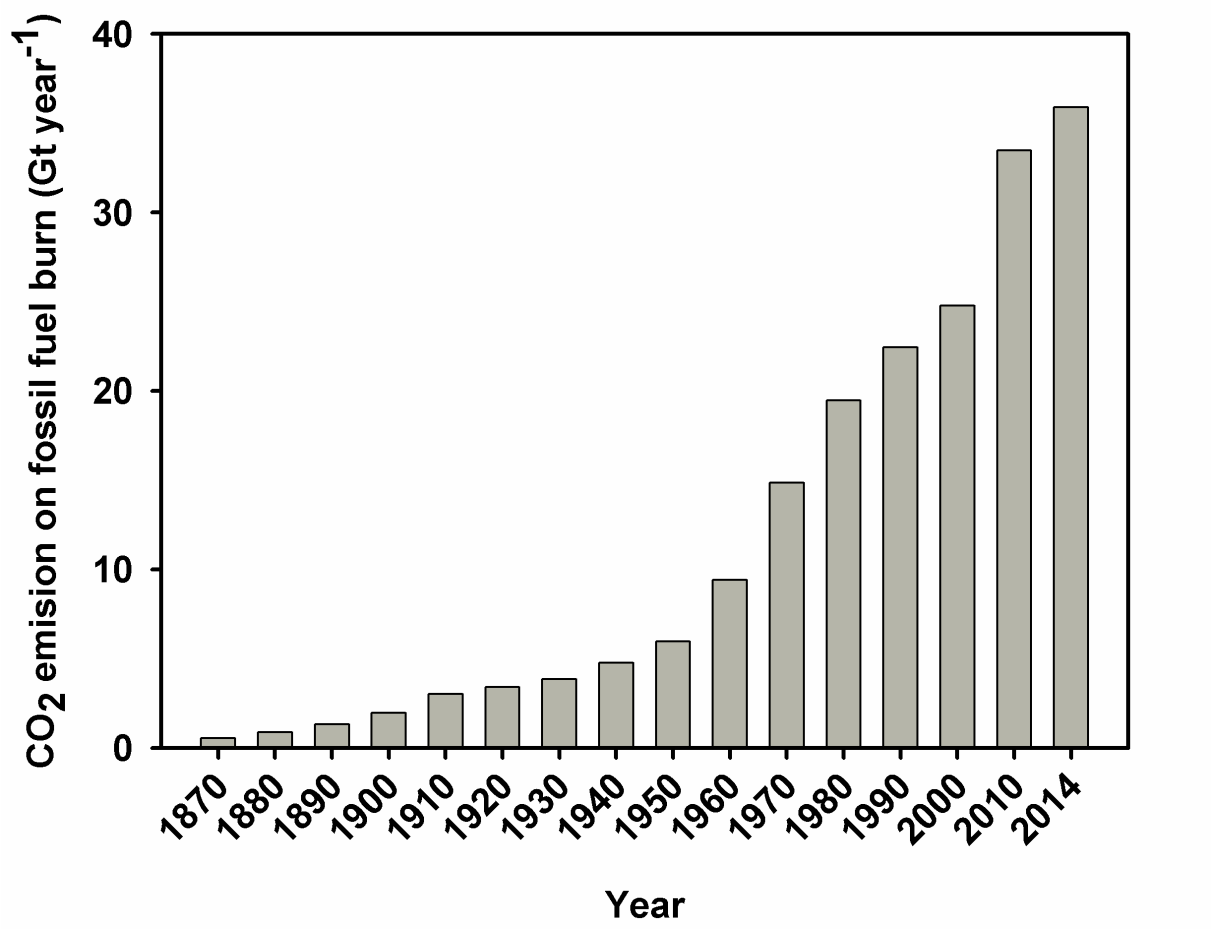

Fig. 2.1 The emission of carbon dioxide (Gt year^{-1}) from fossil fuel from pre-industrial era to 2014 (data source: Le Quéré et al., 2015).

Renewable energy sources such as hydroelectric power, solar, wave, wind, geothermal and biofuels are carbon neutral alternative energy sources (Panwar et al., 2011). Current usage of renewable energy is contributed by hydroelectric power (73.4%), wind (13.4%), biofuels (5.9%) and others (Fig. 2.2). The renewable sources but biofuels can be used in restricted areas where real time energy is required and immovable or less machinaries are employed. This is attributed to the difficulties associated with storage of their energy for futuristic use and their dependency on climatic variations. To that extent,

the solar energy can be harvested in the form of biomass of photosynthetic microorganisms and plants which in turn can be derived into biofuels as per requirement. Biofuels can be produced in gaseous phase (methane, hydrogen), liquid phase (biodiesel, bioethanol, bio-butanol, bio-oil etc.) and solid phase (high calorific dry biomass like microalgae, wood). Synthesis of biofuels from biomass can be classified into three generations based on the source of biomass utilized (Fig. 2.3).

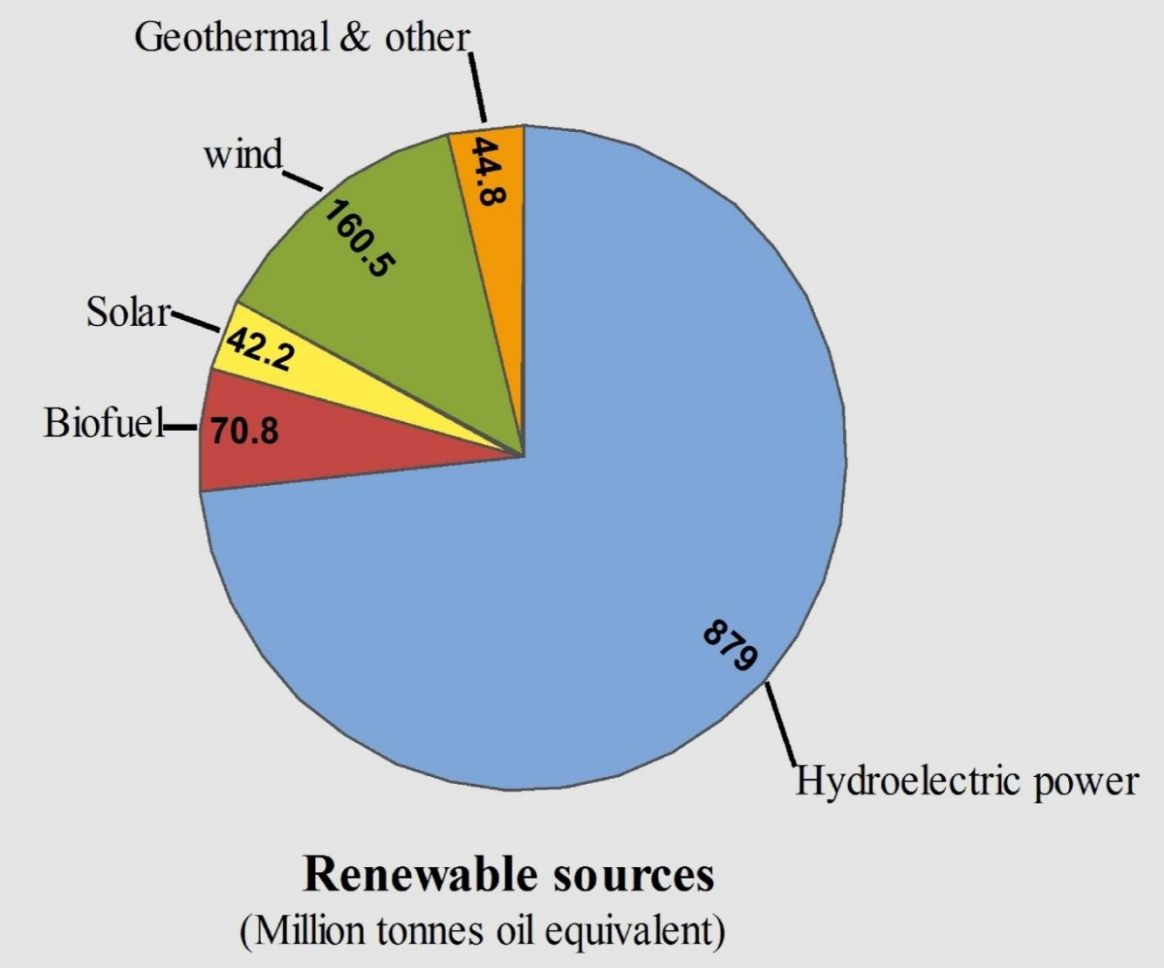

Fig. 2.2 Current statistical distribution of the global renewable energy consumption annually (data source: British Petroleum, 2015).

The first generation biofuels are mainly produced from food crops such as soybean, corn, rapeseed, palm, mustard, etc. The process for production of biofuels from these feed-stocks is economically feasible through advanced downstream technology. However, major disadvantage remains food vs fuel debate with serious ethical issues in

the form of global food supply. This may divert food crops from the human diet chain; potentially leading to food, land shortages and/or price hikes. Loss of biodiversity and excessive utilization of land are certain minor issues which collectively make the process unsustainable (Dragone et al., 2010; Naik et al., 2010).

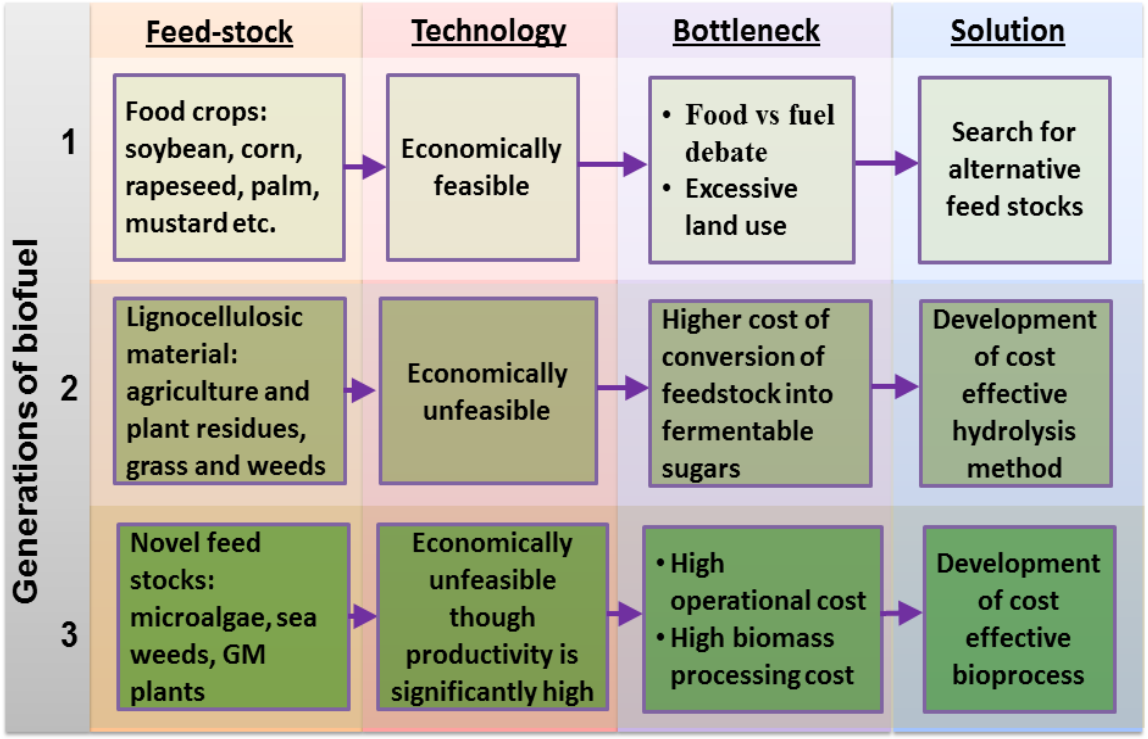

Fig. 2.3 Schematic representation of generations of biofuel production from corresponding feed stocks with existing bottlenecks and solutions (data source: Chisti, 2013; Dragone et al., 2010; Naik et al., 2010).

The second generation biofuels production uses the lignocellulosic materials and novel crops which can be grown easily with higher starch or oil content. Agricultural residues, weeds, plant parts, forest biomass, wood chips, etc. can be used as lignocellulosic material while non- food crops like Jatropha and Miscanthus are identified as novel crops for biofuel production (Dragone et al., 2010). However, the major constraint associated with second generation fuels are the extraction of fermentable sugars from rigid lignocellulosic structures. The lignin content of biomass being a phenolic compound restricts the complete hydrolysis of cellulose and hemicellulose (Taherzadeh and Karimi, 2008). Physico-chemical and enzymatic pre-treatments are effective for hydrolysis of

lignocellulosic biomass, but they are an expensive process and also suffer from several technical challenges.

On the other hand, third generation biofuels are produced from high productivity feed stocks such as algae, recombinant plants, seaweeds and microbes (Dragone et al., 2010). The high productivity is attributed to richness of lipid or cellulose in biomass along with their higher growth rate. The lipid rich microalgal biomass is one of the most promising feedstocks for biofuel production. The intracellular lipid content of biomass is trans-esterified and converted into fatty acid methyl esters which can be used as biodiesel.

2.2. Outline of microalgae and its metabolism

2.2.1. Overview of microalgae

Algae are primitive photosynthetic organism having capacity to carry out all cellular functions individually. Algae may also form multicellular structure with cell differentiation; however the degree of differentiation is very less in comparison to plants (Barsanti and Gualtieri, 2014). Algae exist as simple unicellular structures to complex multicellular masses; hence they were segregated into two groups namely microalgae and macroalgae. Algal size varies from 0.2 μm (diameter) in case of microalgae to 60 m (length) in case of giant macroalgae (Chiaramonti et al., 2015). Macroalgae are mostly found in seawater or large water reservoirs while microalgae can grow in many areas including seawater. This is attributed to the polyphyletic nature of algae which means organism evolved from different origins and attained similar kind of features (Barsanti and Gualtieri, 2014). Algae belong to 11 different divisions on their classification including two divisions of prokaryotes (Fig. 2.4). Algae exist in various forms such as tiny single cell, giant multicellular kelp, filamentous, matted colonies, branched connection, complex leafy or blade kind of forms (Chiaramonti et al., 2015). Microalgae have higher lipid content and growth rate than macroalgae (Behera et al., 2014) and is also easily cultivated

in submerged water (Rodolfi et al., 2009). Hence, research has been mainly focused on microalgal biotechnology rather than macroalgae.

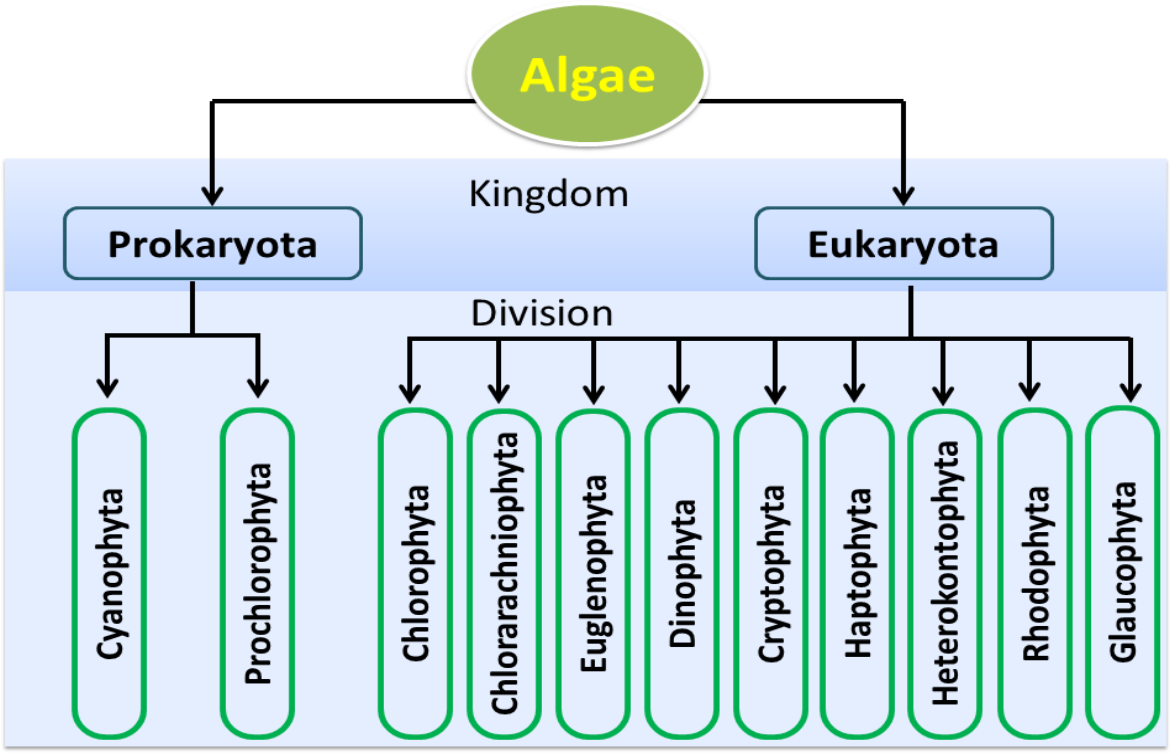

Fig. 2.4 Classification of algal systems based on their evolution from different origins (data source: Barsanti and Gualtieri, 2014).

Microalgae are microscopic unicellular organisms with varying their size from 0.2 micrometres to around hundred micrometres (Milledge et al., 2014). They can be used for the production of various products like carotenoids, phycobilin, biofuels etc. and hence exhibit multiproduct paradigm (Fig. 2.5). Phycobilins (phycocyanin, phycoerythrin and allophycocyanin), single cell protein and carotenoids (β-Carotene and astaxanthin) are commercially produced by microalgae since many years (Anupama and Ravindra, 2000; Borowitzka, 2013). The cost of production of poly unsaturated fatty acids (PUFA) such as γ-linolenic acid, arachidonic acid, eicosapentaenoic acid (EPA) and docosahexaenoic acid (DHA) from microalgae is significantly higher than fish oil based production. In spite of high cost, DHA is commercially being produced from algal platform for infant formulas,

food for pregnant and nursing woman etc. as fish oil based DHA contains mixed fatty acids and may leads to less suitable for application. DHA with various brand names (DHASCO, DHA Gold, DHActive) produced by many industries such as Martek (Columbia, MD, USA), OmegaTech (USA), Nutrinova process (Frankfurt, Germany), etc. (Borowitzka, 2013). Further, polysaccharide, bioplastic, bioactive compound and biofuel production technology are yet to be developed for commercial scale (Borowitzka, 2013). About 15,000 chemical components were extracted from microalgae and chemically identified for their commercial significance (Tabatabaei et al., 2011). Hence, microalgae can be regarded as 'cell factories' for many products. Microalgal cultivation can be advantageous as it can also be grown in marginal lands (desert, semiarid regions, hill area), brackish, saline and waste water (Pandey et al., 2013). Further, some microalgae can grow in organic carbon sources in absence of light which is regarded as heterotrophic growth. Additionally, microalgae may result in 25-100 times higher biofuel productivity than *Jatropha* based biodiesel production (Khan et al., 2009). This is credited to their higher lipid content and higher specific growth rate in comparison with the conventional crops (Becker, 1994).

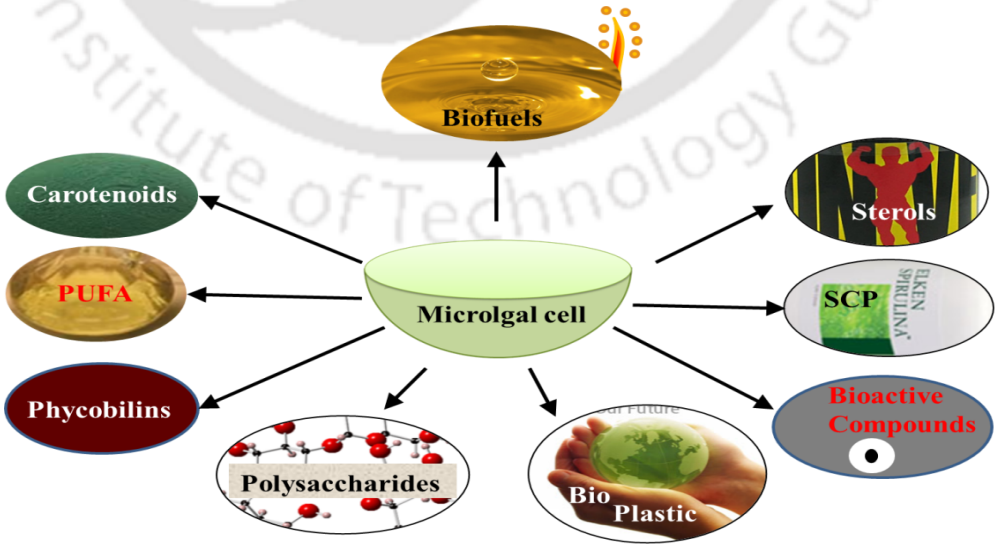

Fig. 2.5 Schematic representation of multi-product paradigm of microalgae as per up to date findings. PUFA and SCP represent poly unsaturated fatty acid and single cell protein respectively (data source: Borowitzka, 2013).

2.2.2. Nutrition

Majority of microalgae show autotrophic growth however some exhibit dependency on organic compounds for their growth and hence they are classified into three groups depending on their nutritional strategies as follows:

- Obligate autotrophic algae: Organism uses CO_2 as sole carbon source and either light or a reduced inorganic compound as energy source for growth and metabolism. E.g. *Porphyridium cruentum, Anacystis nidulans* (Richmond, 2008; Smith et al., 1967)
- Facultative heterotrophic algae: They usually grow autotrophically, however they can consume organic compounds as energy and carbon sources when the light is limiting or surrounded by high concentration of organic materials. E.g. Euglena (Bellinger and Sigee, 2010).
- Obligate heterotrophic algae: These organisms can use only organic materials as carbon and energy sources for their growth. Plastids or chlorophyll content of cell was lost during the evolution and hence they are not able to carry out photosynthesis. E.g. *Petalomonas, Prototheca zopfii* (Bellinger and Sigee, 2010; Zajic and Chiu, 1970).

2.2.3. Cell biology and structure

Microalgal reproduction method varies among species to species as they are polyphyletic in nature. It may be vegetative by the division of a single cell or fragmentation of a colony or asexual by the production of motile spore or sexual by the union of gametes (Barsanti and Gualtieri, 2014). Autosporulation is an asexual reproduction method which is mainly observed in green algae such as *Chlorella* sp. (Chlorophyta) and *Nannochloropsis* (Heterokontophyta). Four daughter cells are formed within the cell wall of mother cell. They reside within mother's cell wall until they form

separate cell wall and attain maturity. After maturation they are released outside with the rupture of mother's cell wall and feed on the residual debris of the mother's cell (Safi et al., 2014). In case of *Chlamydomonas* sp., motile gametes, termed as zoospores, are formed inside the vegetative mother cell; their locomotion being facilitated by the presence of flagella. The binary fission is also a mode of asexual reproduction where the mother cell divides into two equal parts with same nucleic acid contents to form two daughter cells (e.g. *Ceratium* sp.). Sexual reproduction characteristics are also observed in many algal species where distinct gametes are formed with haploid genome via meotic cell division (e.g. Bacillariophyceae).

The microalgae show different kinds of cellular structure based on their phylogenetic links; however common generalized structures for prokaryotic and eukaryotic cells are presented in Fig. 2.6. The prokaryotic cells lack many intracellular organelles such as mitochondria, chloroplast, etc. and a prominent nuclear membrane (Fig. 2.6 A). It performs photosynthesis in thylakoid membranes where phycobilisomes are arranged on their outer surface in order to harvest the light. As storage pockets of energy and carbon, starch granules and lipid bodies are found in the cytoplasm. The cell is covered with three types of layers which are cell membrane as an innermost layer, cell wall in the middle and mucilage layer as an outermost layer. On the other hand, eukaryotic algae contain the chloroplast which comprises of pigments, thylakoid membranes, some DNA sequences and starch granules (Fig. 2.6 B). The intracellular organelles such as endoplasmic reticulum, golgi bodies, mitochondria, etc. are present in eukaryotic microalgal cell. In prokaryotic algae, oxidative phosphorylation and photophosphorylation takes place in thylakoid membranes only. However, in case of eukaryotic microalgae; mitochondria and chloroplast host oxidative phosphorylation and photophosphorylation respectively. Eukaryotic algae may or may not contain mucilage layers as outermost

protective layer and they are present in specific type of species (Barsanti and Gualtieri, 2014; Bellinger and Sigee, 2010).

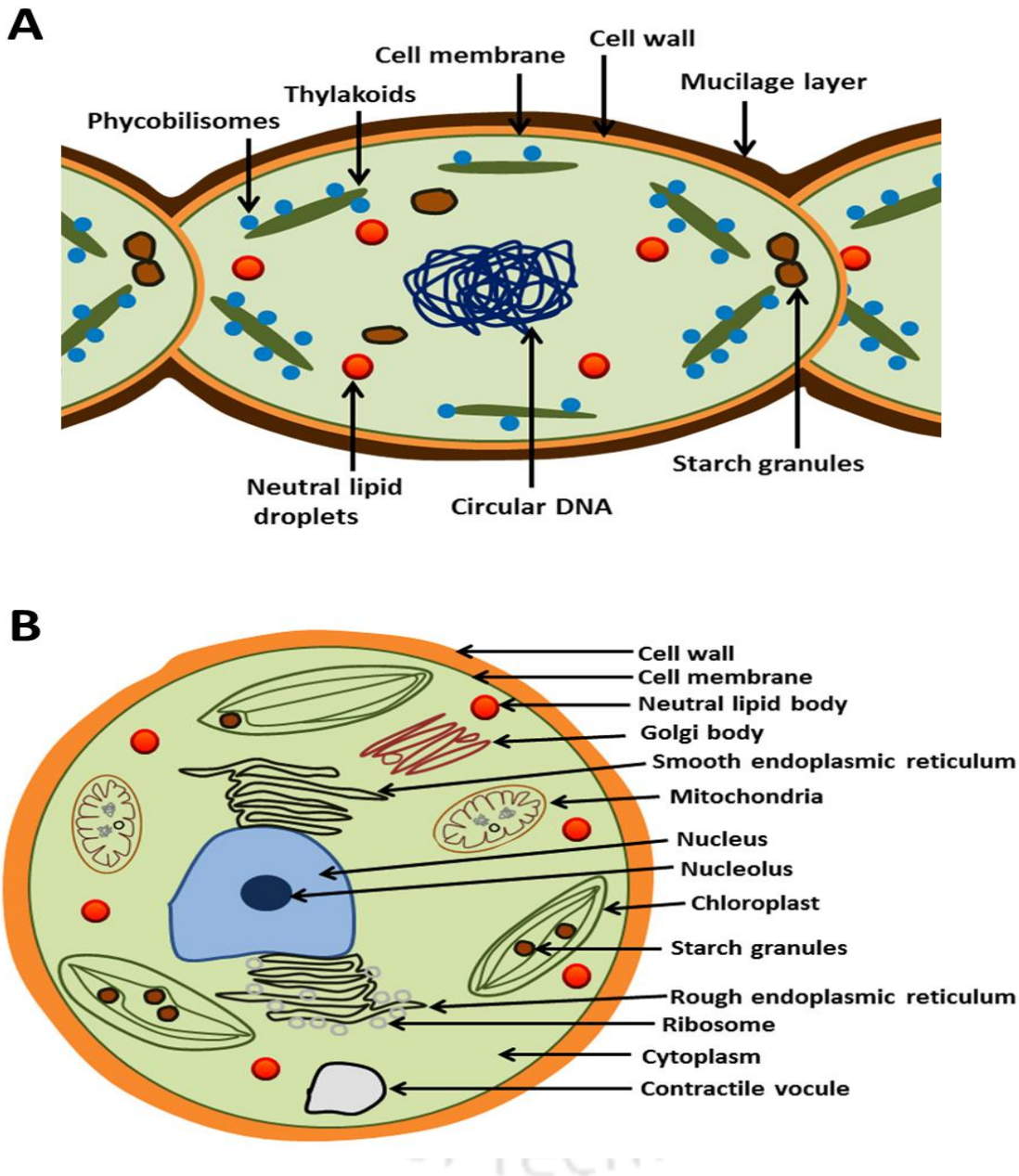

Fig. 2.6 Structural morphology of (A) prokaryotic blue-green algae and (B) eukaryotic green algae based on information obtained from Barsanti and Gualtieri (2014).

2.2.4. Photosynthesis

The electromagnetic radiations from sun are the universal source of energy in the biosphere. Phototrophic organisms harvest this light energy for their cellular mechanism (e.g. plants, algae and some bacteria). Microalgae can absorb the light from 400 nm to 700

nm which is termed as photosynthetically active radiation (PAR). Microalgae account for more than 50% of world's photosynthesis. Photosynthesis starts with the excitation of antenna molecules present in thylakoid membrane by irradiation of light (Barsanti and Gualtieri, 2014). Chlorophyll (Chlorophyll a, chlorophyll b etc.), carotenoids (β- carotene, lutein etc.) and other accessory pigments (phycobilins etc.) work as antenna molecules and transfer the energy reaction centers. These molecules and specific protein complexes together form photosystems (PSI and PSII) for conversion of light energy into chemical energy such as ATP and NADPH (Fig. 2.7). Photosystem I (PSI) contains higher concentration of chlorophyll a in comparison to chlorophyll b and in case of photosystem II (PSII) both are in equal concentration. The concentration of carotenoids and other accessory pigments is lesser in comparison to chlorophylls. Reaction center chlorophylls (P680 in PSII and P700 in PSI) are excited by either direct absorption light or absorption of energy from excited neighboring antenna molecules (Fig. 2.7). The photosystems work complementary to each other and have distinct functions.

Under light condition, P680 absorbs electron from water on photolysis ($2H_2O \rightarrow 4e^- + 4H^+ + O_2$) and attains high energy excited state (redox potential -0.6 eV). In few picoseconds, the electron is transferred to series of protein complexes where energy is dissipated to create proton gradient and concurrently redox potential increases to positive values (Fig. 2.7). The electron gets transferred to reaction center P700 at redox potential of 0.45 eV. On light irradiation, P700 gets excited and possesses a redox potential of more than -1 eV. Thus this whole reaction scheme follows Z type pathway in terms of redox potential and hence it is termed as Z- scheme of photosynthesis (Barsanti and Gualtieri, 2014; Nelson and Cox, 2012). The electron from excited P700 transfers to various protein carriers and finally gets utilized in the formation of NADPH. So, the formation of NADPH from photolysis of water is termed as non-cyclic phosphorylation.

When an end electron acceptor NADP is not available, the ferredoxin of PSI donates its electron back to Cyt b_6f complex and a proton gradient is generated to produce ATP which is termed as cyclic phosphorylation. The overall non-cyclic phosphorylation is expressed as equation 2.1.

$$2\,H_2O + 4\,NADP^+ + 4\,ADP + 4\,Pi + 8\,Photons \rightarrow O_2 + 4\,NADPH + 4\,ATP \qquad (2.1)$$

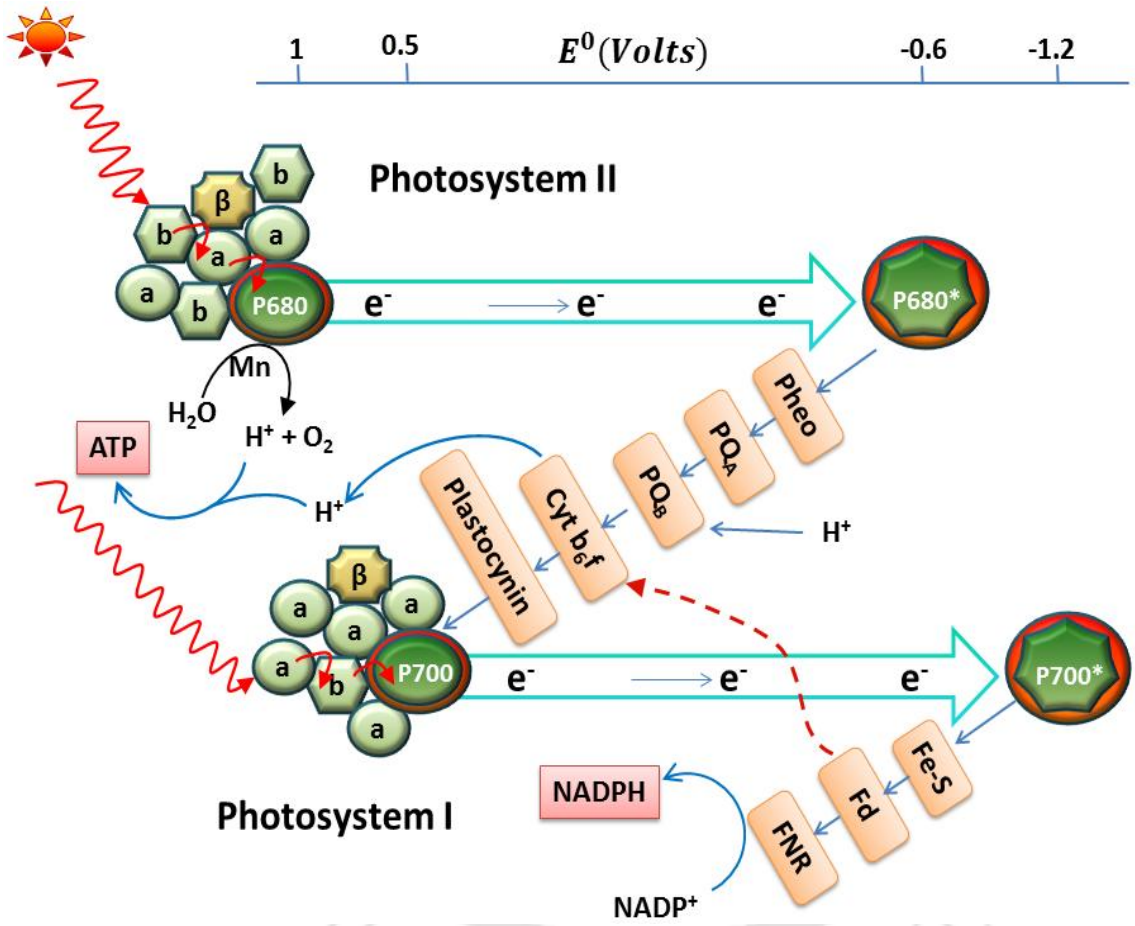

Fig. 2.7 Z-scheme of photosynthesis where redox potential of photosystems (PSII and PSI) oscillates in Z pattern. FNR-ferredoxin reduction complex, FD – ferredoxin, Fe-S – membrane bound ferrous sulfate complex, a – chlorophyll a, b – chlorophyll b, β – β carotene, Pheo – pheophytin, PQ_A – plastoquinone A, PQ_B – plastoquinone B. The * represents the excited state of the reaction center chlorophyll. The dotted line from FD represents the cyclic photophosphorylation. The representation was obtained and modified from Barsanti and Gualtieri (2014) and Nelson and Cox (2012).

2.2.5. Lipid biosynthesis

The biosynthesis of lipid in algae is assumed to be similar to plant metabolism as homologous sequences are observed in respective gene area of both the systems (Hu et al.,

2008). The *de novo* synthesis of lipid can be divided into fatty acid biosynthesis and formation of macromolecules. Fatty acid synthesis mainly takes place in chloroplast by using acetyl CoA as main precursor. Lipid biosynthesis starts with the conversion of acetyl CoA to malonyl CoA by the action of acetyl CoA carboxylase (ACCase). Acetyl CoA is a two carbon molecule which can be generated by series of reactions from extracellular carbon dioxide assimilation under photoautotrophic growth and organic carbon sources like glucose in case of heterotrophic growth (Fig. 2.8). Acyl carrier protein (ACP) carries the malonyl moiety of malonyl CoA in the set of four reactions (condensation, reduction, dehydration and reduction) for the formation of fatty acids. Fatty acid chain is elongated by adding a malonyl group in every cycle of four set of reactions. The enzyme stearoyl ACP desaturases also contributes its activity in the formation of double bonds in required place of fatty acid chain. The chain elongation is terminated with detachment of ACP from acyl group by action of acyl-ACP-hydrolases to form free fatty acids. The specific action of these enzymes controls composition of fatty acids in the neutral lipids and phospholipids (Hu et al., 2008; Kanehisa et al., 2016).

Phospholipid and neutral lipid (triacylglycerol) can be synthesized from free fatty acids at the surface of endoplasmic reticulum which lies in cytoplasm. Two fatty acids are transferred to 1st and 2nd position of glycerol-3-phosphate to form 1, 2 diacyl glycerol by action of three enzymes. This is used for synthesis of neutral lipid by addition of one more fatty acid in the enzymatic reaction of diacylglycerol acyltransferase (DGAT). The phospholipid is formed by various combinations of 1, 2 diacyl glycerol, serine, choline, inositol, ethanol amine, etc. (Hu et al., 2008; Kanehisa et al., 2016). Phospholipids play a significant role in formation of cellular structure like lipid bilayer of cell membrane and they comprise of various classes such as monogalactosyldiacylglycerol, digalactosyldiacylglycerol, sulfoquinovosyldiacylglycerol, phosphatidylglycerol,

phosphatidylethanolamine, etc. Phospholipid content of a cell falls in the range of 5–20% of dry cell weight to maintain the structural integrity of cell (Hu et al., 2008).

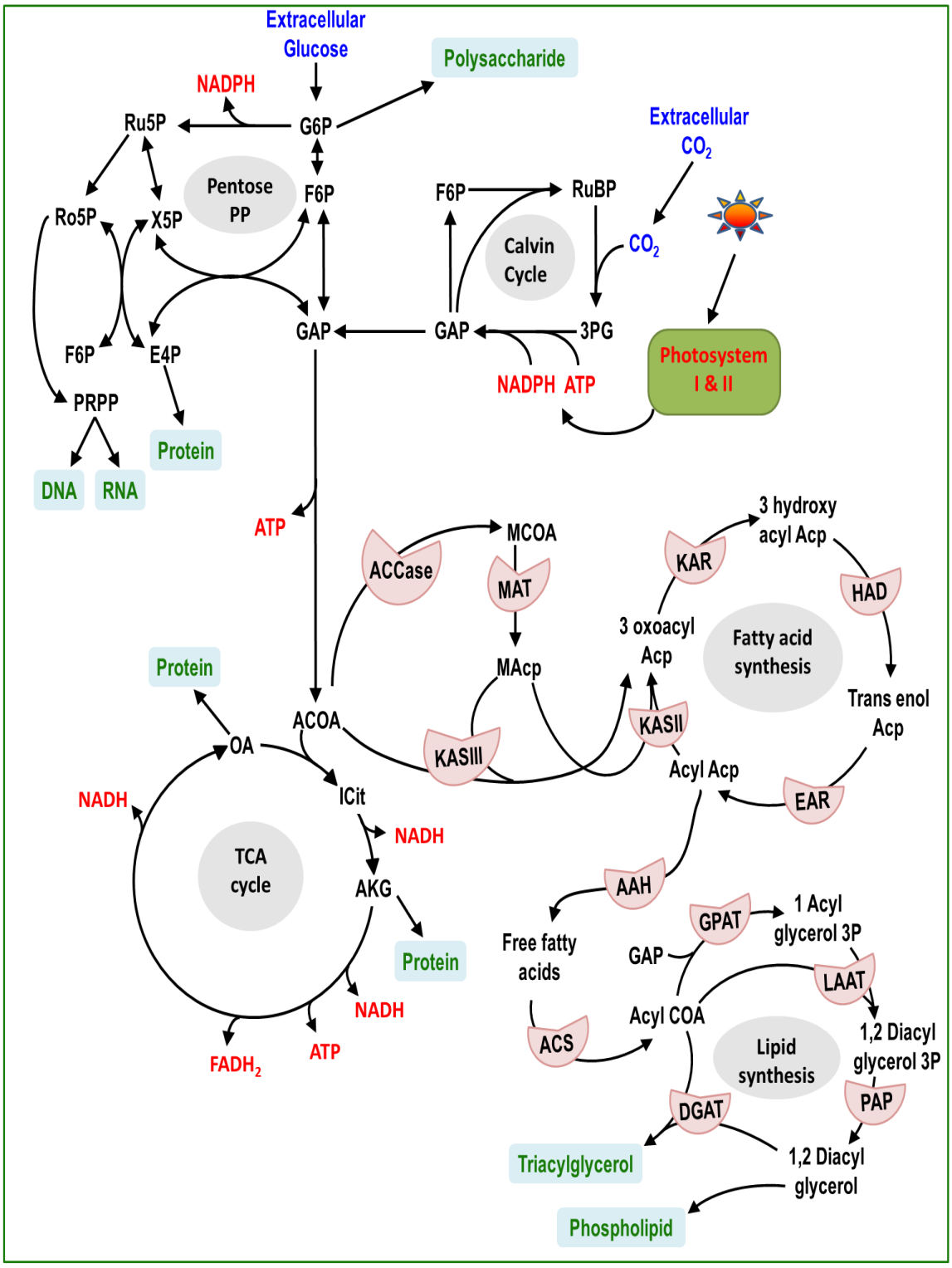

Fig. 2.8 Overview of lipid biosynthesis pathway in microalgae based on information obtained from Kanehisa et al. (2016) and Hu et al. (2008). Where, ACCase – acetyl CoA carboxylase; ACP-acyl carrier protein; CoA-coenzyme A; MAT- malonyl CoA ACP

transacylase; KAS- 3 ketoacyl ACP synthase; KAR- 3 ketoacyl ACP reductase; HAD- 3 hydroxyacyl ACP dehydratase; EAR- enoyl ACP reductase; AAH- acyl ACP hydrolase; ACS- acyl CoA synthetase; GPAT- glycerol 3 phosphate 1acyltransferase; LAAT- lysophosphatidic acid acyltransferase; PAP- phosphatic acid phosphohydrolase; DGAT- diacylglycerol acyltransferase; G6P- glucose 6 phosphate; F6P- fructose 6 phosphate; GAP- glyceraldehyde 3 phosphate; 3PG- 3 phospho glycerate; RuBP- ribulose 1,5 biphosphate; Ru5P- ribulose 5 phosphate; Ro5P- ribose 5 phosphate; X5P- xylulose 5 phosphate; E4P- erythrose 4 phosphate; PRPP- phospho ribosyl pyrophosphate; ACOA- acetyl COA; ICit- isocitrate; AKG- alpha keto glutarate; OA- oxalo acetate; MCOA- malonyl COA; MAcp- malonyl ACP; 1 Acyl glycerol 3P- 1 acyl glycerol 3 phosphate; 1,2 Diacyl glycerol 3P- 1,2 diacyl glycerol 3 phosphate.

The active growing cells of microalgae contain neutral lipid of around 5% DCW, however it may increase to 85% DCW during unfavorable growth conditions such as nutrient starvation, high intensity light irradiance, etc. (Rodolfi et al., 2009). Neutral lipid especially triacylglycerol is accumulated in cells as a storage packet of energy and carbon under unfavorable condition to rebuild the cell after stress (Roessler, 1990).

2.3. Lipid induction strategies

During the growth of organism, phospholipid is synthesized to meet the structural requirement of biomass formation. Microalgae are known to accumulate neutral lipid up to 70% of cell weight (Hu et al., 2008; Rodolfi et al., 2009); hence phospholipid majorly cannot be targeted for biodiesel production. Neutral lipid (TAG) is superior to phospholipid as all three binding sites of glycerol are occupied by fatty acids (Hu et al., 2008; Williams and Laurens, 2010). Fortunately, it can be accumulated in the cell as a storage compound and can be used as potential source of biodiesel production. Many researchers have reported that TAG can be significantly synthesized during non-growth supporting condition as both are mutually exclusive in nature (Xiao et al., 2013). Physical or chemical stimuli such as nutrient starvation, elevated temperature, pH, light intensity, lipid elicitor supplementation shows an enhanced biosynthesis of neutral lipid in oleaginous microalgae (Hu et al., 2008; Kim et al., 2013). Neutral lipid was found to accumulate in biomass in compensation with other macromolecular components under

nitrogen starvation (Rodolfi et al., 2009; Zhu et al., 2014). Synthesis of protein, chlorophyll, nucleic acids and other pigments suffer from nitrogen limitation as they are nitrogenous compounds. These being structural molecules, hinder the growth of organism and hence organism tries to accommodate carbon and energy flux into some other metabolites. To that end, organism shifts its flux towards the formation of either neutral lipid bodies or starch granules in the cytoplasm. The accumulation of neutral lipid bodies or starch granules in the cytoplasm of *Symbiodinium* spp. under nitrogen deprivation was revealed through transmission electron micrographs (Jiang et al., 2014). The synthesis of neutral lipid is prominent in oleaginous microalgae under nutrient starvation as it can accommodate more energy and carbon element in its molecule in comparison with starch (Rodolfi et al., 2009). This is a secondary metabolite and can be used to rebuild the cell in support of growth after the deprival of stress (Roessler, 1990). Similarly, the deprivation of medium components such as phosphate (Liang et al., 2013), silicate in case of diatoms (Jiang et al., 2015), iron (Urzica et al., 2013), zinc (Kropat et al., 2011), sulfur (Deng et al., 2011), calcium (Gorain et al., 2013), etc. also resulted in enhancement of neutral lipid synthesis in microalgae. These are important elements for the growth of an organism and play role in the formation of structural molecules of biomass. During unfavorable growth condition due to ceased formation of structural molecule, organism metabolically activates the fatty acid biosynthesis pathway.

The elevated light intensity may trigger higher production of neutral lipid in order to avoid any photochemical damage to cellular structure (Atta et al., 2013). The light energy is absorbed to synthesize a large amount of ATP & NADPH which is then directed towards formation of fatty acids. However, in some microalgae it may not induce the lipid as it is specific to species, wavelength of light and magnitude of light intensity (Chen et al., 2011) which may damage the photosynthesis system of organism. Microalgae also

show variation in their lipid content along with change in the temperature (Xin et al., 2011). For instance, *Nannochloropsis salina* showed increased lipid content with an increase in temperature (Converti et al., 2009). Recently supplementation of lipid elicitor for biosynthesis of neutral lipid is turning out as an effective method. *Scenedesmus* sp. CCNM 1077 showed 1.8 fold enhanced lipid content with increased levels of reactive oxygen species and malondialdehyde concentration at hyper saline condition with 400 mM of sodium chloride concentration as compared to control condition (Pancha et al., 2015). The action of this oxidative stress on lipid biosynthesis is not clearly understood, however it is believed that it acts as a mediator in fatty acid biosynthesis pathway. Brefeldin A was also used as elicitor as it led to rapid formation of lipid droplets in *Chlamydomonas reinhardtii* and *Chlorella vulgaris* (Kim et al., 2013). It disturbs the homeostasis responsible for lipid in endoplasmic reticulum ER and other extra-plastidial membrane and induces the lipid accumulation in cytoplasm (Fei et al., 2009). Similarly, acetate was also found as one of the effective elicitors in many microalgal strains (Kumar et al., 2016; Qiao and Wang, 2009). Being a simple structured molecule with two carbon atoms, it can be easily assimilated by the cell and converted into acetyl coenzyme A which is the main precursor in fatty acid biosynthesis pathway (Qiao and Wang, 2009). Therefore, nutritional conditions, environmental parameters, lipid elicitors may show the impact towards biodiesel production.

2.4. Carbon assimilation

Microalgae can use various carbon sources depending on the type of strain or growth condition. As most of the microalgae grow autotrophically, they use inorganic carbon and CO_2 for cellular requirements. The CO_2 is fixed into organic compounds (3-phosphoglycerate) by using ATP and NADPH generated from photophosphorylation in the stroma region of the chloroplast of eukaryotic cells or in the cytoplasm of prokaryotes.

This CO_2 fixation pathway does not require light and commonly termed as the Calvin Benson Bassham cycle. The ribulose-1,5-bisphosphate carboxylase/oxygenase (RuBisCO) and phosphorybulokinase (PRK) are the most unique enzymes among 13 enzymes that take part in CO_2 fixation. The carbon fixation rate depends on the activity of RuBisCO enzyme (Spreitzer et al., 2005).

In case of organic carbon source, microalgae can grow on a wide variety of organic substrates; however particular strain can use specific set of carbon sources. Generally glucose is used as carbon source by most of the heterotrophic microalgae (Perez-Garcia et al., 2011). Glucose was found to support higher growth rate and metabolism in comparison to other carbon sources such as monosaccharides, disaccharides, poly saccharides, sugar alcohols, organic acids, and monohydric alcohols (Griffiths et al., 1960). Glucose can be transported into cell through hexose/H^+ symport membrane transporter. These may exist in three different forms which are expressed by hexose uptake protein genes such as hup1, hup2, and hup3 (Caspari et al., 1994; Sauer and Tanner, 1989). The transportation of glucose is carried out along with proton in 1:1 ratio and then converted into glucose- 6- phosphate in its first reaction. Several algae may consume glycerol as carbon source via simple diffusion and convert it into glyceraldehyde-3-phosphate as an important glycolytic intermediate (Perez-Garcia et al., 2011). Acetate is also one of the most commonly used carbon sources for microalgal metabolism. Acetate is consumed in cell through monocarboxylic/proton transporter protein present in the cell membrane. Acetyl CoA was formed after consumption and conversion of acetate in the microalgae, which is a key precursor for lipid biosynthesis and TCA cycle (Boyle and Morgan, 2009). Other carbon sources such as sucrose, lactate, lactose, ethanol, pentose sugars, etc. are not significantly consumed by microalgae due their inhibitory or very low activity as substrate (Perez-Garcia et al., 2011).

2.5. Cultivation of microalgae

2.5.1. Mode of nutrition

The cultivation of microalgae can be carried out under various modes such as photoautotrophic, heterotrophic, mixotrophic and photoheterotrophic conditions (Table 2.1). Mainly large scale cultivation of microalgae has been carried out in open race way ponds under photoautotrophic conditions (Shen et al., 2010). Photoautotrophic cultivation utilizes solar radiation as a source of energy and photosynthetic machinery to convert inorganic carbon into diverse organic matters to satisfy the requirements of microorganism. Lipid productivity of the algal strains varies significantly from species to species (15 to 61 mg L^{-1} day^{-1}) under autotrophic cultivation condition. Major advantages of photoautotrophic condition are lesser capital investment and operational cost (Rodolfi et al., 2009). However, this suffers with several bottlenecks such as narrow light penetration, fluctuating environmental conditions, cell shading effects and high chances of contamination (Chae et al., 2006; Chinnasamy et al., 2010; Shen et al., 2010). It results in reduced biomass concentration and growth rate which in turn increases the operational, harvesting and downstream processing costs (Xiong et al., 2008).

Table 2.1 Different cultivation modes with their respective carbon and energy sources utilized for algal growth

Mode of nutrition	Carbon source	Energy source
Photoautotrophy	Inorganic CO_2	Light
Heterotrophy	Organic carbon	Organic carbon
Mixotrophy	Mainly inorganic CO_2 during illumination and organic carbon during dark hours	Mainly light during illumination and organic carbon during dark hours
Photoheterotrophy	Mainly organic carbon	Mainly light and organic carbon on light limitation

Under heterotrophic growth condition, microalgal strains grow by utilizing organic carbon source as the source of energy and carbon in the absence of light. Heterotrophic cultivation is usually performed in a closed bioreactor which offers consistent and

improved biomass and lipid productivity by eliminating the chances of cross-species contamination and ease of controlling process parameters (Shen et al., 2010). Biomass and lipid productivity can be enhanced upto 12 g L^{-1} day^{-1} and 3 g L^{-1} day^{-1} under heterotrophic batch cultivation (Li et al., 2013). Nevertheless, the cost of organic carbon sources utilized in heterotrophic condition remains an unsolved issue (Turon et al., 2015). One of the alternatives is exploitation of suitable lignocellulosic biomass and other cheaper carbon sources for the growth of microalgal systems, however much attention is still required to achieve feasible process for high biomass and lipid productivity.

Mixotrophic cultivation is another mode of nutrition which involves both photoautotrophic and heterotrophic condition. It provides an opportunity for the strain to utilize both inorganic and organic carbon sources along with light energy (Wang et al., 2014). However design of bioreactor for the efficient utilization of sunlight and maintaining contamination free condition on organic nutrients addition, still remains unachieved. Photoheterotrophic cultivation uses light as the main energy source and organic carbon compounds as the source of carbon (Chen et al., 2011). It also suffers from some disadvantages similar to mixotrophic cultivation since it uses both light and organic carbon source. Various designs involving hybrid systems of these cultivation conditions were reported for biodiesel production. However, a development of sustainable process for commercial scale biodiesel production still remains unachieved.

Mode of operation was also found to effect growth and lipid productivity in all the nutritional conditions. For instance, *Chlorella sorokiniana* was reported to show biomass productivity of 24.2 g L^{-1} day^{-1} under heterotrophic fed-batch mode however it was only 10.7 g L^{-1} day^{-1} under batch cultivation (Zheng et al., 2013).

2.5.2. Cultivation of microalgae in various reactor systems

Open raceway ponds are the commonly used system for photoautotrophic cultivation. These are designed as oval shaped with a depth of 0.2 to 0.5 m containing paddles for proper mixing and sparger for proper CO_2 supply (Fig. 2.9). The operational and installation cost of open raceway pond is less in comparison to photobioreactors. *Dunaliella salina* is being cultivated for β-carotene production in open the pond which spreads for 200 ha in Australia (Borowitzka and Hallegraeff, 2007). The problems associated with open raceway pond are poor light penetration, low biomass titer, high chance of contamination by protozoans and other microbes such as microalgae, bacterial and fungal species (Doucha and Lívanský, 2012; Shen et al., 2010).

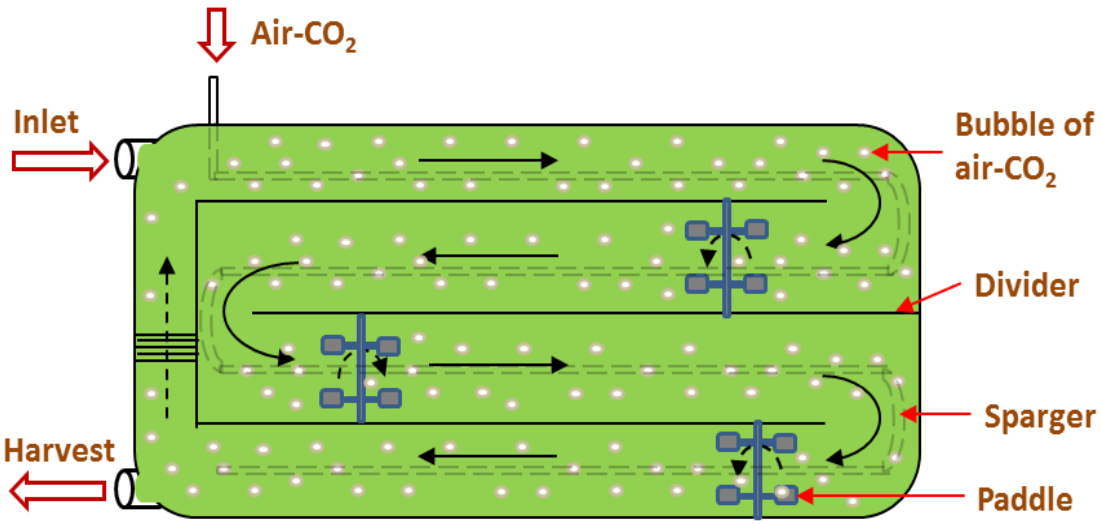

Fig. 2.9 Schematic representation of the open raceway ponds which can be used for large scale cultivation of microalgae

Closed photobioreactor technologies were developed in order to overcome the hurdles associated with outdoor open pond systems. These technologies offer advantages such as contamination free monoculture cultivation, high productivity. To that end, tubular, flat panel and column photobioreactors are developed as closed systems. Tubular photobioreactor is designed with an array of tubes arranged horizontally, vertically or

inclined with land surface and are connected to a reactor for proper mixing of nutrients, gases and pH control (Fig. 2.10). The tubes are usually made up of transparent glass or acrylic or plastic materials with a diameter of about 0.1 m in order to ensure proper light penetration (Chisti, 2007). The major disadvantage of this system is associated with large scale cultivation such as restriction of tube length by O_2 accumulation, CO_2 depletion, and pH variations. Therefore, multiple reactor units with lesser surface area are required for commercial scale production.

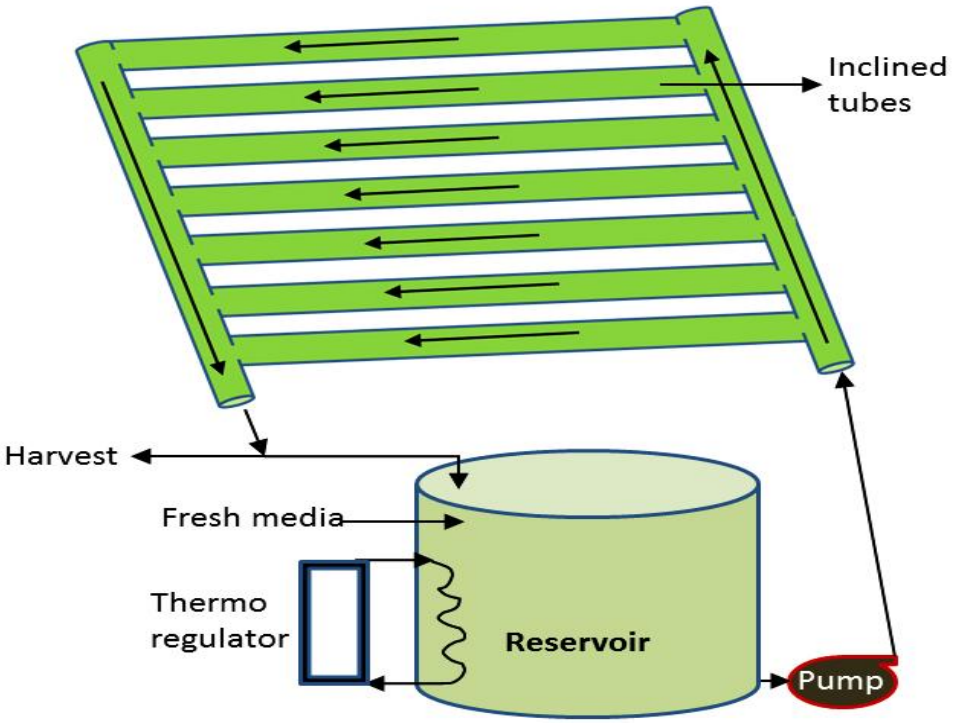

Fig. 2.10 Schematic representation of an inclined tubular photobioreactor which can be used for outdoor microalgal cultivation

Column photo-bioreactor is constructed by hanging a polyethylene bag vertically on a framework or in a support. The bag is usually maintained with inner diameter of 0.3 to 0.5 m and height of 1 to 2.5 m. Along the same lines, flat panel (or flat plate) photo-bioreactors are developed to achieve high cell densities with better mass transfer capabilities. These are made up of two transparent glass panels or polyacrylic sheets arranged with a width of 10-20 mm (Sierra et al., 2008) for proper light penetration even

at high cell density (Fig. 2.11). The cell density of 80 g L^{-1} was reported in flat panel bioreactor (Hu et al., 1998). Requirement of large surface area under large scale cultivation of microalgae in column or flat panel photobioreactors and associated additional capital cost has limited its use.

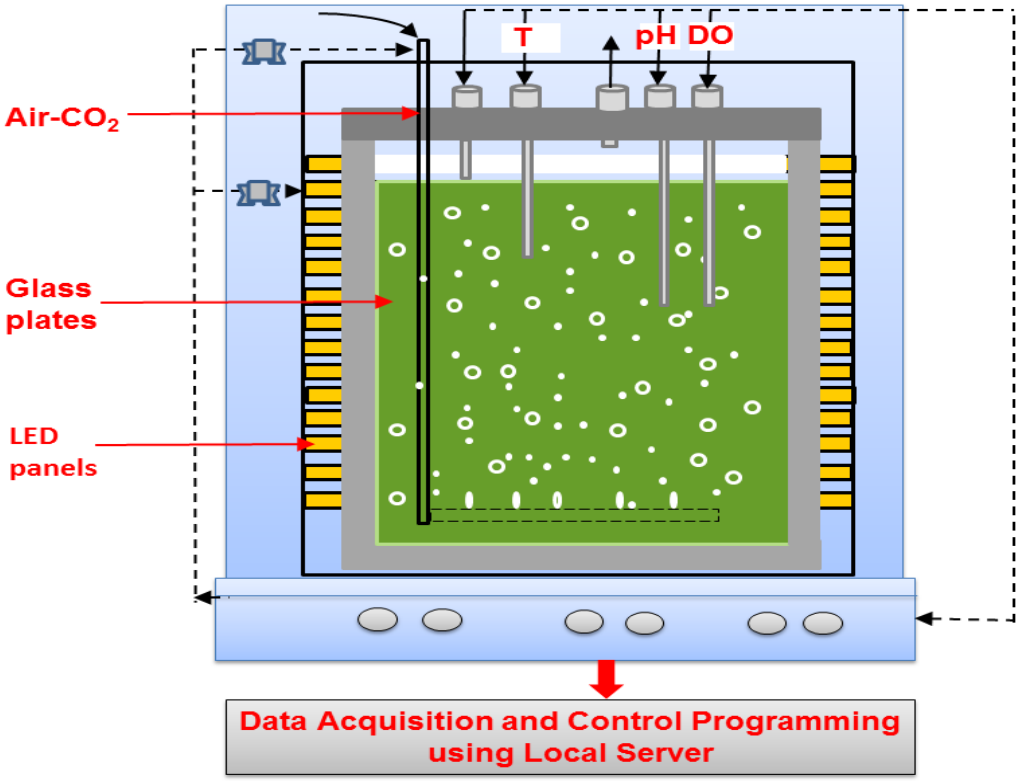

Fig. 2.11 Schematic view of a closed flat panel photo-bioreactor designed for high cell density cultivation

Commonly continuous stirred tank reactor (CSTR) is used for heterotrophic cultivation of microalgae (Doucha and Lívanský, 2012; Xiong et al., 2008). These reactors are easily scalable for industrial scale application. They offer advantages such as proper mixing, aeration, automatic control of process parameters and ease of cultivation with any mode of operation (Fig. 2.12). A CSTR is made up of transparent glass for laboratory scale usage and stainless steel in case of pilot or industrial scale of reactor (Stanbury et al., 2003). The maximum biomass concentration of 117 g L^{-1} was also reported when the microalgae were grown in CSTR on fed-batch mode (Doucha and Lívanský, 2012). Major limitation of this system is non-suitability for autotrophic growth by natural sunlight.

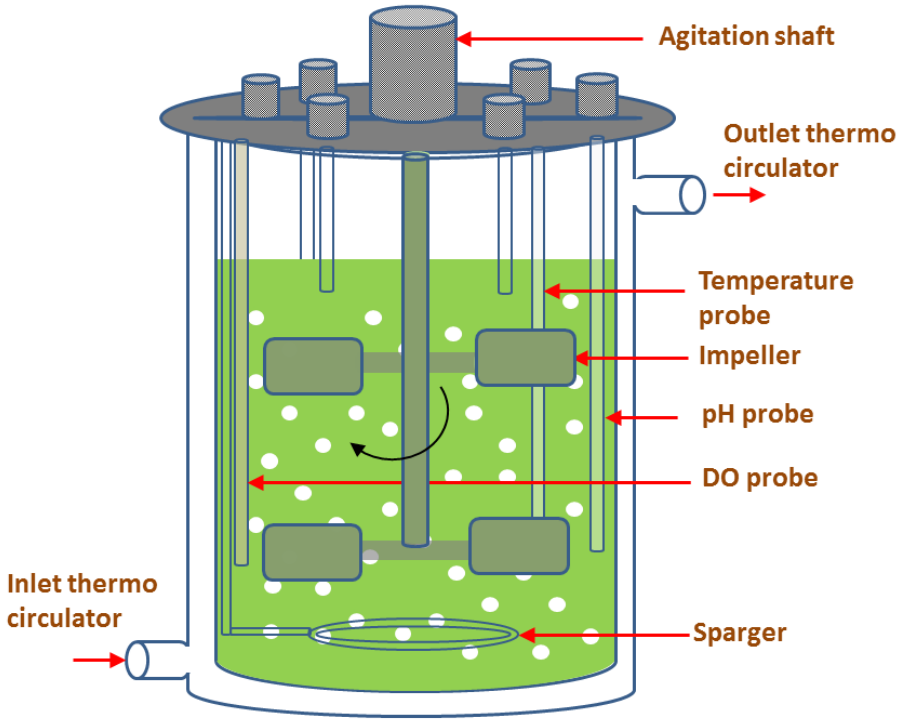

Fig. 2.12 Schematic representation of a continuous stirred tank reactor designed for heterotrophic cultivation

2.6. Biomass to biodiesel conversion technologies

Intracellular lipid content of biomass is converted into fatty acid methyl esters by transesterification method (Fig. 2.13). Fatty acid methyl ester (FAME) can be used as alternative of diesel, hence termed as biodiesel.

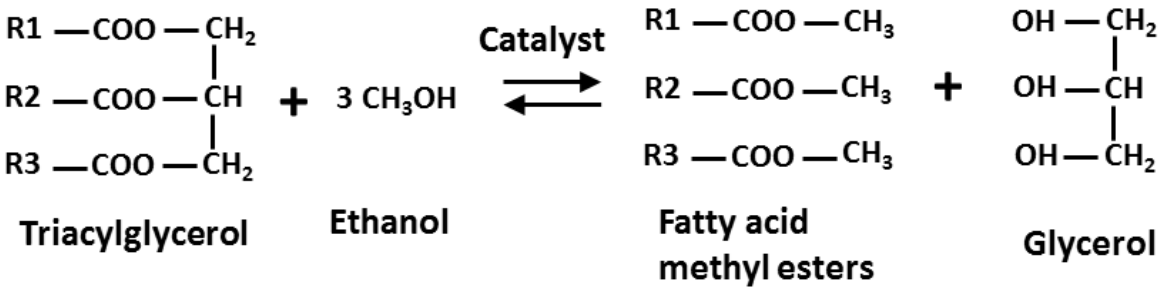

Fig. 2.13 Transesterification of triacylglycerol for the production of fatty acid methyl esters in presence of catalyst and methanol as reactant

Transesterification is performed after the lipid and fatty acid content of biomass is extracted outside the cell. Lipid extraction is an energy demanding step as proper

pretreatment and cell disruption are required to be carried out before the lipid extraction (Hidalgo et al., 2013). The cell disruption can be performed with several physical and chemical methods. While physical method involves grinding, homogenization, microwave processing, sonication, bead beating, freeze drying, etc. and chemical method comprises of solvent mediated cell lysis, supercritical fluids, ionic liquids, direct transesterification methods, etc. (Parmar et al., 2011). Bligh and Dyer method is the commonly used for extracting intracellular lipid by a mixture of chloroform and methanol following which the lipid is transesterified in the presence of catalysts such as sodium hydroxide (Griffiths et al., 2010). It is used in large scale transesterification process due to lesser energy requirement. However, extraction efficiency is very less which may account to only 60% of cellular lipid content.

Other methods involving supercritical fluids, microwave radiations and sonication assisted extraction methods are reported to show improved efficiency with high processing costs which results in economical infeasibility of process (Hidalgo et al., 2013). The *in situ* transesterification method is developed in order to avoid loss due to improper extraction and bypasses the requirement of a separate extraction process (Griffiths et al., 2010). The process uses methanol as an extracting solvent as well as acyl acceptor along with a catalyst which acts as a hydrolyzing agent. The most important problem is the high water content of the wet algal biomass which affects the overall catalyst availability and transesterification efficiency (Kumar et al., 2014). Thus, drying of biomass remains the major issue involving energy consuming drying steps. Usually water content in the algal biomass is removed by spray drying, drum drying and sun drying methods (Pragya et al., 2013). These work on the basis of evaporation of water by heat and hence they may lead into lower yield due to oxidation of fatty acids (Oehrl et al., 2001). Unsaturated fatty acids are more susceptible to oxidation on heat based drying in comparison to saturated fatty

acids. Recently, the sequential two stage *in situ* transesterification method is reported with efficiency of 98.9% by using freeze dried biomass. This method can be used for accurate quantification of intracellular lipid content however is not suitable for large scale biodiesel production due to usage of freeze dried biomass. Therefore, it is imperative to develop efficient and economical transesterification method for commercial scale biodiesel production.

2.7. Mathematical modeling of microalgae as a biological system

Microalgal modeling comprises of all the areas related to microalgal cultivation such as fluid dynamics model (Hall et al., 2003), growth kinetics (Alagesan et al., 2013), metabolic modeling (Shastri and Morgan, 2005), life cycle assessment model (Quinn et al., 2014), etc. Fluid dynamics model can be used for bioreactor design in order to achieve high biomass, productivity, proper light utilization and proper gas exchange. Interestingly, unlike other microbial systems, algae are known to continue to their growth even after exhaustion of nutrients from the medium by using stored intracellular nutrients (Bernard, 2011). The classical Monod model was found to be inadequate to capture microalgal growth kinetics as they vary their yield coefficient depending on substrate concentration (Lemesle and Mailleret, 2008). An alternate approach consisting of variable yield and cell quota theory was employed to model growth of microalga *Monochrysis lutheri* under different concentration regimes of vitamin B_{12} (Droop, 1975, 1968). According to cell quota theory, microalga consumes nutrient at higher rate during nutrient sufficient condition and a portion of it is stored as intracellular nutrient pool. Organism consumes the intracellular stored nutrient during nutrient limited or starved conditions. Some of the variables lack their biological and physical meaning which have been used in Droop's model (Lemesle and Mailleret, 2008). To that end, some literatures have been reported with proper re-interpretation of Droop's cell quota model by providing biological sense to

variables (Lemesle and Mailleret, 2008). In Droop's cell quota model, an internal pool of a nutrient was considered as a single variable for simulation. However, model is upgraded in terms of phosphate transport and assimilation by compartmentalizing single internal pool into three different pools (John and Flynn, 2000). The compartmentalized pools are polyphosphate bodies, soluble inorganic phosphate and structural & other organic phosphate content. Further, no meaningful basis was observed in formulated equation for non-limiting nutrients and hence equation was restructured for proper prediction of utilization profile of non-limiting substrates (Zonneveld, 1996). Two different formats of rate equations for limiting and non-limiting substrates were used in Droop model and thus the model may face difficulties in prediction of microalgal growth kinetics during fed-batch cultivation due to continuous switching of limiting and non-limiting nutrients on their addition. Therefore, well-structured and biologically meaningful kinetic model need to be developed or cell quota model is required to be improvised for accurate prediction of microalgal growth kinetics. These kinetic models can be used as a tool for understanding microbial and animal systems at metabolic level, process optimization, biochemical phenomena, monitoring and control of bioreactors (Béchet et al., 2013; Kumar et al., 2009; Pandey, 2003). These kinetic models can be used to design the feeding recipe in fed-batch and continuous mode of operation for enhanced biomass or lipid productivity (Alagesan et al., 2013; De la Hoz Siegler et al., 2011).

Metabolic modeling is used to understand the complex interplay between genotypic alterations and the corresponding phenotypic response (Boyle and Morgan, 2009; Shastri and Morgan, 2005) through quantification of carbon flux distribution in the metabolic network. It can also be used to simulate the behavior of desired mutant before development of mutant and further construction of mutant can be optimized for the product of interest (de Oliveira Dal'Molin et al., 2011). It can be used to uncover the

underlying mechanism in circadian rhythms, nitrogen assimilation, carbon sequestration, lipid biosynthesis, photosynthesis and stress related responses in microalgae. The constraint based metabolic models can quantitatively predict the responses of the cells with respect to the changes in environmental conditions (Kauffman et al., 2003). Flux balance analysis (FBA) is one of such constraint based mathematical modeling tool which works based on pseudo steady state condition. This is defined as all the intermediate compounds that maintain their concentration same during pathway operation along with changing concentration of substrate and product only. Many studies have been reported for comparative analysis of pathway regulation via flux balance analysis for autotrophic, heterotrophic and mixotrophic growth of microalgae (Boyle and Morgan, 2009; de Oliveira Dal'Molin et al., 2011; Shastri and Morgan, 2005; Yang et al., 2000). Metabolic modeling is not yet studied under different phases of microalgal cultivation such as growth and lipid induction phase which is very important towards biodiesel production.

2.8. Current challenges

At present microalgae based biodiesel production suffers from economical infeasibility (Chisti, 2013) and low marginal net energy ratio (NER) of biomass production (Slade and Bauen, 2013) due to several hurdles in present proven technologies. These include (i) lack of optimal nutrient feeding strategy in batch, fed-batch and continuous cultivation; (ii) lack of sustainable bioprocess for high cell density lipid rich cultivation with high net lipid productivity; (iii) Optimal regulation of carbon flux between lipid production and other storage molecules under various nutritional conditions remain unexplained; (v) Cost and energy effective lipid extraction and transesterification process which may lead towards sustainability of the process are yet to be developed; (v) Commercialization of residual components of biomass which is obtained from lipid extraction remains unexplained. Therefore, the present study aimed to develop a

sustainable bioprocess via high cell density lipid rich cultivation of microalgae with high productivity. This would be achieved via combined strategy of media optimization, designing of model guided feeding recipe of limiting nutrients, supplementation of lipid inducer instead of nutritional stress and substrate driven pH control.

2.9. References

1. Alagesan S., Gaudana S.B., Krishnakumar S., Wangikar P.P., 2013. Model based optimization of high cell density cultivation of nitrogen-fixing cyanobacteria. Bioresource Technology. 148, 228–233.
2. Anupama, Ravindra P., 2000. Value-added food: Single cell protein. Biotechnology Advances. 18, 459–479.
3. Atta M., Idris A., Bukhari A., Wahidin S., 2013. Intensity of blue LED light: a potential stimulus for biomass and lipid content in fresh water microalgae *Chlorella vulgaris*. Bioresource Technology. 148, 373–378.
4. Barsanti L., Gualtieri P., 2014. Algae: anatomy, biochemistry, and biotechnology. CRC Press, Taylor & Francis, Boca Raton, Florida.
5. Béchet Q., Shilton A., Guieysse B., 2013. Modeling the effects of light and temperature on algae growth: State of the art and critical assessment for productivity prediction during outdoor cultivation. Biotechnology Advances. 31, 1648–1663.
6. Becker E.W., 1994. Microalgae: biotechnology and microbiology. Cambridge University Press, Cambridge, New York.
7. Behera S., Singh R., Arora R., Sharma N.K., Shukla M., Kumar S., 2014. Scope of algae as third generation biofuels. Frontiers in Bioengineering and Biotechnology. 2, 90.

8. Bellinger E.G., Sigee D.C., 2010. Freshwater Algae: Identification and Use as Bioindicators. John Wiley & Sons Ltd, Chichester, UK.

9. Bernard O., 2011. Hurdles and challenges for modelling and control of microalgae for CO_2 mitigation and biofuel production. Journal of Process Control. 21, 1378–1389.

10. Borowitzka M.A., 2013. High-value products from microalgae—their development and commercialisation. Journal of Applied Phycology. 25, 743–756.

11. Borowitzka M., Hallegraeff G.M., 2007. Economic importance of algae. In: McCarthy P.M. & Orchard A.E. (eds.) Algae of Australia: Introduction. ABRS, Canberra, 594-622.

12. Boyle N.R., Morgan J.A., 2009. Flux balance analysis of primary metabolism in *Chlamydomonas reinhardtii*. BMC System Biology. 3, 4.

13. Dudley B., 2015. BP Statistical Review of World Energy. 64th ed. Pureprint Group Limited, UK. (http://www.bp.com/statisticalreview)

14. Caspari T., Will A., Opekarova M., Sauer N., Tanner W., 1994. Hexose/H^+ symporters in lower and higher plants. Journal of Experimental Biology. 196, 483–491.

15. Chae S.R., Hwang E.J., Shin H.S., 2006. Single cell protein production of *Euglena gracilis* and carbon dioxide fixation in an innovative photo-bioreactor. Bioresource Technology 97, 322–329.

16. Chen C.-Y., Yeh K.-L., Aisyah R., Lee D.-J., Chang J.-S., 2011. Cultivation, photobioreactor design and harvesting of microalgae for biodiesel production: a critical review. Bioresource Technology. 102, 71–81.

17. Chiaramonti D., Tredici M.R., Prussi M., Biondi N., 2015. Algae Biofuels. Handbook of Clean Energy Systems. 1-16.

18. Chinnasamy S., Bhatnagar A., Claxton R., Das K.C., 2010. Biomass and bioenergy production potential of microalgae consortium in open and closed bioreactors using untreated carpet industry effluent as growth medium. Bioresource Technology. 101, 6751–6760.

19. Chisti Y., 2013. Constraints to commercialization of algal fuels. Journal of biotechnology. 167, 201–214.

20. Chisti Y., 2007. Biodiesel from microalgae. Biotechnology advances. 25, 294–306.

21. Converti A., Casazza A.A., Ortiz E.Y., Perego P., Del Borghi M., 2009. Effect of temperature and nitrogen concentration on the growth and lipid content of *Nannochloropsis oculata* and *Chlorella vulgaris* for biodiesel production. Chemical Engineering and Processing: Process Intensification. 48, 1146–1151.

22. De la Hoz Siegler H., Ben-Zvi A., Burrell R.E., McCaffrey W.C., 2011. The dynamics of heterotrophic algal cultures. Bioresource Technology. 102, 5764–5774.

23. Deng X., Fei X., Li Y., 2011. The effects of nutritional restriction on neutral lipid accumulation in *Chlamydomonas* and *Chlorella*. African Journal of Microbiology Research. 5, 260–270.

24. de Oliveira Dal'Molin C.G., Quek L.-E., Palfreyman R.W., Nielsen L.K., 2011. AlgaGEM–a genome-scale metabolic reconstruction of algae based on the *Chlamydomonas reinhardtii* genome. BMC Genomics 12, S5.

25. Doucha J., Lívanský K., 2012. Production of high-density *Chlorella* culture grown in fermenters. Journal of Applied Phycology. 24, 35–43.

26. Dragone G., Fernandes B.D., Vicente A.A., Teixeira J.A., 2010. Third generation biofuels from microalgae. Current research technology and education topics in

applied microbiology and microbial biotechnology. Formatex Research Center, Badajoz.

27. Droop M.R., 1975. The nutrient status of algal cells in batch culture. Journal of Marine Biological Association of the UK. 55, 541–555.

28. Droop M.R., 1968. Vitamin B12 and marine ecology. IV. The kinetics of uptake, growth and inhibition in *Monochrysis lutheri*. Journal of Marine Biological Association of the UK. 48, 689–733.

29. Fei W., Wang H., Fu X., Bielby C., Yang H., 2009. Conditions of endoplasmic reticulum stress stimulate lipid droplet formation in *Saccharomyces cerevisiae*. Biochemical Journal. 424, 61–67.

30. Gorain P.C., Bagchi S.K., Mallick N., 2013. Effects of calcium, magnesium and sodium chloride in enhancing lipid accumulation in two green microalgae. Environmental Technology. 34, 1887–1894.

31. Griffiths D.J., Thresher C.L., Street H.E., 1960. The heterotrophic nutrition of *Chlorella vulgaris* (Brannon No. 1 strain): with two figures in the text. Annals of Botany. 24, 1–11.

32. Griffiths M.J., Van Hille R.P., Harrison S.T.L., 2010. Selection of direct transesterification as the preferred method for assay of fatty acid content of microalgae. Lipids 45, 1053–1060.

33. Hall D.O., Acién Fernández F.G., Guerrero E.C., Rao K.K., Grima E.M., 2003. Outdoor helical tubular photobioreactors for microalgal production: Modeling of fluid-dynamics and mass transfer and assessment of biomass productivity. Biotechnology and Bioengineering. 82, 62–73.

34. Hidalgo P., Toro C., Navia R., 2013. Advances in direct transesterification of microalgal biomass for biodiesel production. Reviews in Environmental Science and Bio/Technology. 12, 179–199.

35. Hu Q., Kurano N., Kawachi M., Iwasaki I., Miyachi S., 1998. Ultrahigh-cell-density culture of a marine green alga *Chlorococcum littorale* in a flat-plate photobioreactor. Applied Microbiology and Biotechnology. 49, 655–662.

36. Hu Q., Sommerfeld M., Jarvis E., Ghirardi M., Posewitz M., Seibert M., Darzins A., 2008. Microalgal triacylglycerols as feedstocks for biofuel production: perspectives and advances. The Plant Journal. 54, 621–639.

37. Jiang P.-L., Pasaribu B., Chen C.-S., 2014. Nitrogen-deprivation elevates lipid levels in *Symbiodinium* spp. by lipid droplet accumulation: morphological and compositional analyses. PloS ONE. 9, e87416.

38. Jiang Y., Laverty K.S., Brown J., Brown L., Chagoya J., Burow M., Quigg A., 2015. Effect of silicate limitation on growth, cell composition, and lipid production of three native diatoms to Southwest Texas desert. Journal of Applied Phycology. 27, 1433–1442.

39. John E.H., Flynn K.J., 2000. Modelling phosphate transport and assimilation in microalgae; how much complexity is warranted?. Ecological Modelling. 125, 145–157.

40. Kanehisa M., Sato Y., Kawashima M., Furumichi M., Tanabe M., 2016. KEGG as a reference resource for gene and protein annotation. Nucleic Acids Research. 44, D457–D462.

41. Kauffman K.J., Prakash P., Edwards J.S., 2003. Advances in flux balance analysis. Current Opinions in Biotechnology. 14, 491–496.

42. Khan S.A., Hussain M.Z., Prasad S., Banerjee U.C., 2009. Prospects of biodiesel production from microalgae in India. Renewable and Sustainable Energy Reviews. 13, 2361–2372.

43. Kim S., Kim H., Ko D., Yamaoka Y., Otsuru M., Kawai-Yamada M., Ishikawa T., Oh H.-M., Nishida I., Li-Beisson Y., 2013. Rapid induction of lipid droplets in *Chlamydomonas reinhardtii* and *Chlorella vulgaris* by Brefeldin A. PLoS ONE. 8, e81978.

44. Kropat J., Hong-Hermesdorf A., Casero D., Ent P., Castruita M., Pellegrini M., Merchant S.S., Malasarn D., 2011. A revised mineral nutrient supplement increases biomass and growth rate in *Chlamydomonas reinhardtii*. The Plant Journal. 66, 770–780.

45. Kumar A., Singh L.K., Ghosh S., 2009. Bioconversion of lignocellulosic fraction of water-hyacinth (*Eichhornia crassipes*) hemicellulose acid hydrolysate to ethanol by *Pichia stipitis*. Bioresource Technology. 100, 3293–3297.

46. Kumar V., Muthuraj M., Palabhanvi B., Das D., 2016. Synchronized growth and neutral lipid accumulation in *Chlorella sorokiniana* FC6 IITG under continuous mode of operation. Bioresource Technology. 200, 770–779.

47. Kumar V., Muthuraj M., Palabhanvi B., Ghoshal A.K., Das D., 2014. Evaluation and optimization of two stage sequential *in situ* transesterification process for fatty acid methyl ester quantification from microalgae. Renewable Energy. 68, 560–569.

48. Lemesle V., Mailleret L., 2008. A mechanistic investigation of the algae growth "Droop" model. Acta Biotheoretica. 56, 87–102.

49. Le Quéré C., Moriarty R., Andrew R.M., Canadell J.G., Sitch S., Korsbakken J.I., Friedlingstein P., Peters G.P., Andres R.J., Boden *et al.*, 2015. Global Carbon Budget 2015. Earth System Science Data. 7, 349–396.

50. Liang K., Zhang Q., Gu M., Cong W., 2013. Effect of phosphorus on lipid accumulation in freshwater microalga *Chlorella* sp. Journal of Applied Phycology. 25, 311–318.

51. Li T., Zheng Y., Yu L., Chen S., 2013. High productivity cultivation of a heat-resistant microalga *Chlorella sorokiniana* for biofuel production. Bioresource Technology. 131, 60–67.

52. Met Office, 2015. Global climate in context as the world approaches 1°C above pre-industrial for the first time. UK. (http://www.metoffice.gov.uk/research/news/2015/global-average-temperature-2015)

53. Milledge J.J., Smith B., Dyer P.W., Harvey P., 2014. Macroalgae-derived biofuel: a review of methods of energy extraction from seaweed biomass. Energies. 7, 7194–7222.

54. Naik S.N., Goud V.V., Rout P.K., Dalai A.K., 2010. Production of first and second generation biofuels: a comprehensive review. Renewable and Sustainable Energy Reviews. 14, 578–597.

55. Nelson D.L., Cox M.M., 2012. Lehninger Principles of Biochemistry. 6th ed. W H Freeman and Company, New York.

56. Oehrl L.L., Hansen A.P., Rohrer C.A., Fenner G.P., Boyd L.C., 2001. Oxidation of phytosterols in a test food system. Journal of the American Oil Chemist's Society. 78, 1073–1078.

57. Pancha I., Chokshi K., Maurya R., Trivedi K., Patidar S.K., Ghosh A., Mishra S., 2015. Salinity induced oxidative stress enhanced biofuel production potential of microalgae *Scenedesmus* sp. CCNM 1077. Bioresource Technology. 189, 341–348.

58. Pandey A., 2003. Solid-state fermentation. Biochemical Engineering Journal. 13, 81–84.

59. Pandey A., Lee D.-J., Chisti Y., Soccol C.R., 2013. Biofuels from algae. Newnes. Elsevier, Amsterdam.

60. Panwar N.L., Kaushik S.C., Kothari S., 2011. Role of renewable energy sources in environmental protection: a review. Renewable and Sustainable Energy Reviews. 15, 1513–1524.

61. Parmar A., Singh N.K., Pandey A., Gnansounou E., Madamwar D., 2011. Cyanobacteria and microalgae: a positive prospect for biofuels. Bioresource Technology. 102, 10163–10172.

62. Perez-Garcia O., Escalante F.M., de-Bashan L.E., Bashan Y., 2011. Heterotrophic cultures of microalgae: metabolism and potential products. Water Research. 45, 11–36.

63. Pragya N., Pandey K.K., Sahoo P.K., 2013. A review on harvesting, oil extraction and biofuels production technologies from microalgae. Renewable and Sustainable Energy Reviews. 24, 159–171.

64. Qiao H., Wang G., 2009. Effect of carbon source on growth and lipid accumulation in *Chlorella sorokiniana* GXNN01. Chinese Journal of Oceanology and Limnology. 27, 762–768.

65. Quinn J.C., Smith T.G., Downes C.M., Quinn C., 2014. Microalgae to biofuels lifecycle assessment—multiple pathway evaluation. Algal Research. 4, 116–122.

66. Richmond A., 2008. Handbook of microalgal culture: biotechnology and applied phycology. Blackwell Publishing, Oxford, UK.

67. Rodolfi L., Chini Zittelli G., Bassi N., Padovani G., Biondi N., Bonini G., Tredici M.R., 2009. Microalgae for oil: Strain selection, induction of lipid synthesis and

outdoor mass cultivation in a low-cost photobioreactor. Biotechnology and Bioengineering. 102, 100–112.

68. Roessler P.G., 1990. Environmental control of glycerolipid metabolism in microalgae: commercial implications and future research directions. Journal of Phycology. 26, 393–399.

69. Safi C., Zebib B., Merah O., Pontalier P.-Y., Vaca-Garcia C., 2014. Morphology, composition, production, processing and applications of *Chlorella vulgaris*: A review. Renewable and Sustainable Energy Reviews. 35, 265–278.

70. Sauer N., Tanner W., 1989. The hexose carrier from *Chlorella*. FEBS Letters. 259, 43–46.

71. Shastri A.A., Morgan J.A., 2005. Flux balance analysis of photoautotrophic metabolism. Biotechnology Progress. 21, 1617–1626.

72. Shen Y., Yuan W., Pei Z., Mao E., 2010. Heterotrophic culture of *Chlorella protothecoides* in various nitrogen sources for lipid production. Applied Biochemistry and Biotechnology. 160, 1674–1684.

73. Sierra E., Acién F.G., Fernández J.M., García J.L., González C., Molina E., 2008. Characterization of a flat plate photobioreactor for the production of microalgae. Chemical Engineering Journal. 138, 136–147.

74. Slade R., Bauen A., 2013. Micro-algae cultivation for biofuels: cost, energy balance, environmental impacts and future prospects. Biomass and Bioenergy. 53, 29–38.

75. Smith A.J., London J., Stanier R.Y., 1967. Biochemical basis of obligate autotrophy in blue-green algae and thiobacilli. Journal of Bacteriology. 94, 972–983.

76. Spreitzer R.J., Peddi S.R., Satagopan S., 2005. Phylogenetic engineering at an interface between large and small subunits imparts land-plant kinetic properties to algal Rubisco. Proceedings of the National Academy of Science. U. S. A. 102, 17225–17230.

77. Stanbury P.F., Whitaker A., Hall S.J., 2003. Principles of fermentation technology. 2nd ed. Butterworth-Heinemann, Oxford, UK.

78. Tabatabaei M., Tohidfar M., Jouzani G.S., Safarnejad M., Pazouki M., 2011. Biodiesel production from genetically engineered microalgae: Future of bioenergy in Iran. Renewable and Sustainable Energy Reviews. 15, 1918–1927.

79. Taherzadeh M.J., Karimi K., 2008. Pretreatment of lignocellulosic wastes to improve ethanol and biogas production: a review. International Journal of Molecular Sciences. 9, 1621–1651.

80. Turon V., Trably E., Fayet A., Fouilland E., Steyer J.-P., 2015. Raw dark fermentation effluent to support heterotrophic microalgae growth: microalgae successfully outcompete bacteria for acetate. Algal Research. 12, 119–125.

81. Urzica E.I., Vieler A., Hong-Hermesdorf A., Page M.D., Casero D., Gallaher S.D., Kropat J., Pellegrini M., Benning C., Merchant S.S., 2013. Remodeling of membrane lipids in iron-starved *Chlamydomonas*. Journal of Biological Chemistry. 288, 30246–30258.

82. Wang J., Yang H., Wang F., 2014. Mixotrophic cultivation of microalgae for biodiesel production: status and prospects. Applied Biochemistry and Biotechnology. 172, 3307–3329.

83. Williams P.J. le B., Laurens L.M., 2010. Microalgae as biodiesel & biomass feedstocks: review & analysis of the biochemistry, energetics & economics. Energy and Environmental Science. 3, 554–590.

84. Xiao M., Shin H.-J., Dong Q., 2013. Advances in cultivation and processing techniques for microalgal biodiesel: A review. Korean Journal of Chemical Engineering. 30, 2119–2126.

85. Xin L., Hong-Ying H., Yu-Ping Z., 2011. Growth and lipid accumulation properties of a freshwater microalga *Scenedesmus* sp. under different cultivation temperature. Bioresource Technology. 102, 3098–3102.

86. Xiong W., Li X., Xiang J., Wu Q., 2008. High-density fermentation of microalga *Chlorella protothecoides* in bioreactor for microbio-diesel production. Applied Microbiology and Biotechnology. 78, 29–36.

87. Yang C., Hua Q., Shimizu K., 2000. Energetics and carbon metabolism during growth of microalgal cells under photoautotrophic, mixotrophic and cyclic light-autotrophic/dark-heterotrophic conditions. Biochemical Engineering Journal. 6, 87–102.

88. Zajic J.E., Chiu Y.S., 1970. Heterotrophic culture of algae, in: Properties and Products of Algae. Springer, USA.

89. Zheng Y., Li T., Yu X., Bates P.D., Dong T., Chen S., 2013. High-density fed-batch culture of a thermotolerant microalga *Chlorella sorokiniana* for biofuel production. Applied Energy. 108, 281–287.

90. Zhu S., Huang W., Xu J., Wang Z., Xu J., Yuan Z., 2014. Metabolic changes of starch and lipid triggered by nitrogen starvation in the microalga *Chlorella zofingiensis*. Bioresource Technology. 152, 292–298.

91. Zonneveld C., 1996. Modelling the kinetics of non-limiting nutrients in microalgae. Journal of Marine Systems. 9, 121–136.

CHAPTER 3

Characterization of FC2 under wide ranges of pH, temperature, carbon and nitrogen sources

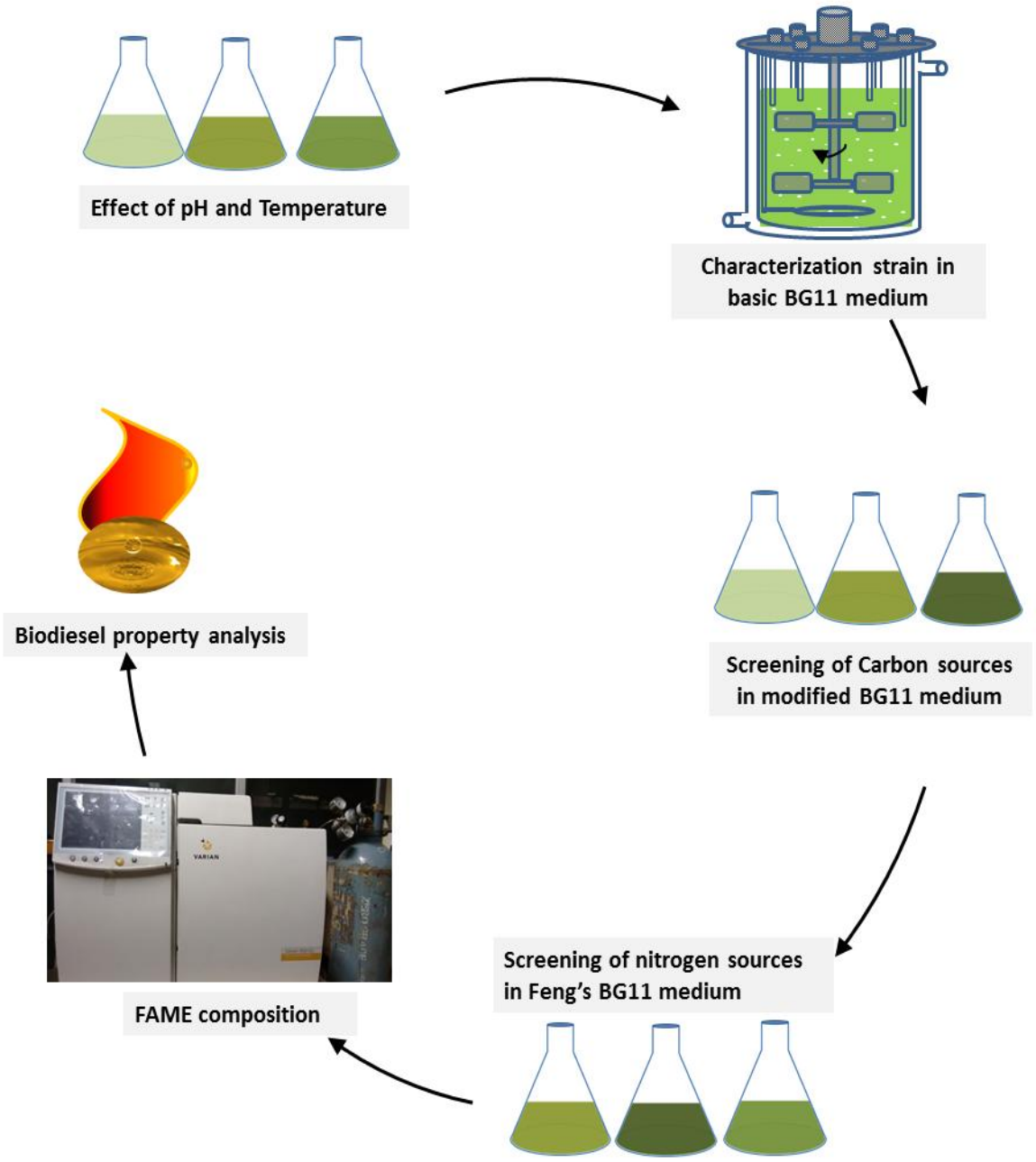

Characterization of *Chlorella* sp. FC2 IITG under wide ranges of pH, temperature, carbon and nitrogen sources

3.1. Background and motivation

Commercialization of microalgae based biodiesel production is still at dormancy due to economical infeasibility (Chisti, 2013) and low marginal net energy ratio (NER) of biodiesel production from microalgae (Slade and Bauen, 2013). This is attributed to low biomass titer, lipid productivity and associated higher harvesting & downstream processing cost in the photoautotrophic open race way pond systems which are largely used for commercial scale cultivation of microalgae (Chae et al., 2006; Chinnasamy et al., 2010; Shen et al., 2010). Interestingly, heterotrophic cultivation supports consistent biomass or lipid productivity, improved cell density and easy scale up (Shen et al., 2010). However the cost of organic carbon remains unsolved issue in heterotrophic cultivation (Turon et al., 2015). High cell density with improved lipid productivity may reduce the batch run time, harvesting and other down-stream processing cost (Xiong et al., 2008). To that end, organism needs to be characterized under wide physiological conditions and various types of nutrition in order to find out the best condition and nutrition for growth which in turn aids in the development of a suitable bioprocess. The microalgal growth varies rapidly with media pH and temperature (Converti et al., 2009; Lundholm et al., 2004) and hence selection of best condition is prerequisite for a technology development.

Microalgal growth and lipid content can vary with various carbon and nitrogen sources (Qiao and Wang, 2009; Xiong et al., 2008). Growth and lipid content are mutually exclusive in nature (Rodolfi et al., 2009) and hence identification of growth supportive and lipid inducing compounds is an important step towards enhancement of respective productivity. In case of lipid induction, it can be carried out by exposing cells into nutrient starved condition (Negi et al., 2015) or lipid elicitor supplemented media (Kim et al., 2013). However, starvation based lipid induction is the traditional method which employs two stage cultivation and hence requires high energy for harvesting, dewatering and re-

suspension of biomass from nutrient sufficient to starvation stages. On the contrary, addition of lipid inducers during the end of nutrient sufficient phase avoids requirement of harvesting and re-suspension thereby minimizing the power inputs in the process. *Chlamydomonas reinhardtii* and *Chlorella vulgaris* were reported to enhance their lipid accumulation by addition of Brefeldin A as an inducer (Kim et al., 2013). However, removal of such complex lipid inducers from the broth is difficult and remains unfeasible; thus necessitates the use of inducers that can be metabolized by microalgae to achieve feasibility. The search of inducer among various carbon or nitrogen sources could yield better metabolizable lipid elicitors as they are major metabolic nutrients of organism.

In the present study, growth supportive and lipid inducing nutrients were identified and their effects on biodiesel properties were also assessed under heterotrophic cultivation of the strain. The study involves evaluation of effect of media pH & temperature on growth, characterization of strain under basic BG11 medium in order to determine growth kinetics, screening of growth promoting/ lipid inducing carbon & nitrogen source, and evaluating biodiesel properties under various nutritional conditions.

3.2. Material and methods

3.2.1. Inoculum preparation and growth condition

The inoculum was prepared by transferring two loops full of slant culture to 250 mL Erlenmeyer flask with 100 mL medium and incubated at 28ºC, 150 rpm in an incubator shaker (ORBITEK® LETT Scigenics Biotech Pvt. Ltd., India). The inoculum preparation for the experiments such as study of initial media pH & temperature effect on growth and determination of growth kinetics was carried out in basic BG11 media with composition mentioned in Table 3.1. Early exhaustion of phosphate from media (Section 3.3.2) was observed in growth kinetics experiment due to very low concentration of phosphate (0.004 g L^{-1}) in BG11 medium. This early exhaustion of phosphate was

expected to mask the effect of carbon and nitrogen sources on growth and lipid accumulation. Hence a modified BG11 medium composition containing 10 times higher phosphate concentration (0.04 g L^{-1}), was adopted from Rippka et al. (1979) for screening of carbon and nitrogen sources. Inoculum was prepared in heterotrophic growth mode with the supplementation of 15 g L^{-1} glucose in the media. In all the experiments, 1% (v/v) of active mid-log phase culture with cell density of 0.23 g L^{-1} was used as inoculum.

Table 3.1 Composition of basic BG11 media for microalgal cultivation (source: Barsanti and Gualtieri, 2014)

Group name	Compounds	Composition
Nitrogen (g L^{-1})	$NaNO_3$	1.5
Phosphorous (g L^{-1})	K_2HPO_4	0.004
Trace elements (g L^{-1})	$MgSO_4.7H_2O$	0.075
	$CaCl_2.2H_2O$	0.036
	Na_2CO_3	0.02
	Citric acid	0.006
	Ferric ammonium citrate	0.006
	EDTA	0.001
Micro elements (mg L^{-1})	H_3BO_3	2.86
	$MnCl_2.H_2O$	1.81
	$ZnSO_4.7H_2O$	0.222
	$CuSO_4.5H_2O$	0.079
	$Na_2MoO_4.2H_2O$	0.390
	$Co(NO_3)_2.6H_2O$	0.049

3.2.2. Effect of media pH and Temperature

These experiments were carried out in 250 mL conical flask containing 100 mL basic BG11 medium and 15 g L^{-1} glucose. In order to assess the effect of initial medium pH on microalgal growth, pH of the media was adjusted to 2, 4, 6, 8 and 10 by the addition of acid or alkali and incubated at similar condition as mentioned for inoculum preparation. Optimal temperature for growth of FC2 was determined by growing the organism at different temperatures (20, 24, 28, 32, 36 and 44°C) with all other growth parameters same

as inoculum preparation. A known amount of sample was taken at regular intervals of 24 h to monitor growth of the organism.

3.2.3. Determination of growth kinetics in an automated bioreactor in basic BG11 medium

In this experiment, organism was characterized under heterotrophic condition in a 3 L automated bioreactor (Bio Console ADI 1025, Applikon Biotechnology, Holland) containing 1.25 L basic BG11 medium supplemented with 15 g L^{-1} glucose. The reactor was operated at 28 °C, agitator speed of 400 rpm and aeration at 1vvm. The medium pH was maintained in between 6.0 to 8.0 by the addition of 0.25 M NaOH or HCl throughout the batch. Sampling was done at every 24 h time interval to monitor the growth, lipid content and substrate utilization profile of the organism. The batch was terminated once the neutral lipid percentage of the biomass reached its maximum and started decreasing thereafter.

3.2.4. Screening of growth promoting and/or lipid inducing carbon and nitrogen sources

The organism was characterized under different carbon sources (glucose, fructose, sucrose, lactose, maltose, sodium acetate, mannitol, starch, carboxy methyl cellulose sodium salt, glycerol, citric acid and lactic acid) to identify the ones which were growth promoting and/or lipid inducing. The experiments were performed in 250 mL conical flask containing modified BG11 medium supplemented with different carbon sources containing equimolar concentration of carbon (6 g L^{-1}). Similarly, organism was cultivated in different nitrogen sources such as sodium nitrate, yeast extract, casein enzyme hydrolysate, peptone, meat extract, glycine, urea, ammonium chloride, ammonium sulfate, tri-ammonium citrate and sodium nitrite. These nitrogenous compounds were supplemented in modified BG11 medium in place of sodium nitrate with equimolar

concentration of nitrogen (0.247 g L^{-1}). These experiments were supplemented with 15 g L^{-1} glucose to grow the organism in heterotrophic condition. The growth conditions were kept same as that for inoculum preparation. Sampling was carried out at regular time intervals for determination of biomass and intracellular lipid content of the cells.

3.2.5. Analysis of growth, lipid and substrates utilization

Estimation of growth, lipid content and substrate utilization profile were carried out at every sampling time point. The collected sample was centrifuged at 8000 × g for 10 minutes at 4°C and the supernatant was collected for extracellular substrates analyses (glucose, nitrate and phosphate). The pellet was utilized for the measurement of biomass, intracellular lipid content.

3.2.5.1. Analysis of growth

The pellet obtained during sample processing was re-suspended in normal saline (0.8 % w/v sodium chloride) and growth of microalgae was monitored in terms of dry cell weight (DCW) by measuring the absorbance (O.D) at 690 nm (A_{690}) using a UV-Visible spectrophotometer (Cary 50, Varian, Australia). Absorbance values were converted into DCW with help of appropriate calibration equations which were determined by comparing absorbance and DCW values at various biomass concentrations. A known volume of sample was centrifuged at 8000 × *g*, 4°C for 10 minutes and obtained pellet was washed with normal saline to make the cells free from adhered media components. Further, pellet was exposed to hot air at a temperature of 60°C to attain constant dry weight which was measured gravimetrically. Thus, two calibration curves were obtained (Fig. 3.1A and 3.1B) where one is for active phase of the growth: one O.D= 0.23 g L^{-1} DCW (R^2 = 0.99) and another for stationary phase of the growth: one O.D = 0.241g L^{-1} DCW (R^2 = 0.97). The biomass productivity (BP) of organism was calculated by using equation 3.1.

$$BP\ (g\ L^{-1} day^{-1}) = \frac{X_f - X_0}{t_f - t_0} \qquad (3.1)$$

Where, X_f and X_0 are biomass concentration (g L^{-1}) at final (t_f) and initial (t_0) time points (days).

Similarly, specific growth rate of organism was determined as per equation 3.2.

$$\mu\ (day^{-1}) = \frac{\ln\frac{x_f}{x_0}}{t_f - t_0} \qquad (3.2)$$

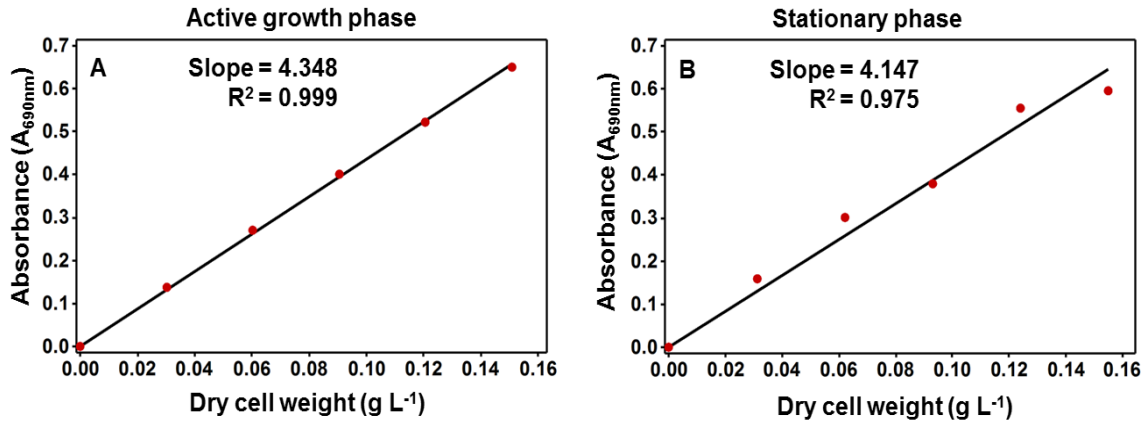

Fig. 3.1 Graphical representation of correlation between the dry cell weight and absorbance measured at 690 nm in a spectrophotometer with use of (A) active growth phase and (B) stationary phase culture of organism grown under heterotrophic condition.

3.2.5.2. Estimation of nitrate by salicylic acid method

Nitrate concentration was estimated using salicylic acid method (Cataldo et al., 1975) with sodium nitrate as standard. Sample of 100 µL was allowed to react with 0.4 mL of 5% (w/v) salicylic acid in sulfuric acid for 20 min at 25°C. The reaction compound turned into yellow color after the addition of 9.5 mL NaOH (2M) and its absorbance was measured at 410 nm wavelength. A correlation standard curve was obtained: One absorbance ($A_{410\ nm}$) corresponding to 0.932 g L^{-1} of nitrate (Fig. 3.2 A).

3.2.5.3. Analysis of glucose utilization profile

Glucose concentration in the medium was monitored by the dinitrosalicyclic acid method (Miller, 1959). Di-nitrosalicylic acid (DNS) reagent of 1 mL was treated with 1 mL sample for 15 minutes in a boiling water bath. DNS reagent consist (w/v) of 1% DNS powder, 1% NaOH, and 0.05% sodium sulfite. Potassium sodium tartrate (40% w/v) was

added to the solution for stabilization of color and absorbance was taken at 575 nm wavelength. The standard curve was developed using dextrose anhydrous and used for glucose concentration determination (Fig. 3.2 B). One absorbance at 575 nm was found to represent 1.87 g L^{-1} of glucose.

3.2.5.4. Biochemical estimation of phosphate utilization profile

The phosphate concentration was estimated using ascorbic acid method with potassium hydrogen phosphate (dibasic) as standard (Parsons et al., 1984). Sample of 2 mL was allowed to react with 0.32 mL combined reagent for 10 minute at room temperature and absorbance was taken at 880 nm wavelength. Combined reagent comprised of (5 N) sulfuric acid, (0.018 M) antimony potassium tartrate, (0.102 M) ammonium molybdate and (0.1 M) ascorbic acid. The correlation between phosphate concentration and corresponding absorbance was constructed where one absorbance at 880 nm corresponded to 10.6 mg L^{-1} of phosphate (Fig. 3.2 C).

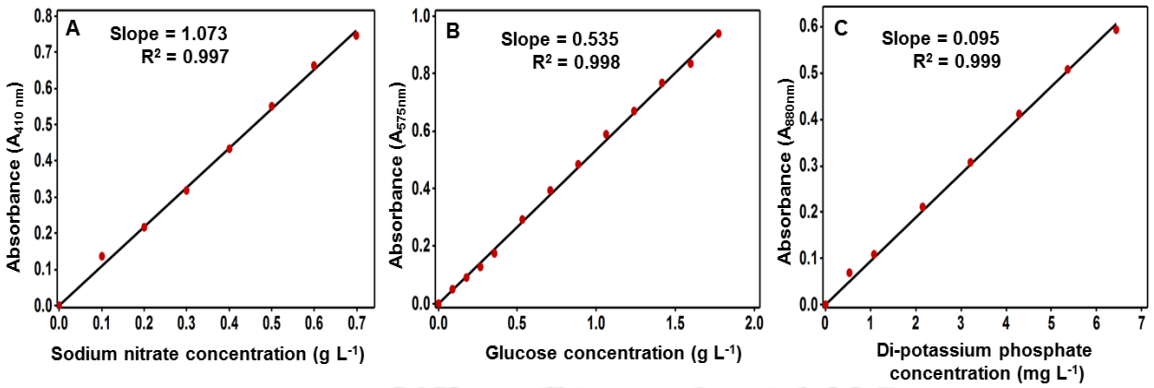

Fig. 3.2 Graphical representation of correlation between concentration of substrates and their respective absorbance in spectrophotometer for the estimation of (A) sodium nitrate (B) glucose and (C) di potassium phosphate.

3.2.5.5. Estimation of intracellular neutral lipid

The intracellular neutral lipid content was quantified using Nile red method (Muthuraj et al., 2014). Cell pellet was re-suspended in 25% (v/v) dimethyl sulfoxide to attain cell density of 0.7 at 690 nm wavelength. The Nile red was added to 1 mL sample in order to attain final concentration of 4 µg mL^{-1} and incubated at 50°C in a water bath for

one minute. The fluorescence emission spectra (550 to 650 nm) were recorded in a spectrophotometer (Fluoromax 3, Horiba, USA) with an excitation wavelength of 480 nm. The auto-fluorescence of cell mass, 25% (v/v) dimethyl sulfoxide and 4 µg mL^{-1} Nile red was subtracted from the fluorescence of Nile red-neutral lipid complex obtained at 580 nm. The correlation graph between fluorescence and lipid concentration (10^5 a.u fluorescence intensity = 26.5 mg L^{-1} neutral lipid) was developed by using Triolein (Supelco, USA) as standard (Fig. 3.3 A).

3.2.5.6. Estimation of intracellular total lipid

The total lipid content of the cells was measured in terms of fatty acid methyl ester (FAME) using a gas chromatograph (GC, Varian 450, Netherlands) equipped with SLB-IL100 column (30 × 0.25 mm i.d., 0.20-µm film thickness) and flame ionization detector in accordance to the method reported by Kumar et al. (2014). The biomass harvested from broth was freeze dried and used for two-step direct transesterification method involving sequential alkali and acid treatment to convert intracellular lipid into FAME. In the first step of direct transesterification, 1.0 mL of 2% (w/v) NaOH in methanol was added to 30 mg lyophilized biomass followed by incubation at 90°C in a shaking water bath at 150 rpm for 20 minutes. In the second step, 1.0 mL 5% (v/v) H_2SO_4 in methanol was added to the mixture and was further incubated at the same condition for 20 minutes. The converted FAME was cooled down to room temperature and equal volume of deionized water and hexane were added to obtain the FAME in hexane layer. The aqueous impurities were removed from hexane extract by washing with water and sample was filtered through 0.2 µm membrane before subjecting to analysis in GC. The GC was operated at a nitrogen constant flow rate of 0.4 m s^{-1} as the carrier gas, split ratio of 1:20, oven temperature 140°C (5 min) followed by ramping at a rate of 3°C min^{-1} till 220°C followed by 5 minutes holding. The injector and detector temperature was maintained at 250°C and the

sample volume of 1 µL was used for injection. Correlation curve (10^5 mV min^{-1} area = 16.826 g L^{-1} total lipid) was prepared with use of FAME mix C14–C22 (Supelco, USA) as the standard (Fig. 3.3 B).

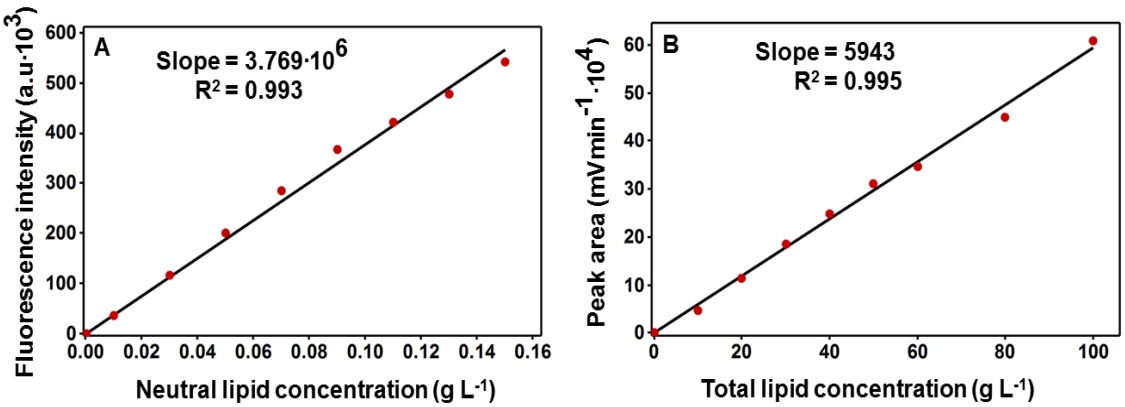

Fig. 3.3 Standard correlation graph for the estimation of (A) neutral lipid by Nile red based assay method in fluorescent spectrophotometer and (B) total lipid as fatty acid methyl esters assayed in gas chromatograph with standard FAME mix C14-C22.

3.2.5.7. Determination of biodiesel properties

Biodiesel (FAME) properties were estimated using empirical formulas developed on the basis of FAME composition. The properties such as viscosity, cetane number, pour point, cloud point, flash point, iodine value, degree of unsaturation, saponification value and highest heating value decide the quality of biodiesel to be used for commercial supplications. The empirical equations developed with experimental validation were extracted from the literature for present work. The equation 3.3 – 3.7 were adopted from Su et al. (2011). Similarly equations 3.8 – 3.10 and equation 3.11 were taken from Francisco et al. (2010) and Ramírez-Verduzco et al. (2012) respectively.

Viscosity, $\eta = 0.235W_C - 0.468\, W_{db}$ (3.3)

Cetane number, $CN = 3.93W_C - 15.93\, W_{db}$ (3.4)

Flash point, $T_f = 23.362W_C + 4.854\, W_{db}$ (3.5)

Cloud point, $T_c = 18.134W_C - 0.79\, W_{US}$ (3.6)

Pour point, $T_p = 18.88W_C - 1\, W_{US}$ (3.7)

Saponification value, $SV = \sum 560P_{FA}/MW$ (3.8)

Iodine value, $IV = \sum 254P_{FA}N_D/MW$ (3.9)

Degree of unsaturation, $DU = W_{MUFA} + 2W_{PUFA}$ (3.10)

Highest heating value, $HHV = 46.19 - \frac{1794}{MW_i} - 0.21N_D$ (3.11)

Where, W_C- weighted average number of carbon atoms, W_{db} - weighted-average number of double bonds, W_{US} - total unsaturated FAME content (weight %), P_{FA} - percentage of each fatty acid, MW - molecular mass of individual fatty acids, N_D - number of double bonds, W_{MUFA} - monounsaturated fatty acids in weight percentage, W_{PUFA} - polyunsaturated fatty acids in weight percentage, MW_i - molecular weight of the i^{th} FAME component.

3.3. Results and discussion

3.3.1. Effect of initial pH of the media and temperature on growth of the organism

The strain was able to grow over a wide range of pH 4 to 10 and its optimal growth was observed in between pH 6 and 8 (Fig. 3.4 A). Microalga *Chlamydomonas reinhardtii* has also been reported to show its maximal growth at pH 7.5 (Kong et al., 2010). The survival of the organism over wide pH range points towards metabolic flexibility of the strain to adapt with external conditions. The cultivation of microalgae in alkali pH may control contamination from other organisms (Touloupakis et al., 2016) as most of the bacteria and fungi grow in acidic or neutral environment.

FC2 was found to grow in wide range of temperature however maximal biomass concentration was observed at 28ºC (Fig. 3.4 B) which was lower than many other *Chlorella* sp. reported in the literatures (Wan et al., 2012). This shows that FC2 can be grown in different geographical locations where average temperature varies from 20ºC to 35ºC. Biomass titer was maximal when microalga *Chlorella sorokiniana* was grown at 30ºC temperature (Wan et al., 2012). Hereafter all the experiments were carried out at 6-8

pH and 28ºC temperature. Previous studies with FC2 in autotrophic mode of cultivations also exhibited similar growth profile under wide range of pH and temperatures (Muthuraj et al., 2014) however, with lower cell densities as compared to the present study.

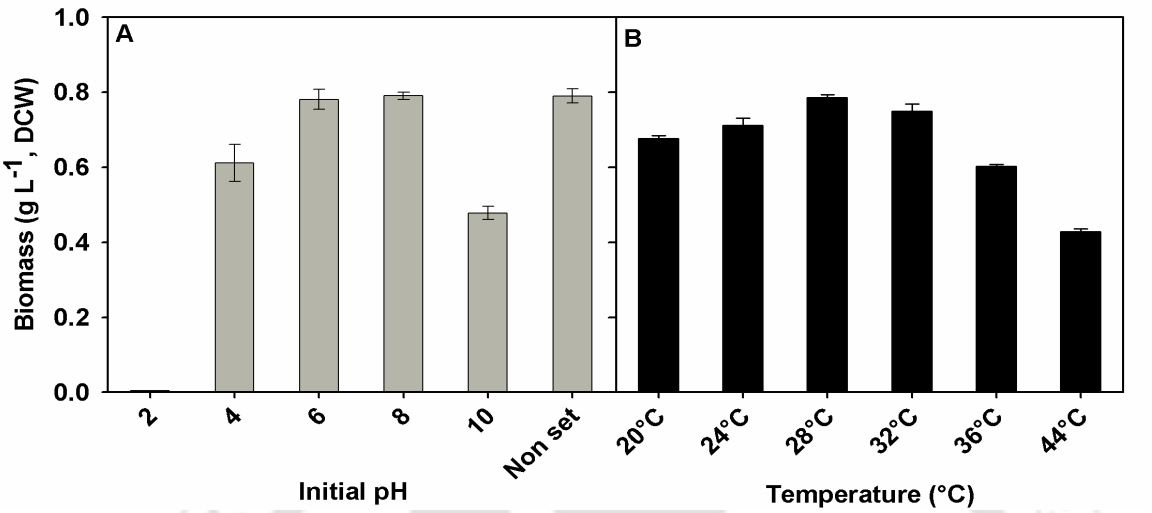

Fig. 3.4 Effect of (A) initial media pH and (B) temperature on growth of FC2 in glucose supplemented basic BG11 media under dark heterotrophic cultivation condition

3.3.2. Characterization of growth and lipid production under basic BG11 medium

The cultivation of microalga in basic BG11 medium under heterotrophic mode yielded biomass concentration of 0.673 g L^{-1} with maximal lipid content of 59.69% (w/w, DCW) (Fig. 3.5 A). While many microalga such as *Chlorella protothecoides* (Shen et al., 2010), *Chlorella kessleri* (Wang et al., 2012) etc. have shown higher biomass titer, lipid content of FC2 was found to be higher comparatively. This shows that organism's lipid biosynthesis pathway can be tuned up for accumulation via process engineering strategies. Lower biomass titer was attributed to early depletion phosphate from the media at 72 h of cultivation (Fig. 3.5 B). The organism showed the extended growth with slower specific growth rate even after exhaustion of extracellular phosphate along with concomitant induction of neutral lipid. The similar phenomenon was observed when *Nannochloropsis* sp. F&M-M24 exhibited an intracellular lipid content of 60% (w/w, DCW) under nitrogen starvation (Rodolfi et al., 2009). This heterotrophic cultivation of the organism in basic

BG11 medium resulted in biomass and lipid productivity of 132 mg L^{-1} day^{-1} and 48.8 mg L^{-1} day^{-1} respectively (Table 3.2). Previously in case of autotrophic and mixotrophic cultivation of FC2, relatively lower lipid productivity of 28.8 mg L^{-1} day^{-1} and 44.9 mg L^{-1} day^{-1} respectively was reported (Muthuraj et al., 2014). However, mixotrophic cultivation gave higher biomass productivity (155.6 mg L^{-1} day^{-1}) when compared with the present study (Muthuraj et al., 2014). *Chlorella vulgaris* has also been reported to show 151 mg L^{-1} day^{-1} biomass productivity and 35 mg L^{-1} day^{-1} lipid productivity under glucose supplemented heterotrophic cultivation (Liang et al., 2009). However biomass and lipid productivities of present study are lower than many other strains reported in the literatures (Xiong et al., 2008) which may be attributed to early exhaustion of phosphate from the media.

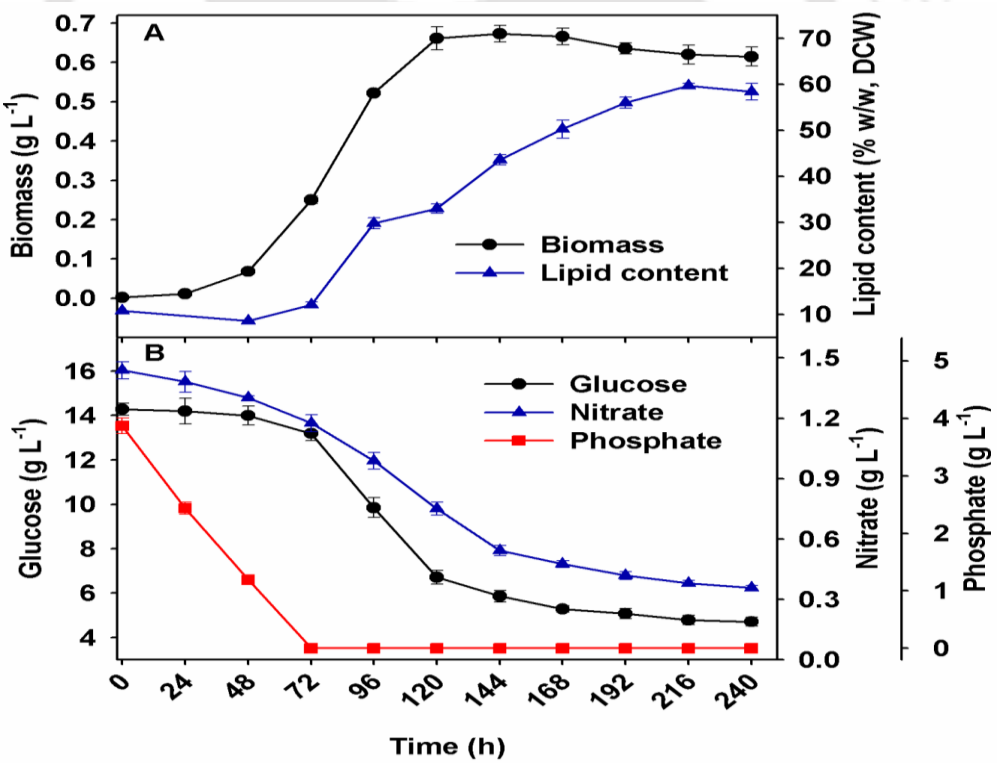

Fig. 3.5 Dynamic profiles for (A) growth & lipid content of biomass, and (B) utilization of glucose, nitrate & phosphate, when FC2 was grown in 3 L automated bioreactor with basic BG11 medium.

Further improvement in biomass and lipid productivity is possible via optimization and process engineering strategies for optimal nutrition for the organism growth.

Microalga FC2 showed several advantageous features such as huge neutral lipid accumulation potential in biomass, shorter lag phase and high specific growth even under phosphate limited condition.

Table 3.2 Kinetic parameters for growth and lipid formation of organism cultivated under heterotrophic basic BG11 medium.

Parameters	**Values**	**Parameters**	**Values**
Specific growth rate (day $^{-1}$)	1.817	Total lipid content (% w/w, DCW)[a]	64.52
Biomass titer (g L^{-1})	0.673	Biomass productivity (mg L^{-1} day^{-1})	132
Neutral lipid content (% w/w, DCW)	59.69	Neutral lipid productivity (mg L^{-1} day^{-1})	48.8

[a] Total lipid content was estimated at last sampling point while all other parameters represents their maximum values during fermentation.

3.3.3. Screening of growth promoting and/or lipid inducing carbon and nitrogen sources

From the previous experiment (section 3.3.2), phosphate was observed to be exhausted soon as the medium contained only 0.004 g L^{-1} of phosphate. This early phosphate limitation may mask the effect of carbon and nitrogen sources on growth and lipid accumulation. Hence BG11 medium containing high concentration of phosphate (0.04 g L^{-1}) was adopted from the literature (Rippka et al., 1979) and used for screening experiments. The strain FC2 showed considerable growth by utilizing glucose and sodium acetate under dark heterotrophic cultivation condition (Fig. 3.6 A). However, the organism failed to grow on other carbon substrates which could be attributed to the lack of membrane transporters or metabolizing enzymes (Morales-Sánchez et al., 2013). Highest biomass titer of 3.88 g L^{-1} was achieved in the presence of glucose while, in case of sodium acetate biomass titer was reduced to 2.6 g L^{-1}. However, accumulation of intracellular neutral lipid was found to be maximal in case of sodium acetate with a lipid content of 66% (w/w, DCW) which was 48.35% higher than that achieved in case of

glucose (Fig. 3.6 A). In accordance with the present observation, *Chlorella sorokiniana* GXNN01 was found to accumulate maximum amount of neutral lipid on supplementation of sodium acetate as carbon source (Qiao and Wang, 2009). It is important to note that these experiments were conducted under batch mode and no intermittent feeding of the limiting nutrients e.g. nitrate and phosphate was provided to maintain nutrient sufficient condition for the cells. It is a well-known fact that the nitrate and/or phosphate starvation can act as the triggers for neutral lipid accumulation in microalgae (Menon et al., 2013) and there may be a significant change in biomass and lipid productivity in response to nutritional starvation. Hence, there was a need to confirm whether accumulation of neutral lipid on glucose and sodium acetate was a consequence of nutritional starvation or was it due to their effect as a lipid inducer.

To that end, the sole effect of carbon sources on lipid induction was determined by growing the organism in their respective carbon sources under nutrient sufficient condition with intermittent feeding of nitrate and phosphate throughout the cultivation period. Interestingly, the organism exhibited improved growth with very less accumulation of neutral lipid (~3% w/w, DCW) in the presence of glucose as carbon source under nutrient sufficient condition (Fig. 3.6 B). In contrast, significant accumulation of neutral lipid (55% w/w, DCW) was observed when the organism was grown on sodium acetate under nutrient sufficient condition. In this case, biomass titer was reduced by 57% as compared to the batch grown on glucose under nutrient sufficient condition. These results reveal that while glucose can act as a growth promoting carbon source, sodium acetate can be considered as an effective lipid inducer. Microalga *Chlorella vulgaris* showed maximum growth on glucose supplemented media in comparison to other carbon sources such as sugar alcohols, sugar phosphates, organic acids, and monohydric alcohols (Griffiths et al., 1960). Glucose is a simple sugar which is easily taken up by microalgae (Morales-Sánchez

et al., 2013) and readily converted into glucose 6 phosphate (G6P), a precursor for glycolysis and pentose phosphate pathway (Shastri and Morgan, 2005). On the other hand, sodium acetate, being a simple structured molecule with two carbon atoms can be easily assimilated by the cell and converted into acetyl coenzyme A, main precursor for lipid biosynthesis (Qiao and Wang, 2009). This increased concentration of acetyl CoA facilitates the increased the flux towards lipid biosynthesis pathway resulting in enhanced accumulation of neutral lipid in microalgae. Further, based on these experimental observations we can conclude that lipid induction in glucose supplemented medium was due to the effect of nitrate or phosphate starvation (Fig. 3.6 A) whereas in case of sodium acetate supplemented medium, induction of neutral lipid was due to the combined effect of sodium acetate as lipid inducer (predominant) and nutritional starvation (Fig. 3.6 A).

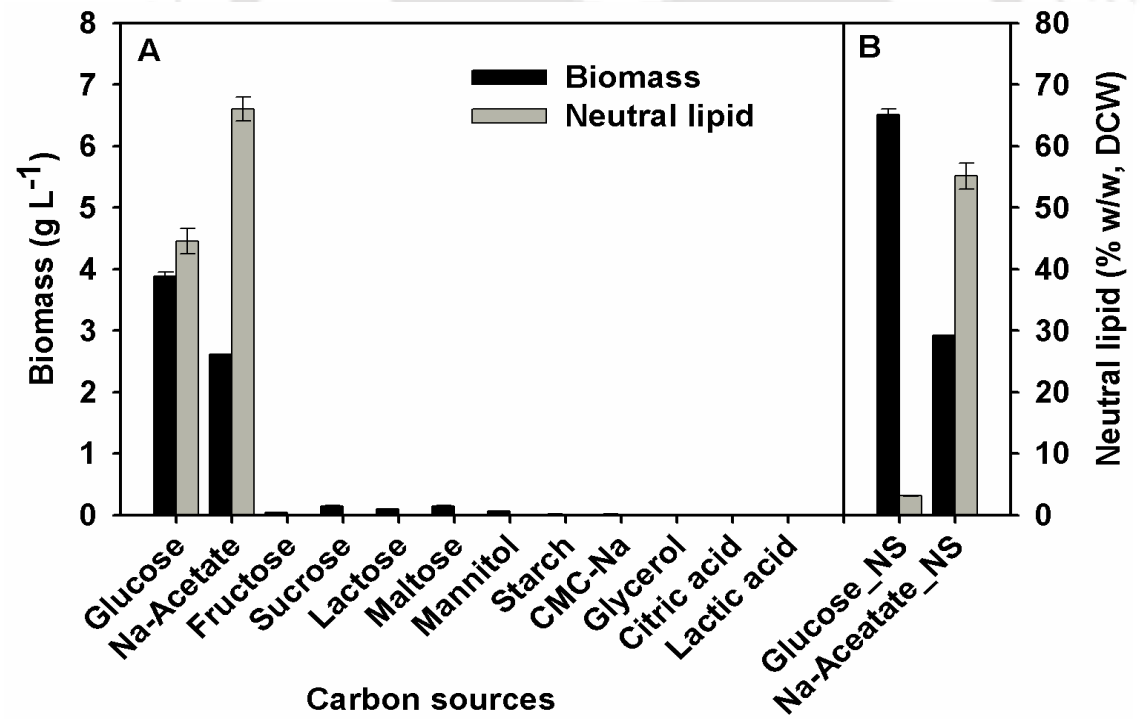

Fig. 3.6 Characterization of FC2 in terms of growth and neutral lipid accumulation under (A) different carbon sources at equimolar concentration of carbon (6 g L^{-1}) in batch mode of operation, (B) glucose and sodium acetate as carbon source in nutrient sufficient condition maintained through intermittent feeding of nitrate and phosphate.

Biomass titer and lipid content were found to be similar across various nitrogen sources (Fig 3.7) however organism failed to grow significantly in case of ammonium

chloride, ammonium sulfate and sodium nitrite. Microalgae *Hillea* sp. and *Prorocentrum minimum* were also exhibited no growth in the presence of ammonium (Lourenco et al., 2002) which is in accordance with present findings. Similarly, no significant growth was observed in autotrophic cultivation of FC2 under these nitrogen sources as also reported earlier (Muthuraj et al., 2014). Thus ammonium shows negative effect on growth as higher concentration of ammonium is toxic for microalgae. Similarly lower growth of *Haematococcus pluvialisin* was reported in sodium nitrite as nitrogen source than urea and nitrate (Harker et al., 1995). This may be due to inhibition of photosynthetic electron transport chain by nitrite (Loranger and Carpentier, 1994). In the remaining nitrogen sources, slightly enhanced growth was observed in case of sodium nitrate, glycine and yeast extract (Fig 3.7). Similarly, *Chlorella protothecoides* was reported to exhibit higher growth in presence of nitrate and yeast extract than urea as a nitrogen source (Shen et al., 2010). This may be attributed to full expression of nitrate reductase in case of sodium nitrate (Perez-Garcia et al., 2011) and supply of readily available amino acids in case of yeast extract and glycine. According to the previous study on nitrogen screening in autotrophic growth condition, maximal growth was observed in nitrate and urea than glycine (Muthuraj et al., 2014). However present study exhibited lower growth with urea in comparison to glycine and nitrate as nitrogen sources. This depicts that growth supporting nitrogen sources may vary with cultivation conditions of the organism. The significantly higher lipid induction was not observed in any nitrogen sources as they support growth rather than lipid production. Sodium nitrate was selected as growth supporting nitrogen source for successive studies owing to cost and availability of nitrate in comparison with yeast extract and glycine. It is known fact that nitrogen limitation enhances the lipid induction in microalgae (Rodolfi et al., 2009) and hence no nitrogen source was found to act as lipid inducer.

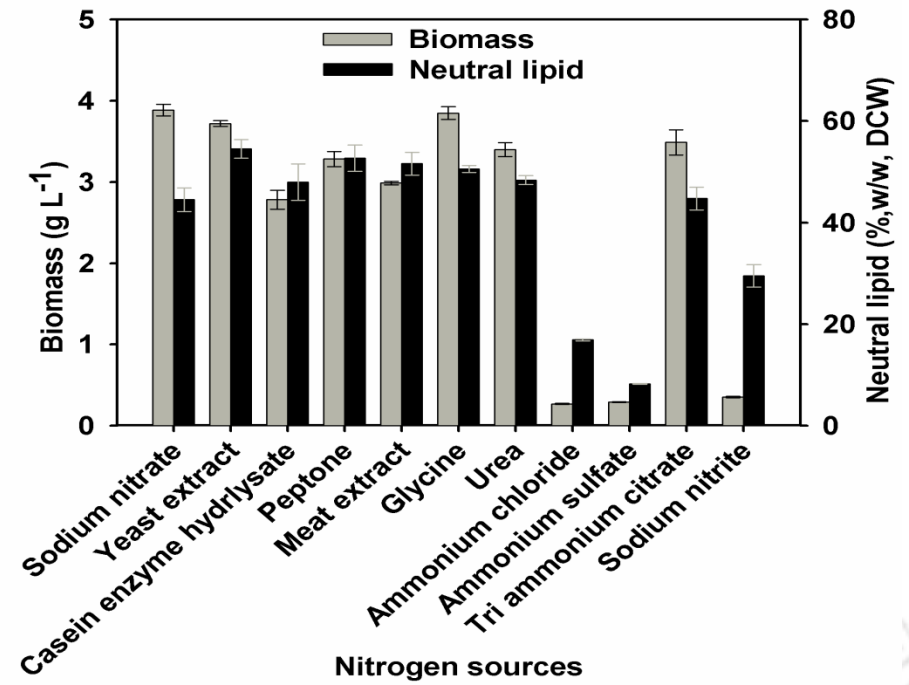

Fig. 3.7 Characterization of FC2 in terms of growth and neutral lipid accumulation under different nitrogen sources at equimolar concentration of nitrogen (0.247 g L^{-1}) in batch mode of operation.

3.3.4. Fatty acid methyl esters (FAME) composition and evaluation of biodiesel properties of FC2 grown under various carbon and nitrogen sources

FAME composition of FC2 under various carbon and nitrogen sources exhibited moderate variation in fatty acid chain lengths especially in oleic acid (C18:1) and linoleic acid (C18:2) composition (Fig. 3.8). Organic nitrogen sources were found to support enhanced synthesis of oleic acid in comparison with linoleic acid. In case of inorganic nitrogen sources, linoleic acid was the major component among the total FAME composition. Modulation of this composition with organic and inorganic nitrogen sources is a unique characteristic of FC2 which has not been reported in the literature. This may be due to enhanced expression of fatty acid desaturase enzyme under inorganic nitrogen sources. Palmitic acid (C16:0), oleic acid and linoleic acid contribute around 80% of total FAME composition across the various carbon and nitrogen sources. Similarly *Chlorella zofingiensis* was reported to exhibit higher composition of C16:0, C18:1 and C18:2 in the total FAME (Liu et al., 2011). The total FAME was found to constitute fatty acid chain

lengths from C16 to C18 and it is similar to petroleum based diesel comprising of the alkane molecules in the ranges of C15 - C19 (McArthur and Spalding, 2004).

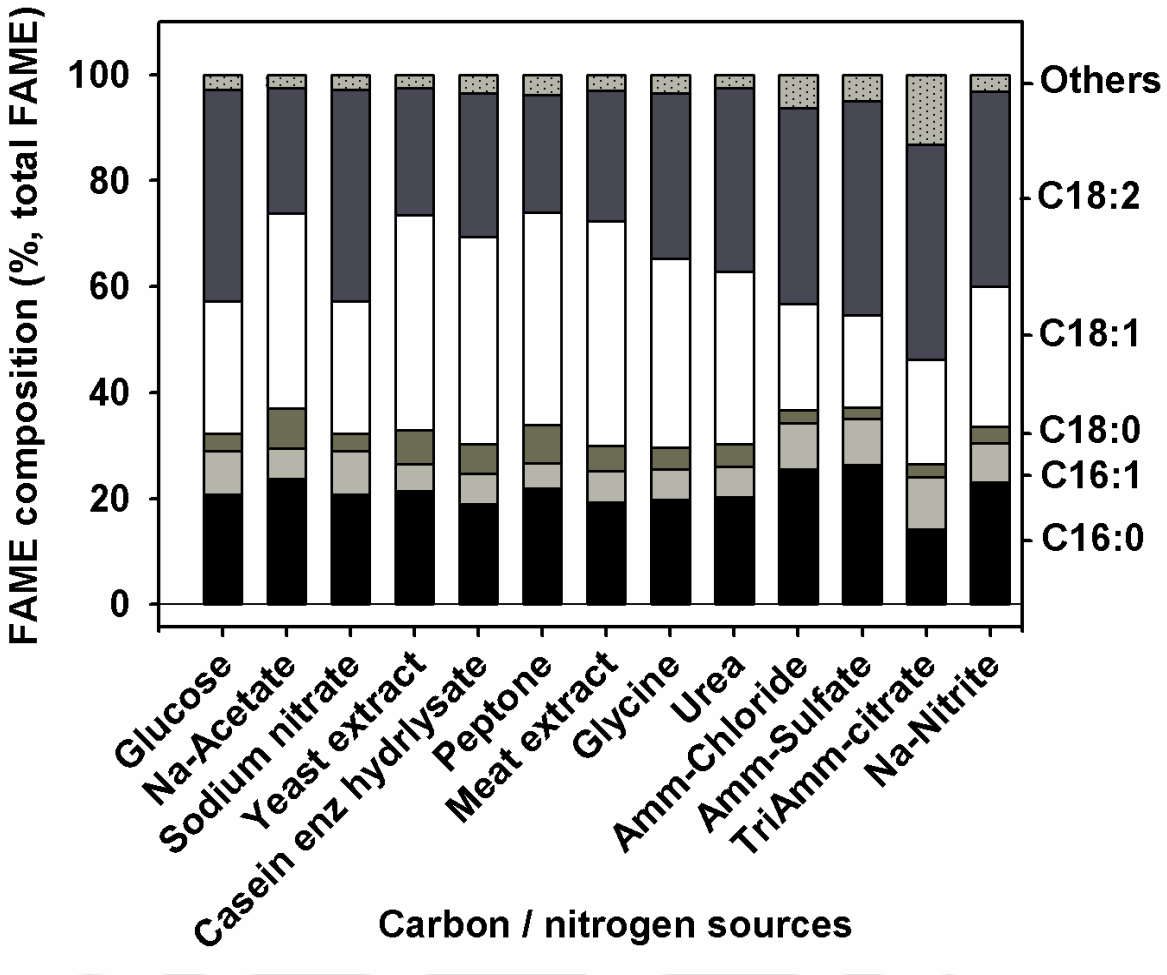

Fig. 3.8 Effect of different carbon and nitrogen sources on FAME composition when FC2 was grown at various carbon and nitrogen sources under heterotrophic condition.

FAME composition was used to calculate biodiesel properties with the help of empirical formulas for carbon and nitrogen screening experiment (Table 3.3). Kinematic viscosity was found to vary from 4.27 cSt to 4.5 cSt in various carbon and nitrogen sources. This value is appropriate for commercial purpose as higher viscosity may block the fuel filter and injection system in engines (Tat and Van Gerpen, 1999) while lower values fails to provide proper lubrication for moving parts of engine. The ignition delay and engine knocking problems can be eliminated by elevating the cetane values and interestingly these values fall in the range of 52.4–57.9 which were higher than both

American and European standards. The transportation safety is indicated by minimum flammable temperature termed as flash point value. This was found much higher (>152.57°C) than American and European standards and hence can be used as suitable transportation fuel. Cloud point values show the cold flow property of oil where oil starts appearing cloudy. These values were observed in the range of 0.7°C to 6.8°C in various carbon and nitrogen sources which depicts that this biodiesel can be used as transportation fuel till 0.7°C. Hence, biodiesel obtained from microalga FC2 can be used for commercial purpose irrespective of supplementation of carbon and nitrogen sources.

Table 3.3 Biodiesel properties obtained from FC2 biomass grown in a various carbon and nitrogen sources. Properties are calculated using empirical formulas based on experimentally determined FAME compositions and compared with ASTM D6751–15a and EN14214

Standard	**Viscosity**	**Cetane number**	**Flash point**	**Cloud point**	**Saponification value**	**Iodine value**
ASTM D6751–15a	1.9 - 6	>47	>93	ND	ND	ND
EN 14214	3.5 - 5	>51	>101	ND	ND	<120
Carbon or nitrogen sources						
Glucose	4.34	54.12	159.71	0.96	203.57	102.89
Na-Acetate	4.49	57.73	159.15	6.67	202.03	81.86
Sodium nitrate	4.34	54.12	159.71	0.96	203.57	102.89
Yeast extract	4.48	57.39	160.67	4.97	202.05	85.17
Casein enzyme hydrolysate	4.44	56.45	161.04	3.28	200.67	90.03
Peptone	4.5	57.88	160.22	6.82	199.55	81.04
Meat extract	4.46	56.75	161.45	2.84	200.77	88.8
Glycine	4.41	55.68	161.51	2.9	200.23	94.43
Urea	4.39	55.19	161.28	2.35	202.18	97.81
Amm-Chloride	4.32	54.6	153.56	2.41	201.36	93.47
Amm-Sulfate	4.29	53.99	152.57	0.76	204.96	97.61
TriAmm-citrate	4.27	52.4	160.42	3.22	182.57	101.34
Na-Nitrite	4.35	54.76	157.89	1.66	203.86	97.83

ND-not defined

3.4. Conclusions

In the present study, growth supportive and lipid inducing conditions/nutrients were screened among various physiological and nutritional conditions. The study showed that organism can grow in wide range of initial media pH and temperature with maximum growth was observed at pH 6-8 and 28°C. While glucose was found to support growth, sodium acetate was observed as lipid inducing carbon source. In case of nitrogen sources, no significant change in growth was observed however owing to its cheaper cost sodium nitrate was selected for cultivation. The biodiesel produced from microalga FC2 was found to follow the American and European standards among all nutritional values which is a prerequisite condition for biodiesel production. These results were used for further optimization and process development experiments.

3.5. References

1. Barsanti L., Gualtieri P., 2014. Algae: anatomy, biochemistry, and biotechnology. CRC Press, Taylor & Francis, Boca Raton, Florida.
2. Cataldo D.A., Maroon M., Schrader L.E., Youngs V.L., 1975. Rapid colorimetric determination of nitrate in plant tissue by nitration of salicylic acid. Communications in Soil Science & Plant Analysis. 6, 71–80.
3. Chae S.R., Hwang E.J., Shin H.S., 2006. Single cell protein production of *Euglena gracilis* and carbon dioxide fixation in an innovative photo-bioreactor. Bioresource Technology. 97, 322–329.
4. Chinnasamy S., Bhatnagar A., Claxton R., Das K.C., 2010. Biomass and bioenergy production potential of microalgae consortium in open and closed bioreactors using untreated carpet industry effluent as growth medium. Bioresource Technology. 101, 6751–6760.

5. Chisti Y., 2013. Constraints to commercialization of algal fuels. Journal of Biotechnology. 167, 201–214.

6. Converti A., Casazza A.A., Ortiz E.Y., Perego P., Del Borghi M., 2009. Effect of temperature and nitrogen concentration on the growth and lipid content of *Nannochloropsis oculata* and *Chlorella vulgaris* for biodiesel production. Chemical Engineering and Processing: Process Intensification. 48, 1146–1151.

7. Francisco E.C., Neves D.B., Jacob-Lopes E., Franco T.T., 2010. Microalgae as feedstock for biodiesel production: carbon dioxide sequestration, lipid production and biofuel quality. Journal of Chemical Technology and Biotechnology. 85, 395–403.

8. Griffiths D.J., Thresher C.L., Street H.E., 1960. The heterotrophic nutrition of *Chlorella vulgaris* (Brannon No. 1 strain): with two figures in the text. Annals of Botany. 24, 1–11.

9. Harker M., Tsavalos A.J., Young A.J., 1995. Use of response surface methodology to optimise carotenogenesis in the microalga, *Haematococcus pluvialis*. Journal of Applied Phycology. 7, 399–406.

10. Kim S., Kim H., Ko D., Yamaoka Y., Otsuru M., Kawai-Yamada M., Ishikawa T., Oh H.-M., Nishida I., Li-Beisson Y., 2013. Rapid induction of lipid droplets in *Chlamydomonas reinhardtii* and *Chlorella vulgaris* by Brefeldin A. PLoS ONE. 8, e81978.

11. Kong Q., Li L., Martinez B., Chen P., Ruan R., 2010. Culture of microalgae *Chlamydomonas reinhardtii* in wastewater for biomass feedstock production. Applied Biochemistry and Biotechnology. 160, 9–18.

12. Kumar V., Muthuraj M., Palabhanvi B., Ghoshal A.K., Das D., 2014. Evaluation and optimization of two stage sequential in situ transesterification process for fatty acid methyl ester quantification from microalgae. Renewable Energy. 68, 560–569.

13. Liang Y., Sarkany N., Cui Y., 2009. Biomass and lipid productivities of *Chlorella vulgaris* under autotrophic, heterotrophic and mixotrophic growth conditions. Biotechnology Letters. 31, 1043–1049.

14. Liu J., Huang J., Sun Z., Zhong Y., Jiang Y., Chen F., 2011. Differential lipid and fatty acid profiles of photoautotrophic and heterotrophic *Chlorella zofingiensis*: assessment of algal oils for biodiesel production. Bioresource Technology. 102, 106–110.

15. Loranger C., Carpentier R., 1994. A fast bioassay for phytotoxicity measurements using immobilized photosynthetic membranes. Biotechnology and Bioengineering. 44, 178–183.

16. Lourenco S.O., Barbarino E., Mancini-Filho J., Schinke K.P., Aidar E., 2002. Effects of different nitrogen sources on the growth and biochemical profile of 10 marine microalgae in batch culture: an evaluation for aquaculture. Phycologia 41, 158–168.

17. Lundholm N., Hansen P.J., Kotaki Y., 2004. Effect of pH on growth and domoic acid production by potentially toxic diatoms of the genera *Pseudo-nitzschia* and *Nitzschia*. Marine Ecology Progress Series. 273, 1-15.

18. McArthur H., Spalding D., 2004. Engineering materials science: Properties, uses, degradation, remediation. Woodhead Publishing, Cambridge.

19. Menon K.R., Balan R., Suraishkumar G.K., 2013. Stress induced lipid production in *Chlorella vulgaris*: relationship with specific intracellular reactive species levels. Biotechnology and Bioengineering. 110, 1627–1636.

20. Miller G.L., 1959. Use of dinitrosalicylic acid reagent for determination of reducing sugar. Analytical Chemistry. 31, 426–428.

21. Morales-Sánchez D., Tinoco-Valencia R., Kyndt J., Martinez A., 2013. Heterotrophic growth of *Neochloris oleoabundans* using glucose as a carbon source. Biotechnology for Biofuels. 6, 1–13.

22. Muthuraj M., Kumar V., Palabhanvi B., Das D., 2014. Evaluation of indigenous microalgal isolate *Chlorella* sp. FC2 IITG as a cell factory for biodiesel production and scale up in outdoor conditions. Journal Industrial Microbiology and Biotechnology. 41, 499–511.

23. Negi S., Barry A., Friedland N., Sudasinghe N., Subramanian S., Pieris S., Holguin F.O., Dungan B., Schaub T., Sayre R., 2015. Impact of nitrogen limitation on biomass, photosynthesis, and lipid accumulation in *Chlorella sorokiniana*. Jornal of Applied Phycology. 28, 803–812.

24. Parsons T.R., Maita Y., Lalli C.M., 1984. A Manual of Chemical & Biological Methods for Seawater Analysis. Pergamon Press, Oxford.

25. Perez-Garcia O., Escalante F.M., de-Bashan L.E., Bashan Y., 2011. Heterotrophic cultures of microalgae: metabolism and potential products. Water research. 45, 11–36.

26. Qiao H., Wang G., 2009. Effect of carbon source on growth and lipid accumulation in *Chlorella sorokiniana* GXNN01. Chineese Journal of Oceanology Limnology. 27, 762–768.

27. Ramírez-Verduzco L.F., Rodríguez-Rodríguez J.E., del Rayo Jaramillo-Jacob A., 2012. Predicting cetane number, kinematic viscosity, density and higher heating value of biodiesel from its fatty acid methyl ester composition. Fuel. 91, 102–111.

28. Rippka R., Deruelles J., Waterbury J.B., Herdman M., Stanier R.Y., 1979. Generic assignments, strain histories and properties of pure cultures of *cyanobacteria*. Journal of General Microbiology. 111, 1-61.

29. Rodolfi L., Chini Zittelli G., Bassi N., Padovani G., Biondi N., Bonini G., Tredici M.R., 2009. Microalgae for oil: Strain selection, induction of lipid synthesis and outdoor mass cultivation in a low-cost photobioreactor. Biotechnology and Bioengineering. 102, 100–112.

30. Shastri A.A., Morgan J.A., 2005. Flux balance analysis of photoautotrophic metabolism. Biotechnology Progress. 21, 1617–1626.

31. Shen Y., Yuan W., Pei Z., Mao E., 2010. Heterotrophic culture of *Chlorella protothecoides* in various nitrogen sources for lipid production. Applied Biochemistry Biotechnology. 160, 1674–1684.

32. Slade R., Bauen A., 2013. Micro-algae cultivation for biofuels: cost, energy balance, environmental impacts and future prospects. Biomass and Bioenergy. 53, 29–38.

33. Su Y.-C., Liu Y.A., Diaz Tovar C.A., Gani R., 2011. Selection of prediction methods for thermophysical properties for process modeling and product design of biodiesel manufacturing. Industrial and Engineering Chemistry Research. 50, 6809–6836.

34. Tat M.E., Van Gerpen J.H., 1999. The kinematic viscosity of biodiesel and its blends with diesel fuel. Journal of the American Oil Chemists' Society. 76, 1511–1513.

35. Touloupakis E., Cicchi B., Benavides A.M.S., Torzillo G., 2016. Effect of high pH on growth of *Synechocystis* sp. PCC 6803 cultures and their contamination by

golden algae (*Poterioochromonas* sp.). Applied Microbiology and Biotechnology. 100, 1333–1341.

36. Turon V., Trably E., Fayet A., Fouilland E., Steyer J.-P., 2015. Raw dark fermentation effluent to support heterotrophic microalgae growth: microalgae successfully outcompete bacteria for acetate. Algal Research. 12, 119–125.

37. Wang Y., Chen T., Qin S., 2012. Heterotrophic cultivation of *Chlorella kessleri* for fatty acids production by carbon and nitrogen supplements. Biomass and Bioenergy. 47, 402–409.

38. Wan M.-X., Wang R.-M., Xia J.-L., Rosenberg J.N., Nie Z.-Y., Kobayashi N., Oyler G.A., Betenbaugh M.J., 2012. Physiological evaluation of a new *Chlorella sorokiniana* isolate for its biomass production and lipid accumulation in photoautotrophic and heterotrophic cultures. Biotechnology and Bioengineering. 109, 1958–1964.

39. Xiong W., Li X., Xiang J., Wu Q., 2008. High-density fermentation of microalga *Chlorella protothecoides* in bioreactor for microbio-diesel production. Applied Microbiology and Biotechnology. 78, 29–36.

CHAPTER 4

Optimization of nutrients concentration for maximization of growth and lipid content

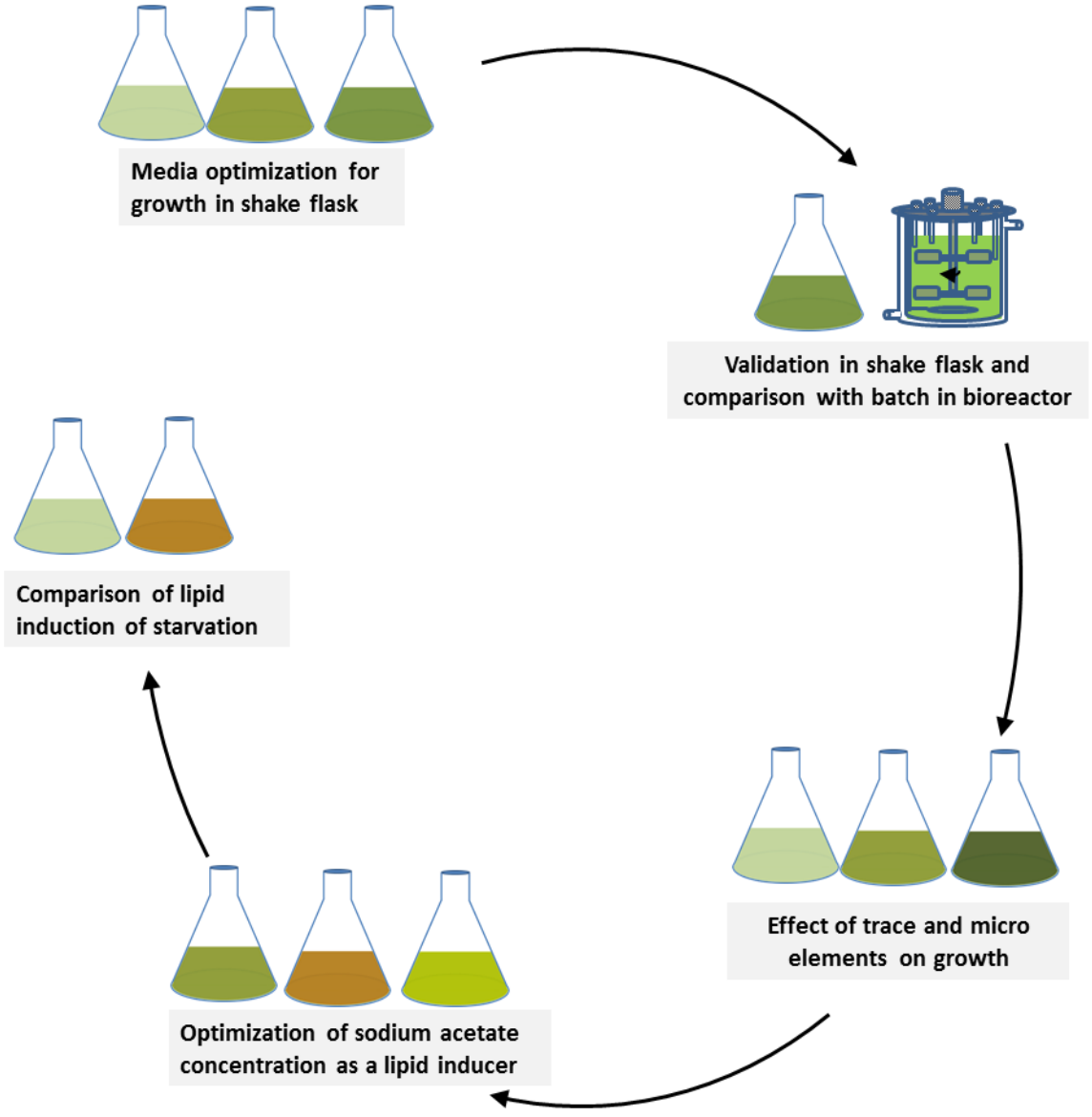

Optimization of nutrients concentration for maximization of growth and lipid content of FC2 in batch cultivation

4.1. Background and motivation

In the previous chapter (Chapter 3), microalga FC2 was found to accumulate 66 % (w/w, DCW) intracellular neutral lipid which makes biomass a potential feedstock for biodiesel production. However, organism showed lower biomass titer when cultivated in BG11 medium under heterotrophic condition. On the other hand, 5.7 fold increment was observed in biomass concentration of FC2 grown with modified BG11 medium as compared to basic BG11 media where elevated concentration of phosphate was used. This suggested that optimization of the media components may lead to enhancement of biomass titer. Microalga *Chlorella protothecoides* was reported to exhibit 1.8 times increment in biomass titer on optimization of nutrient concentrations in the media (Cheng et al., 2013). Similarly *Chlorella minutissima* showed 3.7 times higher biomass productivity at optimal concentration of carbon, nitrogen and phosphorous sources (Li et al., 2011). The changes in concentration of carbon and nitrogen sources were found to result in a significant variation (9 g L^{-1} to 21 g L^{-1}) in biomass concentration (Xiong et al., 2008). Along the similar line, growth of organism also varies with concentration of trace and microelements (Xiong et al., 2008). Therefore, characterization and optimization of key nutrients are important in order to develop a process for high cell density cultivation.

High cell density cultivation may hinder the accumulation of intracellular lipid in cells due to mutually exclusive nature of growth and lipid content (Rodolfi et al., 2009). The lipid induction in *Scenedesmus* sp. was reported to vary rapidly with concentration of sodium chloride which was supplemented as a lipid inducer (Pancha et al., 2015). Maximum lipid accumulation in *Chlorella sorokiniana* was observed at 20 g L^{-1} sodium acetate when it was used as lipid elicitor (Kumar et al., 2016). Thus, optimization of lipid inducing condition is also necessary in view of biodiesel production.

The classical method of 'one variable at a time' can be used for optimization of single variable processes however in case of multivariable systems it is time consuming and expensive due to design of large number of experiments (Bezerra et al., 2008; Stanbury et al., 2003). Hence, statistical methods such as response surface methodology (RSM), Genetic algorithm, Taguchi method, etc. are being employed to find out the optimal solution with minimal amount of experiments (Kalil et al., 2000; Li et al., 2013). RSM coupled with factorial design is widely used for optimization of media and other biological processes as it also determines the interaction effect between two variables (Bezerra et al., 2008).

The present study focused on optimization of media compositions and lipid inducers for growth and lipid content of the organism FC2. The study covers RSM based optimization of media components for growth, evaluation of effect of trace and microelements (TME) on growth, and optimization of sodium acetate concentration as lipid inducer. In the first step, concentration of glucose, nitrate and phosphate was optimized by using central composite design (CCD) and RSM. This was performed with individual two objective functions such as specific growth rate and biomass titer. In the second step, effect of different concentrations of TME on specific growth rate was assessed. Finally, sodium acetate concentration was optimized using one variable at a time strategy for higher accumulation of intracellular neutral lipid.

4.2. Material and methods

4.2.1. Growth condition

Inoculum was prepared as described in the section 3.2.1. Modified BG11 media adopted from Rippka et al. (1979) was used along with 15 g L^{-1} glucose supplementation for inoculum preparation in case of optimization of media components for growth and validation. All successive experiments (effect of TME and optimization of sodium acetate)

and their inoculum preparation were carried out in optimized BG11 medium (detail in section 4.3.1). All the experiments were inoculated with 1% (v/v) of active mid-log phase culture and were carried out in 250 mL shake flask under the conditions mentioned for inoculum preparation in the section 3.2.1. The growth of the organism under optimized BG11 medium was also characterized in 3 L automated bioreactor (Bio Console ADI 1025, Applikon Biotechnology, Holland) and compared with shake flask data. The reactor was operated at 28°C, agitator speed of 400 rpm and aeration rate of 1vvm. Sampling was done at regular intervals of time for determination of biomass, lipid content and specific growth rate.

4.2.2. Optimization of media composition for maximization of specific growth rate and biomass titer

The concentrations of key rate limiting nutrients such as glucose, nitrate and phosphate for the growth of FC2 were selected as the target parameters for optimization using RSM. Three parameters and five level central composite design was formulated using the software Design Expert 8.0.0 (Stat-Ease Inc, Minneapolis, USA). The levels of these factors and CCD design for 17 experiments are shown in Table 4.1 and Table 4.2 respectively.

Table 4.1 Actual and coded levels of the selected BG11 media components for the maximizations of specific growth rate and biomass titer of FC2.

Factors		Levels and corresponding actual values				
Code	**Name**	**-2**	**-1**	**0**	**1**	**2**
X_1	Initial glucose concentration (g L^{-1})	5	12.5	20	27.5	35
X_2	Initial nitrate concentration (g L^{-1})	0.3	0.65	1	1.35	1.7
X_3	Initial phosphate concentration (mg L^{-1})	20	60	100	140	180

Table 4.2 CCD matrix of the media components used in RSM with corresponding experimental and predicted measurements for specific growth rate (μ) and biomass titer

Std. No.	Glucose (g L^{-1})	Nitrate (g L^{-1})	Phosphate (mg L^{-1})	μ (day^{-1})		Biomass titer (g L^{-1})	
				Exp.	Pred.	Exp.	Pred.
1	12.5	0.65	60	1.993	1.979	4.01	3.92
2	27.5	0.65	60	2.003	2.012	4.56	4.54
3	12.5	1.35	60	2.052	2.055	4.22	4.20
4	27.5	1.35	60	2.050	2.052	5.25	5.45
5	12.5	0.65	140	2.046	2.049	4.50	4.46
6	27.5	0.65	140	2.017	2.018	5.43	5.61
7	12.5	1.35	140	2.090	2.084	6.02	6.19
8	27.5	1.35	140	2.000	2.017	7.72	7.96
9	5	1	100	1.994	2.003	3.39	3.46
10	35	1	100	1.982	1.969	6.08	5.85
11	20	0.3	100	1.995	1.998	3.28	3.34
12	20	1.7	100	2.079	2.073	6.19	5.97
13	20	1	20	1.990	1.992	3.35	3.39
14	20	1	180	2.032	2.027	6.64	6.44
15	20	1	100	2.101	2.102	6.91	6.94
16	20	1	100	2.111	2.102	7.14	6.94
17	20	1	100	2.098	2.102	6.93	6.94

Remaining all other media components such as trace elements and microelements were used in same concentrations as mentioned in basic BG11 medium. Maximizations of specific growth rate (M_μ) and maximization of biomass titer (M_X) were used as the individual objective functions in the model and the responses were expressed as second order polynomial equation (Equation 4.1). While media optimized for M_μ of the organism is essential in fed batch and chemostat to attain enhanced biomass productivity, media

optimized for M_X is useful for batch cultivation of the organism. Therefore two objective functions were used in optimization of media components.

$$Y = \beta_0 + \sum_{i=1}^{k} \beta_i X_i + \sum_{i=1}^{k} \beta_{ii} X_i^2 + \sum_{i=1,i<j}^{k-1} \sum_{j=2}^{k} \beta_{ij} X_i X_j \quad (4.1)$$

Where, Y is response (specific growth rate or biomass titer), X_i is the i^{th} parameter, k is the total number of parameters and β_0, β_i, β_{ii} and β_{ij} are the regression coefficients. Variable i =1, 2, 3 represents glucose, nitrate and phosphate respectively.

The equation 4.1 consist linear, quadratic and interaction effect of initial concentration of glucose, nitrate and phosphate on the responses. This was carried out by RSM which depends on the design of proper experimental points. Usually central composite design was used predominantly in optimization problems which cover the factorial points, axial points, and central points of design. In the present design, these points consist of eight, six, and three experiments respectively. Sampling was done at regular intervals of time for determination of biomass and specific growth rate for all 17 experiments.

4.2.3. Effect of trace elements and microelements on specific growth rate and biomass titer

BG11 medium consist of 6 trace elements and 6 microelements as shown in the Table 3.1. The total composition of trace elements and micro elements per liter of BG11 medium was considered as one unit (U) of TME per liter. In the first step, effect of TME on specific growth rate was assessed under different concentrations of TME such as 0.05, 0.15, 0.3, 0.45, 0.6, 0.9, 1.2, 1.5, 1.8, 2.1, 3 and 1 U L^{-1}. 1 U L^{-1} TME concentration in the BG11 medium was used as control experiment. The experiments were performed in the BG11 medium optimized for M_μ, with different amount of TME in each flask under batch

mode of operation. In the next step, similar experiments were carried out using BG11 medium optimized for maximization of biomass titer M_X.

In case of fed-batch or continuous operation, feeding of TME along with glucose, nitrate and phosphate is necessary however obtaining real time utilization profile of all twelve components of TME is a difficult task. As an alternative, yield coefficient of TME may guide in designing of TME feeding strategy. The yield coefficient was calculated by determining the amount of TME required for generation of one gram of biomass without loss of maximal specific growth rate at nutrient sufficient condition. To that end, a shake flask experiment was carried out with 1 unit L^{-1} of TME along with intermittent feeding of nitrate, phosphate and glucose to maintain nutrient sufficient condition. Here, intermittent feeding refers to addition of nitrate, phosphate and glucose at regular time interval in order to maintain the broth concentration of these nutrients more than 50% of their respective initial concentration. Experiment was carried out in BG11 medium optimized for M_μ as this media was potentially used for fed-batch and continuous cultivation to maintain higher maximum specific growth rate and in turn high biomass productivity. Sampling was carried out at regular intervals of time to determine biomass concentration and specific growth rate of the organism.

4.2.4. Effect of sodium acetate concentration as an inducer of intracellular neutral lipid in FC2

From screening of various carbon sources (Section 3.3.3) it was found that sodium acetate could act as an effective inducer for accumulation of intracellular neutral lipid in FC2. Concentration of sodium acetate was optimized with one at a time strategy with the objective function of maximization of intracellular neutral lipid. The organism was grown in the bioreactor in order to achieve significant amount of cells (~ 4 g L^{-1}) under nutrient sufficient condition by intermittent feeding of limiting substrates. This was followed by

harvesting of the cells under aseptic condition through centrifugation at 8000 $\times g$ for 10 minutes at 4°C. Cell pellet was washed in saline (0.9% w/v of sodium chloride) and then distributed to 10 Erlenmeyer flasks containing 0, 2, 4, 6, 8, 12, 16, 20, 24, and 28 g L^{-1} of sodium acetate in BG11 medium optimized for M_μ (Fig. 4.1). The process development for high biomass titer or productivity was to be carried out in BG11 medium optimized for M_μ due to its maximal growth rate and hence optimal concentration of sodium acetate for lipid induction was also determined in the same media composition. Effect of sodium acetate on lipid induction was determined by maintaining media components such as nitrate, phosphate, glucose, TME at their optimal concentrations via intermittent feeding throughout fermentation and thereby avoiding the effects of nutrient starvation on the lipid induction in FC2. Extent of lipid accumulation through addition of sodium acetate was also compared with the lipid accumulation under nitrate and phosphate starvations via inoculating the cells into the BG11 medium optimized for M_μ and devoid of nitrate or phosphate source. In all the experiments, sampling was carried out at regular time intervals to obtain dynamic profile of biomass, substrate utilization and lipid content of the cells.

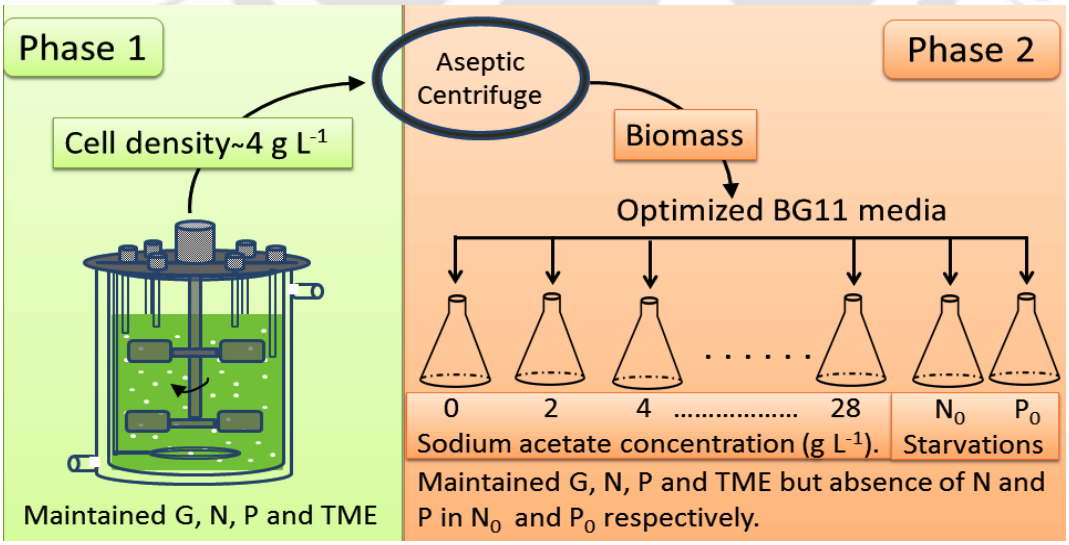

Fig. 4.1 Schematic representation of the two-phase cultivation process designed for optimization of sodium acetate concentration targeted towards maximization of neutral lipid content of the strain FC2 grown in optimized BG11 medium under heterotrophic condition. Phase 1 represents, organism growth in a 7.5 L automated bioreactor with

nutrient sufficient condition by maintaining glucose (G), nitrate (N), phosphate (P), trace and microelements (TME) in order to achieve 4 g L^{-1} biomass. Phase 2 represents optimization of sodium acetate concentration and characterization of strain under nutrient starvation by transferring the first phase biomass into shake flasks. The strain was characterized for effect of sodium acetate by growing it in BG11 medium with different concentration of sodium acetate and for nutrient starvation by growing it in BG11 medium devoid of nitrate or phosphate. In the second phase of sodium acetate experiments N, P, G and TME was maintained throughout the batch by intermittent feeding.

4.2.5. Analyses of biomass, lipid and substrate concentration

The sample collected at regular time intervals was centrifuged at 8000 × g for 10 minutes at 4°C to separate supernatant and pellet. While the pellet was used for estimation of growth and lipid content measurement, the supernatant was used for the analyses of substrate utilization. Cell growth was obtained by measuring optical density of the cells as mentioned in section 3.2.5.1. The neutral lipid content of biomass was measured by Nile red method as explained in 3.2.5.5. The utilization profile of substrates such as glucose, nitrate and phosphate were carried out through the method described in sections 3.2.5.3, 3.2.5.2 and 3.2.5.4 respectively.

4.3. Results and discussion

4.3.1. Maximization of specific growth rate and biomass titer of FC2 via media optimization

Based on the results observed in previous chapter (chapter 3), optimization was carried out for initial concentrations of glucose, nitrate and phosphate. A total of 17 experiments were carried out as per the CCD design and corresponding specific growth rate and biomass titer was used as the response in developing RSM based quadratic model which was analyzed by multiple regression analysis. Maximization of specific growth rate (M_μ) and biomass titer (M_μ) were used as objective functions to obtain two optimal media compositions. Effect of parameters and their significance were examined through analysis of variance (ANOVA) as shown in Table 4.3.

Table 4.3 Analyses of variance for the quadratic regression model obtained from RSM based optimization of media components for maximization of specific growth rate and biomass titer FC2 grown heterotrophically in shake flask

Parameters	Maximization of specific growth rate					Maximization of biomass titer				
	Sum of Squares	DOF	Mean Square	F value	p-value*	Sum of Squares	DOF	Mean Square	F Value	p-value*
Model	0.031	9	3.44E-03	23.16	0.0002	33.26	9	3.70	73.81	< 0.0001
X_1	1.15E-03	1	1.15E-03	7.73	0.0273	5.75	1	5.75	114.74	< 0.0001
X_2	5.66E-03	1	5.66E-03	38.08	0.0005	6.92	1	6.92	138.23	< 0.0001
X_3	1.26E-03	1	1.26E-03	8.47	0.0227	9.33	1	9.33	186.37	< 0.0001
X_1^2	0.016	1	0.016	108.98	< 0.0001	6.31	1	6.31	126.11	< 0.0001
X_2^2	5.34E-03	1	5.34E-03	35.95	0.0005	6.31	1	6.31	125.97	< 0.0001
X_3^2	0.01	1	0.01	69.62	< 0.0001	4.96	1	4.96	98.99	< 0.0001
X_1*X_2	6.54E-04	1	6.54E-04	4.4	0.0741	0.20	1	0.20	3.92	0.0882
X_1*X_3	2.04E-03	1	2.04E-03	13.75	0.0076	0.14	1	0.14	2.77	0.1402
X_2*X_3	7.88E-04	1	7.88E-04	5.3	0.0548	1.05	1	1.05	20.88	0.0026
Residual	1.04E-03	7	1.49E-04			0.35	7	0.050		
Lack of fit	9.50E-04	5	1.90E-04	4.18	0.2041	0.32	5	0.064	3.90	0.2166
Pure Error	9.08E-05	2	4.54E-05			0.033	2	0.016		
Total	0.032	16				33.61	16			
	R^2 = 0.97	Signal to noise ratio = 11.18				R^2 = 0.99	Signal to noise ratio = 26.93			

* - p value >0.1 is considered as insignificant

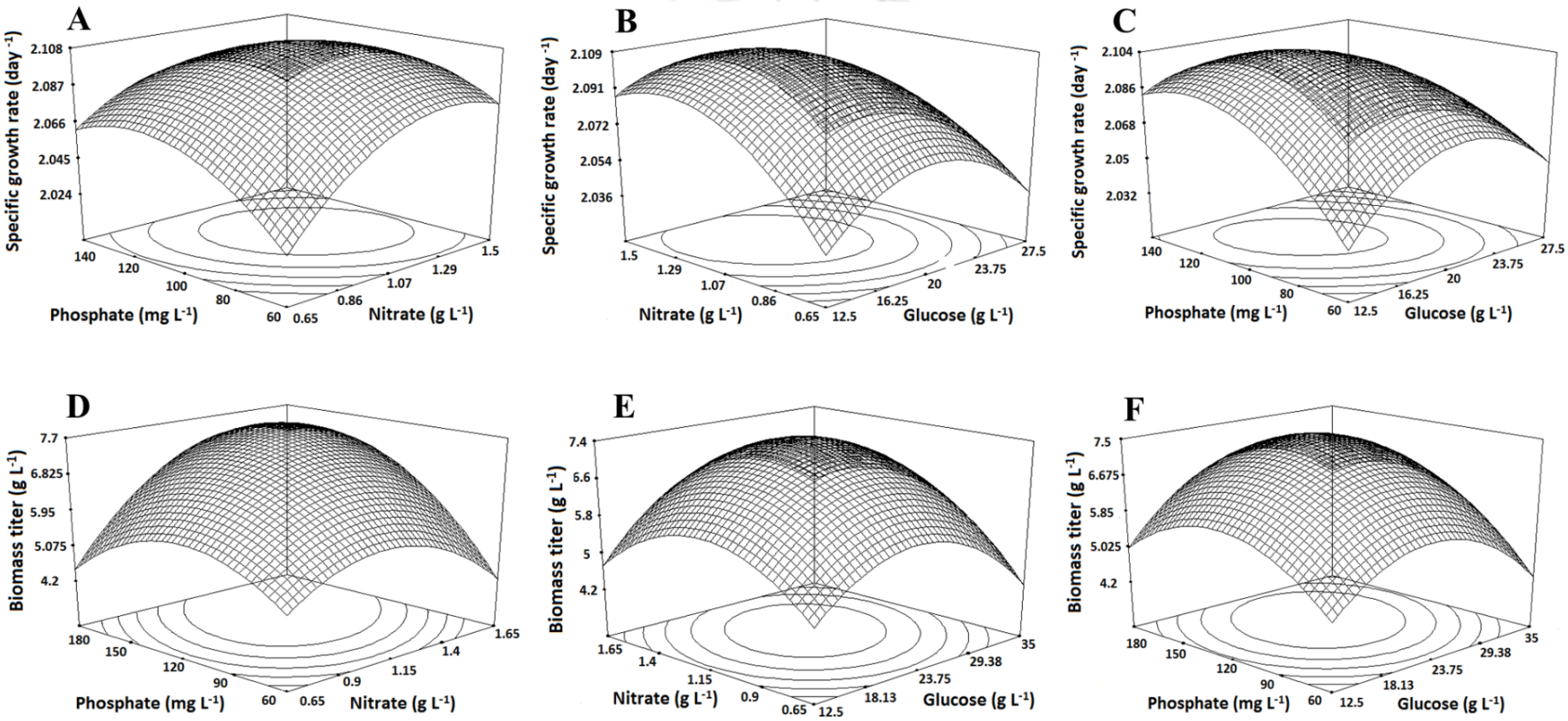

Fig. 4.2 Response surface plots representing the interaction effect of (A) phosphate & nitrate, (B) nitrate & glucose, & (C) phosphate & glucose on specific growth rate and (D) phosphate & nitrate, (E) nitrate & glucose, & (F) phosphate & glucose on biomass titer of organism. In above two variable interactions, third variable kept at constant middle value. The middle values of glucose, nitrate and phosphate were 20 g L^{-1}, 1 g L^{-1} and 100 mg L^{-1} respectively.

From the ANOVA analysis, linear, quadratic and interaction effect of all parameters of model were found significant for both the optimization models. The noise disturbance in the models was found to be negligible as the signal to noise ratio values of 14.18 and 26.93 were observed in optimization models for maximization of specific growth rate and biomass titer respectively. Regression coefficient (R^2) values were also found to be higher than 0.97 which depicts that the model can predict the response with 97% accuracy. The M_μ and M_X can be predicted using the model equations 4.2 and 4.3 respectively.

$$Specific\ growth\ rate\ (day^{-1})$$
$$= 1.31647 + 0.028206 * X_1 + 0.46473 * X_2 + 0.00488 * X_3 - 5.14 * 10^{-4} * {X_1}^2 - 0.13559 * {X_2}^2 - 1.44 * 10^{-5} * {X_3}^2 - 0.00344 * X_1 * X_2 - 5.327 * 10^{-5} * X_1 * X_3 - 7.09 * 10^{-4} * X_2 * X_3 \quad (4.2)$$

$$Max\ cell\ density\ (g\ L^{-1})$$
$$= -5.67563 + 0.38240 * X_1 + 7.42098 * X_2 + 0.047734 * X_3 - 0.010151 * {X_1}^2 - 4.65865 * {X_2}^2 - 3.16 * 10^{-4} * {X_3}^2 + 0.059671 * X_1 * X_2 + 4.39 * 10^{-4} * X_1 * X_3 + 0.025821 * X_2 * X_3 \quad (4.3)$$

Where, X_1, $X_2$and X_3 are the concentration of glucose (g L^{-1}), nitrate (g L^{-1}) and phosphate (mg L^{-1}) respectively.

The interaction effect of all the model parameters showed that their optimum values lie within the considered parameters range (Fig. 4.2). Each plot of response is a representation of different combinations of two media components while keeping the third component constant at its middle value (Fig. 4.2 A – 4.2 F). The models were validated by comparing model predicted responses with the corresponding experimental values at their optimal media composition (Table 4.4). The specific growth rate at optimized BG11 media for M_μ was moderately increased in comparison with the basic BG11 media (1.6 day^{-1}).The concentrations of the key nutrients in the optimized BG11 media were not

found to vary much as compared to basic BG11 media with the exception of phosphate concentration which is considerably higher in case of optimized media composition. In case of BG11 media optimized for M_X, biomass titer of 7.81 g L^{-1} was achieved which was 10 fold higher than the basic BG11 medium. Earlier, similar optimization of media composition with respect to maximization of specific growth rate and biomass titer was demonstrated for microalga *Haematococcus pluvialis* (Gong and Chen, 1997). RSM based optimization for growth of FC2 under photoautotrophic condition showed 2.21 fold improved biomass titer in comparison to growth in unoptimized medium (Muthuraj et al., 2014). Organism characterization in automated bioreactor with optimal media composition showed that biomass titer was not improved in comparison to shake flask, however increment in specific growth rate was observed in both the media composition (Table 4.5). This might be attributed to aeration and proper mixing in bioreactor.

Table 4.4 Values of media components & responses at optimal conditions obtained from maximization specific growth rate and biomass titer

Media components & responses	**Values at optimal condition**	
	specific growth rate	**biomass titer**
Initial glucose concentration	17.73 g L^{-1}	26.21 g L^{-1}
Initial nitrate concentration	1.2 g L^{-1}	1.37 g L^{-1}
Initial phosphate concentration	107.2 mg L^{-1}	149.3 mg L^{-1}
Model predicted response	2.11 day^{-1}	8.01 g L^{-1}
Experimental response	2.115 day^{-1}	7.81 g L^{-1}

Table 4.5 Comparison of kinetic parameters of FC2 grown in optimal media compositions for maximization of specific growth rate and biomass titer

Parameter	**Optimal media for specific growth rate**	**Optimal media for biomass titer**
Specific growth rate (h^{-1})	0.12	0.112
Biomass titer (g L^{-1})	5.65	7.8
Neutral lipid content (% w/w, DCW)	48	44
Biomass productivity (g L^{-1} day^{-1})	2.27	2.45
Neutral lipid productivity (g L^{-1} day^{-1})	0.5	0.56

4.3.2. Effect of trace and micro elements on the growth of FC2

Organism was characterized in terms of its specific growth rate under varying concentrations of TME in optimized BG11 medium for M_μ (Table A6 in appendix A). The composition of trace elements and micro elements per liter of optimized BG11 medium was considered as one unit (U) of TME per liter. Specific growth rate of the organism remained unchanged when TME concentration in the BG11 medium was varied from 0.15 U L^{-1} to 1.5 U L^{-1} (Fig. 4.3 A). In comparison to control experiment, organism showed reduced specific growth rate at TME concentration higher than 1.5 U L^{-1} which may be due to inhibitory effect of TME on organism metabolism. Some metals such as copper act as toxic material at their higher concentrations which are component elements of TME (Barsanti and Gualtieri, 2014). The similar experiment carried out using BG11 medium optimized for M_X (Table A7 in appendix A), showed maximal cell density of ~7.85 g L^{-1} at supplementation of 1 U L^{-1} to 1.8 U L^{-1} TME (Fig. 4.3 B). The biomass titer was reduced when organism was grown in TME concentration lesser than 1 U L^{-1}. However, supplementation of 1.2 U L^{-1} TME exhibited both higher growth rate and biomass concentration. Microalgae *Cyanothece* sp. was also reported to consume some of the TME components completely to achieve 7 g L^{-1} biomass under mixotrophic growth condition (Alagesan et al., 2013).

Further, it was important to decide the amount of TME required for generation of one gram of biomass which in turn was used for designing of TME feeding strategy in fed-batch and continuous operation. To that end, a shake flask experiment was carried out with 1 U L^{-1} of TME along with intermittent feeding of nitrate, phosphate and glucose. Organism was able to maintain its maximum specific growth rate up to 77 h of fermentation resulting in biomass concentration of 5.17 g L^{-1} (Fig. 4.4 A and 4.4 B). This signifies that 1 unit of TME supports FC2 growth up to 5.17 g DCW with maximum

specific growth rate and hence, feeding of 1 U L^{-1} of TME can be carried out for every 5.17 g L^{-1} of biomass generation. Similar observation was reported for microalga *Chlorella protothecoides* where 2.67 g L^{-1} biomass could be generated from one U L^{-1} of TME (Xiong et al., 2008).

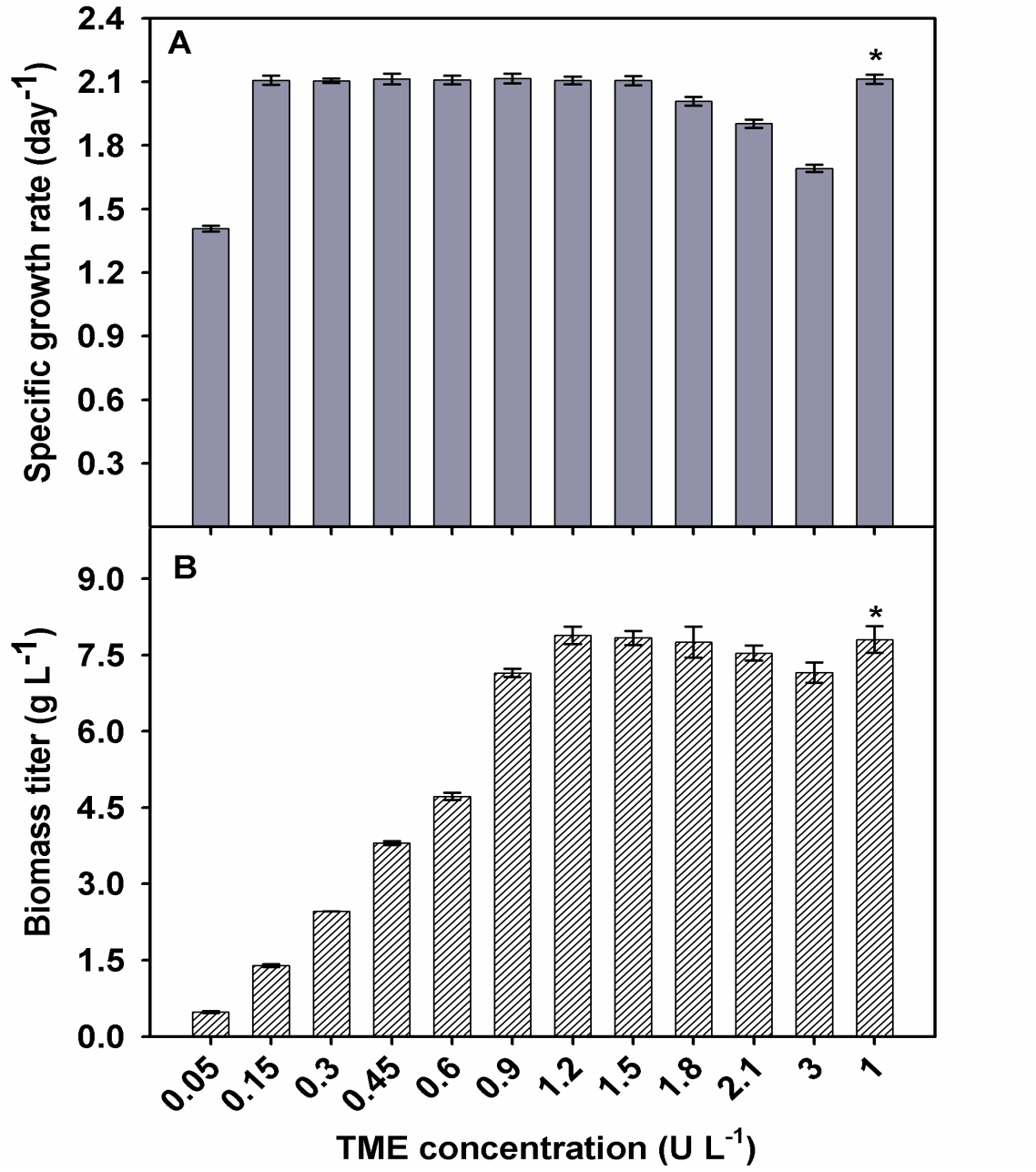

Fig. 4.3 Effect of various concentrations of trace and microelements (TME) on (A) specific growth rate of FC2 grown in optimized BG11 medium (for μ), and (B) growth of FC2 cultivated in BG11 medium optimized for biomass titer. Different TME concentration was achieved via supplementation of TME stock ranging from 0.05 to 3 units per liter of TME. One unit of TME corresponds to the same amount of TME in one liter of BG11 medium. Notation '*' represents the control experiment.

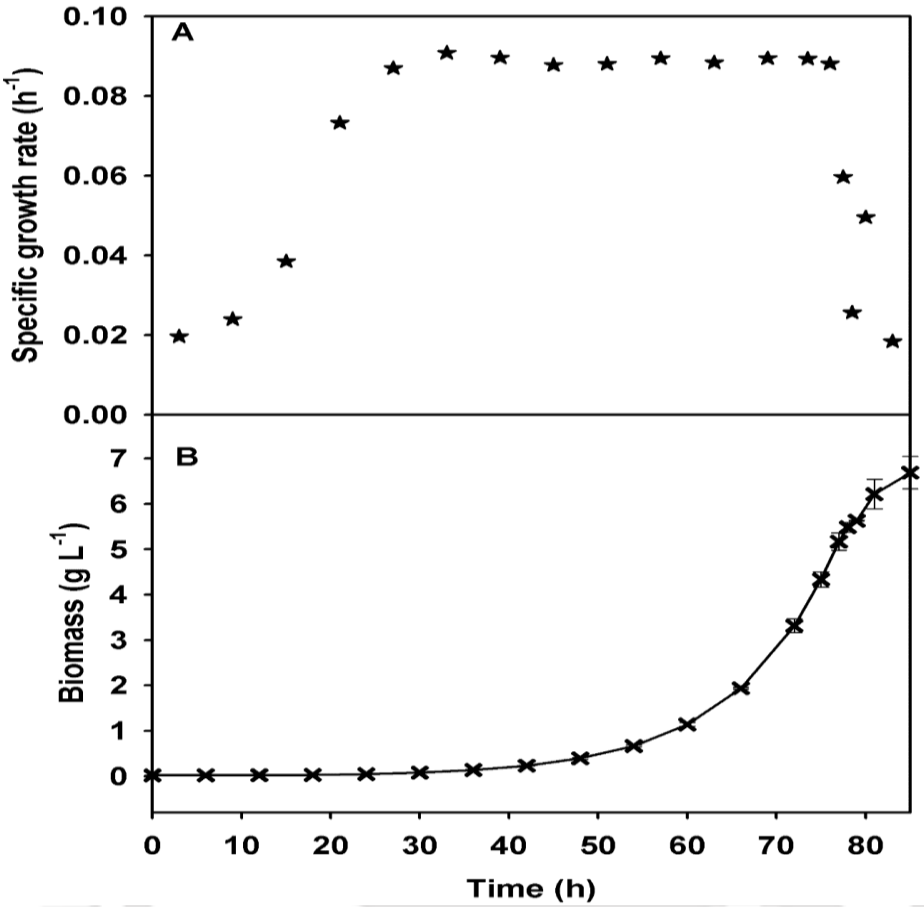

Fig. 4.4 Dynamic profile of (A) specific growth rate and (B) biomass titer of the organism grown in optimized BG11 medium with one unit of TME per liter. In this experiment, nitrate, phosphate and glucose was maintained via intermittent feeding.

4.3.3. Optimization of sodium acetate concentration for maximal lipid induction

The organism FC2 was evaluated under ten different concentration of sodium acetate as an inducer for intracellular neutral lipid. An increase in lipid content was observed with increase in sodium acetate concentration from 6 g L^{-1} and reached a maximum value of ~66% w/w, DCW at a sodium acetate concentration of 24 g L^{-1} (Fig. 4.5 A). Microalga *Chlorella sorokiniana* FC6 IITG was reported to accumulate maximum amount of neutral lipid at a sodium acetate concentration of 20 g L^{-1} (Kumar et al., 2014). Optimum concentration of sodium acetate showed greater potential to induce neutral lipid than nitrogen (~55%, w/w, DCW) or phosphate (~40%, w/w, DCW) starvation (Fig. 4.5 B). In case of phosphorous and/or nitrogen starvation based lipid induction, carbon flux from DNA, RNA, protein biosynthesis are mainly diverted to biosynthesis of neutral lipid

as it is nitrogen and phosphate free, energy rich metabolite (Rodolfi et al., 2009). The starvation in fact simultaneously creates stress on organism and results in enhanced utilization of maintenance energy with concomitant reduction in growth (Section 8.3.3). However, supplementation of sodium acetate in the medium directly increases carbon flux towards acetyl CoA node and in turn, up-regulate the neutral lipid biosynthesis without creating any stress to the organism (Qiao and Wang, 2009). This may be the reason for increased lipid content in sodium acetate supplementation rather than nitrate and phosphate starvations. Hence, usage of acetate for lipid induction is advantageous as it induces higher lipid, bypasses the second stage cultivation and less likely to cause water pollution as it can be completely consumed by the organism before termination of batch.

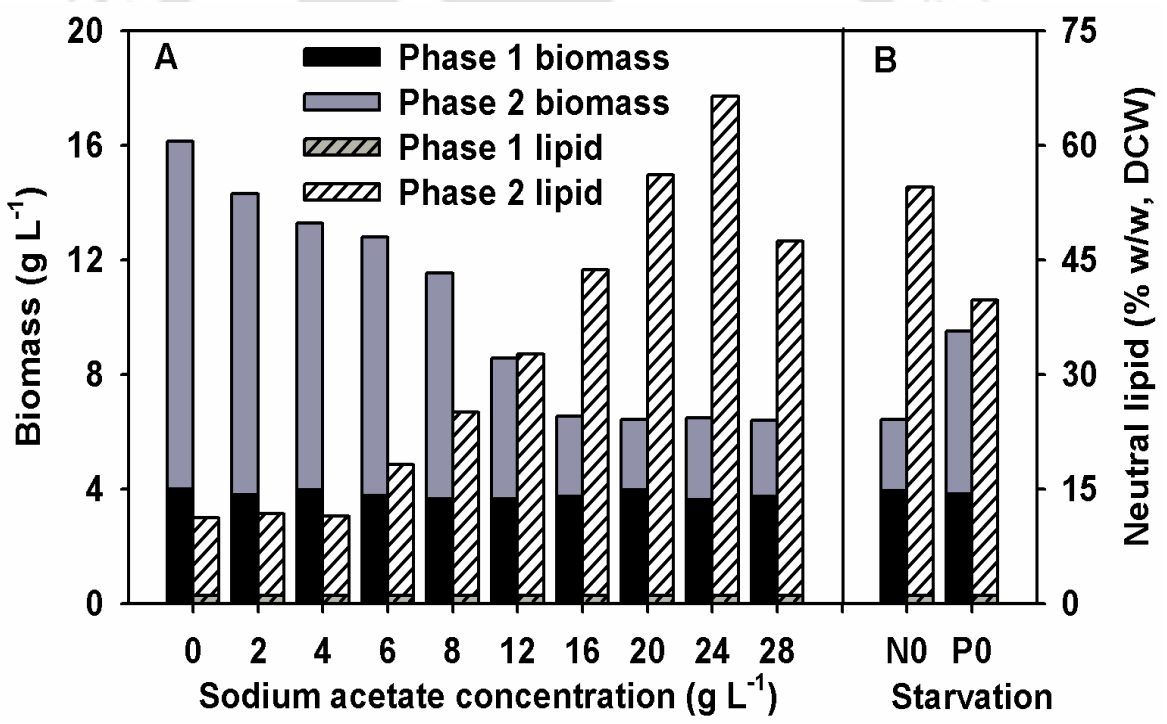

Fig. 4.5 Characterization of the strain FC2 in terms of growth and neutral lipid accumulation under different nutritional conditions: (A) effect of sodium acetate concentration on lipid accumulation in the strain under nutrient sufficient condition achieved with intermittent feeding of limiting nutrients. The organism was grown in the bioreactor (phase 1) in order to achieve significant amount of cells, followed by harvesting and distribution of the cells into shake flasks (phase 2) containing varied concentration of sodium acetate, (B) Evaluation of lipid production potential of the strain FC2 under nitrate (N0) and phosphate (P0) starvation used as control for comparing with aforesaid results. Except desired nutritional stress, concentrations of all other nutrients were maintained via intermittent feeding.

4.4. Conclusions

In the present work, BG11 media components and lipid inducers were optimized for growth and neutral lipid production in the microalga. Two optimal media compositions were obtained for maximization of specific growth rate and biomass titer individually. While maximal specific growth rate is necessary for operation of fed-batch and continuous systems to get high productivity, as much as possible higher biomass need to be attained in batch cultivation. BG11 medium optimized for maximization of specific growth rate is broadly referred as optimized BG11 medium in remaining portion of thesis and medium optimized for maximization of biomass titer is clearly mentioned wherever it is being used. Further yield coefficient of TME was determined in order to design feeding recipe of TME in fed-batch and continuous operations. Similarly sodium acetate concentration was optimized to enhance the lipid accumulation in biomass. This is advantageous due to enhanced induction of neutral lipid, bypass of second stage cultivation and lesser prone to water pollution as being consumed by the organism. These strategies for specific growth rate and lipid induction opens up the scope for development of lipid rich-high cell density cultivation or improved lipid productivity.

4.5. References

1. Alagesan S., Gaudana S.B., Krishnakumar S., Wangikar P.P., 2013. Model based optimization of high cell density cultivation of nitrogen-fixing cyanobacteria. Bioresource Technology. 148, 228–233.
2. Barsanti L., Gualtieri P., 2014. Algae: anatomy, biochemistry, and biotechnology. CRC Press, Taylor & Francis, Boca Raton, Florida.
3. Bezerra M.A., Santelli R.E., Oliveira E.P., Villar L.S., Escaleira L.A., 2008. Response surface methodology (RSM) as a tool for optimization in analytical chemistry. Talanta. 76, 965–977.

4. Cheng K.-C., Ren M., Ogden K.L., 2013. Statistical optimization of culture media for growth and lipid production of *Chlorella protothecoides* UTEX 250. Bioresource Technology. 128, 44–48.

5. Gong X., Chen F., 1997. Optimization of culture medium for growth of *Haematococcus pluvialis.* Journal of Applied Phycology. 9, 437–444.

6. Kalil S.J., Maugeri F., Rodrigues M.I., 2000. Response surface analysis and simulation as a tool for bioprocess design and optimization. Process Biochemistry. 35, 539–550.

7. Kumar V., Muthuraj M., Palabhanvi B., Das D., 2016. Synchronized growth and neutral lipid accumulation in *Chlorella sorokiniana* FC6 IITG under continuous mode of operation. Bioresource Technology. 200, 770–779.

8. Kumar V., Muthuraj M., Palabhanvi B., Ghoshal A.K., Das D., 2014. High cell density lipid rich cultivation of a novel microalgal isolate *Chlorella sorokiniana* FC6 IITG in a single-stage fed-batch mode under mixotrophic condition. Bioresource Technology. 170, 115–124.

9. Li T., Zheng Y., Yu L., Chen S., 2013. High productivity cultivation of a heat-resistant microalga *Chlorella sorokiniana* for biofuel production. Bioresource Technology. 131, 60–67.

10. Li Z., Yuan H., Yang J., Li B., 2011. Optimization of the biomass production of oil algae *Chlorella minutissima* UTEX2341. Bioresource Technology. 102, 9128–9134.

11. Muthuraj M., Chandra N., Palabhanvi B., Kumar V., Das D., 2014. Process Engineering for High-Cell-Density Cultivation of Lipid Rich Microalgal Biomass of *Chlorella* sp. FC2 IITG. BioEnergy Research. 8, 726–739.

12. Pancha I., Chokshi K., Maurya R., Trivedi K., Patidar S.K., Ghosh A., Mishra S., 2015. Salinity induced oxidative stress enhanced biofuel production potential of microalgae *Scenedesmus* sp. CCNM 1077. Bioresource Technology. 189, 341–348.

13. Qiao H., Wang G., 2009. Effect of carbon source on growth and lipid accumulation in *Chlorella sorokiniana* GXNN01. Chinese Journal of Oceanology and Limnology. 27, 762–768.

14. Rippka R., Deruelles J., Waterbury J.B., Herdman M., Stanier R.Y., 1979. Generic assignments, strain histories and properties of pure cultures of *cyanobacteria*. Journal of General Microbiology. 111, 1-61.

15. Rodolfi L., Chini Zittelli G., Bassi N., Padovani G., Biondi N., Bonini G., Tredici M.R., 2009. Microalgae for oil: Strain selection, induction of lipid synthesis and outdoor mass cultivation in a low-cost photobioreactor. Biotechnology and Bioengineering. 102, 100–112.

16. Stanbury P.F., Whitaker A., Hall S.J., 2003. Principles of fermentation technology. 2nd ed. Butterworth-Heinemann, Oxford, UK.

17. Xiong W., Li X., Xiang J., Wu Q., 2008. High-density fermentation of microalga *Chlorella protothecoides* in bioreactor for microbio-diesel production. Applied Microbiology and Biotechnology. 78, 29–36.

CHAPTER 5

Development of multi-nutrient mechanistic model for heterotrophic growth kinetics of FC2

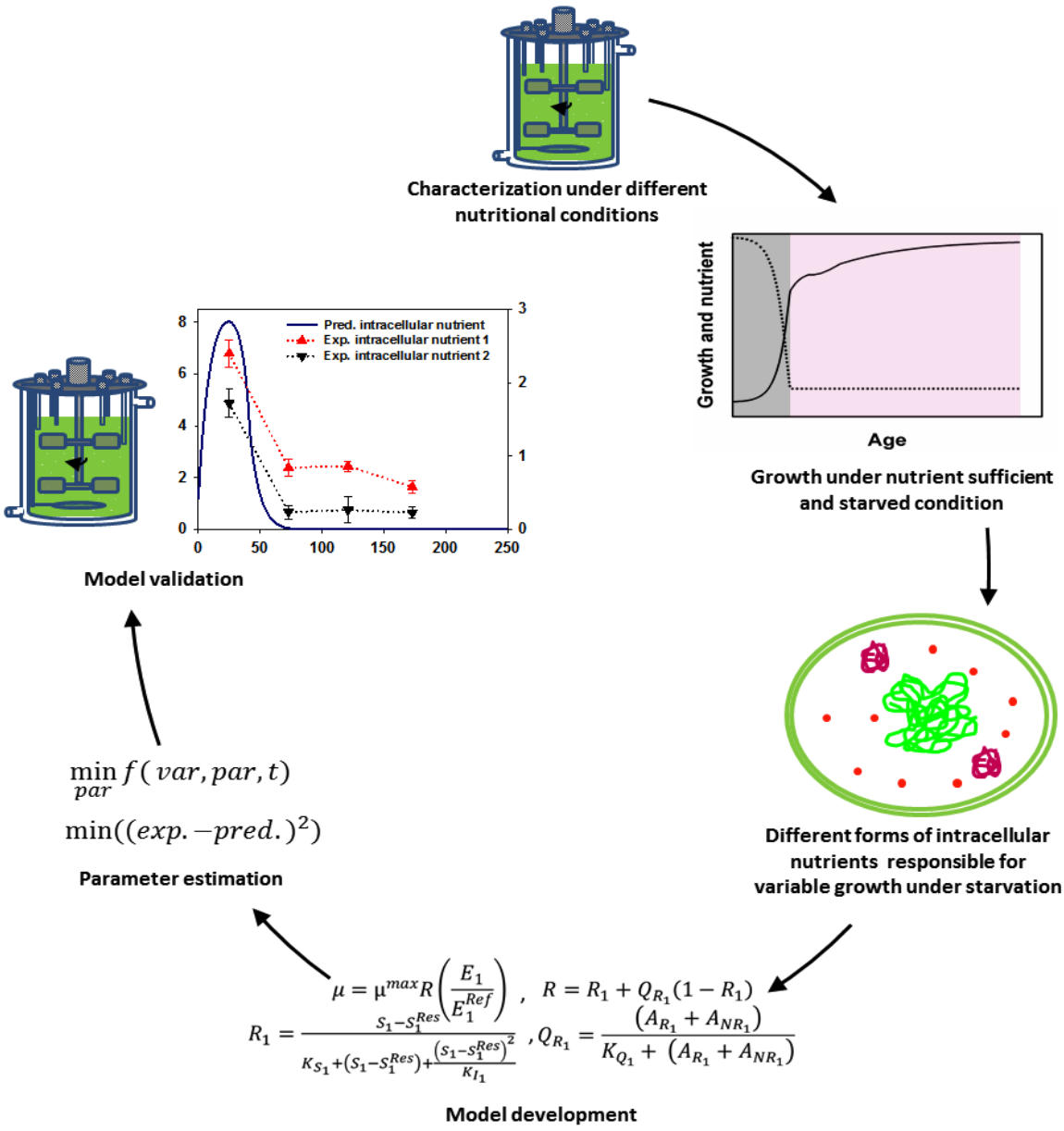

Development of multi-nutrient mechanistic model to predict heterotrophic growth kinetics of *Chlorella* sp. FC2 IITG under both nutrient sufficient and nutrient depleted conditions

5.1. Background and motivation

Lower biomass titer/productivity, understanding of growth kinetics and process control are some of the existing bottlenecks in commercial scale production of biodiesel from microalgae (Rodolfi et al., 2009; Shen et al., 2010; Xiong et al., 2008). Interestingly unlike other microbial systems, microalgae are known to continue to their growth even after exhaustion of nutrients from the medium by using stored intracellular nutrients (Bernard, 2011). For instance, *Chlorella* sp. FC2 IITG has been shown to grow substantially under phosphate and nitrate starvation (Muthuraj et al., 2014). Therefore, understanding microalgal growth kinetics under varied nutritional conditions remains a challenge towards development of a bioprocess for microalgal products. This can be achieved by combining wet lab experiments and *in silico* modeling. To that end, kinetic models have been used as a tool for understanding microbial and animal systems at metabolic level, process optimization, biochemical phenomena, monitoring and control of bioreactors (Béchet et al., 2013; Kumar et al., 2009; Pandey, 2003). Biological systems, involving growing cells are complex in nature and this is even true for microalgal systems which can decouple its growth from nutrient uptake under nutrient deplete conditions (Bernard, 2011).

The classical Monod model is based on the theory of constant yield where substrate utilization rate varies proportionally with organism growth (Lemesle and Mailleret, 2008) and hence, found to be inadequate to explain microalgal growth kinetics. While constant yield assumption may be valid for carbon, the main fraction of algal biomass, the same may not be valid for other nutrients such as phosphate, nitrate and vitamins (Lemesle and Mailleret, 2008). An alternate approach consisting of variable yield and cell quota theory was employed to model growth of microalga *Monochrysis lutheri* under different concentration regimes of vitamin B_{12} (Droop, 1975, 1968). Nutrient quota

is a time dependent variable defined as the amount of total intracellular substrate present in unit amount of biomass. The model relies on the assumption that the growth of the organism depends on nutrient quota which is linked to the specific substrate uptake rate which in turn, depends on the substrate concentration in the medium (Droop, 1968). Therefore, unlike Monod model, organism growth will continue even after exhaustion of key nutrients in the medium till intracellular nutrient quota reaches its critical value. There are literatures which have reported kinetic models for algal growth with proper re-interpretation of Droop's cell quota model (Lemesle and Mailleret, 2008). Further, a model on phosphate transport and assimilation towards microalgal growth was reported which deals with segregation of intracellular phosphate and their utilizations during growth (John and Flynn, 2000). However, development of multi-nutrient mechanistic model taking into account prioritized utilization of different biological forms of intracellular nutrients is sparse in the literature. Existing kinetic models suffer from various bottlenecks which limit their application as a tool for process optimization and control. For instance, Droop's cell quota model may not predict utilization profile of non-limiting substrate accurately (Zonneveld, 1996). Even though Droop's model was demonstrated for microalgal cultivation in batch and continuous mode (Droop, 1975, 1968), it may be difficult for the model to predict growth and substrate utilization kinetics in fed-batch mode of operation due to use of different formats of rate equations for limiting and non-limiting substrates. In the fed batch cultivation, limiting and non-limiting substrates keep on inter changing upon feeding of nutrients. Therefore, there is a need to develop a *mechanistic* model consisting single formatted rate equations for limiting and non-limiting substrate utilization, which can be used as a tool for forecasting microalgal growth kinetics under different nutrient conditions.

The present study was focused on development of multi-nutrient mechanistic model for growth on preferential utilization of extracellular nutrients and different forms of intracellular stored nutrients under heterotrophic cultivation of microalga FC2. The model is based on Monod kinetics with varying yield concept which segregates intracellular nutrient quota into different biological forms and captures their preferential utilizations. The intracellular nutrient is segregated into three different forms: *structural form of nutrient* (SFN), stored *readily utilizable nutrient* (RUN) and stored *non-readily utilizable nutrient* (Non-RUN). The basic premise of our model is that the microorganism growth will take place even after exhaustion of the extracellular nutrients (ECN) by sequential utilization of RUN and Non-RUN. The structural form of nutrient (SFN) is the remaining fraction after exhaustion of both RUN and Non-RUN which is required to maintain integrity of cell structure.

5.2. Material and methods

5.2.1. Growth condition

Inoculum was prepared in optimized BG11 media as explained in section 3.2.1. Active log phase culture (1% of working volume with cell density of 3 g L^{-1}) was used as inoculum for all the experiments of present study. The experiments were carried out in a 3.0 L automated bioreactor (Bio Console ADI 1025, Applikon Biotechnology, Holland) with 1.5 L working volume at 28ºC, 400 rpm and aeration of 1 vvm. The dark heterotrophic condition was maintained by covering black colour paper over reactor jacket to avoid the exposure of cells to light source.

The organism was grown under four different nutritional conditions to characterize its response in terms of growth and substrate utilization pattern in the bioreactor. In the first step, data obtained from three different nutritional conditions were used for the development of the multi-nutrient mechanistic model. These batches were different in

terms of type of nutrient limitations and varied initial concentration of limiting nutrient while keeping all other compositions same as optimized BG11 medium: (i) phosphate limited condition with higher initial phosphate concentration of 107 mg L^{-1} (optimized BG11 medium); (ii) nitrate limited condition with lower initial nitrate concentration of 50 mg L^{-1}; and (iii) phosphate limited condition with lower initial phosphate concentration of 5 mg L^{-1}. In the next step, predictive ability of the model was validated by growing the organism under nitrate limited condition with higher initial nitrate concentration of 170 mg L^{-1}. Sampling was done at regular time interval to monitor growth and nutrient utilization profiles. All the experiments were conducted in triplicates and measurements were expressed in terms of mean values ± standard error.

5.2.2. Analysis of growth, biomass composition and substrates utilization

Estimation of growth and substrate utilization profile were carried out at every sampling time point. Biochemical analysis of intracellular nitrogen containing compounds and phosphorus containing compounds of biomass were performed at four dynamic sampling points. The collected sample was centrifuged at 8000 × g for 10 minutes at 4°C and the supernatant was collected for extracellular substrates analyses (glucose, nitrate and phosphate). The pellet was utilized for measurement of biomass, intracellular nitrogen containing compounds and phosphorous containing compounds. Organism growth was measured by taking optical density of cells as described in section 3.2.5.1. Glucose utilization profile was determined by protocol mentioned in section 3.2.5.3. The phosphate content of the sample was analyzed by method explained in section 3.2.5.4.

5.2.2.1. Analysis of nitrate utilization by HPLC

Nitrate concentration was estimated using high pressure liquid chromatograph (Agilent 1220 Infiniti HPLC, USA) equipped with photo diode array detector (Kumar et al., 2014). The cell free supernatant was injected into a (4.6 x 150 mm, 5µm) Zorbax

Eclipse XDB-C18 column (Agilent, USA) and the detection was at λ = 220 nm. Ammonium dihydrogen phosphate (0.01 M) in 30% (v/v) methanol was used as the mobile phase at a flow rate of 0.8 mL min^{-1}. The standard correlation curve was developed for concentration of nitrate and peak area of chromatogram with use of sodium nitrate as standard (Fig. 5.1 A). From the correlation, 10^8 mAU absorbance was found to depict 0.11 g L^{-1} nitrate.

5.2.2.2. Biochemical analysis of intracellular protein formation

Determination of intracellular protein content was carried out in two-steps; alkali hydrolysis at 100° C followed by quantification with Lowry method (Pruvost et al., 2011). Cell pellets were subjected to alkaline hydrolysis with addition of 2 N NaOH for 15 minutes at boiling water bath (100°C) and then solution pH was reduced to 7.0 by adding 1.6 N HCl. The solution containing intracellular protein was estimated using Lowry's method (Lowry et al., 1951) at 660 nm. The calibration equation was developed by using bovine serum albumin as a standard where one absorbance (A660) corresponds to 2.32 g L^{-1} of protein concentration (Fig. 5.1 B). Quantified intracellular protein was expressed in terms of nitrate quantity (mg nitrate g^{-1} DCW) on basis of equimolar nitrogen content.

5.2.2.3. Estimation of intracellular chlorophyll content

The chlorophyll content was extracted from biomass by incubating the pellet in 100% methanol at 45°C for 30 minutes (Pruvost et al., 2011). Absorbance of extracted chlorophyll measured at 750 nm, 665 nm and 652 nm to quantify chlorophyll a and chlorophyll b with use of equations 5.1 and 5.2 (Ritchie, 2006).

$$Chlorophyll\ a\ (mg\ L^{-1}) = 16.52 \cdot (A_{665} - A_{750}) - 8.09 \cdot (A_{652} - A_{750}) \quad (5.1)$$

$$Chlorophyll\ b\ (mg\ L^{-1}) = 27.44 \cdot (A_{652} - A_{750}) - 12.17 \cdot (A_{665} - A_{750}) \quad (5.2)$$

The intracellular chlorophyll content was expressed in terms of nitrate quantity (mg nitrate g^{-1} DCW).

5.2.2.4. Estimation of intracellular amino acid and free nitrate concentration

Clean pellet (10 mg DCW equivalent) was re-suspended in 5 mL of deionized water and hydrolyzed by autoclaving for 20 minutes at 121°C (Simmon et al., 2004). The lysate was separated from cell debris by centrifugation and filtered with 0.2 µm pore size membrane. The quantity of amino acid in the lysate was determined using ninhydrin based assay method (Nigam and Ayyagari, 2007). The mixture of 2 mL lysate and 2 mL Ninhydrin reagent was allowed to carry out reaction at boiling water bath for 15 min and 3 mL 50% ethanol was added to mixture before measuring the absorbance at 570 nm. The correlation (one O.D. = 0.021 g L^{-1} glycine) between absorbance and concentration of amino acid was developed with use of glycine as standard (Fig. 5.1 C). The intracellular amino acid content was expressed in terms of nitrate quantity (mg nitrate g^{-1} DCW).

The filtered lysate was also used to quantify intracellular free nitrate amount by HPLC method as explained in the section 5.2.2.1.

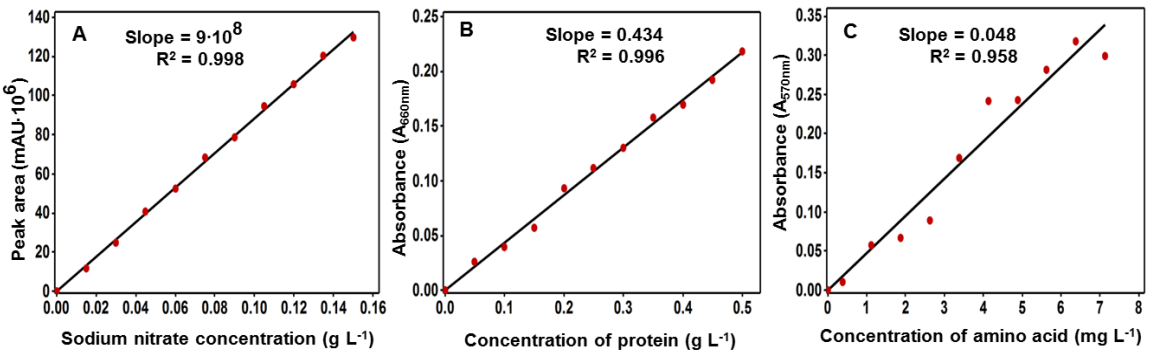

Fig. 5.1 Graphical representation of correlation between concentration of substrates and their respective absorbance for the estimation of (A) sodium nitrate in HPLC (B) protein in spectrophotometer and (C) amino acid in spectrophotometer

5.2.2.5. Extraction of intracellular nucleic acids

The intracellular nucleic acid (RNA and DNA) was extracted from fresh wet algal biomass (3 mg DCW equivalent) by the method reported by Zachleder (1984). The algal cells were treated four times (50 min cycle) with 10 mL 0.2 N perchlroic acid (PCA) in 50% ethanol followed by de-lipidization and de-pigmentation by extraction in a mixture of

3: 1 (v/v) ethanol: ethyl ether. The pellet obtained was further hydrolyzed using 0.5 N PCA followed by incubation at 70°C for 2 hours. The contents were centrifuged to obtain the supernatant and the absorbance was measured at 260 nm and the nucleic acid concentration was determined using the following calibration equation 5.3.

$$NA\ (mg\ L^{-1}) = 45.5\ \times absorbance\ at\ 260nm \quad (5.3)$$

Where, NA represents the total nucleic acid concentration. The intracellular nucleic acid content was expressed in terms of both nitrate quantity (mg nitrate g^{-1} DCW) and phosphate quantity (mg phosphate g^{-1} DCW) as it contains both nitrogen and phosphorus.

5.2.2.6. Extraction of intracellular phosphorus containing compounds

The extraction of intracellular phosphate containing compounds was carried out from fresh wet algal biomass (25 mg DCW equivalent) by the Sicko-Goad and Jensen (1976) method. To the wet cells, 5 mL of 5% cold tri-chloro acetic acid (TCA) was added and incubated for 30 minutes at 4°C for extraction of acid soluble form of intracellular phosphate. Additional 5 mL of TCA was added and incubated for more 30 minutes. The contents were centrifuged at 12,000 × g at 4°C for 10 minutes and the supernatant (extract 1) was used for phosphate estimation.

Subsequently, phospholipid was extracted from residual biomass by addition of absolute ethanol followed by incubation for 30 minutes and then 5 mL of 3:1 mixture of ethanol-ethyl ether was added to the contents. The mixture was heated for 1 minute in a boiling water bath and then the supernatant (extract 2) was collected for phosphate analysis after 20 minutes incubation at room temperature.

The residual biomass was heated at 70°C for drying and then used for extraction of acid insoluble form of phosphate in the next step. 5 mL of 5% TCA was added twice to the dried biomass at 70°C, in a 15 minutes interval time followed by centrifugation to obtain the supernatant (extract 3) for total phosphate analysis. All three extracts were digested by

Menzel and Corwin (1965) potassium persulfate method and analyzed for total phosphate content of each extract using ascorbic acid method as explained in section 3.2.5.4. The free phosphate content from extract 1 was determined by ascorbic acid method before digestion. Major fraction of the acid soluble extract contains smaller chain length polyphosphates while acid insoluble extract consist higher chain length polyphosphate with polymerization grades of order 10 and 50 respectively (Krishnan et al., 1957). The intracellular phosphorus containing compounds were expressed in terms of phosphate quantity (mg phosphate g^{-1} DCW).

5.2.3. Model development

The conceptual representation of the model is shown in Fig. 5.2. It has been assumed that the microorganism grow primarily by utilizing extracellular substrates under nutrient replete condition. However, the strain continues to grow even under exhaustion of limiting nutrient(s) from the medium and the growth was supported by the stored intracellular nutrient(s). Further, total intracellular nutrient was assumed to exist in three different forms (Fig. 5.2 A): (i) structural form of nutrient, SFN (structural protein, DNA, rRNA, etc.); (ii) readily utilizable nutrient, RUN (inorganic phosphate, nitrate, ammonia etc.) and (iii) non-readily utilizable nutrient, Non-RUN (some protein, mRNA, polyphosphate bodies etc.) (Dortch et al., 1984; John and Flynn, 2000). RUN and Non-RUN were considered as intracellular stored nutrients. The utilization of Non-RUN results in slower growth rate attributed to the delayed degradation of the complex polymeric substances into simpler molecules followed by its utilization for growth. RUN is utilized directly by the organism without any lag leading to moderate growth rates. Hence, the growth of the microorganism was assumed to take place in three sequential phases (Fig. 5.2 B): (i) first phase of the growth takes place through utilization of the extracellular nutrients (ECN); (ii) second phase of the growth is supported by RUN after exhaustion of

the limiting ECN; and (iii) the final phase of the growth is based on utilization of Non-RUN. The remaining amount of intracellular nutrients after the complete consumption of RUN and Non-RUN was termed as structural form of nutrient which is the minimum required nutrient for maintenance of cell structure integrity. The complete consumption of intracellular stored nutrients will result in the cessation of growth. Thus, first phase corresponds to the growth under nutrient sufficient condition; the second and third phase corresponds to growth under nutrient starvation.

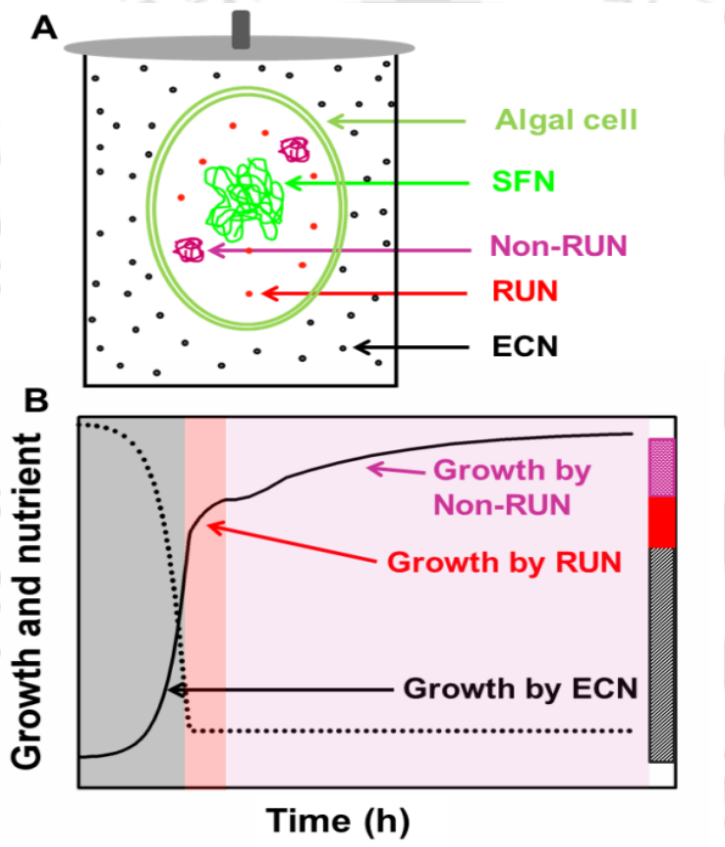

Fig. 5.2 Schematic representation of the proposed kinetic model. (A) Different available forms of extracellular and intracellular nutrients supporting microalgal growth: SFN, structural form of intracellular nutrient; RUN, intracellular stored readily utilizable nutrient; Non-RUN, intracellular stored non-readily utilizable nutrient and ECN, extracellular nutrient; (B) Representation of different growth phases supported by utilization of different form of nutrients. The microalgal growth assumed to take place in three sequential phases: phase 1 - growth through utilization of ECN, phase 2 - growth supported by RUN after exhaustion of the limiting ECN and phase 3 - growth based on the utilization of Non-RUN after exhaustion of RUN. SFN is the remaining fraction of intracellular nutrients after complete utilization of RUN and Non-RUN, necessary for maintenance of cellular integrity

5.2.4. Model equations

Earlier, the strain FC2 has shown its growth even after exhaustion of extracellular phosphate (Section 3.3.2). Therefore in the present study, the experiments were designed to achieve different nutritional conditions in terms of nitrate or phosphate limitations by adjusting their initial concentration in the medium. Hence, the proposed model is expected to predict growth kinetics and uncover the underlying mechanism supporting the microalgal growth under nitrate or phosphate limitations. The growth of the strain was modelled taking into account combinatorial effect of following two substrate combinations: (i) extracellular limiting nutrient and extracellular non-limiting nutrient and (ii) extracellular non-limiting nutrient and intracellular stored nutrient (Equation 5.4 and 5.5). Note that the concentration of glucose was maintained relatively higher than the other nutrients present in the medium and hence, was never consumed completely till the end of the batch. The carbon source glucose was therefore considered as non-limiting nutrient and the growth on glucose was assumed to be based only on the extracellular concentration. The initial lag phase of growth was attributed to the induction of enzymes (E_1) for nutrients uptake and assimilation, which was represented in the ratio with theoretical maximum induction of enzyme $\left(E_1^{Ref}\right)$ at that condition (Bapat et al., 2006). The enzymes E_2 and E_3 were considered as hydrolytic enzymes for degradation of Non-RUN of nitrate and phosphate respectively. Further, growth on extracellular nutrients was modeled using Monod kinetics (Equation 5.6 A, 5.6 B and 5.6 C) with incorporation of substrate inhibition (K_{I_i}). Growth under nutrient exhaustion condition (Equation 5.7 A and 5.7 B) was based on available RUN $\left(A_{R_i}\right)$ and Non-RUN $\left(A_{NR_i}\right)$ form of nitrate or phosphate. Under this condition intracellular nutrient quota (Q_i) decreases with the consumption of RUN and Non-RUN, hence A_{R_i} and A_{NR_i} were represented in terms of Q_i in the model. Organism was assumed to grow until intracellular nutrient quota (Q_i) reaches

the threshold values T_{R_i} and further T_{NR_i} by utilizing RUN and Non-RUN respectively (Equation 5.8 A, 5.8 B, 5.9 A, 5.9 B, 5.10 A and 5.10 B). The threshold intracellular nutrient quotas T_{R_i} and T_{NR_i} represent complete utilization of RUN and Non-RUN respectively.

$$\mu = \mu^{max} R \left(\frac{E_1}{E_1^{Ref}}\right) \tag{5.4}$$

$$R = R_1\left[R_2 + Q_{R_2}(R_2^m - R_2)/R_2^m\right]\left[R_3 + Q_{R_3}(R_3^m - R_3)/R_3^m\right] \tag{5.5}$$

$$R_1 = \frac{S_1 - S_1^{Res}}{K_{S_1} + (S_1 - S_1^{Res}) + \frac{(S_1 - S_1^{Res})^2}{K_{I_1}}} \tag{5.6 A}$$

$$R_2 = \frac{S_2 - S_2^{Res}}{K_{S_2} + (S_2 - S_2^{Res}) + \frac{(S_2 - S_2^{Res})^2}{K_{I_2}}} \tag{5.6 B}$$

$$R_3 = \frac{S_3 - S_3^{Res}}{K_{S_3} + (S_3 - S_3^{Res}) + \frac{(S_3 - S_3^{Res})^2}{K_{I_3}}} \tag{5.6 C}$$

$$Q_{R_2} = \frac{(A_{R_2} + A_{NR_2})}{K_{Q_2} + (A_{R_2} + A_{NR_2})} \tag{5.7 A}$$

$$Q_{R_3} = \frac{(A_{R_3} + A_{NR_3})}{K_{Q_3} + (A_{R_3} + A_{NR_3})} \tag{5.7 B}$$

$$A_{R_2} = Q_2 - T_{R_2} \tag{5.8 A}$$

$$A_{R_3} = Q_3 - T_{R_3} \tag{5.8 B}$$

$$A_{NR_2} = (T_{R_2} - T_{NR_2})\left(\frac{E_2}{E_2^{Ref}}\right) \tag{5.9 A}$$

$$A_{NR_3} = (T_{R_3} - T_{NR_3})\left(\frac{E_3}{E_3^{Ref}}\right) \tag{5.9 B}$$

$$Q_2 = \frac{S_2^0 - S_2 + Q_2^0 X^0}{X} \tag{5.10 A}$$

$$Q_3 = \frac{S_3^0 - S_3 + Q_3^0 X^0}{X} \tag{5.10 B}$$

5.2.4.1. Mass balance equations

The microalgal growth was assumed to follow first order kinetics and accordingly formation of biomass (X) was represented by Equation 5.11. Growth dependent utilization of substrates was considered with variable yield coefficients $(Y_{S_i/X})$ until the exhaustion of extracellular substrates (Equation 5.12, 5.13 and 5.14). Maintenance coefficient with a constraint $(R_2 > 0)$ was incorporated in the differential equation of glucose (Equation 5.12) based on observed experimental evidence for higher consumption rate of glucose in presence of extracellular nitrate. In the present study, while nitrate utilization was found to be independent, phosphate uptake was dependent on availability of extracellular nitrate. Therefore, phosphate utilization was subjected to an additional constraint $R_2R_3 > 0$ (Equation 5.14). The inducible enzyme E_1 (Equation 5.15) was assumed to be synthesized as a component of biomass with net rate of synthesis dependent on the nutrient concentration in medium and enzyme degradation constant (β_1). The rate of synthesis of inducible enzymes E_2 and E_3 was dependent on available Non-RUN for nitrate and phosphate in the cell respectively (Equation 5.16 and 5.17).

$$\frac{dX}{dt} = \mu X \tag{5.11}$$

$$\frac{dS_1}{dt} = \begin{cases} -\mu X Y_{S_1/X} - m_s X, & R_2 > 0 \\ -\mu X Y_{S_1/X} \end{cases} \tag{5.12}$$

$$\frac{dS_2}{dt} = \begin{cases} -\mu X Y_{S_2/X}, & R_2 > 0 \\ 0 \end{cases} \tag{5.13}$$

$$\frac{dS_3}{dt} = \begin{cases} -\mu X Y_{S_3/X}, & R_2R_3 > 0 \\ 0 \end{cases} \tag{5.14}$$

$$\frac{d\left(\frac{E_1}{E_1^{Ref}}\right)}{dt} = (\mu^{max}R + \beta_1) - (\mu^{max}R + \beta_1)\left(\frac{E_1}{E_1^{Ref}}\right) \tag{5.15}$$

$$\frac{d\left(\frac{E_2}{E_2^{Ref}}\right)}{dt} = \begin{cases} 0, & Q_2 > T_{R_2} \\ \left((T_{R_2} - Q_2)\mu^{max} + \beta_2\right) - \left((T_{R_2} - T_{NR_2})\mu^{max} + \beta_2\right)\left(\frac{E_2}{E_2^{Ref}}\right) \end{cases} \tag{5.16}$$

$$\frac{d\left(\frac{E_3}{E_3^{Ref}}\right)}{dt} = \begin{cases} 0, & Q_3 > T_{R_3} \\ \left((T_{R_3} - Q_3)\mu^{max} + \beta_3\right) - \left((T_{R_3} - T_{NR_3})\mu^{max} + \beta_3\right)\left(\frac{E_3}{E_3^{Ref}}\right) \end{cases} \quad (5.17)$$

5.2.4.2. Variability in yield coefficients

Owing to their metabolic flexibility, microalgae exhibit variability in nutrient yield coefficients ($Y_{S_i/X}$) with dynamic change in extracellular nutrient concentrations (Lemesle and Mailleret, 2008). In the present model, overall yield coefficient ($Y_{S_i/X}$) was segregated into two parts i.e. variable fraction and non-variable fraction, hence changes in $Y_{S_i/X}$ were modeled by combining variable fraction and non-variable fraction. In case of nitrate and phosphate, the non-variable fraction of yield coefficient corresponds to minimum yield coefficient $\left(Y_{S_i/X}^{min}\right)$ which is achieved when extracellular nutrient concentration tends to zero. Variable fraction of yield coefficient is dependent on extracellular concentration of nitrate and phosphate which changes over the time of cultivation. Therefore, the variable fraction of yield coefficient was modeled in the form of Michaelis Menten kinetics and expressed as a function of extracellular substrate concentration (Equation 5.19 and 5.20). In case of glucose, its yield coefficient was assumed to vary inversely with those of nitrate and phosphate to balance total contribution in the biomass (Eq. 5.18). The threshold values of intracellular nitrate and phosphate quotas (T_{R_2}, T_{NR_2} and T_{R_3}, T_{NR_3}) were determined based on initial yield coefficients $\left(Y_{S_i/X}^{0}\right)$ and maximum nutrient storing capacity of cell $\left(K_{T_{Ri}}, K_{T_{NRi}}\right)$ as given in Equation 5.21 A, 5.21 B, 5.22 A and 5.22 B.

$$Y_{S_1/X} = Y_{S_1/X}^{min} + Y_{S_1/X}^{var}\left(\frac{Y_{S_2/X}^{min} + Y_{S_2/X}^{var} - Y_{S_2/X}}{Y_{S_2/X}^{var}}\right)\left(\frac{Y_{S_3/X}^{min} + Y_{S_3/X}^{var} - Y_{S_3/X}}{Y_{S_3/X}^{var}}\right) \quad (5.18)$$

$$Y_{S_2/X} = Y_{S_2/X}^{min} + Y_{S_2/X}^{var}\left(\frac{S_2 - S_2^{Res}}{K_{Y_2} + (S_2 - S_2^{Res})}\right) \quad (5.19)$$

$$Y_{S_3/X} = Y_{S_3/X}^{min} + Y_{S_3/X}^{var}\left(\frac{S_2 - S_2^{Res}}{K_{Y_2} + (S_2 - S_2^{Res})}\right)\left(\frac{S_3 - S_3^{Res}}{K_{Y_3} + (S_3 - S_3^{Res})}\right), \quad (5.20)$$

$$T_{R_2} = Y_{S_2/X}^{0} - K_{T_{R2}} \quad (5.21\ A)$$

$$T_{R_3} = Y^0_{S_3/X} - K_{T_{R3}} \quad (5.21\ B)$$

$$T_{NR_2} = Y^0_{S_2/X} - \left(K_{T_{R2}} + K_{T_{NR2}}\right) \quad (5.22\ A)$$

$$T_{NR_3} = Y^0_{S_3/X} - \left(K_{T_{R3}} + K_{T_{NR3}}\right) \quad (5.22\ B)$$

These model equations were solved using ODE solver ode23s available in the MATLAB (Mathworks, Natick, MA) for the simulation of growth and substrate utilization profiles.

5.2.5. Estimation of model parameters

The model parameter values were determined by fitting simulated dynamic profiles of biomass, glucose, nitrate and phosphate with corresponding experimental data. This was carried out by constrained based linear optimization algorithm '*fmincon*' available in Matlab (Mathworks, Natick, MA, USA). The minimization of deviation between predicted and corresponding experimental values was used as objective function for this linear optimization problem. Even though linear optimization finds the local optima instead of global optimum, it can be used to avoid the drawbacks of global optimization algorithms such as complexity in solving problems and infeasibility of using multiple variables (Das et al., 2011). The regression analysis was performed through analysis of variance (ANOVA) approach to find degree of fit with experimental values in MINITAB (Version 16.1.1, Minitab Inc., USA).

5.3. Results and discussion

Three batch runs used for the model development differ in terms of type of nutrient limitation and initial concentration of limiting nutrient. The model parameters were estimated by fitting simulated profile of growth and substrate utilization with the corresponding experimental values. The model prediction was validated by growing the microorganism under nitrate limitation with initial nitrate concentration of 170 mg L^{-1}.

5.3.1. Model fit and model validation under phosphate and nitrate limited conditions

Growth of the strain FC2 was observed to continue even after exhaustion ($R_i = 0$) of limiting substrate phosphate (Fig. 5.3 and 5.4) or nitrate (Fig. 5.5) from the extracellular medium. This extended growth of the organism was supported by the intracellular stored nutrients under the condition of nutrient depletion (Droop, 1968). Interestingly, under phosphate limited condition with higher initial concentration of phosphate (Fig. 5.3), organism exhibited two-stage growth with first growth stage of 56 h followed by a distinct lag phase of 25 h and the second growth stage started at 81 h (Fig. 5.3). This two-stage growth profile is similar to the diauxic growth exhibited by many microorganisms under multiple carbon sources (Misi and Forster, 2001). As per the model assumptions (Fig. 5.2 B) while first stage of growth was supported by the easily usable form of nutrients which include extracellular nutrients, ECN (phase 1) and intracellular RUN (phase 2), the second stage of growth was achieved via utilization of intracellular Non-RUN (phase 3).

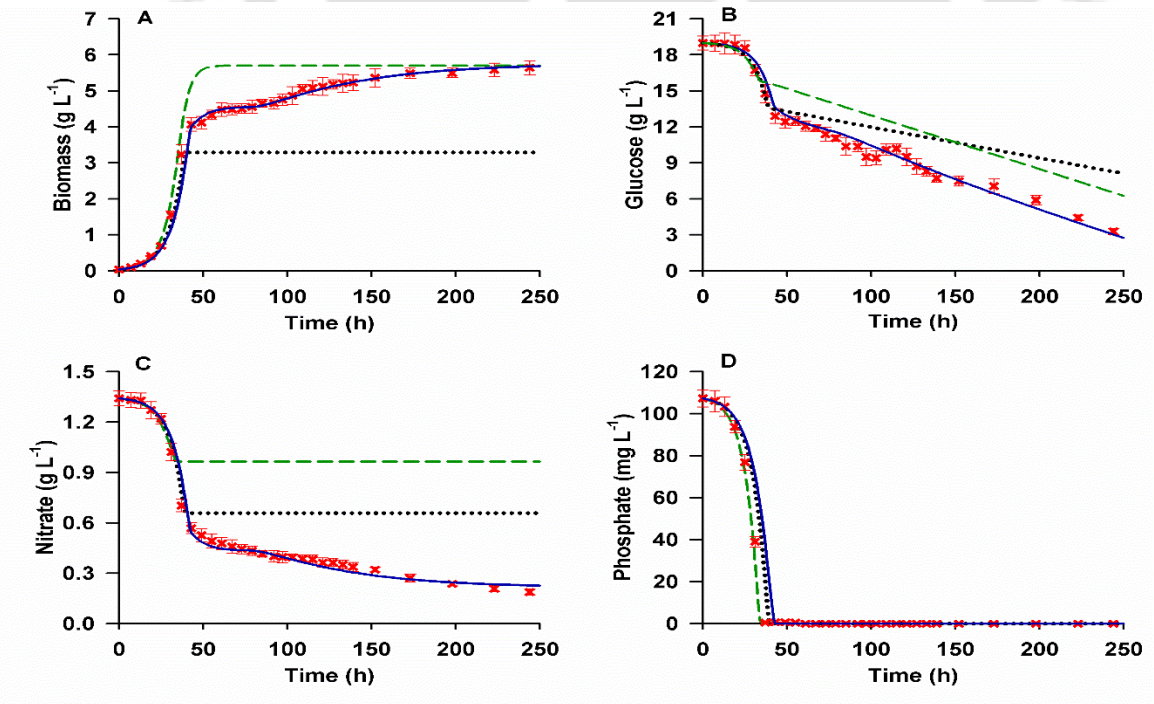

Fig. 5.3 Dynamic profiles for growth and substrate utilization of the strain *Chlorella* sp. FC2 IITG grown in a 3.0 L automated bioreactor under phosphate limited heterotrophic

condition with high initial concentration of phosphate (107 mg L^{-1}). Initial concentration of glucose and nitrate was 18 g L^{-1} and 1.3 g L^{-1} respectively. Predictions by the present model (—), Monod kinetics (⋯) and Droop's cell quota model (---) were compared with experimental data (×). (A) biomass synthesis, (B) glucose concentration, (C) nitrate concentration and (D) phosphate concentration

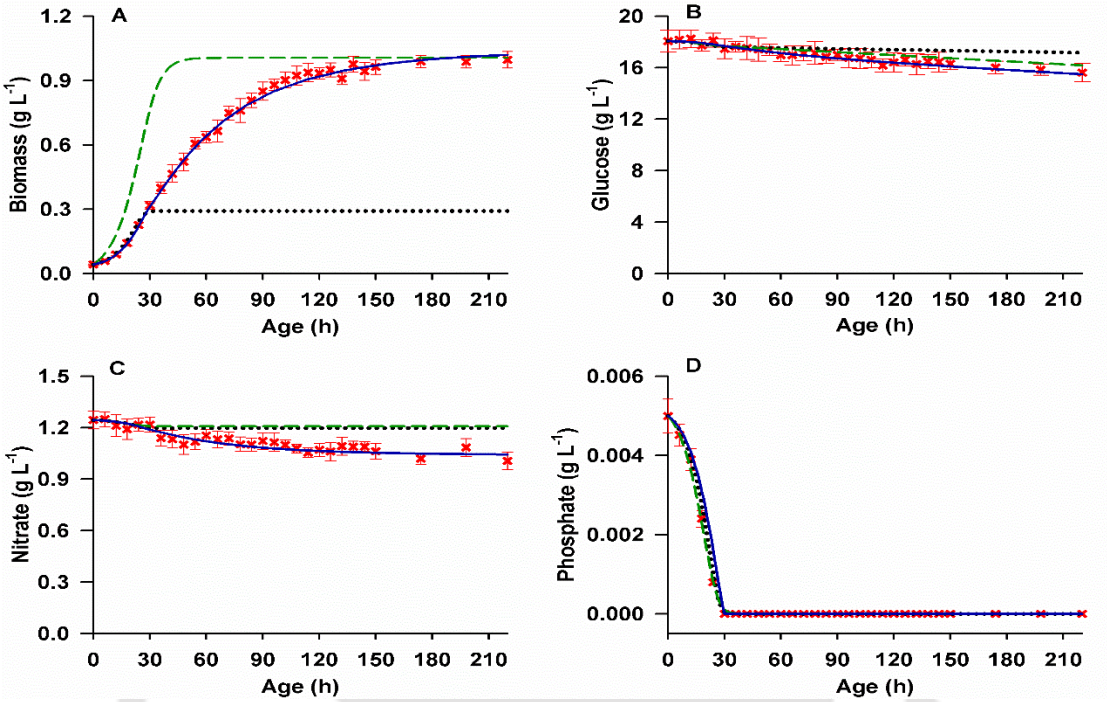

Fig. 5.4 Dynamic profiles for growth and substrate utilization of the strain grown under phosphate limited heterotrophic condition with very low initial phosphate concentration 5 mg L^{-1}. The other nutrients were same as that of the optimized BG11 media in both the batches. Predictions by proposed model (—), Monod kinetics (⋯) and Droop's cell quota model (---) were compared with experimental data (×). (A) biomass synthesis, (B) glucose concentration, (C) nitrate concentration and (D) phosphate concentration

In the present study, intracellular free phosphate, phospholipid, low molecular weight polyphosphates and nucleic acid were experimentally identified as readily utilizable phosphate, while high molecular weight polyphosphate was recognized as non-readily utilizable phosphate. The simulated profiles for preferential utilizations of RUN and Non-RUN form of phosphate were found to be in agreement with the corresponding experimental values (Fig. 5.6). Non-RUN form of phosphate (Fig. 5.6 B) exhibited a delayed utilization kinetics which may be due to the additional enzymatic hydrolysis required to yield simpler molecules from the complex ones that are further utilized by the organism for extended growth. For instance, high molecular weight polyphosphate can be

degraded into low molecular weight fractions by hydrolytic action of polyphosphate de-polymerase (Rose et al., 1983) which can be easily utilized by the organism. Therefore, in our study the intermediate lag phase observed under phosphate limited condition could be attributed to the synthesis of Non-RUN hydrolytic enzymes (E_2, E_3) which were inducible after exhaustion of RUN (Fig. 5.3 A and 5.3 D). Simulated profiles of the growth and substrates utilization obtained from the current model were compared with the corresponding profiles obtained from Droop kinetics and Monod kinetics. While Droop kinetics failed to capture the two stage growth, Monod kinetics did not predict the extended growth of the microorganism under nutrient exhaustion condition (Fig. 5.3 A). In contrast to the two-stage growth observed under higher initial concentration of phosphate (Fig. 5.3), a single staged growth was evident in the batches with lower initial concentration of both phosphate and nitrate (Fig. 5.4 A and 5.5 A). In case of lower initial concentration of limiting substrates, the organism could have experienced nutritional stress at initial stage of growth which might have led to early synthesis of hydrolytic enzymes and hence, no intermediate lag phase was observed. A short initial lag phase was observed for the growth of the organism under different nutritional conditions (Fig. 5.4 and 5.5). This lag phase corresponds to the adaptation of the microorganism to the growth environment different from inoculum (Robinson et al., 1998). These distinct features of growth kinetics were modeled using modified Monod equation (Equation 5.4 and 5.5) which includes contribution from both stored intracellular nutrients (Q_{R_i}) and extracellular nutrients (R_i) towards its extended growth under nutrient starvation. The length of the first lag phase was modeled by an inducible enzyme E_1 and the intermediate lag phase was modeled by hydrolytic enzymes E_2 and E_3 for breakdown of Non-RUN.

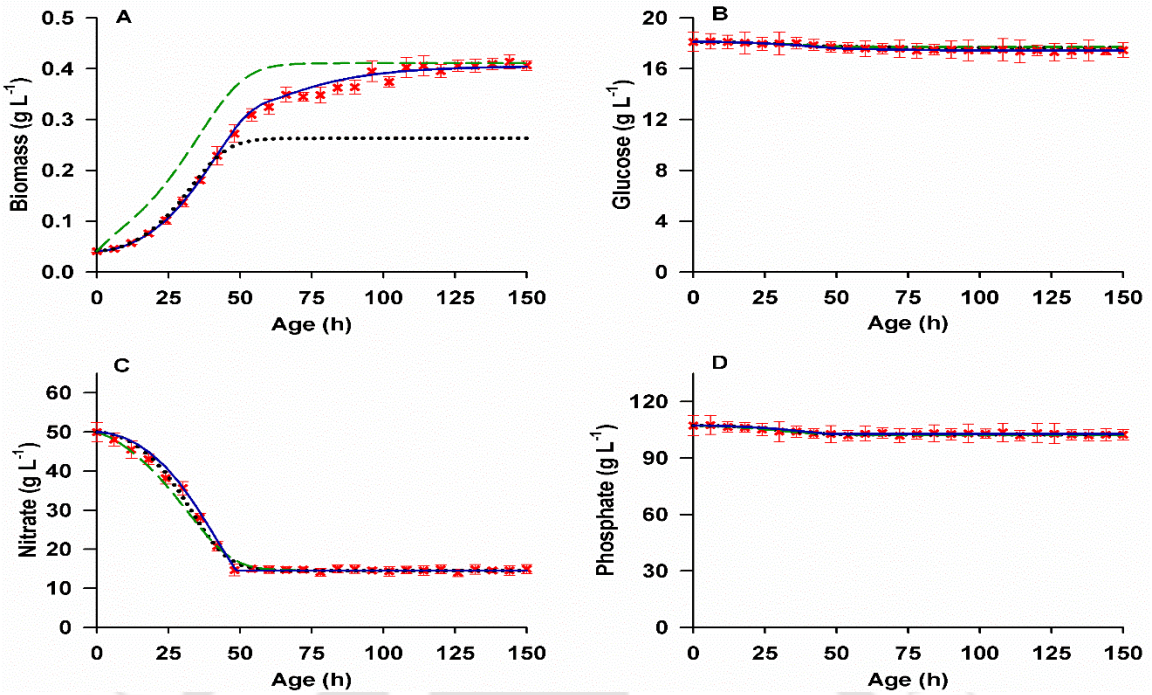

Fig. 5.5 Dynamic profiles for growth and substrate utilization of the strain grown under nitrate limited heterotrophic condition with very low initial nitrate concentration 50 mg L^{-1}. The other nutrients were same as that of the optimized BG11 media in both the batches. Predictions by proposed model (—), Monod kinetics (⋯) and Droop's cell quota model (- - -) were compared with experimental data (×). (A) biomass synthesis, (B) glucose concentration, (C) nitrate concentration and (D) phosphate concentration

It is interesting to note that in case of phosphate limited conditions (Fig. 5.3 and 5.4), even after exhaustion of phosphate, microorganism still continues to utilize nitrate from extracellular medium. This phenomenon was more prominent for higher initial concentration of phosphate in fermentation medium (Fig. 5.3). However, in case of nitrate limited condition, as soon as nitrate was exhausted from the medium and reached its residual concentration, phosphate uptake was stopped completely (Fig. 5.5). Therefore, while phosphate uptake kinetics was found to be dependent on the presence of extracellular nitrate, nitrate uptake kinetics was free from the influence of phosphate. A similar observation was reported for the growth of *M. lutheri* where uptake of phosphorous was inhibited in the absence of vitamin B_{12} and vice versa (Droop, 1975). Although nitrate (Daniel-Vedele et al., 1998) and phosphate (Chung et al., 2003) transporters are different, it was assumed that transportation of nitrate favored the

condition for phosphate uptake. In the present model, this phenomena was captured by incorporating an additional constraint ($R_2 > 0$) in the phosphate uptake kinetics (Equation 5.14). Therefore, in case of phosphate limited condition (Fig. 5.3 and 5.4) the extended growth of the organism under phosphate starvation was achieved by utilization of intracellular phosphate and extracellular nitrate. However, in case of nitrate limitation the extended growth under nitrate starvation was achieved by utilization of intracellular stored nitrate and phosphate compounds (Fig. 5.5).

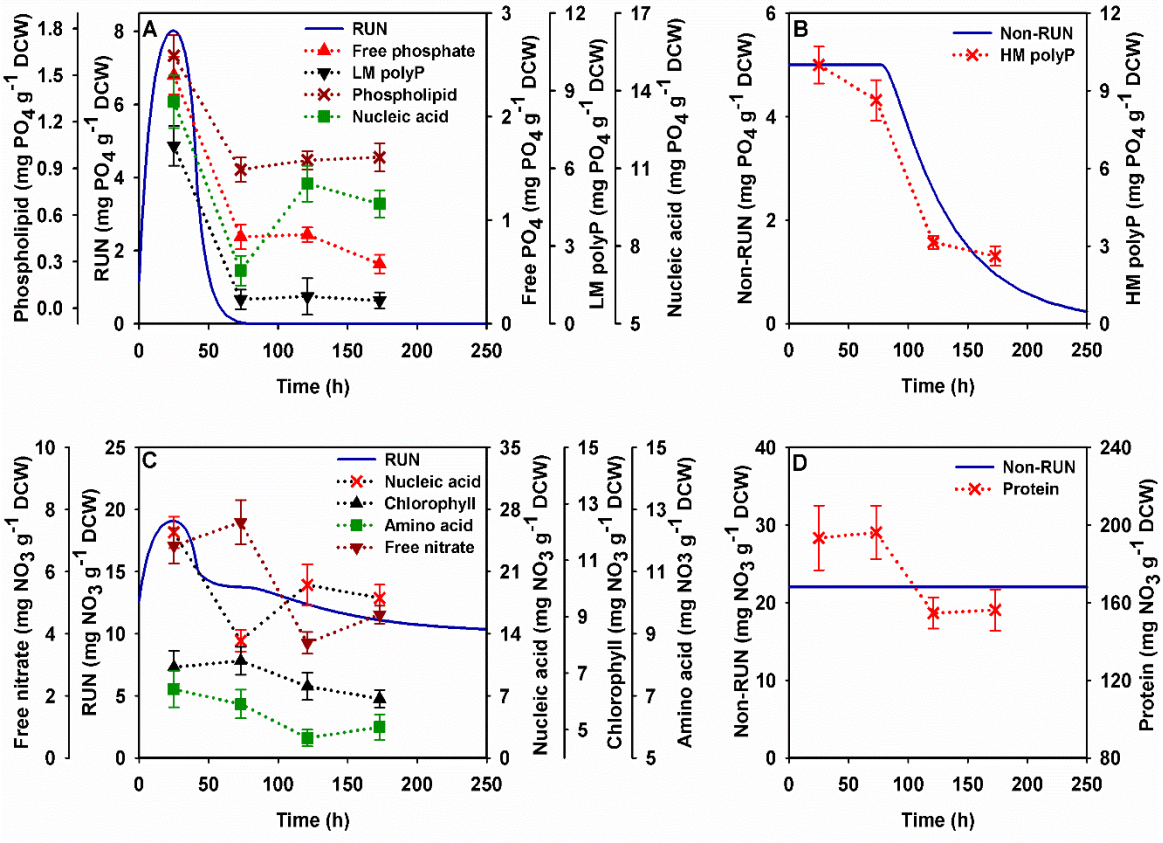

Fig. 5.6 Validation of simulated profiles of RUN and Non-RUN form of phosphate and nitrate under phosphate limiting condition: (A) validation of RUN form of phosphate via experimentally determined free phosphate, nucleic acid, phospholipid and low molecular weight polyphosphate (LM polyP); (B) validation of Non-RUN form of phosphate via experimentally determined high molecular weight polyphosphate (HM polyP); (C) validation of RUN form of nitrate via quantification of free nitrate, nucleic acid, chlorophyll and amino acid; (D) validation of Non-RUN form of nitrate via quantification of protein. The strain was grown under phosphate limited heterotrophic condition with high initial concentration of phosphate (107 mg L^{-1}). Initial concentration of glucose and nitrate was 18 g L^{-1} and 1.3 g L^{-1} respectively. All the phosphate and nitrate compounds are expressed in terms of phosphate quantity (mg phosphate g^{-1} DCW) and nitrate quantity (mg nitrate g^{-1} DCW) respectively

The present model exhibited improved predictions for utilization profiles of different substrates as compared to Droop and Monod kinetics (Fig. 5.3, 5.4 and 5.5). The degree of model fit was checked by estimating the coefficient of determinant (R^2) for experimental and predicted data in MINITAB software. Regression values for model fit were calculated by averaging the R^2 values of biomass formation and nutrient (glucose, nitrate and phosphate) utilization profiles. The goodness of the fit was evident from higher value of R^2 in the range of 0.95 to 0.98 for all the batches. Further, the predictive ability of the model was validated by comparing simulated profile for growth and substrates utilization with the corresponding experimental values obtained by growing the culture under nitrate limited condition with initial nitrate concentration of 170 mg L^{-1} (Fig. 5.7).

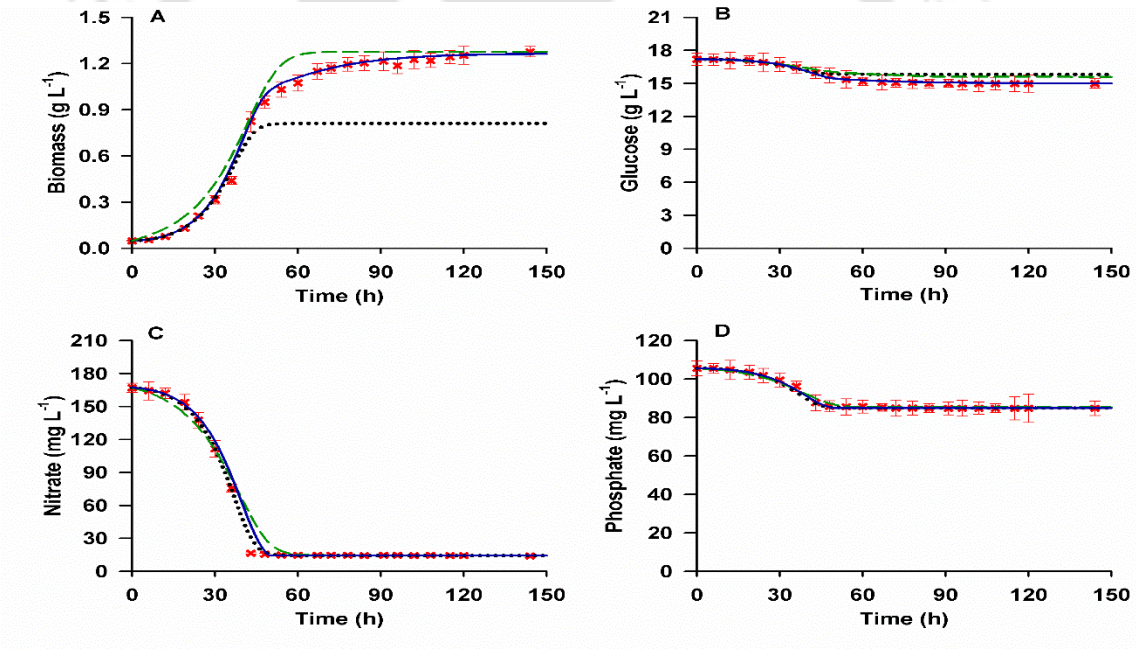

Fig. 5.7 Validation of the proposed model by comparing model predicted (—) profiles for growth and substrate utilizations with corresponding experimental data (×). Proposed model predictions were also compared with Monod kinetics (···) and Droop's cell quota model (---). The strain was grown under nitrate limited heterotrophic condition with initial nitrate concentration of 170 mg L^{-1}. Initial concentration of glucose and phosphate was 18 g L^{-1} and 107 mg L^{-1} respectively. (A) biomass synthesis, (B) glucose concentration, (C) nitrate concentration and (D) phosphate concentration

The model was able to predict the growth and nutrient utilization kinetics accurately with an average R^2 value of 0.99. The simulated profiles of intracellular nitrate

or phosphate in the form of RUN and Non-RUN were also validated with the corresponding experimental values for nitrate limited conditions (Fig. 5.8) which were found to be in agreement with the predicted profiles. Intracellular free nitrate, amino acids, nucleic acids and chlorophyll were found to be the readily utilizable nitrate those were preferentially utilized first during the nutrient limitation. Intracellular proteins were identified as the Non-RUN nitrate which was utilized after the exhaustion of RUN nitrate. The preferential utilization of RUN followed by Non-RUN during the nitrate limited condition shows that the model assumptions were in accordance with the experimental observations. The RUN and Non-RUN fractions of nitrate (Fig. 5.8 C and 5.8 D) were found to be utilized along with RUN fraction of phosphate (Fig. 5.8 A). However, in case of phosphate limited condition only the RUN and Non-RUN fractions of phosphate were found to get utilized.

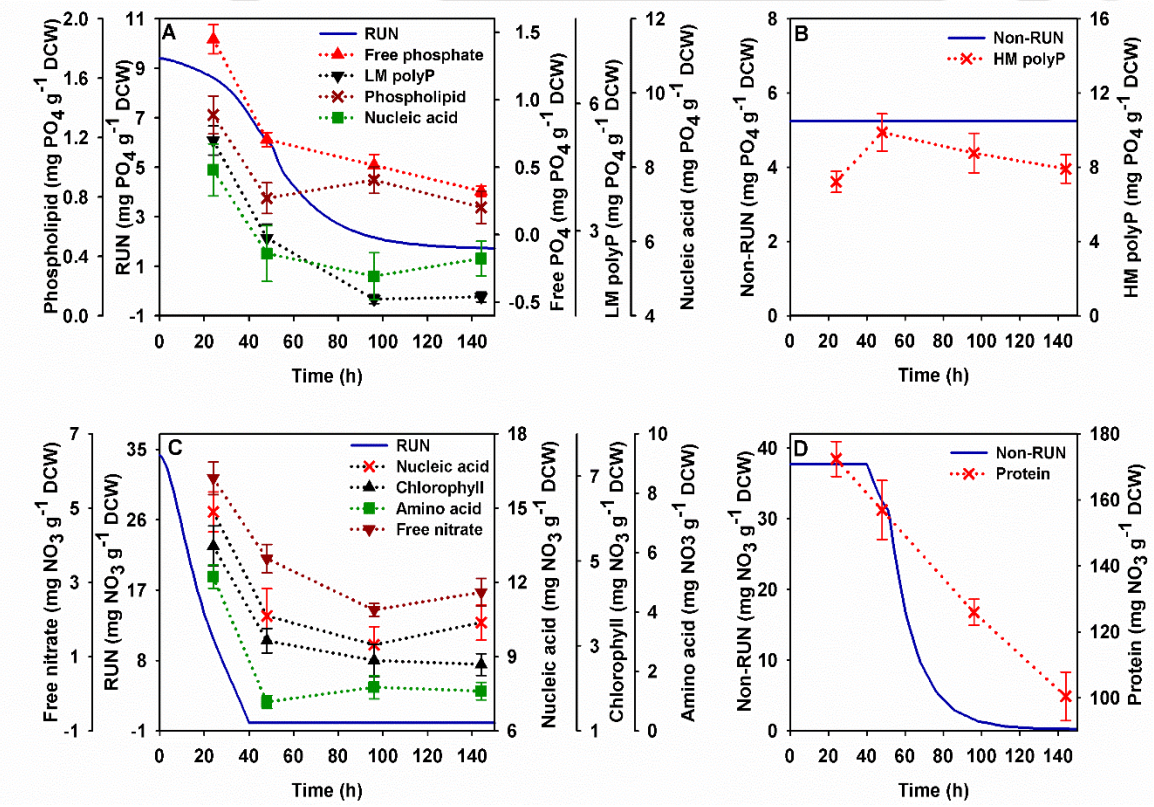

Fig. 5.8 Validation of model prediction of RUN and Non-RUN form of phosphate and nitrate under nitrate limiting condition: (A) experimental validation of RUN form of phosphate via quantification of free phosphate, nucleic acid, phospholipid and low

molecular weight polyphosphate (LM polyP); (B) experimental validation of Non-RUN form of phosphate via quantification of high molecular weight polyphosphate (HM polyP); (C) validation of RUN form of nitrate via quantification of free nitrate, nucleic acid, chlorophyll and amino acid; (D) validation of Non-RUN form of nitrate via quantification of protein. The strain was grown under nitrate limited heterotrophic condition with initial nitrate concentration of 170 mg L^{-1}. Initial concentration of glucose and phosphate was 18 g L^{-1} and 107 mg L^{-1} respectively. All the phosphate and nitrate compounds are expressed in terms of phosphate quantity (mg phosphate g^{-1} DCW) and nitrate quantity (mg nitrate g^{-1} DCW) respectively

5.3.2. Significance of model parameters

The model parameters were estimated by fitting simulated profiles of growth and substrate utilization to the corresponding experimental values obtained from different batch runs (Table 5.1) as discussed in the previous section 5.2.5. Substrate inhibition constant (K_I) for glucose, nitrate and phosphate was estimated to be much higher than their respective concentrations used in the experiments. Therefore, no or less substrate inhibition was expected from any of these nutrients (Andrews, 1968). Half saturation constant (K_S) for glucose, nitrate and phosphate were found to be minimal and hence, organism was able to maintain the higher growth rate till the ECN reached very low concentration in the medium (Bapat et al., 2006). In case of intracellular nutrient quota, half saturation constant (K_Q) was found to be considerably high with respect to available nutrient quota for growth ($A_{R_i} + A_{NR_i}$), resulting in reduced growth rate under nutrient exhaustion. The degradation constant (β_i) for hydrolytic enzymes (0.02-0.05 h^{-1}) was estimated to be higher than ECN transportation related enzymes (0.005 h^{-1}). This indicates that these hydrolytic enzymes induced under nutritional stress condition have to be degraded faster which otherwise will degrade structural form of nutrients (SFN) required for cell viability. A considerably high maintenance energy (m_s) of $7.8 \times 10^{-3}\ h^{-1}$ was estimated by the model in presence of nitrate in the medium ($R_2 > 0$). We hypothesized that transport and assimilation of nitrate and phosphate were active only when nitrate was present in the medium. Therefore, a significant amount of energy was invested for these

transportation processes resulting in noticeable maintenance energy in presence of nitrate. A similar observation of high maintenance energy of 1.5 mmol ATP g^{-1} biomass h^{-1} ($m_s = 9 \times 10^{-3}\ h^{-1}$) was reported for the growth of microalga *Chlamydomonas reinhardtii* (Boyle and Morgan, 2009).

Table 5.1 Estimated model parameters for prediction of heterotrophic growth and substrate utilization by microalga *Chlorella* sp. FC2 IITG under different nutritional conditions

Parameter	Value	Parameter	Value
$\mu^{max}(h^{-1})$	0.145	$Y_{S_1/X}^{min}$	1.18
R_2^m	0.88	$Y_{S_2/X}^{min}$	0.14
R_3^m	0.94	$Y_{S_3/X}^{min}$	17.5 x10^{-3}
$K_{S_1}(g\ L^{-1})$	0.2	$Y_{S_1/X}^{var}$	0.7
$K_{S_2}(g\ L^{-1})$	0.07	$Y_{S_2/X}^{var}$	0.08
$K_{S_3}(g\ L^{-1})$	2 x10^{-3}	$Y_{S_3/X}^{var}$	25 x10^{-3}
$K_{I_1}(g\ L^{-1})$	350	$S_1^{Res}(g\ L^{-1})$	0.64
$K_{I_2}(g\ L^{-1})$	15	$S_2^{Res}(g\ L^{-1})$	0.0145
$K_{I_3}(g\ L^{-1})$	1.73	$S_3^{Res}(g\ L^{-1})$	0
K_{Q_2}	0.08	K_{Y_2}	0.25
K_{Q_3}	0.02	K_{Y_3}	0.04
$m_s(h^{-1})$	7.8x10^{-3}	$K_{T_{R2}}$	0.02
$\beta_1(h^{-1})$	0.005	$K_{T_{R3}}$	0.009
$\beta_2(h^{-1})$	0.05	$K_{T_{NR2}}$	0.022
$\beta_3(h^{-1})$	0.02	$K_{T_{NR3}}$	0.005

The residual concentrations of glucose (S_1^{Res}), nitrate (S_2^{Res}) and phosphate (S_3^{Res}) were found to be 0.64 g L^{-1}, 0.014 g L^{-1} and 0 g L^{-1} respectively. Uptake of these nutrients from extracellular medium continued until the respective residual concentration was reached after which sufficient driving force might not exist for plasma membrane transportation of nutrients into cell. Microalga *M. lutheri* was reported to exhibit a residual phosphate concentration of 0.7 µg L^{-1} (Droop, 1975). In the present study, maximum amount of RUN that can be stored in biomass $K_{T_{Ri}}$, (g of RUN g^{-1} of biomass) for nitrate and phosphate was found to be 0.02 and 0.009 respectively. Further, maximum amount of Non-RUN that can be stored in biomass $K_{T_{NRi}}$ (g of Non-RUN g^{-1} of biomass) for nitrate and phosphate was estimated to be 0.022 and 0.005 respectively.

5.3.3. Variable yield coefficients

The maximum value of overall yield coefficients $Y_{S_i/X}$ was achieved at very high concentration of nitrate and phosphate which was represented as the sum of $Y_{S_i/X}^{min}$ and $Y_{S_i/X}^{var}$ (maximum value of the variable fraction of the yield). Note that minimum value of $Y_{S_i/X}$ was obtained when the concentration of nitrate and phosphate in the medium was negligible and was equal to $Y_{S_i/X}^{min}$. In the present study, the overall yield coefficient for nitrate was found to vary from 0.14 to 0.22 g of NO_3 g^{-1} of biomass and the corresponding values for phosphate was found to be in the range 0.017 to 0.042 g of PO_4 g^{-1} of biomass. The phosphate yield was observed to vary with both phosphate and nitrate concentration in the medium (Fig. 5.9) while, nitrate yield was independent of the extracellular phosphate concentration (Fig. 5.9 A and 5.9 C). Interestingly, the glucose yield coefficient was found to vary inversely with nitrate and phosphate yield coefficients. Under nitrate or phosphate limitation, organism consumed more glucose per unit mass of cell as a source of carbon. Earlier it was shown that the organism triggers neutral lipid accumulation under phosphate and nitrate starvation (Menon et al., 2013; Muthuraj et al., 2014). Further, under lower

concentration of nitrate and phosphate (lower yield coefficient), microorganism would require higher maintenance energy to combat nutritional stress (Section 8.3.3). Under this condition, additional glucose was expected to get utilized for the synthesis of carbon rich neutral lipid and maintenance of cellular processes.

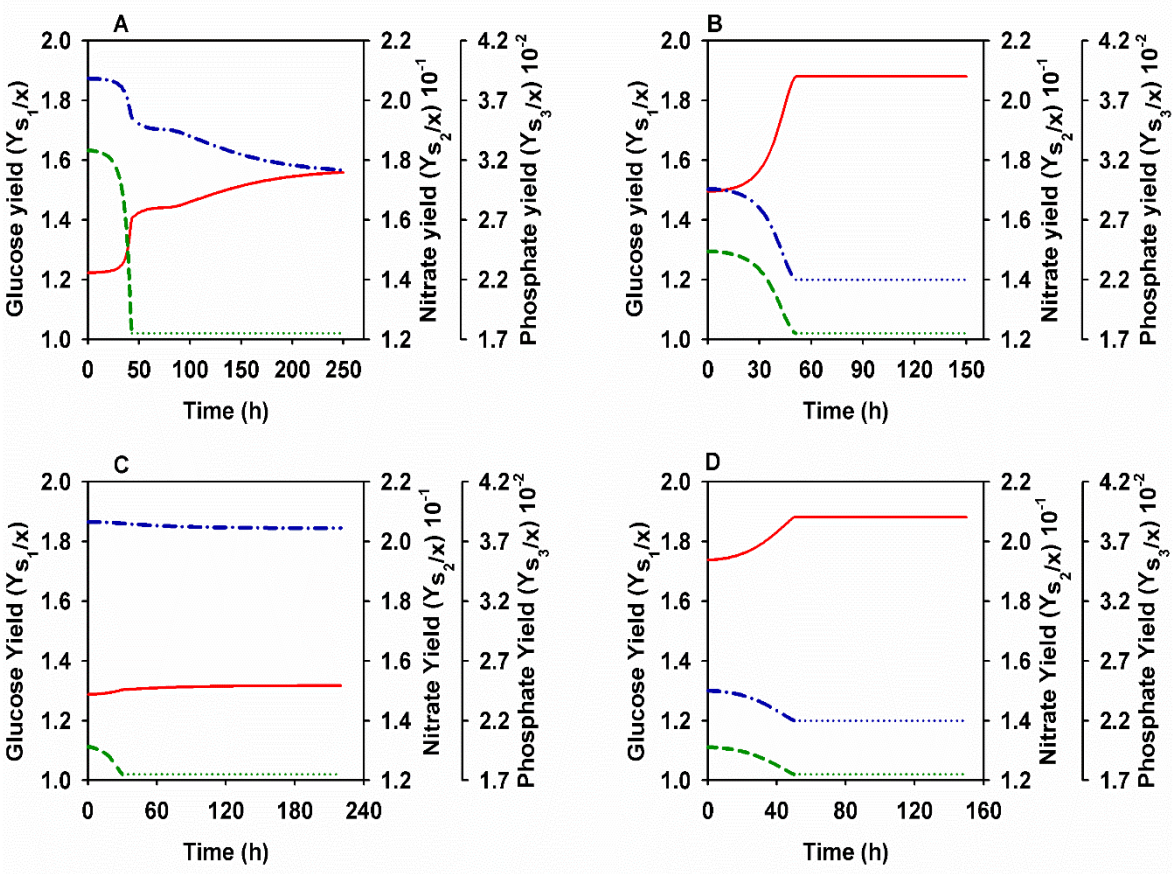

Fig. 5.9 Dynamic changes in model predicted glucose yield (—), nitrate yield (− · −) and phosphate yield (− −) under different nutritional conditions. The dotted line (···) represents the exhaustion of corresponding nutrient from the medium. The batches differ in terms of varied initial concentration of phosphate and nitrate: (A) phosphate limited batch with 107 mg L^{-1} phosphate and 1.3 g L^{-1} nitrate; (B) nitrate limited batch with 170 mg L^{-1} nitrate and 107 mg L^{-1} phosphate; (C) phosphate limited batch with 5 mg L^{-1} phosphate and 1.3 g L^{-1} nitrate; (D) nitrate limited batch with 50 mg L^{-1} nitrate and 107 mg L^{-1} phosphate. Glucose (18 g L^{-1}) was used as carbon source.

5.3.4. Intracellular nutrient quota and their role on microalgal growth under nutrient limitation

From our simulation, it was observed that the intracellular nutrient quota (Q_i) for nitrate or phosphate decreased gradually with time course of fermentation (Fig. 5.10).

However, an initial increase in intracellular nitrate quota was observed when the organism was grown on relatively higher initial concentration of nitrate (Fig. 5.10 A and 5.10 C).

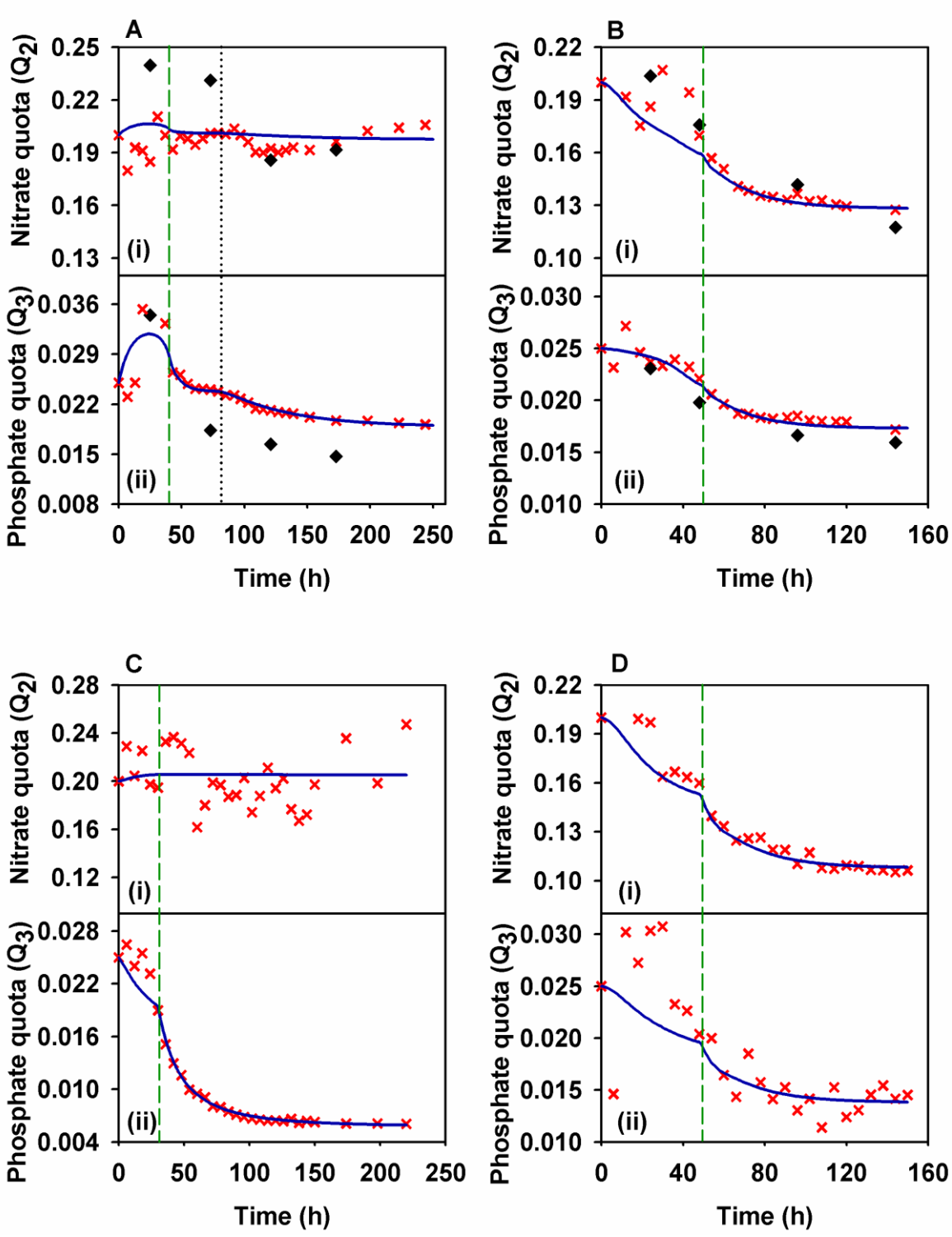

Fig. 5.10 Dynamic changes in intracellular (i) nitrate quota and (ii) phosphate quota obtained from proposed model predictions (—), experimental data based on ECN consumption (×) and experimental data based on extraction of intracellular components (♦) under different nutritional conditions. The batches differ in terms of varied initial

concentration of phosphate and nitrate: (A) phosphate limited batch with 107 mg L^{-1} phosphate and 1.3 g L^{-1} nitrate; (B) nitrate limited batch with 170 mg L^{-1} nitrate and 107 mg L^{-1} phosphate; (C) phosphate limited batch with 5 mg L^{-1} phosphate and 1.3 g L^{-1} nitrate; (D) nitrate limited batch with 50 mg L^{-1} nitrate and 107 mg L^{-1} phosphate. Glucose (18 g L^{-1}) was used as carbon source. Exhaustion of extracellular nutrient (ECN) and onset of utilization of intracellular stored utilizable nutrient was marked with dashed line (---). The dotted line (⋯) represents the complete consumption of intracellular readily utilizable stored nutrients (RUN) just before the onset of intracellular non-readily utilizable stored nutrients (Non-RUN) consumption

It is important to note that because of nitrate dependent uptake of phosphate, similar increase in intracellular phosphate quota was observed only when both nitrate and phosphate concentration was higher (Fig. 5.10 A). Irrespective of nutritional conditions a phase transition was observed at around ~40-50 h (dashed line ---) in the dynamic profile of intracellular nutrient quota (Fig. 5.10 B, 5.10 C and 5.10 D). This phase transition represents exhaustion of extracellular nutrient and onset of utilization of intracellular stored nutrients. However, in case of growth on higher initial concentration of phosphate and nitrate (Fig. 5.10 A), two phase transitions were evident in the profile of intracellular phosphate quota. In this case, the first phase transition represents exhaustion of extracellular phosphate and onset of intracellular readily utilizable phosphate (RUN) consumption. The second transition corresponds to exhaustion of RUN and initiation of Non-RUN utilization (dotted line ⋯). The double phase transition was attributed to the delayed induction of Non-RUN hydrolyzing enzymes (E_2 *and* E_3) at higher initial concentration of nitrate and phosphate. This phenomenon was not observed in other batches with lower or moderate initial concentration of nitrate or phosphate (Fig. 5.10 B, 5.10 C and 5.10 D) which might be due to probably early induction of hydrolytic enzymes as explained earlier. The growth ceases as soon as nutrient quota reaches its threshold value (T_{NR_3}) at which Non-RUN gets utilized completely.

5.4. Conclusions

A multi-nutrient mechanistic model was developed to capture the heterotrophic growth kinetics of FC2 under both nutrient sufficient and nutrient depleted conditions. Model segregated the intracellular nutrients into SFN, RUN and Non-RUN. This preferential utilization of ECN under nutrient sufficient condition followed by RUN and then Non-RUN leaving behind SFN for cellular integrity under nutrient deplete condition, was modeled and experimentally validated. The variability in yield coefficient for substrate consumption was modeled by expressing the coefficient in terms of Michaelis Menten kinetics. Model demonstrates improved predictability over existing growth kinetics such as Monod, Droop models. This model can be used as a tool to accurately predict microalgal growth kinetics and intracellular nutrient status. As the model consist uniform equations for limiting and non-limiting substrates, it can be easily used for optimization of substrate concentration and feeding rate in case of fed-batch and continuous operations.

5.5. Nomenclature

Abbreviations	Descriprtion
A_{R_2}	Amount of intracellular stored readily utilizable nutrient (RUN) form of NO_3 $\left(\frac{g\ RUN\ NO_3\ L^{-1}}{g\ biomass\ L^{-1}}\right)$
A_{R_3}	Amount of intracellular RUN PO_4 $\left(\frac{g\ RUN\ PO_4\ L^{-1}}{g\ biomass\ L^{-1}}\right)$
A_{NR_2}	Amount of intracellular stored non-readily utilizable nutrient (Non-RUN) form of NO_3 $\left(\frac{g\ NonRUN\ NO_3\ L^{-1}}{g\ biomass\ L^{-1}}\right)$
A_{NR_3}	Amount of intracellular Non-RUN PO_4 $\left(\frac{g\ NonRUN\ PO_4\ L^{-1}}{g\ biomass\ L^{-1}}\right)$
E_1	Induction of nutrient uptake and assimilation related enzyme (U g^{-1}

	biomass)
E_1^{Ref}	Theoretical maximum induction of enzyme E_1 (U g^{-1} biomass)
E_2	Induction of Non-RUN NO_3 hydrolyzing enzyme (U g^{-1} biomass)
E_2^{Ref}	Theoretical maximum induction of enzyme E_2 (U g^{-1} biomass)
E_3	Induction of Non-RUN PO_4 hydrolyzing enzyme (U g^{-1} biomass)
E_3^{Ref}	Theoretical maximum induction of enzyme E_3 (U g^{-1} biomass)
K_{I_1}	Inhibition constant of glucose for growth (g L^{-1})
K_{I_2}	Inhibition constant of NO_3 for growth (g L^{-1})
K_{I_3}	Inhibition constant of PO_4 for growth (g L^{-1})
K_{Q_2}	Half saturation constant of Q_2 for growth $\left(\frac{g\ intracellular\ NO_3\ L^{-1}}{g\ biomass\ L^{-1}}\right)$
K_{Q_3}	Half saturation constant of Q_3 for growth $\left(\frac{g\ intracellular\ PO_4\ L^{-1}}{g\ biomass\ L^{-1}}\right)$
K_{S_1}	Half saturation constant of glucose for growth (g L^{-1})
K_{S_2}	Half saturation constant of NO_3 for growth (g L^{-1})
K_{S_3}	Half saturation constant of PO_4 for growth (g L^{-1})
$K_{T_{R2}}$	Maximum amount of RUN NO_3 that can be stored in biomass (g RUN NO_3 g^{-1} biomass)
$K_{T_{R3}}$	Maximum amount of RUN PO_4 that can be stored in biomass (g RUN PO_4 g^{-1} biomass)
$K_{T_{NR2}}$	Maximum amount of Non-RUN NO_3 that can be stored in biomass (g Non-RUN NO_3 g^{-1} biomass)
$K_{T_{NR3}}$	Maximum amount of Non-RUN PO_4 that can be stored in biomass (g Non-RUN PO_4 g^{-1} biomass)
K_{Y_2}	Half saturation constant of NO_3 for variable fraction of $Y_{S_2/X}$ (g NO_3 g^{-1}

	biomass)
K_{Y_3}	Half saturation constant of PO_4 for variable fraction of $Y_{S_3/X}$ (g PO_4 g^{-1} biomass)
m_s	Maintenance coefficient (g glucose g^{-1} biomass h^{-1})
Q_2	Intracellular NO_3 quota $\left(\frac{g\ intracellular\ NO_3\ L^{-1}}{g\ biomass\ L^{-1}}\right)$
Q_2^0	Initial value of intracellular NO_3 quota Q_2
Q_3	Intracellular PO_4 quota $\left(\frac{g\ intracellular\ PO_4\ L^{-1}}{g\ biomass\ L^{-1}}\right)$
Q_3^0	Initial value of intracellular PO_4 quota Q_3
R_2^m	Maximum value of fractional growth rate (R_2) contributed by NO_3
R_3^m	Maximum value of fractional growth rate (R_3) contributed by PO_4
S_1	Extracellular glucose concentration in medium (g L^{-1})
S_1^{Res}	Residual value of S_1 beyond which glucose will not be consumed (g L^{-1})
S_2	Extracellular NO_3 concentration in medium (g L^{-1})
S_2^0	Initial value of NO_3 concentration S_2 in medium (g L^{-1})
S_2^{Res}	Residual value of S_2 beyond which NO_3 will not be consumed (g L^{-1})
S_3	Extracellular PO_4 concentration in medium (g L^{-1})
S_3^0	Initial value of PO_4 concentration S_3 in medium (g L^{-1})
S_3^{Res}	Residual value of S_3 beyond which PO_4 will not be consumed (g L^{-1})
T_{R_2}	Threshold intracellular NO_3 quota Q_2, at which RUN NO_3 gets exhausted
T_{R_3}	Threshold intracellular PO_4 quota Q_3, at which RUN PO_4 gets exhausted
T_{NR_2}	Threshold intracellular NO_3 quota Q_2, at which Non-RUN NO_3 gets exhausted
T_{NR_3}	Threshold intracellular PO_4 quota Q_3, at which Non-RUN PO_4 gets

	exhausted
X	Biomass concentration in broth (g L^{-1})
X^0	Initial biomass concentration in the broth (g L^{-1})
$Y_{S_1/X}$	Yield coefficient of glucose (g glucose consumed g^{-1} biomass formed)
$Y_{S_1/X}^{min}$	Non variable fraction of glucose yield coefficient $Y_{S_1/X}$
$Y_{S_1/X}^{var}$	Maximum value of variable fraction of glucose yield coefficient $Y_{S_1/X}$
$Y_{S_2/X}$	Yield coefficient of NO_3 (g NO_3 consumed g^{-1} biomass formed)
$Y_{S_2/X}^{min}$	Non variable fraction of NO_3 yield coefficient $Y_{S_2/X}$
$Y_{S_2/X}^{var}$	Maximum value of variable fraction of NO_3 yield coefficient $Y_{S_2/X}$
$Y_{S_2/X}^{0}$	Initial value of yield coefficient of NO_3
$Y_{S_3/X}$	Yield coefficient of PO_4 (g PO_4 consumed g^{-1} biomass formed)
$Y_{S_3/X}^{min}$	Non variable fraction of PO_4 yield coefficient $Y_{S_3/X}$
$Y_{S_3/X}^{var}$	Maximum value of variable fraction of PO_4 yield coefficient $Y_{S_3/X}$
$Y_{S_3/X}^{0}$	Initial value of yield coefficient of PO_4
β_1	Degradation constant of enzymes E_1 (h^{-1})
β_2	Degradation constant of enzymes E_2 (h^{-1})
μ	Specific growth rate (h^{-1})
μ^{max}	Maximum specific growth rate (h^{-1})

5.6. References

1. Andrews J.F., 1968. A mathematical model for the continuous culture of microorganisms utilizing inhibitory substrates. Biotechnology and Bioengineering. 10, 707–723.

2. Bapat P.M., Sohoni S.V., Moses T.A., Wangikar P.P., 2006. A cybernetic model to predict the effect of freely available nitrogen substrate on rifamycin B production in complex media. Applied Microbiology and Biotechnology. 72, 662–670.

3. Béchet Q., Shilton A., Guieysse B., 2013. Modeling the effects of light and temperature on algae growth: State of the art and critical assessment for productivity prediction during outdoor cultivation. Biotechnology Advances. 31, 1648–1663.

4. Bernard O., 2011. Hurdles and challenges for modelling and control of microalgae for CO_2 mitigation and biofuel production. Journal of Process Control. 21, 1378–1389.

5. Boyle N.R., Morgan J.A., 2009. Flux balance analysis of primary metabolism in *Chlamydomonas reinhardtii*. BMC Systems Biology. 3, 1.

6. Chung C.-C., Hwang S.-P.L., Chang J., 2003. Identification of a high-affinity phosphate transporter gene in a prasinophyte alga, *Tetraselmis chui*, and its expression under nutrient limitation. Applied and Environmental Microbiology. 69, 754–759.

7. Daniel-Vedele F., Filleur S., Caboche M., 1998. Nitrate transport: a key step in nitrate assimilation. Current Opinion in Plant Biology. 1, 235–239.

8. Das D., Basu A., Nigam A., Phale P.S., Wangikar P.P., 2011. Dynamics of rate limiting enzymes involved in the sequential substrate uptake by *Pseudomonas putida* CSV86: Modeling and experimental validation. Process Biochemistry. 46, 701–708.

9. Dortch Q., Clayton Jr J.R., Thoresen S.S., Ahmed S.I., 1984. Species differences in accumulation of nitrogen pools in phytoplankton. Marine Biology. 81, 237–250.

10. Droop M.R., 1975. The nutrient status of algal cells in batch culture. Journal of the Marine Biological Association of the UK. 55, 541–555.

11. Droop M.R., 1968. Vitamin B 12 and marine ecology. IV. The kinetics of uptake, growth and inhibition in *Monochrysis lutheri*. Journal of the Marine Biological Association of the UK. 48, 689–733.

12. John E.H., Flynn K.J., 2000. Modelling phosphate transport and assimilation in microalgae; how much complexity is warranted? Ecological Modelling. 125, 145–157.

13. Krishnan P.S., Damle S.P., Bajaj V., 1957. Studies on the role of "metaphosphate" in molds. II. The formation of "soluble" and "insoluble" metaphosphates in *Aspergillus niger*. Archives of Biochemistry and Biophysics. 67, 35–52.

14. Kumar A., Singh L.K., Ghosh S., 2009. Bioconversion of lignocellulosic fraction of water-hyacinth (*Eichhornia crassipes*) hemicellulose acid hydrolysate to ethanol by *Pichia stipitis*. Bioresource Technology. 100, 3293–3297.

15. Kumar V., Muthuraj M., Palabhanvi B., Ghoshal A.K., Das D., 2014. High cell density lipid rich cultivation of a novel microalgal isolate *Chlorella sorokiniana* FC6 IITG in a single-stage fed-batch mode under mixotrophic condition. Bioresource Technology. 170, 115–124.

16. Lemesle V., Mailleret L., 2008. A mechanistic investigation of the algae growth "Droop" model. Acta Biotheoretica. 56, 87–102.

17. Lowry O.H., Rosebrough N.J., Farr A.L., Randall R.J., 1951. Protein measurement with the Folin phenol reagent. The Journal of Biological Chemistry. 193, 265–275.

18. Menon K.R., Balan R., Suraishkumar G.K., 2013. Stress induced lipid production in *Chlorella vulgaris*: relationship with specific intracellular reactive species levels. Biotechnology and Bioengineering. 110, 1627–1636.

19. Menzel D.W., Corwin N., 1965. The measurement of total phosphorus in seawater based on the liberation of organically bound fractions by persulfate oxidation. Limnology and Oceanography. 10, 280–282.

20. Misi S.N., Forster C.F., 2001. Batch co-digestion of multi-component agro-wastes. Bioresource Technology. 80, 19–28.

21. Muthuraj M., Kumar V., Palabhanvi B., Das D., 2014. Evaluation of indigenous microalgal isolate *Chlorella* sp. FC2 IITG as a cell factory for biodiesel production and scale up in outdoor conditions. Journal of Industrial Microbiology and Biotechnology. 41, 499–511.

22. Nigam A., Ayyagari A., 2007. Lab manual in biochemistry, immunology and biotechnology. Tata McGraw-Hill Publishing Company Limited, New Delhi.

23. Pandey A., 2003. Solid-state fermentation. Biochemical Engineering Journal. 13, 81–84.

24. Pruvost J., Van Vooren G., Le Gouic B., Couzinet-Mossion A., Legrand J., 2011. Systematic investigation of biomass and lipid productivity by microalgae in photobioreactors for biodiesel application. Bioresource Technology. 102, 150–158.

25. Ritchie R.J., 2006. Consistent sets of spectrophotometric chlorophyll equations for acetone, methanol and ethanol solvents. Photosynthesis Research. 89, 27–41.

26. Robinson T.P., Ocio M.J., Kaloti A., Mackey B.M., 1998. The effect of the growth environment on the lag phase of *Listeria monocytogenes*. International Journal of Food Microbiology. 44, 83–92.

27. Rodolfi L., Chini Zittelli G., Bassi N., Padovani G., Biondi N., Bonini G., Tredici M.R., 2009. Microalgae for oil: Strain selection, induction of lipid synthesis and outdoor mass cultivation in a low-cost photobioreactor. Biotechnology and Bioengineering. 102, 100–112.

28. Rose A.H., Morris J.G., Tempest D.W., 1983. Advances in Microbial Physiology. Academic Press. New York.

29. Shen Y., Yuan W., Pei Z., Mao E., 2010. Heterotrophic culture of *Chlorella protothecoides* in various nitrogen sources for lipid production. Applied Biochemistry and Biotechnology. 160, 1674–1684.

30. Sicko-Goad L., Jensen T.E., 1976. Phosphate metabolism in blue-green algae. II. Changes in phosphate distribution during starvation and the "polyphosphate overplus" phenomenon in *Plectonema boryanum*. American Journal of Botany. 183–188.

31. Simmon K.E., Steadman D.D., Durkin S., Baldwin A., Jeffrey W.H., Sheridan P., Horton R., Shields M.S., 2004. Autoclave method for rapid preparation of bacterial PCR-template DNA. Journal of Microbiological Methods. 56, 143–149.

32. Xiong W., Li X., Xiang J., Wu Q., 2008. High-density fermentation of microalga *Chlorella protothecoides* in bioreactor for microbio-diesel production. Applied Microbiology and Biotechnology. 78, 29–36.

33. Zachleder V., 1984. Optimization of nucleic acids assay in green and blue-green algae: extraction procedures and the light-activated diphenylamine reaction for DNA. Archiv Fur Hydrobiologie. 67, 313–328.

34. Zonneveld C., 1996. Modelling the kinetics of non-limiting nutrients in microalgae. Journal of Marine Systems. 9, 121–136.

CHAPTER 6

Process development for high cell density-lipid rich cultivation in fed-batch operation

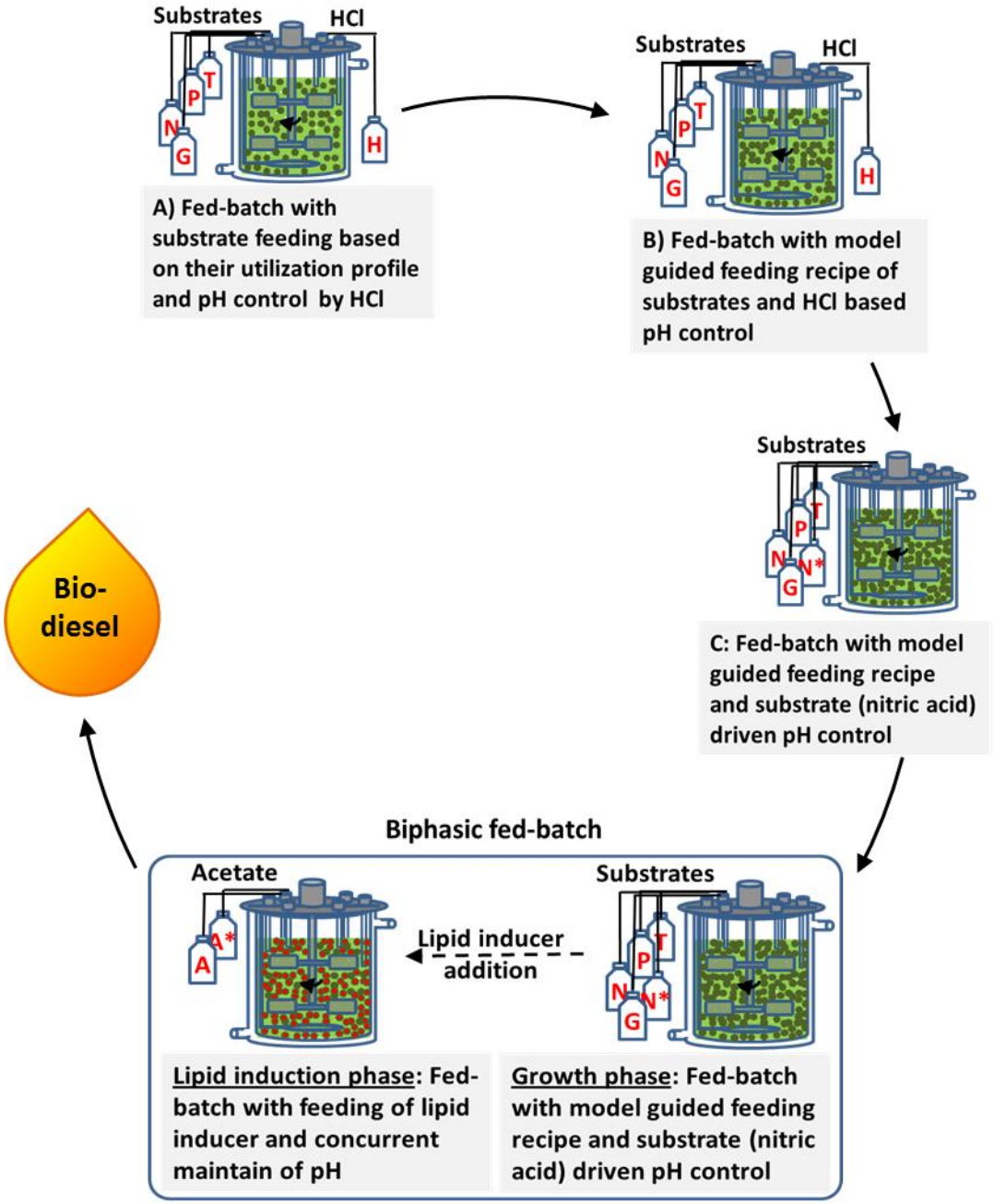

Process development for high cell density-lipid rich cultivation in fed-batch operation via model guided feeding recipe and substrate driven pH control.

6.1. Background and motivation

In comparison to photoautotrophic growth, heterotrophic cultivation is superior in terms of cell density, growth condition maintenance and contamination free cultivation (Shen et al., 2010). Nevertheless, the cost of organic carbon sources utilized in heterotrophic condition remains an unsolved issue (Turon et al., 2015). Current strategies involve exploitation of alternate lignocellulosic biomass and other cheaper carbon sources for the growth of microalgal systems (Turon et al., 2015). Another way to step towards process feasibility is through attaining high cell density cultivation. Thus, success of heterotrophic cultivation is dependent on achieving high biomass yield or productivity and avoiding overconsumption of nutrients. To that end, model guided feeding strategies involving intermittent addition of limiting nutrients could be an effective tool to design optimal substrate feeding recipes for growth thereby avoiding substrate limitation or inhibition (Alagesan et al., 2013). Thus, optimized nourishment is expected to result in the achievement of high cell density ensuring a desired outcome. As explained in chapter 5, various kinetic models have been developed for microalgal growth kinetics which can be employed for optimization of feeding recipes (Droop, 1968; John and Flynn, 2000; Lemesle and Mailleret, 2008). In a similar line, a multi nutrient mechanistic model was developed in previous study (Chapter 5) for the freshwater microalga *Chlorella* sp. FC2 IITG based on preferential utilization of extracellular nutrients and different forms of intracellular stored nutrients. Such structured kinetic model can be a reliable tool for process development through dynamic optimization with control vector parameterization (CVP). CVP is used to solve optimal control problems, where control parameters are discretized and optimized with nonlinear programming techniques (Banga et al., 2005).

Despite the advantages of high cell density cultivation, it may hinder the accumulation of intracellular lipid in cells due to mutually exclusive nature of growth and

lipid content (Muthuraj et al., 2014). Lipid can be accumulated in biomass by exposing cells into nutrient starved condition (Negi et al., 2015) or medium supplemented with lipid inducers (Kumar et al., 2014). Starvation based lipid induction is the traditional method which employs two stage cultivation and hence requires high energy for harvesting, dewatering and re-suspension of biomass from nutrient sufficient to starvation stages. It may also be carried out through single stage strategy with simple nutrient limitation or starvation. However, lipid induction in the biomass will be lesser in quantity and/or slower in rate which leads to reduced lipid productivity. Even though this strategy bypasses the two stage process, it turns ineffective due lower lipid productivity (Rodolfi et al., 2009). Addition of lipid inducers during the end of nutrient sufficient phase also avoids requirement of harvesting and re-suspension thereby minimizing the power inputs in the process. *Chlamydomonas reinhardtii* and *Chlorella vulgaris* were reported to enhance their lipid accumulation by addition of Brefeldin A as an inducer (Kim et al., 2013). However, removal of such complex lipid inducers from the broth is difficult and remains unfeasible; thus necessitating the use of inducers that can be metabolized by microalgae to achieve feasibility. The use of molecule which acts as both lipid inducer and carbon source could be ecofriendly.

In the present study, we have demonstrated a process engineering strategy for high cell density-lipid rich fermentation of the strain FC2 under heterotrophic condition. The strategy involves intermittent feeding of the limiting nutrients through model guided feeding recipe, substrate driven pH control and neutral lipid enrichment through feeding of lipid inducer. In the first step, multi-nutrient mechanistic model developed for batch study was used and their equations were transformed for fed-batch cultivations. In the next step, optimal substrate feeding recipe was designed with help of model via dynamic optimization of the nutrients feeding rates. Finally, a two phase fed-batch cultivation was

demonstrated where first phase was marked as growth phase and the second phase was marked as lipid induction phase. In the growth phase, high cell density was achieved through model based feeding of the limiting nutrients coupled with substrate driven pH control. Lipid induction phase was carried out by addition of lipid inducer.

6.2. Material and methods

6.2.1. Cultivation conditions

Inoculum was prepared as explained in section 5.2.1. In all the experiments, 1% (v/v) of active mid-log phase culture (cell density of 3 g L^{-1}) was used as inoculum. All the experiments were conducted in a 7.5 L automated bioreactor (New Brunswick™ BioFlo®/CelliGen® 115) at 28°C temperature and more than 50% dissolved oxygen (DO) concentration. DO was maintained via varying the aeration rate (1-4 L min^{-1}), agitation speed (250-400 rpm) and by purging pure oxygen (0-2.2 L min^{-1}) in the reactor. The complete dark environment was maintened for the heterotrophic growth of organism.

Three different sets of experiments were conducted aiming at cultivation of FC2 with high biomass titer under fed batch mode of operation. These batches differ in terms of strategy for substrate feeding and controlling of medium pH. Glucose, sodium nitrate, dibasic potassium phosphate and combined solutions of trace elements and microelements (TME) were chosen as the key limiting nutrients to be fed into the bioreactor. In the first experiment, the intermittent feeding of the limiting substrates was done based on their observed consumption profile from the medium. The concentrations of the substrates were maintained above 50% (w/v) of their original concentration throughout the fermentation and the broth pH was maintained at 7.5-8 by addition of 5 N HCl. In the second experiment, the feeding of the limiting nutrients was done as per the model guided optimized feeding rates and the broth pH was maintained at the set value by addition of HCl.

Table 6.1 Concentration, role and feeding strategy of different substrates used in fed-batch operation of strain FC2 grown in a 7.5 L automated bioreactor under heterotrophic mode of operation in optimized BG11 medium via model guided feeding recipe of the nutrients along with concurrent maintenance of broth pH by substrate itself.

SI. No	Substrates	Stock conc.	Main role	Additional role	Feeding strategy	Phase
1	Glucose	3.89 M	Carbon source	Energy source	Model guided	Growth
2	Di potassium hydrogen phosphate	0.143 M	Phosphate source	--	Model guided	Growth
3	Sodium nitrate	1.765 M	Nitrogen source	--	Model guided	Before broth pH reached 8, Growth phase
4	Nitric acid (in place of nitrate)	1.765 M	Nitrogen source	pH maintenance	Model guided	After broth pH reached 8, Growth phase
5	Trace and micro elements (TME)	100 units L^{-1}	Precursor of coenzymes	--	Model guided (converting exponential into step feed)	Growth
6	Sodium acetate	5 M	Carbon source	Lipid inducer	one time feeding	Beginning of lipid phase
7	Acetic acid	8 M	Carbon source	Lipid inducer pH maintenance	In cascade with broth pH to maintain pH and acetate concentration	Lipid

Finally, third experiment was performed by model guided feeding strategy along with concurrent maintenance of broth pH by substrate itself. This batch was divided into two phases: growth phase for high cell density cultivation of FC2 and lipid enrichment phase. In the growth phase, sodium nitrate was used as usual nitrogen source till the medium pH reached a value of 8 followed by addition of nitric acid (instead of sodium nitrate) containing equimolar amount of nitrogen. As per the preliminary studies (Section 3.3.1) growth of FC2 was optimal over an initial broth pH of 6-8 under heterotrophic condition. Nitric acid therefore acts as both nitrogen source and acid source to control the pH shift towards desired pH of the medium. On attaining the maximum biomass titer, a dosing of 24 g L^{-1} sodium acetate was done for the neutral lipid enrichment in cells and then, lipid induction phase was initiated. This concentration was used based on the work carried in section 4.3.3 where 24 g L^{-1} sodium acetate was found to be optimal concentration for lipid induction. In this phase of fermentation, pH of the medium was controlled through addition of acetic acid. The role of various substrates and their feeding strategy is elaborated in Table 6.1. Sampling was done at regular time intervals to obtain dynamic profile of biomass, lipid content and substrate utilization. All the experiments were conducted in triplicate and the data were expressed as mean value ± standard error.

6.2.2. Process model formulation for designing the optimal feeding recipe of limiting nutrients targeted towards high cell density cultivation

Multi nutrient mechanistic model developed in previous study (Chapter 5) was used for optimization of substrate feeding rates in fed batch mode of operation aiming towards high biomass titer. The equations formulated in chapter 5 were adopted and accordingly transformed for fed-batch mode of operations. The intracellular nutrient quota (Q_i) was reformulated taking into account initial substrate content in the medium ($S_i^0 V^0$), substrate content in initial biomass ($Q_i^0 X^0 V^0$) used as inoculum and total substrate

supplemented (TS_i) during fermentation (Equation 6.7). The dilution factor arisen due to supplementation of nutrients was incorporated in the mass balance equation for biomass (Equation 6.8), substrates (Equation 6.10 – 6.12) and enzymes (Equation 6.13 – 6.15). It is important to note that, the model was developed considering three limiting nutrients glucose, nitrate and phosphate. However, growth of the organism was also found to be dependent on the availability of the TME in the broth (Section 4.3.2). In general, growth medium is supplemented with a specific volume of TME stock solution comprising a set of trace elements and microelements. In the present formulation, addition of TME stock solution was represented as a volumetric factor, $\mu XVK_{V/X}$ in the mass balance equation for volume (Equation 6.9). Volumetric factor depends on growth rate of the organism (μXV) and experimentally determined proportionality constant, $K_{V/X}$ (Calculation of $K_{V/X}$ is detailed in section 1 in appendix A). Therefore, temporal changes of the volumetric factor depicts flow rate of TME stock to be fed into bioreactor. Mass balance equations for total supplementation of nitrate and phosphate were added in the model in order to use them in the intracellular nutrient quota calculation (Equation 6.16 – 6.17).

$$\mu = \mu^{max} R \left(\frac{E}{E^{Ref}}\right) \tag{6.1}$$

$$R = R_1\left[R_2 + Q_{R_2}(R_2^m - R_2)/R_2^m\right]\left[R_3 + Q_{R_3}(R_3^m - R_3)/R_3^m\right] \tag{6.2}$$

$$R_i = \frac{S_i - S_i^{Res}}{K_{S_i} + (S_i - S_i^{Res}) + \frac{(S_i - S_i^{Res})^2}{K_{I_i}}} \tag{6.3}$$

$$Q_{R_i} = \frac{\left(A_{R_i} + A_{NR_i}\right)}{K_{Q_i} + \left(A_{R_i} + A_{NR_i}\right)} \tag{6.4}$$

$$A_{R_i} = Q_i - T_{R_i} \tag{6.5}$$

$$A_{NR_i} = \left(T_{R_i} - T_{NR_i}\right)\left(\frac{E_i}{E_i^{Ref}}\right) \tag{6.6}$$

$$Q_i = \frac{(S_i^0 V^0 + TS_i + Q_i^0 X^0 V^0)/V - S_i}{X} \tag{6.7}$$

Where, *i* =1, 2, 3 represents glucose, nitrate and phosphate respectively.

Mass balance equations

Biomass (X)

$$\frac{dX}{dt} = \mu X - \left(\frac{dV}{dt}\right)\frac{X}{V} \tag{6.8}$$

Volume (V)

$$\frac{dV}{dt} = \left(F(1) + F(2) + F(3) + \mu X V K_{V/X}\right) \tag{6.9}$$

Glucose (S_1)

$$\frac{dS_1}{dt} = \begin{cases} \frac{F(1)C_1}{V} - \mu X Y_{S_1/X} - m_s X - \left(\frac{dV}{dt}\right)\frac{S_1}{V}, & R_2 > 0 \\ \frac{F(1)C_1}{V} - \mu X Y_{S_1/X} - \left(\frac{dV}{dt}\right)\frac{S_1}{V} \end{cases} \tag{6.10}$$

Nitrate (S_2)

$$\frac{dS_2}{dt} = \begin{cases} \frac{F(2)C_2}{V} - \mu X Y_{S_2/X} - \left(\frac{dV}{dt}\right)\frac{S_2}{V}, & R_2 > 0 \\ 0 \end{cases} \tag{6.11}$$

Phosphate (S_3)

$$\frac{dS_3}{dt} = \begin{cases} \frac{F(3)C_3}{V} - \mu X Y_{S_3/X} - \left(\frac{dV}{dt}\right)\frac{S_3}{V}, & R_2 R_3 > 0 \\ 0 \end{cases} \tag{6.12}$$

Enzymes (E, E_2 and E_3)

$$\frac{d\left(\frac{E}{E^{Ref}}\right)}{dt} = (\mu^{max} R + \beta) - (\mu^{max} R + \beta)\left(\frac{E}{E^{Ref}}\right) \tag{6.13}$$

$$\frac{d\left(\frac{E_2}{E_2^{Ref}}\right)}{dt} = \begin{cases} 0, & Q_2 > T_{R_2} \\ \left((T_{R_2} - Q_2)\mu^{max} + \beta_2\right) - \left((T_{R_2} - T_{NR_2})\mu^{max} + \beta_2\right)\left(\frac{E_2}{E_2^{Ref}}\right) \end{cases} \tag{6.14}$$

$$\frac{d\left(\frac{E_3}{E_3^{Ref}}\right)}{dt} = \begin{cases} 0, & Q_3 > T_{R_3} \\ \left((T_{R_3} - Q_3)\mu^{max} + \beta_3\right) - \left((T_{R_3} - T_{NR_3})\mu^{max} + \beta_3\right)\left(\frac{E_3}{E_3^{Ref}}\right) \end{cases} \tag{6.15}$$

Total nitrate (TS_2) and phosphate (TS_3) addition

$$\frac{d(TS_2)}{dt} = F(2)C_2 \tag{6.16}$$

$$\frac{d(TS_3)}{dt} = F(3)C_3 \quad (6.17)$$

6.2.3. Dynamic optimization

The maximization of biomass was used as the objective function to optimize the feeding rates of the substrates. The feeding rates $F(1)$, $F(2)$ and $F(3)$ were employed as control variables, while biomass (X), volume of the culture (V), extracellular substrate concentrations (S_i), induction of enzyme $\left(\frac{E}{E^{Ref}}, \frac{E_i}{E_i^{Ref}}\right)$ and amount of substrate addition (TS_i) were used as system state variables. The total estimated time of fed batch was divided into 24 equal intervals with duration of 4 hours each. The control variables were optimized for each interval by control vector parameterization through dynamic optimization. This nonlinear problem was solved using inbuilt subroutine '*fmincon*' available in Matlab (Mathworks, Natick, MA, USA) for the following optimization structures.

Maximization of biomass (X) at final time point t_f

$\max_{t_f} \int_{t_0}^{t_f} \dot{Var}(t) = X(t_f)$, with initial condition S_{var}^0 at $t = 0$

$\dot{Var}(t) = f[S_{var}(t), C_{var}(t)]$

$S_{var}(t) = \left[X, V, S_1, S_2, S_3, \frac{E}{E^{Ref}}, \frac{E_2}{E_2^{Ref}}, \frac{E_3}{E_3^{Ref}}, TS_2, TS_3\right]$

$C_{var}(t) = [F(1), F(2), F(3)]$

Constraints:

$V < V_{max}$

$F_{min} \leq F(t) \leq F_{max}$

Where $S_{var}(t)$ and $C_{var}(t)$ are the system state variables and control variables respectively. The lower and upper bound for different state and control variables are specified in Table 6.2.

Table 6.2 Lower bound (lb) and upper bound (ub) for different state variables and control variables used in dynamic optimization algorithm in order to predict the substrate feeding rate and growth of microalga *Chlorella* sp. FC2 IITG grown under heterotrophic fed-batch mode of operation.

	Variables	lb	ub
Control variables	Glucose feed rate (L h^{-1})	0	0.168
	Nitrate feed rate (L h^{-1})	0	0.168
	Phosphate feed rate (L h^{-1})	0	0.168
State variable	Working volume (L)	0	6.1

6.2.4. Analyses of biomass, lipid and substrate concentration

A known volume of broth was collected at regular time intervals and subjected to centrifugation at 8000 × *g* for 10 minutes at 4°C. While the pellet obtained was used for the growth and lipid content measurements, the supernatant was used for the analyses of substrate utilization. Dry cell weight of culture estimated by measuring the optical density of cells as mentioned in section 3.2.5.1. Ascorbic acid method was used to measure phosphate concentration as explained in section 3.2.5.4. Estimation of glucose concentration was carried out by the dinitrosalicyclic acid method (Detailed in section 3.2.5.3). Nitrate content of the sample was estimated using protocol described in section 3.2.5.2. Neutral lipid content of biomass was estimated using Nile red method as explained in section 3.2.5.5. Similarly intracellular total lipid was quantified using gas chromatography as detailed in section 3.2.5.6. Estimation of acetate concentration was performed by HPLC as per procedure detailed in section 8.2.4.2. Biodiesel properties obtained from FC2 biomass was determined by using empirical formulas as described in section 3.2.5.7.

6.3. Results and discussion

With the aim of high cell density cultivation of FC2, the organism was grown under fed-batch mode of operation with different nutrient feeding strategies and medium

pH controlling mechanisms. In all the experiments glucose, sodium nitrate, dibasic potassium phosphate and combined solutions of trace elements and microelements (TME) were chosen as the key limiting nutrients for growth and hence were fed to maintain the optimal conditions.

6.3.1. Fed-batch with feeding of the nutrients based on their observed utilization profile

In this experiment, the intermittent feeding of the limiting substrates was done as and when the concentration of these nutrients went below 50% (w/v) of their original concentration in the media. The broth pH was maintained at 7.5-8 by the addition of 5 N HCl. Dynamic profile of glucose, nitrate and phosphate was obtained via analysis of sample collected at every four hours interval which was subsequently used for deciding the feeding requirements.

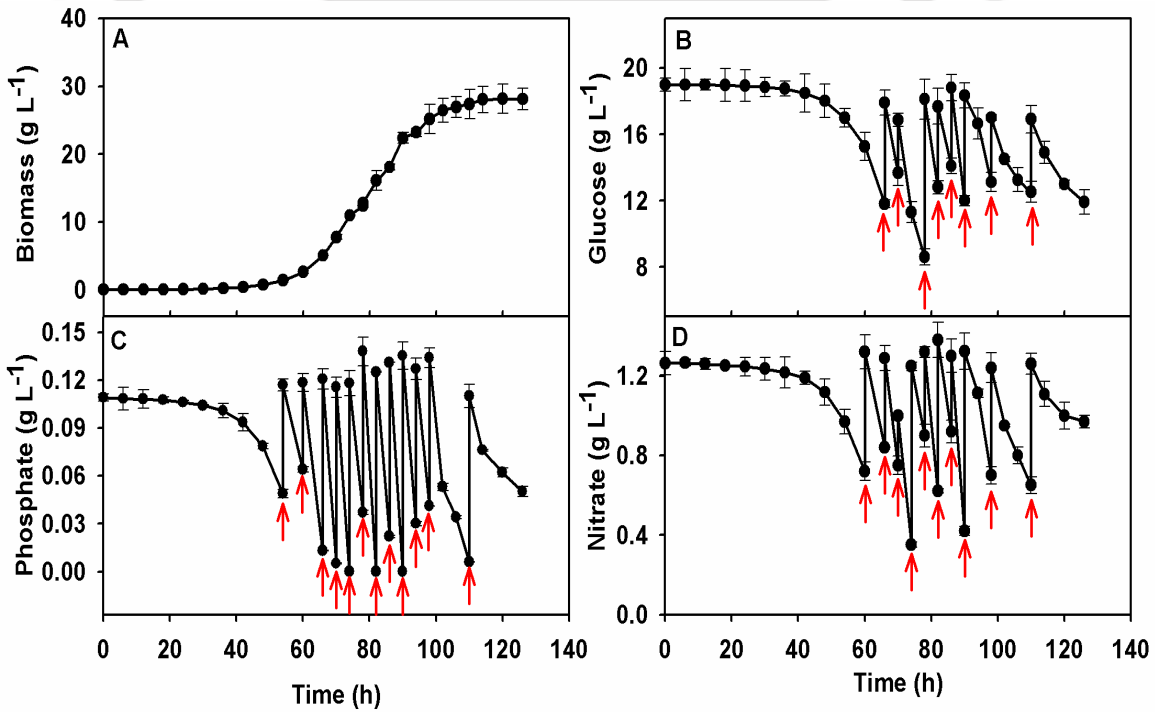

Fig. 6.1 Dynamic profiles for growth and substrate utilization of the strain FC2 grown under heterotrophic fed-batch mode of operation in optimized BG11 medium. The intermittent feeding of the limiting substrates was done based on the observed consumption profile in order to maintain 50% (w/v) of their original concentration in the media. The broth pH was maintained at 7.5-8 by addition of 5N HCl. (A) biomass

formation, (B) glucose concentration, (C) nitrate concentration and (D) phosphate concentration. Solid arrow mark (↑) represents the point of feeding of various substrates.

The fed-batch resulted in a final biomass titer of 28.2 g L^{-1} (Fig. 6.1 A) which was 3.6 times higher than maximal cell density obtained from the batch process (Table 4.4). Biomass productivity of 6.21 g L^{-1} day^{-1} was achieved at the end of 102 h which is considered to be moderately high in case of fed-batch cultivation of microalgae under heterotrophic condition. Biomass titer of 16.8 g L^{-1} with a productivity of ~2.2 g L^{-1} day^{-1} was reported for fed-batch cultivation of *Chlorella protothecoides* in a 5 L bioreactor that supports the present observation (Xiong et al., 2008). Further maximization of biomass titer to 51.2 g L^{-1} was achieved by strict maintenance of the process parameters and substrate concentrations at their optimal values. This shows that strict maintenance of media components at their optimal concentration might enhance the biomass titer and productivity. It is important to note that the concentration of phosphate in the optimized BG11 medium was less in comparison with other nutrients e.g. glucose and nitrate. Therefore, extent of phosphate utilization from the medium was very fast in the exponential phase of the growth making it very difficult to maintain its concentration above 50% of its initial value in the later phase of the fermentation. However, glucose (Fig. 6.1 B) and nitrate (Fig. 6.1 D) concentration could be maintained at their threshold level throughout entire fermentation period. As observed from the analysis of the samples at 74 h, 82 h and 90 h, phosphate was completely exhausted from the medium resulting in a nutritional starvation condition for the organism (Fig. 6.1 C). This repeated exposure of the organism to nutritional stress may retard the growth of organism at its optimum level resulting in a low biomass titer. Microalga *Monodus subterraneus* was also reported to show decreased growth under phosphate limitation (Khozin-Goldberg and Cohen, 2006). Phosphate depletion induces *psr*1 (phosphorus starvation response) gene in *Chlamydomonas reinhardtii* which rebuilds the phosphate pool via reducing the carbon

fluxes towards structural molecule DNA (Yehudai-Resheff et al., 2007). The gene transcript analysis also showed that growth rate retardation was negatively correlated with level of *psr*1 expression (Wykoff et al., 1999). The gene also activates several stress-associated chaperones, proteases and scavenging phosphatases (Moseley et al., 2006) which might have collectively reduced the growth. Thus, it may be hypothesized that the reduction in growth of FC2 may be due to changes in the expression of *psr1* gene. Therefore, feeding of the limiting nutrients based on their observed utilization profile offer drawbacks such as experimental difficulty in maintaining the nutrient concentration with lower optimal value during exponential phase of the growth which in turn causes momentary nutritional stress to the organism leading to lower biomass titer. In order to address these challenges we have further demonstrated a fed-batch where feeding of the key nutrients were designed by a mechanistic model coupled with dynamic optimization algorithm.

6.3.2. Fed-batch with model guided feeding recipe of the nutrients and HCl based pH control

In this fed-batch fermentation the feeding of limiting nutrients was done as per the model guided optimized feeding rates. Interestingly, model guided feeding strategy resulted in a significant increase (71.3%) in biomass titer with a final biomass concentration of 48.3 g L^{-1} (Fig. 6.2 A) when compared with the fed-batch based on observed substrate utilization profile (Fig. 6.1 A). Fed-batch cultivation of *Chlorella pyrenoidosa* with optimal feeding rates designed by hybrid neural network model was reported to produce 5.81 fold higher biomass titer in comparison to preliminary fed-batch operation (Wu and Shi, 2007). Feeding of the key nutrients e.g. nitrate, phosphate, glucose (Fig. 6.2 B) and TME ensures nutrient sufficient condition throughout the fermentation and thereby, maintaining the specific growth rate of the organism at its optimal level.

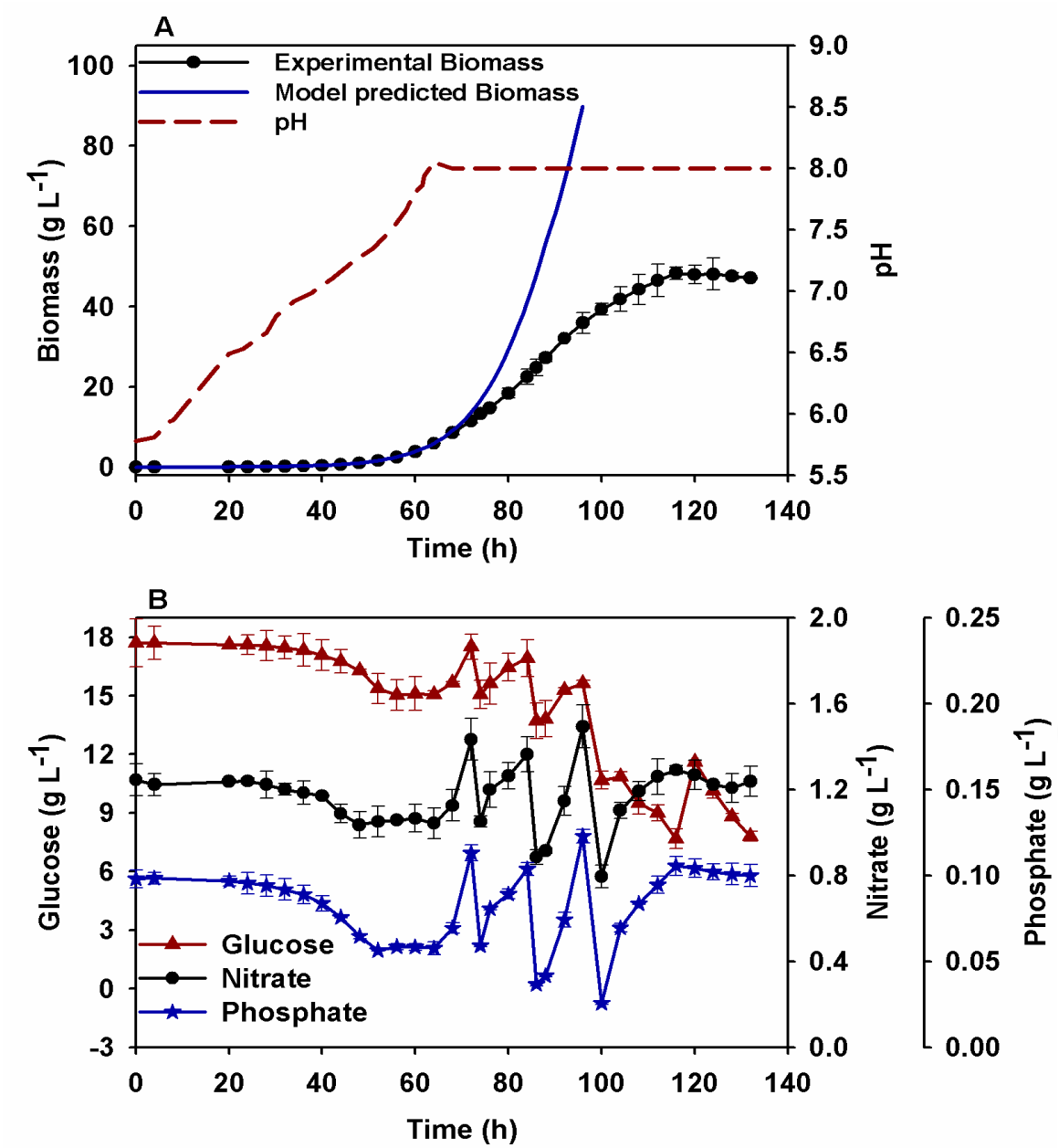

Fig. 6.2 Dynamic profiles for growth, broth pH and substrate utilization of the strain FC2 grown under heterotrophic fed-batch mode of operation in optimized BG11 medium. The feeding of the limiting nutrients were done as per the model guided feeding rates and the broth pH was maintained at 7.5-8 via addition of 5 N HCl. (A) model predicted biomass formation (—), was compared with the experimentally determined values (—●—) and (B) experimentally determined concentrations of glucose (—▲—), nitrate (—●—) and phosphate (—∗—).

It is important to note that during the post 72 h of fermentation, the model predicted profile for the growth of the organism deviated significantly from corresponding experimental values (Fig. 6.2 A). This reduced experimentally observed biomass titer may be attributed to the increasing salinity stress to the organism caused due to the addition of

hydrochloric acid (HCl) in order to maintain the broth pH. The medium pH was found to increase gradually from 5.78 to 8 within 64 h of fermentation and from this point a total of 100 mL 5N HCl was added till the end of fermentation in order to avoid further raise in pH (Fig. 6.2 A). The assimilation of nitrate from extracellular medium into amino acids/proteins consumes equimolar amount of hydrogen ions (H^+) from the surroundings, hence utilization of nitrate resulted in alkalization of media (Ullrich et al., 1998). Addition of HCl has resulted in accumulation of ~130 mM of salt at the end of the batch and hence, causing substantial salinity stress to the organism. The effect of salinity on growth of FC2 was studied by supplementing the optimized BG11 media with 90 mM sodium chloride in a separate experiment (Data is detailed in section 2 of appendix A). A 70% reduction in the biomass titer was observed with 90 mM salinity as compared to the growth in optimal media composition which signifies the negative effect of salinity on growth of FC2. Pancha et al. (2015) also showed 30% reduction in growth of *Scenedesmus* sp. CCNM 1077 under 100 mM salt concentration. The increased salinity induces the accumulation of reactive oxygen species (ROS) thus leading to oxidative stress resulting in the degradation of intracellular macromolecules. To that end, another fed-batch experiment was designed with an alternate pH control strategy coupled with model guided feeding recipe for high cell density cultivation.

6.3.3. High cell density-lipid rich cultivation of FC2 through model guided feeding recipe of the nutrients and substrate driven pH control

The entire fermentation was divided into two phases: growth phase for high cell density cultivation of FC2 and lipid induction phase. In the first phase, high cell density was achieved via coupling model guided feeding of key nutrients e.g. nitrate, phosphate, glucose and TME with substrate (nitric acid) driven pH control. During growth phase sodium nitrate was used as nitrogen source until pH of the medium became 8 and then

subsequent addition of nitric acid was done instead of sodium nitrate which serves a dual purpose of nitrogen source and acid source for maintaining the pH of the medium at its set point. While, concentration of the biomass reached its maximum value, lipid induction phase was initiated through addition of sodium acetate.

6.3.3.1. Growth phase

The fed-batch strategy with model guided feeding recipe and substrate driven pH control resulted in a biomass titer of 87 g L^{-1} with a biomass productivity of 19.75 g L^{-1} day^{-1} (Fig. 6.3 A). This biomass titer was 208% and 80% higher when compared with the fed-batch cultivation based on observed substrate utilization profile (Fig. 6.1) and model guided feeding of the substrate (Fig. 6.2) along with pH control through HCl respectively. The enhancement of biomass titer may be attributed to maintenance of substrates concentration at their optimal values throughout fermentation and control of other process parameters below the toxic level. While there are many microalgae reported with higher biomass titer under heterotrophic condition, present cultivation strategy of the strain FC2 exhibited significantly higher biomass productivity in comparison with the majority of the strain reported in the literature (Table A1 in appendix A). The biomass yield coefficient of the strain FC2 was found to be 0.735 g biomass g^{-1}glucose which was highest among all the strains reported in the literature for high cell density cultivation (Table A1 in appendix A). Thus efficient feeding of glucose avoids overconsumption of the nutrient resulting in significant generation of biomass. In other words, the organism requires less glucose to generate same amount of biomass when the substrates are fed effectively through model guided strategy. This yield coefficient was found to be higher than fed-batch cultivation based on substrate utilization profile (0.649 g biomass g^{-1}glucose) and model guided feeding of substrate (0.67 g biomass g^{-1}glucose) along with HCl based pH control respectively. The improvement in the biomass yield coefficient might be attributed to the

disappearance of phosphate starvation stress and salinity stress which were the governing factors for reduced growth in the earlier discussed fed-batches. Carbon flux shifts its paradigm towards enhanced maintenance of cell (Section 8.3.3), rather than biomass synthesis due to stress (Rajvanshi and Venkatesh, 2011).

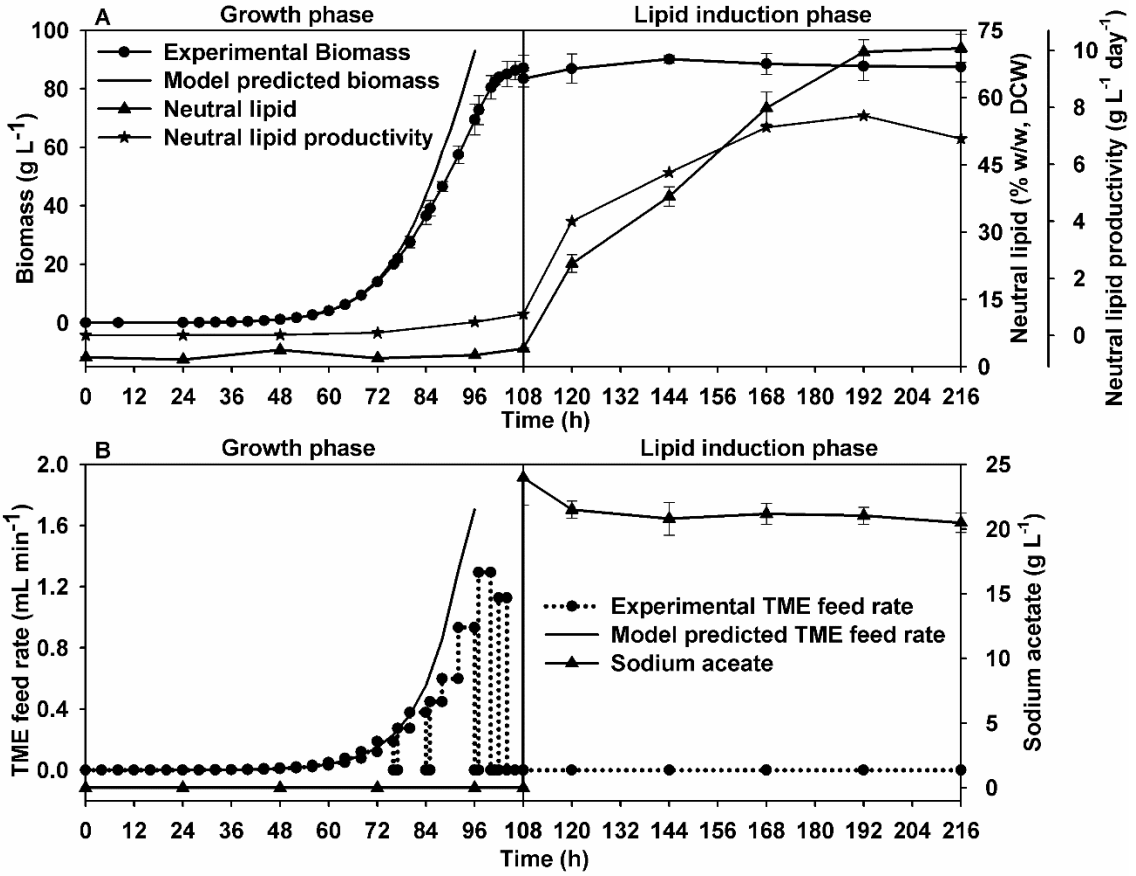

Fig. 6.3 Dynamic profiles for growth, intracellular neutral lipid content & productivity, TME feeding rate and acetate utilization of the strain FC2 grown in a 7.5 L automated bioreactor under heterotrophic fed-batch mode of operation in optimized BG11 medium. The feeding of the limiting nutrients was done as per model guided feeding strategy along with concurrent maintenance of broth pH by substrate itself. (A) model predicted biomass formation (—) was compared with the experimentally determined profile (—●—) in the growth phase of the fermentation, and (B) comparison of model predicted TME feeding rate (—) with the experimentally determined TME feeding rate (···●···)

Interestingly, an oscillation in the utilization profile of glucose (Fig. 6.4 A), nitrate (Fig. 6.5 A) and phosphate (Fig. 6.6 A) was observed once their concentration in the broth reached 15.1 g L^{-1}, 1.04 g L^{-1} and 0.059 g L^{-1} respectively. The specific growth rate of the organism was found to be maximal at these concentrations of the nutrients. Therefore,

frequent substrate feeding was required to maintain the desired concentration of the nutrients leading to an oscillation in their utilization profile. While a better corroboration was observed between the model predicted utilization profiles of nitrate, phosphate and glucose with the corresponding experimental values during the initial phase of fermentation, a deviation was observed with increasingly higher concentration of biomass in the later phase of fermentation. Similarly, an improved growth of the organism was predicted when compared with the experimental values at later time point. Previously, the strain *C. vulgaris* was reported to exhibit similar profile of reduced growth with increase in biomass concentration (Doucha and Lívanský, 2012). This might be attributed by either accumulation of inhibitory metabolic products in fermenter or overcrowding of broth with cells (Özadali and Özilgen, 1988).

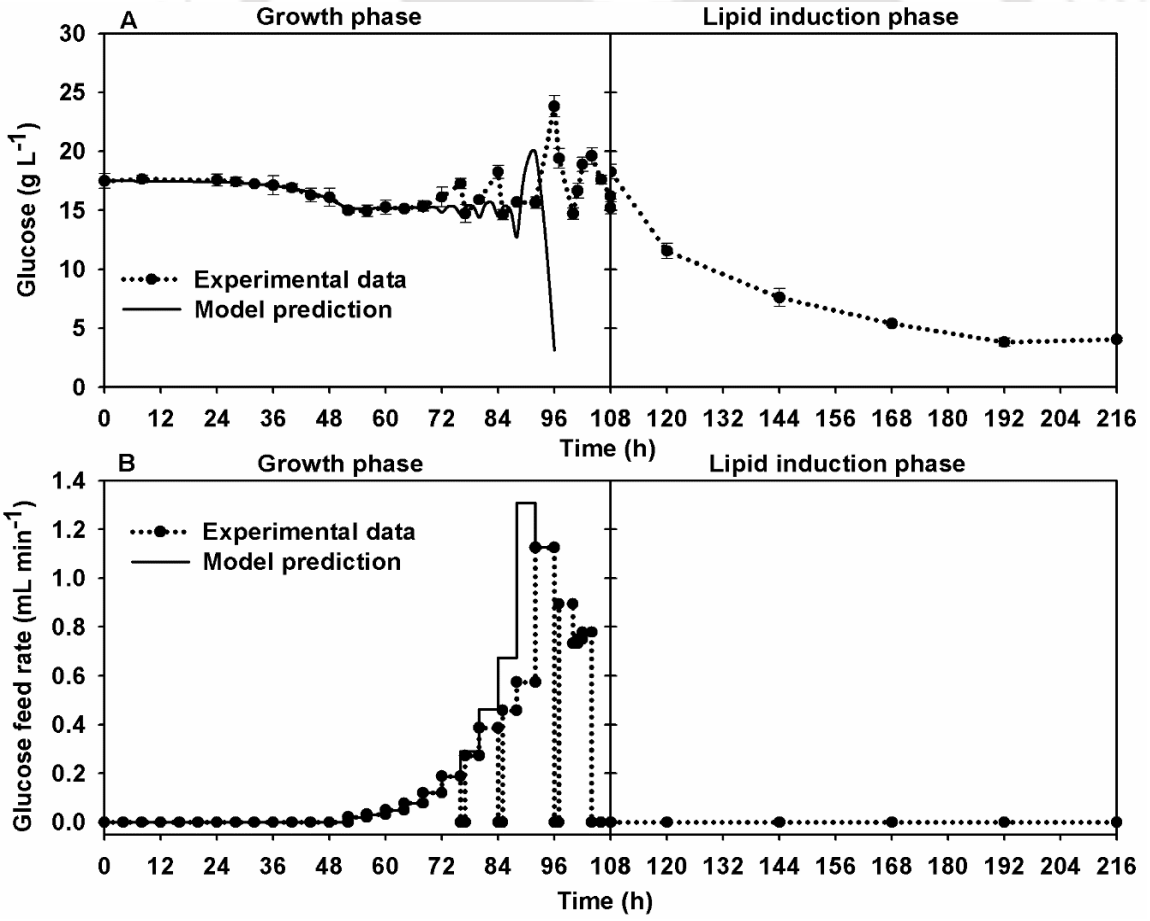

Fig. 6.4 Model predicted (—) dynamic profiles for glucose utilization (A) and feeding rate of glucose (B) were compared with the corresponding experimental values (—●—). The

strain FC2 was grown under heterotrophic fed-batch mode of operation in optimized BG11 medium. The feeding of the limiting nutrients was done as per model guided feeding strategy along with concurrent maintenance of broth pH by substrate itself.

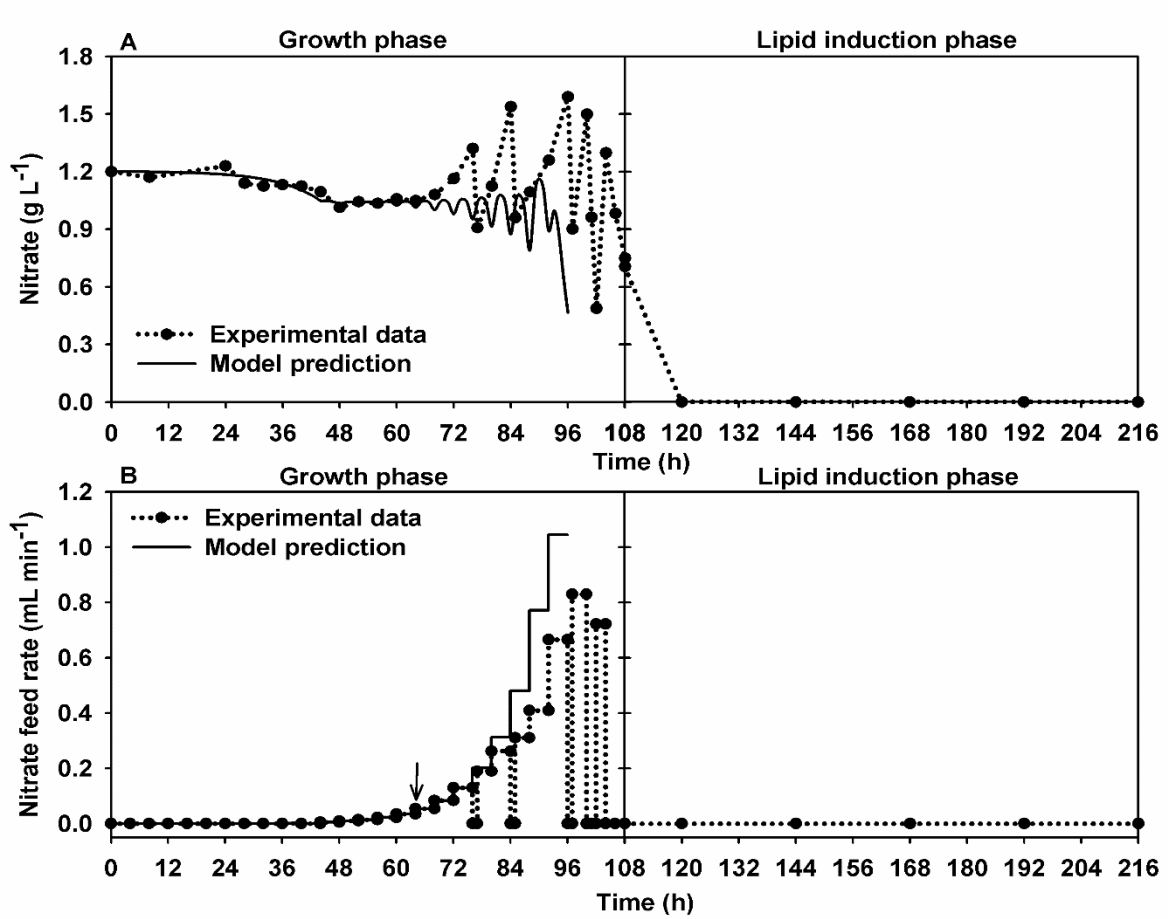

Fig. 6.5 Model predicted (—) dynamic profiles for nitrate utilization (A) and feeding rate of nitrate (B) were compared with the corresponding experimental values (···●···). The strain FC2 was grown under heterotrophic fed-batch mode of operation in optimized BG11 medium. The feeding of the limiting nutrients was done as per model guided feeding strategy along with concurrent maintenance of broth pH by substrate itself. Solid arrow mark (↓) represents the starting point of nitric acid feeding in place of sodium nitrate.

This lesser growth of the organism was linked to the lesser utilization of the substrates from the fermentation broth. Therefore, in the later phase of the fermentation the feed rates of the glucose (Fig. 6.4 B), nitrate (Fig. 6.5 B) and phosphate (Fig. 6.6 B) were readjusted as per the objective of maintaining optimal concentration of the nutrients and not strictly based on model prediction. The readjusted feed rates were calculated based on corresponding model predicted feed rates and the reduction in specific growth rate as

compared to the model predicted. In the present study, TME feeding profile was modeled as per the exponential feed rate. However, maintaining exponential feeding rate was practically difficult. Therefore, the total amount of TME to be fed over each four hour time interval was supplied as constant flow rate which resulted in stepwise feeding pattern instead of exponential one as predicted by the model (Fig. 6.3 B).

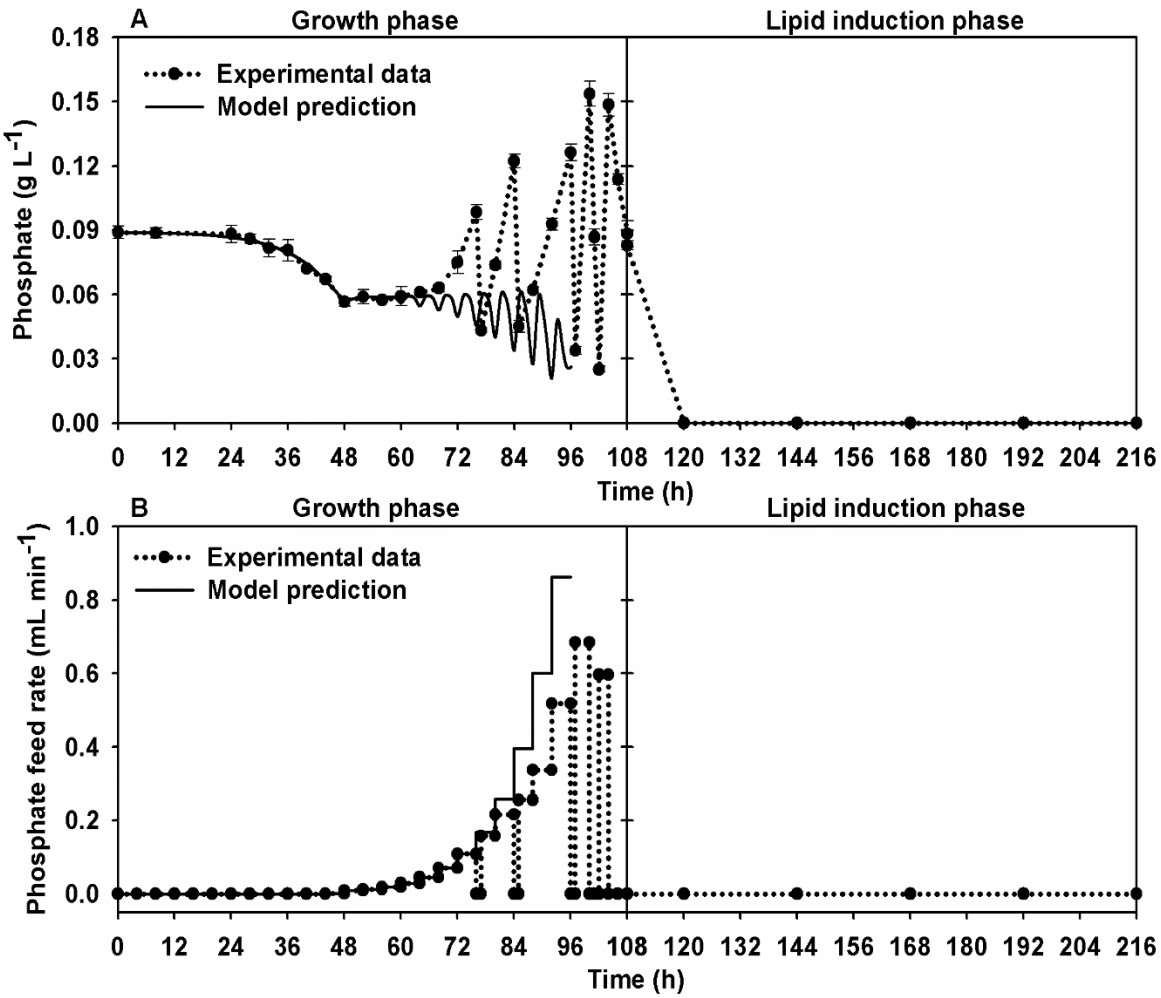

Fig. 6.6 Model predicted (—) dynamic profiles for phosphate utilization (A) and feeding rate of phosphate (B) was compared with the corresponding experimental values (—●—). The strain FC2 was grown under heterotrophic fed-batch mode of operation in optimized BG11 medium. The feeding of the limiting nutrients was done as per model guided feeding strategy along with concurrent maintenance of broth pH by substrate itself.

One of the key process engineering strategies adopted in the present study was the feeding of nitric acid instead of sodium nitrate which serves dual purpose of pH maintenance and nitrogen source in the growth phase of the organism. Patino et al. (2007)

reported that *Chlorella vulgaris* grown on nitric acid concurrently maintained broth pH. Supplementation of nitric acid eliminates the possibility of formation of metal salt in HCl driven pH control and also stabilizes the broth pH (Fig. 6.7 A). Dissolved oxygen concentration was gradually decreased to 50% of its saturation value with the initiation of active growth phase and was maintained thereafter through increase in agitation speed and aeration rate (Fig. 6.7 B). In order to avoid any harsh condition to the organism the maximum limit of the agitation speed and aeration rate was constrained to 400 rpm and 4 L min^{-1} respectively. Once these maximum limits were attained, the DO was maintained by additionally purging pure oxygen, where total flow rate of air and pure oxygen mixture was maintained in the maximum limit of aeration.

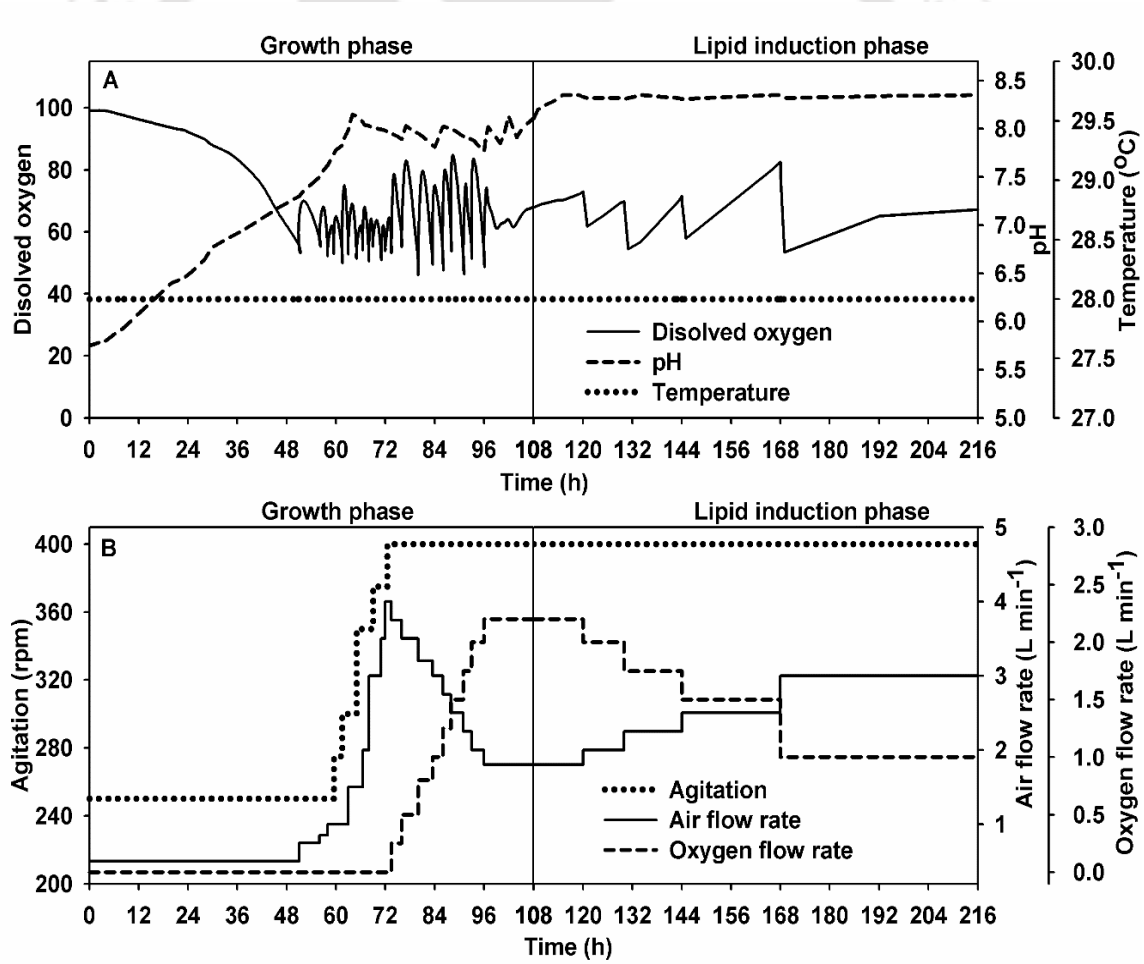

Fig. 6.7 Dynamic profiles of different process parameters obtained during growth of the strain FC2 in a 7.5 L automated bioreactor under heterotrophic fed-batch mode of operation in optimized BG11 medium. The feeding of the limiting nutrients was done as per model guided feeding strategy along with concurrent maintenance of broth pH by

substrate itself. (A) dissolved oxygen (DO) concentration (—), fermentation broth pH (----) & broth temperature (⋯⋯) and (B) aeration rate (—), agitation rate (⋯⋯) & pure oxygen purging rate (-----)

6.3.3.2. Lipid induction phase

At the end of the growth phase when the biomass concentration reached its maximum the lipid induction phase was initiated via addition of sodium acetate as an inducer. From this point onwards feeding of sodium nitrate or nitric acid, phosphate, and TME was completely stopped in order to achieve combined effect of nutritional starvation and lipid inducer on accumulation of neutral lipid in the organism. At the end of the growth phase, an optimum sodium acetate concentration of 24 g L^{-1} was achieved through feeding of 5 M sodium acetate into the bioreactor. Acetate consumption is coupled with consumption of proton (H^+) with a ratio of 1:1 through monocarboxylic/proton transporter (Perez-Garcia et al., 2011) leading to alkalization of broth by reduced H^+ ion and concurrently increased hydroxyl ion. Therefore, acetate consumption was proportional with increase in medium pH. Hence, in order to maintain media pH and optimal acetate concentration in the broth, acetic acid feeding was done which was kept in cascade mode with medium pH. It is important to note that, feeding of sodium acetate was done only once in the beginning of the lipid induction phase, thereafter acetate concentration was maintained through addition of acetic acid. Acetic acid was shown to serve the purpose of both as a carbon source and control of medium pH towards cultivation of *Crypthecodinium cohnii* (De Swaaf et al., 2003). The organism was found to continue its growth in the lipid induction phase and reached a final biomass titer of 90.15 g L^{-1}. Combined effect of lipid inducer and nutritional starvation resulted in lipid enrichment of 70.2% w/w DCW (Fig. 6.3 A), with a net neutral lipid productivity of 7.7 g L^{-1} day^{-1}. Freshwater microalga *Chlorella sorokiniana* FC6 IITG was reported with a lipid enrichment of ~55% w/w, DCW when subjected to sodium acetate dosing under

mixotrophic mode of fermentation (Kumar et al., 2014). This neutral lipid productivity of the strain FC2 was significantly higher than any other strains reported in the literature (Table A2 in appendix A) with the exception of *Chlorella vulgaris* which showed a lipid productivity of 8.19 g L^{-1} day^{-1} (Doucha and Lívanský, 2012). However, as compared to the present study the strain *Chlorella vulgaris* was grown with substantially higher initial concentration of the biomass and higher working volume of 50 L. This resulted in higher biomass titer and increased net lipid productivity in spite of lipid content of only 9.7% w/w, DCW.

6.3.4. Fatty acid methyl esters (FAME) composition and evaluation of biodiesel properties

Lipid rich biomass harvested at the end of the fermentation was processed through two stage sequential *in situ* transesterification method towards conversion of lipid into FAME. Fatty acid chain lengths of C16:0, C16:1, C18:0, C18:1 and C18:2 were found to comprise 99% of FAME composition (Table 6.3). This was found to fall in the range of petroleum based diesel which involves alkanes in the ranges of C15 - C19 (McArthur and Spalding, 2004). In general, higher cetane number of biodiesel is desirable to shorten ignition delay and eliminates engine knocking which is one of the causes of engines tear. In the present study, a higher cetane number of 58.07 was achieved when compared with the ASTM or EN standard (Table 6.4). Flash point value of 159 was found to be much higher than the minimum threshold specific by the ASTM standard (Table 6.4). Hence, the biodiesel obtained in the present study was found to be less flammable. The cold flow properties such as cloud point and pour point were found to be 5.85 and 2.8 respectively which were higher as compared with the other microalgae grown under photoautotrophic or mixotrophic condition (Kumar et al., 2014). Therefore, biodiesel obtained from microalga

FC2 grown under heterotrophic condition can be used for commercial applications as it satisfies overall ASTM D6751–15a and EN 14,214 standards.

Table 6.3 Fatty acid methyl ester (FAME) compositions obtained from the strain FC2 grown under heterotrophic fed-batch mode of operation in optimized BG11 medium via model guided feeding recipe of nutrients along with concurrent maintenance of broth pH by substrate itself.

Fatty acid name	Code	FAME composition (%)	FAME details	% values
Lauric acid	[C12:0]	0.486	Total saturated FAME	32.48
Miristic acid	[C14:0]	0.11	Total monounsaturated FAME	45.59
Palmitic acid	[C16:0]	24.15		
Palmitoleic acid	[C16:1]	5.97	Total polyunsaturated FAME	21.78
Stearic acid	[C18:0]	7.49		
Oleic acid	[C18:1]	39.62	Other FAME	0.15
Linoleic acid	[C18:2]	21.78	Total FAME (w/w DCW)	73.8
Arachidic acid	[C20:0]	0.105		
Behenic acid	[C22:0]	0.138		

Table 6.4 Property of biodiesel obtained from the strain FC2 grown under heterotrophic fed-batch mode of operation in optimized BG11 medium via model guided feeding recipe of nutrients along with concurrent maintenance of broth pH by substrate itself. Properties are calculated using empirical formulas based on experimentally determined FAME compositions and compared with ASTM D6751–15a and EN14214

Biodiesel properties	Units	FC2 values	Standards	
			ASTM D6751–15a	EN 14214
Viscosity (η)	$mm^2\ s^{-1}$	4.48	1.9 - 6	3.5 - 5
Cetane number (CN)		58.07	>47	>51
Flash point (T_f)	^0C	159.09	>93	>101
Cloud point (T_c)	^0C	5.85	ND	ND
Pour point (T_p)	^0C	2.80	ND	ND
Saponification value (SV)	mg KOH g^{-1}	203.63	ND	ND
Iodine value (IV)	% (g I_2 g^{-1} oil)	99.58	ND	<120
Degree of unsaturation (DU)		87.38	ND	ND
Highest Heating value (HHV)	MJ kg^{-1}	39.74	ND	ND

ND-not defined

6.4. Conclusions

The present study has developed an process engineering strategy to obtain high cell density cultivation of the lipid rich oleaginous microalga FC2 via designing a model guided feeding recipe along with substrate driven pH control and using acetate as driver for lipid biosynthesis. The process has shown extremely high lipid and biomass productivity of 7.7 and 19.75 g L^{-1} day^{-1} respectively, which was significantly higher among the other strains characterized for high cell density cultivation. It is also important to mention that, the biomass yield with respect to the glucose consumed was relatively higher than any other studies reported so far for high cell density heterotrophic cultivation and the process has effectively avoided the overconsumption of nutrients. The strategic process engineering approach developed in the preset study can be employed for maximization of product yields and to reduce overconsumption of nutrients. The process strategy also opens up scope for further economic feasibility analysis and scale up for commercial applications.

6.5. References

1. Alagesan S., Gaudana S.B., Krishnakumar S., Wangikar P.P., 2013. Model based optimization of high cell density cultivation of nitrogen-fixing cyanobacteria. Bioresource Technology. 148, 228–233.
2. Banga J.R., Balsa-Canto E., Moles C.G., Alonso A.A., 2005. Dynamic optimization of bioprocesses: Efficient and robust numerical strategies. Journal of Biotechnology. 117, 407–419.
3. De Swaaf M.E., Sijtsma L., Pronk J.T., 2003. High-cell-density fed-batch cultivation of the docosahexaenoic acid producing marine alga *Crypthecodinium cohnii*. Biotechnology and Bioengineering. 81, 666–672.

4. Doucha J., Lívanský K., 2012. Production of high-density *Chlorella* culture grown in fermenters. Journal of Applied Phycology. 24, 35–43.

5. Droop M.R., 1968. Vitamin B 12 and marine ecology. IV. The kinetics of uptake, growth and inhibition in *Monochrysis lutheri*. Journal of the Marine Biological Association of the UK. 48, 689–733.

6. John E.H., Flynn K.J., 2000. Modelling phosphate transport and assimilation in microalgae; how much complexity is warranted? Ecological Modelling. 125, 145–157.

7. Khozin-Goldberg I., Cohen Z., 2006. The effect of phosphate starvation on the lipid and fatty acid composition of the fresh water eustigmatophyte *Monodus subterraneus*. Phytochemistry. 67, 696–701.

8. Kim S., Kim H., Ko D., Yamaoka Y., Otsuru M., Kawai-Yamada M., Ishikawa T., Oh H.-M., Nishida I., Li-Beisson Y., 2013. Rapid induction of lipid droplets in *Chlamydomonas reinhardtii* and *Chlorella vulgaris* by Brefeldin A. PLoS ONE. 8, e81978.

9. Kumar A., Singh L.K., Ghosh S., 2009. Bioconversion of lignocellulosic fraction of water-hyacinth (*Eichhornia crassipes*) hemicellulose acid hydrolysate to ethanol by *Pichia stipitis*. Bioresource Technology. 100, 3293–3297.

10. Kumar V., Muthuraj M., Palabhanvi B., Ghoshal A.K., Das D., 2014. High cell density lipid rich cultivation of a novel microalgal isolate *Chlorella sorokiniana* FC6 IITG in a single-stage fed-batch mode under mixotrophic condition. Bioresource Technology. 170, 115–124.

11. Lemesle V., Mailleret L., 2008. A mechanistic investigation of the algae growth "Droop" model. Acta Biotheoretica. 56, 87–102.

12. McArthur H., Spalding D., 2004. Engineering materials science: Properties, uses, degradation, remediation. Woodhead Publishing, Cambridge.

13. Moseley J.L., Chang C.-W., Grossman A.R., 2006. Genome-based approaches to understanding phosphorus deprivation responses and PSR1 control in *Chlamydomonas reinhardtii*. Eukaryotic Cell. 5, 26–44.

14. Muthuraj M., Kumar V., Palabhanvi B., Das D., 2014. Evaluation of indigenous microalgal isolate *Chlorella* sp. FC2 IITG as a cell factory for biodiesel production and scale up in outdoor conditions. Journal of Industrial Microbiology and Biotechnology. 41, 499–511.

15. Negi S., Barry A., Friedland N., Sudasinghe N., Subramanian S., Pieris S., Holguin F.O., Dungan B., Schaub T., Sayre R., 2015. Impact of nitrogen limitation on biomass, photosynthesis, and lipid accumulation in *Chlorella sorokiniana*. Journal of Applied Phycology. 1–10.

16. Özadali F., Özilgen M., 1988. Microbial growth kinetics of fed-batch fermentations. Applied Microbiology and Biotechnology. 29, 203–207.

17. Pancha I., Chokshi K., Maurya R., Trivedi K., Patidar S.K., Ghosh A., Mishra S., 2015. Salinity induced oxidative stress enhanced biofuel production potential of microalgae *Scenedesmus* sp. CCNM 1077. Bioresource Technology. 189, 341–348.

18. Patino R., Janssen M., von Stockar U., 2007. A study of the growth for the microalga *Chlorella vulgaris* by photo-bio-calorimetry and other on-line and off-line techniques. Biotechnology and Bioengineering. 96, 757–767.

19. Perez-Garcia O., Escalante F.M., de-Bashan L.E., Bashan Y., 2011. Heterotrophic cultures of microalgae: metabolism and potential products. Water Research. 45, 11–36.

20. Rajvanshi M., Venkatesh K.V., 2011. Phenotypic characterization of *Corynebacterium glutamicum* under osmotic stress conditions using elementary mode analysis. Journal of Industrial Microbiology and Biotechnology. 38, 1345–1357.

21. Rodolfi L., Chini Zittelli G., Bassi N., Padovani G., Biondi N., Bonini G., Tredici M.R., 2009. Microalgae for oil: Strain selection, induction of lipid synthesis and outdoor mass cultivation in a low-cost photobioreactor. Biotechnology and Bioengineering. 102, 100–112.

22. Shen Y., Yuan W., Pei Z., Mao E., 2010. Heterotrophic culture of *Chlorella protothecoides* in various nitrogen sources for lipid production. Applied Biochemistry and Biotechnology. 160, 1674–1684.

23. Turon V., Trably E., Fayet A., Fouilland E., Steyer J.-P., 2015. Raw dark fermentation effluent to support heterotrophic microalgae growth: microalgae successfully outcompete bacteria for acetate. Algal Research. 12, 119–125.

24. Ullrich W.R., Lazarova J., Ullrich C.I., Witt F.G., Aparicio P.J., 1998. Nitrate uptake and extracellular alkalinization by the green alga *Hydrodictyon reticulatum* in blue and red light. Journal of Experimental Botany. 49, 1157–1162.

25. Wu Z., Shi X., 2007. Optimization for high-density cultivation of heterotrophic *Chlorella* based on a hybrid neural network model. Letters in Applied Microbiology. 44, 13–18.

26. Wykoff D.D., Grossman A.R., Weeks D.P., Usuda H., Shimogawara K., 1999. Psr1, a nuclear localized protein that regulates phosphorus metabolism in *Chlamydomonas*. Proceedings of the National Academy of Sciences. 96, 15336–15341.

27. Xiong W., Li X., Xiang J., Wu Q., 2008. High-density fermentation of microalga *Chlorella protothecoides* in bioreactor for microbio-diesel production. Applied Microbiology and Biotechnology. 78, 29–36.

28. Yehudai-Resheff S., Zimmer S.L., Komine Y., Stern D.B., 2007. Integration of chloroplast nucleic acid metabolism into the phosphate deprivation response in *Chlamydomonas reinhardtii*. The Plant Cell. 19, 1023–1038.

CHAPTER 7

Process development for high biomass and lipid productivity in continuous cultivation

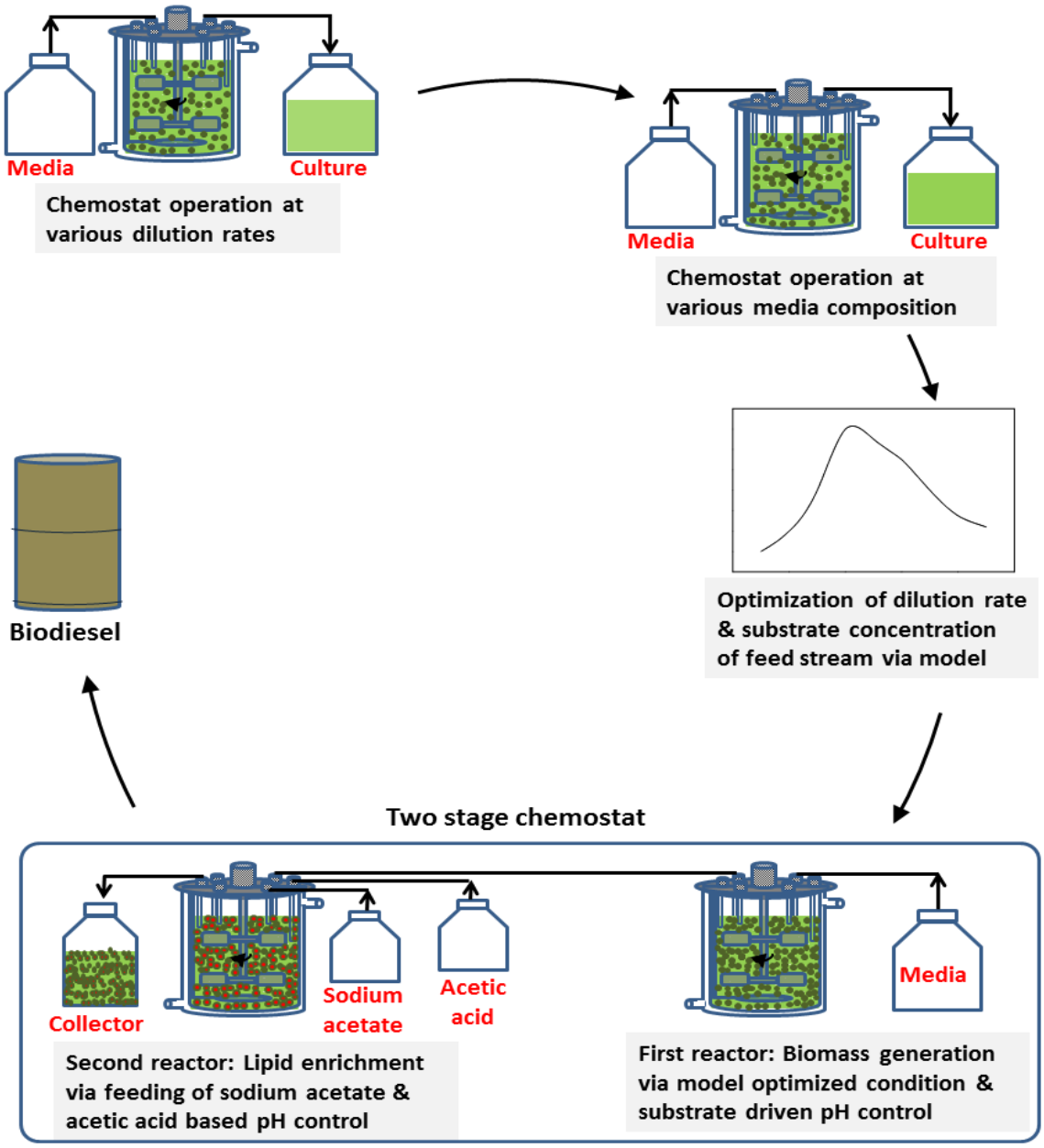

Process development for high biomass and lipid productivity in continuous mode of cultivation via model based optimization of control variables.

7.1. Background and motivation

The high cell density-lipid rich fed-batch cultivation via model guided feeding recipe along with substrate driven pH control, has shown 7.7 and 19.75 g L^{-1} day^{-1} lipid and biomass productivity respectively. This was significantly higher than many reported strains so far, however further enhancement can be expected in continuous mode of operation. Superior biomass productivity can be achieved in continuous cultivation of organism (Chen and Johns, 1995; Stanbury et al., 2003). The biomass productivity of *Chlamydomonas reinhardtii* was reported to vary with dilution rate and substrate concentration of feed stream (Chen and Johns, 1996). Cultivation of organism at optimal condition may result in enhanced biomass and/or lipid productivity. Microalga *Chlorella sorokiniana* FC6 IITG showed maximal biomass and lipid productivity at an optimized dilution rate of 0.54 day^{-1} (Kumar et al., 2016). Model guided optimization of dilution rate and substrate concentrations predicted an improved lipid productivity of 12.27 g L^{-1} day^{-1} in the continuous cultivation of *A. protothecoides,* UTEX 25 (De la Hoz Siegler et al., 2011). Various kinetic models were reported in the literature for the growth kinetics of microorganisms as explained in section 5.1. The multi-nutrient mechanistic model developed in the present study (Chapter 5) showed better predictability of growth kinetics under both nutrient sufficient and starved condition than existing models. Such powerful predictive tools can be used for optimization of substrate concentrations of feed stream and dilutions rate in order to maximize biomass and lipid productivity.

Another potential bottleneck involved in microalgal biofuel technology is mutual exclusivity of biomass production and lipid accumulation (Rodolfi et al., 2009). Nutrient limiting condition may enhance the lipid accumulation in microalgae however, no significant improvement in net lipid productivity can be observed due to reduction of biomass titer or productivity (Xin et al., 2010). Hence, growth and lipid generation phase

need to be decoupled and performed separately by using growth supporting and lipid inducing nutrients separately and efficiently. Previously, high cell density-lipid rich cultivation in fed-batch mode of operation was performed in two phases: growth phase and lipid induction phase (Chapter 6). Similarly, two-stage chemostat may also yield both improved biomass and lipid productivity.

The present study demonstrates a process engineering strategy for continuous cultivation of lipid rich microalgal biomass with high biomass and net lipid productivity. Typically, in a fermentation process multiple rate limiting substrates may co-exists at any instance of time. Hence, in the first step effect of dilution rate and concentration of the limiting substrates in the feed stream was evaluated for biomass productivity as process response. These experiments helped in identification of key parameters having significant impact on biomass productivity which were further optimized using model based optimization algorithm with the objective function of maximization of cell mass productivity. Finally, a process was demonstrated for continuous production of lipid rich algal biomass with high productivity in two sequential bioreactors: first reactor was used for the generation of biomass followed by intracellular lipid enrichment in the second reactor through addition of lipid inducer.

7.2. Material and methods

7.2.1. Cultivation conditions

Inoculum preparation was carried out as explained in section 5.2.1. Active mid-log phase culture of cell density of 3 g L^{-1} was inoculated (1%, v/v) in all the experiment. The experiments were carried out in 7.5 L automated bioreactor (New Brunswick™ BioFlo®/CelliGen® 115) at 28°C temperature. Dissolved oxygen (DO) concentration was maintained more than 50% of saturation with varying the aeration rate (1-4 L min^{-1}), agitation rate (250-400 rpm) and by changing pure oxygen supply rate (0-1.75 L min^{-1}) in

order to avoid any effect arising from DO limitation. Inoculum preparation and bioreactor experiments were carried out under heterotrophic condition under complete dark environment.

7.2.2. Effect of dilution rate and feed stream substrate concentration on biomass productivity

In the first step, effect of different dilution rates on biomass productivity was assessed using optimal media composition under heterotrophic growth condition. Initially, organism was grown under batch mode till biomass concentration reaches 1.2 g L^{-1} and then continuous mode of operation was initiated. The optimized media supports generation of 1.2 g L^{-1} of biomass without any substrate limitation (Section 5.3.1) and hence mode of operation was changed at this concentration of biomass. Four different dilution rates 0.03 h^{-1}, 0.05 h^{-1}, 0.08 h^{-1} and 0.1 h^{-1} were chosen to evaluate biomass productivity.

In the next step, effect of varied feed stream composition on biomass productivity was evaluated at the best dilution rate (0.08 h^{-1}) obtained from previous experiments. Evaluation was carried out for three different feed stream compositions which differed in terms of concentration of limiting nutrients nitrate and phosphate while concentration of all other nutrients remained same. Nitrate and phosphate concentration in the feed stream composition C1, C2 and C3 are mentioned in Table 7.1.

Table 7.1 Substrate concentrations in feed-streams used for cultivation of stain under various dilution rates and feed-stream compositions

Feed concentration	**C1**	**C2**	**C3**
Phosphate (mg L^{-1})	107	200	200
Nitrate (g L^{-1})	1.2	1.2	1.6
Glucose (g L^{-1})	17.73	17.73	17.73
Trace and micro elements	Same as BG11 media		

Sampling was carried out at regular time intervals for determination of growth and substrate utilization profile.

7.2.3. Formulation of multi-nutrient mechanistic model for optimization of feed stream composition and dilution rate towards high biomass productivity

From the preliminary characterization, it was found that the control variables such as concentration of the limiting nutrients in the feed stream and dilution rate, significantly influence biomass productivity in a chemostat. Therefore, optimization of these control variables was expected to result in high algal biomass productivity, one of the important criteria towards development of sustainable bioprocess. In the present study, optimization of feed stream composition and dilution rate was performed using a multi-nutrient mechanistic model. It was developed (chapter 5) and demonstrated to capture growth kinetics of strain under nutrient sufficient and nutrient starved condition in batch cultivation mode. The model equations were obtained from previous work (chapter 5) and modified for continuous cultivation of microalgae. Further, specific growth rate (μ) of the organism was found to decrease with the increase in biomass titer as observed in high cell density fed-batch cultivation (Fig. 6.5 A). This phenomenon was more prominent at higher concentration of cell mass in the broth. Therefore, equation of specific growth rate was re-modeled taking into account biomass inhibition in the form of Hill's equation with a maximum attainable biomass concentration of 91 g L^{-1} (equation 7.1). It is important to note that the maximum achievable biomass titer was found to be 91 g L^{-1} during high cell density cultivation of FC2 in model guided fed-batch operation (Fig. 6.5 A). In continuous cultivation, intracellular nutrient quota (Q_i) is equal to yield coefficient $\left(Y_{S_i/X}\right)$ at steady state condition and hence Q_i equation was modified as shown in equation 7.7.

$$\mu = \mu^{max} R \left(\frac{E}{E^{Ref}}\right)\left(\frac{(91-X)^n}{K_x^n+(91-X)^n}\right) \tag{7.1}$$

$$R = R_1\left[R_2 + Q_{R_2}(R_2^m - R_2)/R_2^m\right]\left[R_3 + Q_{R_3}(R_3^m - R_3)/R_3^m\right] \quad (7.2)$$

$$R_i = \frac{S_i - S_i^{Res}}{K_{S_i} + (S_i - S_i^{Res}) + \frac{(S_i - S_i^{Res})^2}{K_{I_i}}} \quad (7.3)$$

$$Q_{R_i} = \frac{\left(A_{R_i} + A_{NR_i}\right)}{K_{Q_i} + \left(A_{R_i} + A_{NR_i}\right)} \quad (7.4)$$

$$A_{R_i} = Q_i - T_{R_i} \quad (7.5)$$

$$A_{NR_i} = \left(T_{R_i} - T_{NR_i}\right)\left(\frac{E_i}{E_i^{Ref}}\right) \quad (7.6)$$

$$Q_i = Y_{S_i/X} \quad (7.7)$$

Where, i =1, 2, 3 represents glucose, nitrate and phosphate respectively.

Mass balance equations

The mass balance for biomass (equation 7.8) and substrates utilization profile (equation 7.9-7.11) was modified in order to incorporate the effect of dilution rate. The ratio of inducible enzymes $\left(\frac{E_i}{E_i^{Ref}}\right)$ is dependent on substrate concentration rather than dilution rate hence equations 7.12-7.14 were expressed in original form.

Biomass (X)

$$\frac{dX}{dt} = \mu X - DX \quad (7.8)$$

Glucose (S_1)

$$\frac{dS_1}{dt} = \begin{cases} DS_1^F - \mu X Y_{S_1/X} - m_s X - DS_1, & R_2 > 0 \\ DS_1^F - \mu X Y_{S_1/X} - DS_1 \end{cases} \quad (7.9)$$

Nitrate (S_2)

$$\frac{dS_2}{dt} = \begin{cases} DS_2^F - \mu X Y_{S_2/X} - DS_2\,, & R_2 > 0 \\ 0 \end{cases} \quad (7.10)$$

Phosphate (S_3)

$$\frac{dS_3}{dt} = \begin{cases} DS_3^F - \mu X Y_{S_3/X} - DS_3, & R_2 R_3 > 0 \\ 0 \end{cases} \quad (7.11)$$

Enzymes (E, E_2 and E_3)

$$\frac{d\left(\frac{E}{E^{Ref}}\right)}{dt} = (\mu^{max}R + \beta) - (\mu^{max}R + \beta)\left(\frac{E}{E^{Ref}}\right) \quad (7.12)$$

$$\frac{d\left(\frac{E_2}{E_2^{Ref}}\right)}{dt} = \begin{cases} 0, & Q_2 > T_{R_2} \\ \left((T_{R_2} - Q_2)\mu^{max} + \beta_2\right) - \left((T_{R_2} - T_{NR_2})\mu^{max} + \beta_2\right)\left(\frac{E_2}{E_2^{Ref}}\right) \end{cases} \quad (7.13)$$

$$\frac{d\left(\frac{E_3}{E_3^{Ref}}\right)}{dt} = \begin{cases} 0, & Q_3 > T_{R_3} \\ \left((T_{R_3} - Q_3)\mu^{max} + \beta_3\right) - \left((T_{R_3} - T_{NR_3})\mu^{max} + \beta_3\right)\left(\frac{E_3}{E_3^{Ref}}\right) \end{cases} \quad (7.14)$$

7.2.4. Estimation of model parameters

The newly introduced parameters (n and K_x) in equation 7.1 were estimated by comparing simulated dynamic profile of growth with the corresponding experimental value adopted from high cell density cultivation of FC2 in fed-batch (Fig. 6.5 A). The minimization of difference between simulated values and corresponding experimental data was employed as objective function in the optimization of control variables. The estimated values of n and K_x were found to be 1.71 and 11.56 respectively. Rest of the model parameters were obtained from the previous study (Table 5.1). The experimental data of biomass formation obtained from high cell density cultivation of FC2 in fed-batch was compared with model predictions carried out by original form of equation for μ (equation 6.1) and modified form of equation for μ (equation 7.1) as shown in Fig. 7.1. The higher difference was observed between experimental data and model predictions with original equation as p-value (0.683) was found to be lesser than confidence interval (0.95) while p-value 0.997 was observed in case of modified equation making it better fit with experimental data. Hence modified equation was used in process development for high biomass productivity under continuous mode of cultivation.

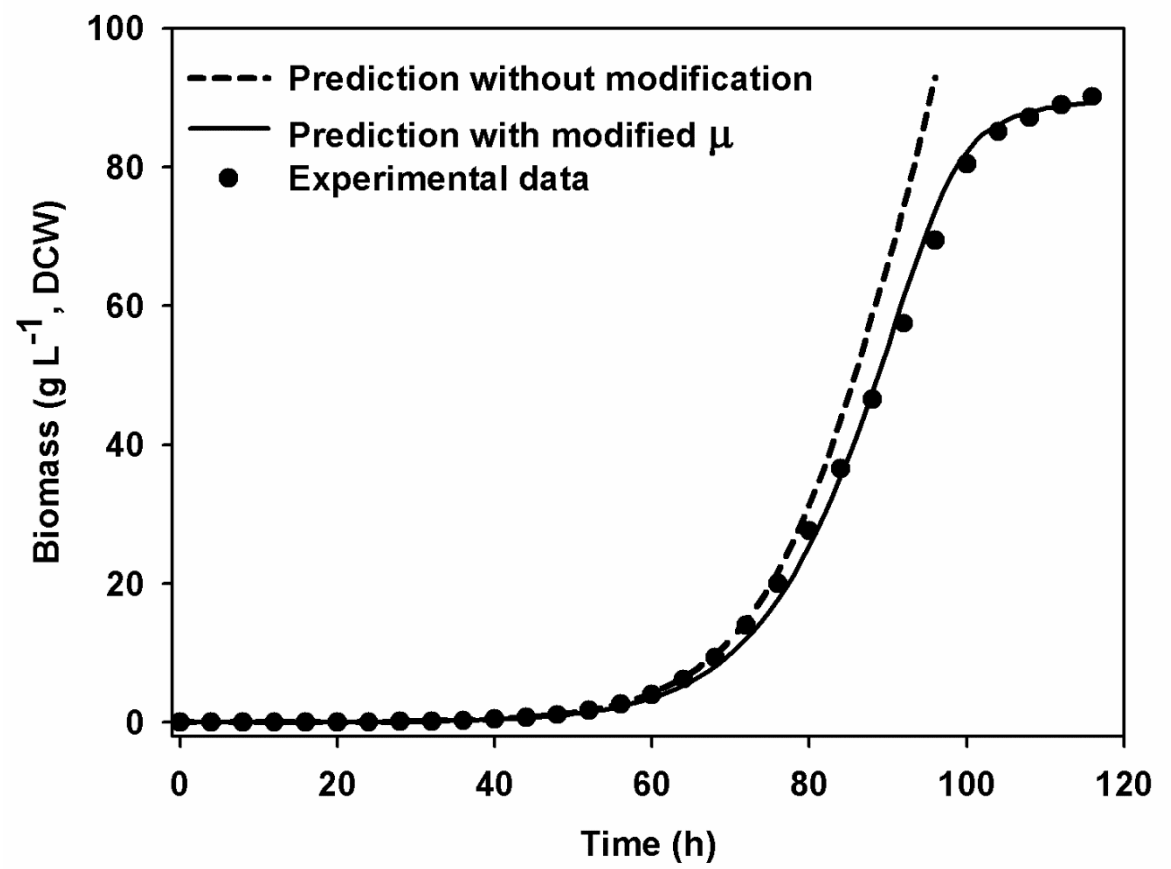

Fig. 7.1 Comparison of experimental data of biomass formation obtained from previous work (Section 6.3.3) on high cell density fed-batch cultivation with model predictions performed by original form of specific growth rate equation (equation 6.1) and modified form of equation (equation 7.1).

7.2.5. Optimization of control variables

The control variables such as dilution rate, concentration of glucose (S_1^F), nitrate (S_2^F) and phosphate (S_3^F) in the feed stream were optimized for maximal biomass productivity (DX) using inbuilt subroutine '*fmincon*' available in Matlab (Mathworks, Natick, MA, USA). Biomass (X), concentration of glucose (S_1), nitrate (S_2) and phosphate (S_3) in the fermentation broth and inducible enzymes concentration $\left(\frac{E}{E^{Ref}}, \frac{E_2}{E_2^{Ref}} \text{ \& } \frac{E_3}{E_3^{Ref}}\right)$ were expressed as state variables.

7.2.6. Demonstration of two stage chemostat fermentation for higher productivity of lipid rich algal biomass

A two-stage chemostat process was developed for continuous production of lipid rich algal biomass with higher productivity by connecting two reactors in series (Fig. 7.2). Initially, the organism was grown in the first reactor through intermittent feeding of the limiting nutrients in order to achieve high biomass concentration. The glucose, nitrate (sodium nitrate & nitric acid), phosphate, trace elements and microelements were supplemented as per the model guided feeding recipe as was demonstrated in the previous study (section 6.3.3). When the biomass concentration of ~60 g L^{-1} was achieved, the operation of first reactor was shifted from fed-batch to continuous mode at model optimized feed stream substrate concentration and narrowly varied optimal dilution rate in order to achieve steady state. During chemostat operation a mixture of nitric acid and sodium nitrate in a molar ratio of 6.31 was used in the feed stream which serves the dual purpose of pH maintenance and source of nitrogen for the organism. Under steady state, the exit stream from the first reactor containing high concentration of biomass was redirected into the second reactor with concomitant continuous addition of sodium acetate resulting in its final broth concentration of 24 g L^{-1} which acts as lipid inducer in the organism (Section 4.3.3). It is important to note that only a fraction of the exit broth stream from the first reactor was redirected into the second reactor which in turn resulted in lower dilution rate and hence sufficient residence time of three days for induction of intracellular neutral lipid in the algal biomass. Previously, the organism FC2 was shown to accumulate intracellular lipid of 60-70% (w/w, DCW) over a time period of three days when exposed to acetate moieties (Section 6.3.3.2). Maintenance of broth pH at ~8 and acetate concentration in the second reactor was performed by supplying 10 M acetic acid in cascade mode. Sampling was done from both the reactors at regular intervals of time to

determine growth, biomass productivity, lipid content of biomass and substrate utilization profiles.

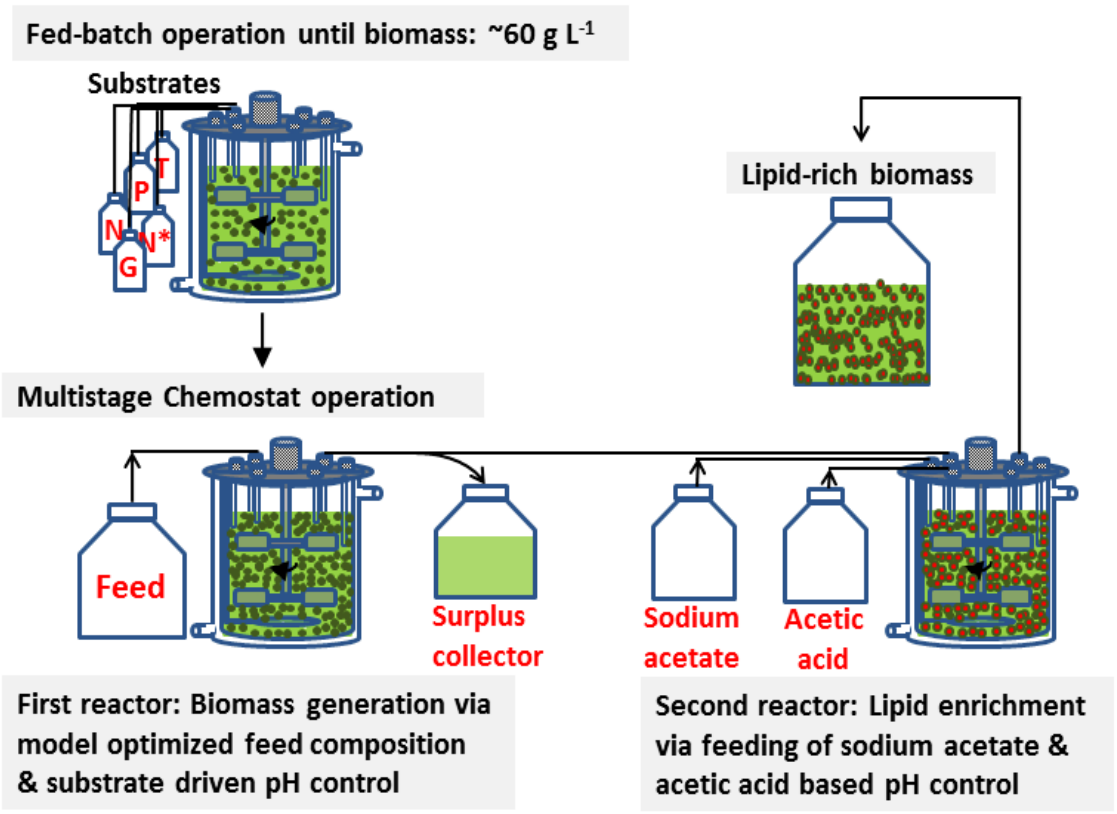

Fig. 7.2 Schematic representation of the two stage chemostat operation for continuous production of lipid rich algal biomass with higher productivity by connecting two reactors in series. Initially, the organism was grown in the first reactor through intermittent feeding of the limiting nutrients in order to achieve biomass concentration of 60 g L^{-1}. In the next step, the operation of first reactor was shifted from fed-batch to continuous mode at model optimized substrate concentrations in feed stream and narrowly varied dilution rate in order to achieve steady state. Under steady state, the fraction of exit stream from the first reactor was redirected into the second reactor with concomitant continuous addition of sodium acetate as lipid inducer. Maintenance of broth pH and acetate concentration in the second reactor was performed by supplying acetic acid in cascade mode.

7.2.7. Analysis of biomass, lipid and substrate concentration

A known amount of sample was centrifuged at 8000 × *g* for 10 minutes at 4°C to collect pellet for the growth, biomass productivity and lipid content measurements while substrate utilization profiles were determined from supernatant. Growth was determined by measuring the optical density (OD) of the cells at 690 nm (A_{690}) in a UV-Visible spectrophotometer (Detailed in Section 3.2.5.1). Nitrate concentration of broth was

analyzed by use of salicylic acid method as explained in section 3.2.5.2. Phosphate concentration was estimated through ascorbic acid based colorimetric method as explained in section 3.2.5.4. Dinitrosalicyclic acid method was employed to estimate the glucose concentration as detailed in section 3.2.5.3. Nile-red dye based quantification method was used to determine intracellular neutral lipid content of biomass (Detailed in 3.2.5.5). Total lipid was quantified using sequential two-step direct transesterification method as mentioned in section 3.2.5.6. Biodiesel properties were determined by using empirical formulas obtained from literature as explained in section 3.2.5.7. Sodium acetate content of sample was analyzed by method described in section 8.2.4.2. All the experiments were performed in triplicate and the results were expressed as mean value ± standard error.

7.3. Results and discussion

7.3.1. Effect of dilution rate and feed stream substrate concentration on biomass productivity

In the first step, biomass productivity of FC2 was evaluated under four different dilution rates 0.03 h^{-1}, 0.05 h^{-1}, 0.08 h^{-1} and 0.1 h^{-1} (Fig. 7.3). In all these experiments the organism was grown on optimized BG11 medium (C1). Maximum biomass productivity of 5.3 g L^{-1} day^{-1} was achieved when grown on a dilution rate of 0.08 h^{-1} (Fig. 7.3 A). However, 74% of steady state biomass concentration was washed out over a time period of 50 h when dilution rate was increased from 0.08 h^{-1} to 0.1 h^{-1} (Fig. 7.3 A). Therefore, all the nutrients remained unutilized resulting in sharp increase in their respective concentration (Fig. 7.3 B – 7.3 D). The bacteria *Aerobacter cloacae* also showed wash out phenomenon under chemostat mode at dilution rate of 1.2 h^{-1} (Herbert et al., 1956). While, step wise increase in dilution rate from 0.03 h^{-1} to 0.08 h^{-1} resulted in slight decrease in biomass titer from 3.3 g L^{-1} to 2.78 g L^{-1}, the productivity was significantly increased from 2.4 g L^{-1} day^{-1} to 5.3 g L^{-1} day^{-1}. Similar observation was reported for continuous

cultivation of *Chlamydomonas reinhardtii* when dilution rate was increased from 0.02 to 0.045 h^{-1} (Chen and Johns, 1996).

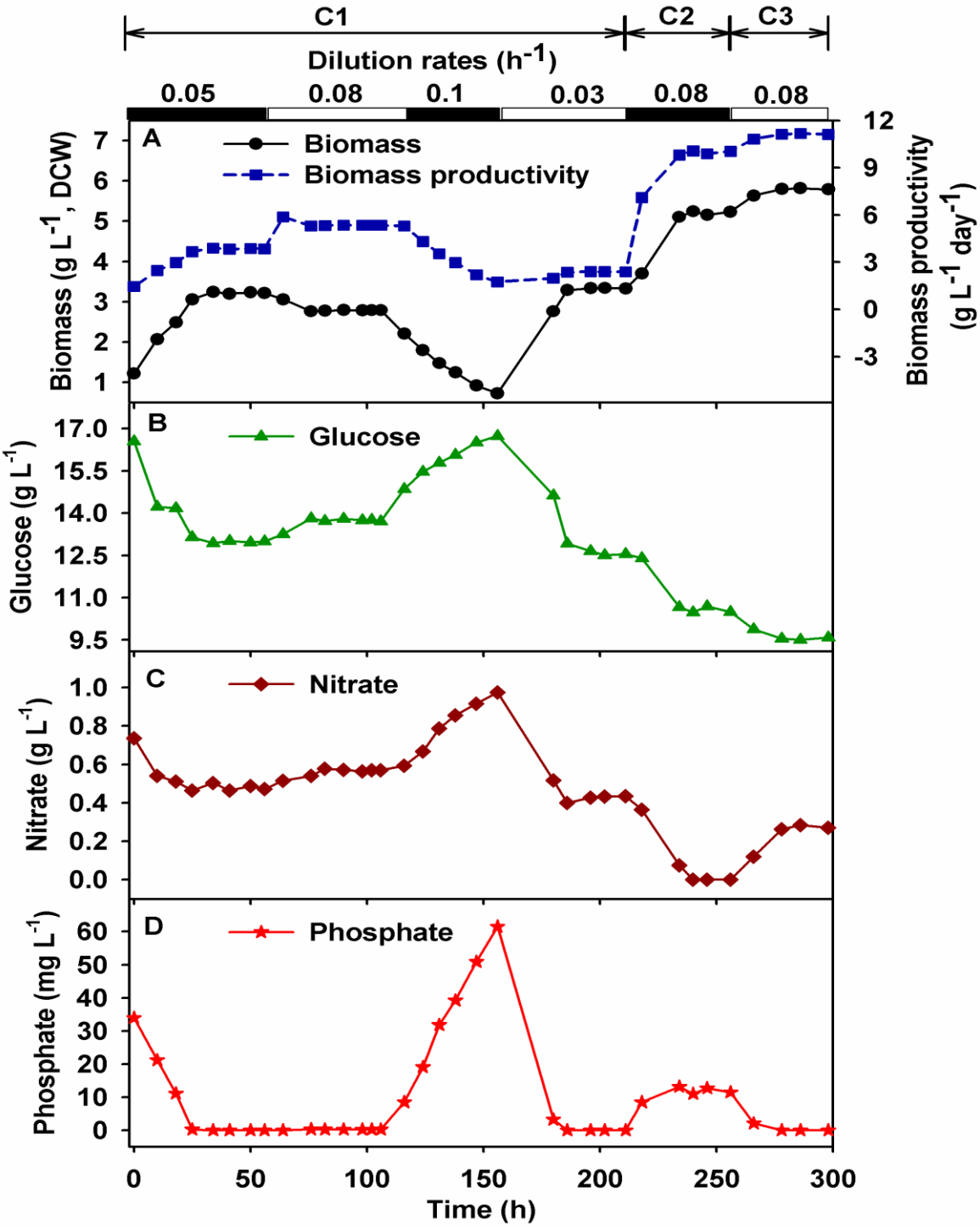

Fig. 7.3 Dynamic profiles for growth, biomass productivity and substrate utilization of organism grown under various dilution rates and feed stream substrate compositions in heterotrophic continuous mode of operation. Filled and non-filled bars on the top of graph represent dilution rates and similarly C1, C2 & C3 depicts the three different feed stream substrate compositions. (A) biomass formation & productivity, (B) residual glucose concentration, (C) residual nitrate concentration and (D) residual phosphate concentration

It is interesting to note that in all the steady state conditions, phosphate was completely utilized by the organism and hence may be limiting towards further improvement in biomass titer or productivity. Therefore, in the next step cultivation of the organism was shifted to C2 medium which had elevated phosphate concentration 0.2 g L^{-1} at the dilution dilution rate of 0.08 h^{-1}. This resulted in an improved steady state biomass titer and productivity of 5.2 g L^{-1} and 10 g L^{-1} day^{-1} respectively (Fig. 7.3 A). However, in this batch, nitrate concentration was found to be limiting as was observed from its concentration profile (Fig. 7.3 C). Cultivation of the organism was further shifted to C3 medium containing elevated nitrate concentration of 1.6 g L^{-1} at the same dilution rate. Biomass productivity was further increased to 11.2 g L^{-1} day^{-1}. The microalga *Chlamydomonas reinhardtii* reported to show enhanced growth and biomass productivity under chemostat operation when the acetate concentration was varied from 1.7 g L^{-1} to 3.4 g L^{-1} in the feed stream (Chen and Johns, 1996). The improvement in biomass productivity is the result of increased specific growth rate in case of increasing dilution rate while it is attributed to higher biomass titer by enhanced feed stream substrate concentration. The results suggest that the concentration of limiting nutrient in the feed stream and the dilution rate serve as the critical parameters which have significant effect on the biomass productivity. Optimization of these parameters is therefore expected to yield higher biomass productivity. With the change in feed stream composition from C1 to C3 through C2, the broth pH was increased from 7.98 to 8.43 resulting in pH drift towards alkali (Fig. 7.4). This is attributed to the uptake of nitrate molecule along with a proton moiety which results in increment of hydroxyl ions (Ullrich et al., 1998) and eventually raises the broth pH (Section 6.3.2). Hence, maintenance of pH was also necessary for development of a process with high biomass productivity.

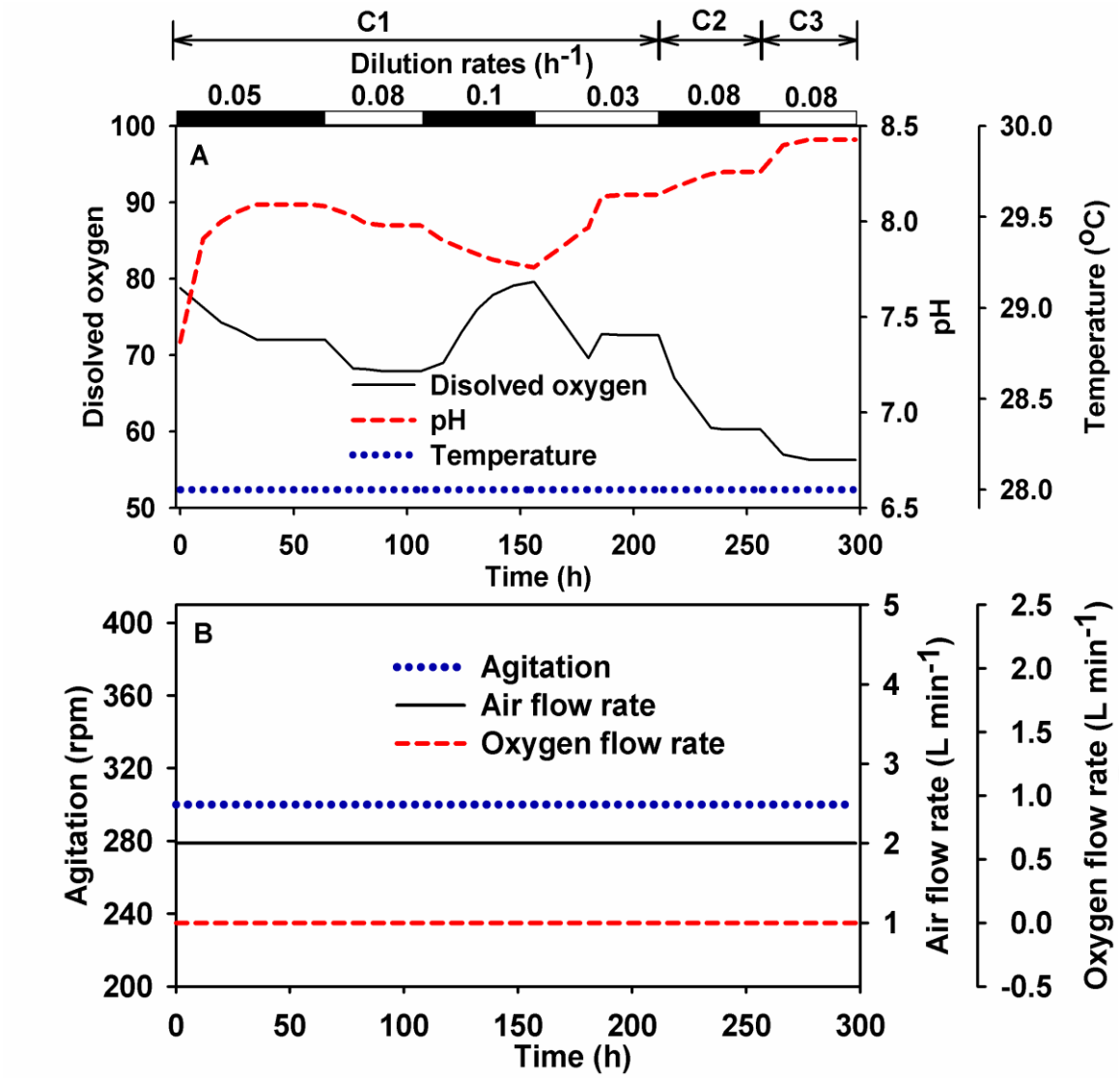

Fig. 7.4 Dynamic profiles of different process parameters obtained during growth of the strain under various dilution rates and feed stream substrate compositions in heterotrophic continuous mode of operation. Filled and non-filled bars on the top of graph represent dilution rates and similarly C1, C2 & C3 depicts the three different feed stream substrate compositions. (A) dissolved oxygen (DO) concentration (—), fermentation broth pH (-----) & broth temperature (……) and (B) aeration rate (—), agitation rate (……) & pure oxygen purging rate (-----).

7.3.2. Optimization of dilution rate and feed stream substrate concentration for high biomass productivity

From section 7.3.1 it can be concluded that dilution rate and substrates concentration in the feed stream were found to be the important control variables. These variables were therefore optimized using the multi-nutrient mechanistic model with the objective of improved biomass productivity. The sequential quadratic programming based

optimization predicted the maximal biomass productivity of 137.93 g L^{-1} day^{-1} with biomass concentration of 66.44 g L^{-1}. The model predicted optimal values of glucose, nitrate and phosphate concentrations in the feed stream and dilution rate were represented in Table 7.2. In order to maintain media pH in desired range and to concurrently provide nitrogen source, a mixture of nitric acid and sodium nitrate was supplemented in place of sodium nitrate. The ratio of nitric acid and sodium nitrate was calculated based on model prediction and data obtained from previous experiment (Section 7.3.1).

The amount of sodium nitrate was calculated to be 2 g L^{-1} based on its consumption of ~1 g L^{-1} to reach pH 8 (Section 7.3.1) and 1.04 g L^{-1} was predicted to be the steady state value (Table 7.2). In order to maintain the media pH around 8, remaining part of the nitrogen requirement was provided by nitric acid. Hence, mixture of nitric acid and sodium nitrate with a molar ratio of 6.3 was used in the feed stream.

Table 7.2 Model optimized parameter values for maximization of biomass productivity in continuous cultivation of FC2 under heterotrophic condition.

S.No.	Parameters	Model optimized values
1	Dilution rate (h^{-1})	0.0865
2	Glucose concentration in feed (g L^{-1})	104.32
3	Nitrate concentration in feed (g L^{-1})	14.61
4	Phosphate concentration in feed (g L^{-1})	2.02
5	Steady state glucose concentration of broth (g L^{-1})	15.1
6	Steady state nitrate concentration of broth (g L^{-1})	1.04
7	Steady state phosphate concentration of broth (g L^{-1})	0.059
8	Steady state biomass titer of broth (g L^{-1})	66.44

Supplementation of appropriate concentration of trace and micro elements (TME) along with the optimized feed composition is essential towards optimal growth of the organism. TME stock consists of a complex mixture of six trace elements and six microelements which makes kinetic modeling of utilization profile of TME a difficult task.

Hence, their concentrations were determined manually based on predicted steady state concentration of biomass and data obtained from previous study of TME effect on growth organism (Section 4.3.2). The study showed that biomass concentration of 5.17 g can be generated from one unit of TME (one unit corresponds to amount present in 1 L basic BG11 medium) with maximal specific growth rate which implied that the yield coefficient $\left(Y_{TME/X}\right)$ of TME for growth is equal to 0.193. In the present study, the biomass concentration of 66.44 g L^{-1} was predicted on optimization control variables (Table 7.2). TME concentration of 0.75 unit L^{-1} was assumed to be a steady state value as specific growth rate was observed to be maximum in TME concentration range of 0.15 – 1.5 unit L^{-1} (Section 4.3.2). The TME concentration in feed was calculated as shown in equation 7.15 – 7.17.

$$\frac{d(TME)}{dt} = DC_{TME\ of\ feed} - \mu XY_{TME/X} - DC_{TME\ of\ broth} \quad (7.15)$$

$$0 = 0.0865 \cdot C_{TME\ of\ feed} - 0.0865 \cdot 66.44 \cdot 0.193 - 0.0865 \cdot 0.75 \quad (7.16)$$

$$C_{TME\ of\ feed} = 13.57 \quad (7.17)$$

TME concentration of 13.57 unit L^{-1} was used along with other optimized substrates concentration in feed of continuous cultivation.

7.3.3. Process development for generation of lipid rich algal biomass with higher productivity via two-stage chemostat cultivation

Generation of lipid rich algal biomass with higher productivity was achieved via connecting two reactors in series. Algal biomass was generated in the first reactor expected to be operated under model based optimized control variable values. The second reactor was dedicated for enrichment of neutral lipid in the cell mass. However, operation of the first reactor at model predicted dilution rate of 0.086 h^{-1} resulted in wash out of biomass. The phenomenon was evident from the observed substantial drop in biomass concentration (Fig. 7.5 A) coupled with concomitant increase in residual concentrations of

substrates (Fig. 7.6 A) with respect to their optimal broth concentration (Table 7.2). Therefore, a hit and trial method was applied and at a dilution rate of 0.066 h^{-1}, the system was able to reach stable steady state. Therefore, the first reactor was operated at this particular dilution rate instead of model predicted one.

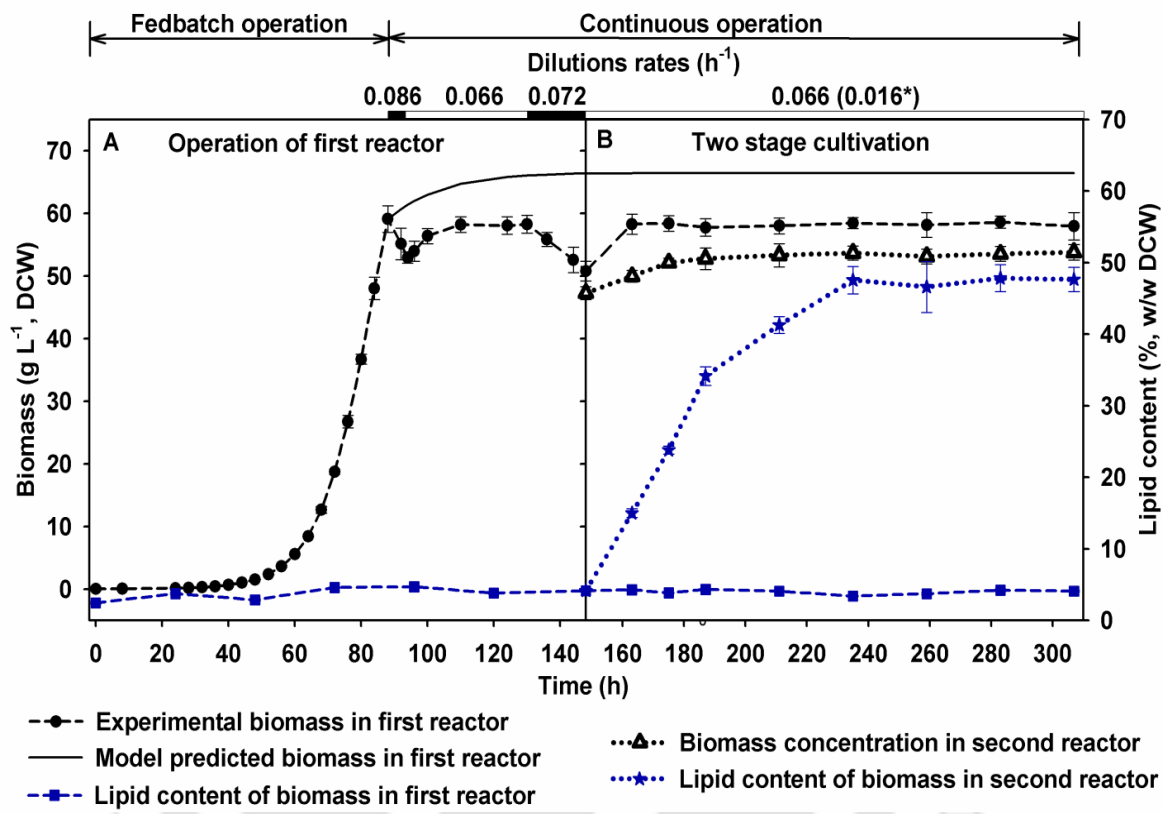

Fig. 7.5 Dynamic profiles for growth and intracellular lipid content of the strain FC2 grown under two stage chemostat operation for continuous production of lipid rich algal biomass with maximal productivity by connecting two reactors in series. (A) The strain was grown in the first reactor through fed-batch mode in order to achieve significantly high biomass and then shifted to continuous mode at model optimized substrate concentrations in feed stream or varied dilution rate in order to achieve steady state. After obtaining stable steady state, (B) the operation of second reactor was started by redirecting the fraction of exit stream from the first reactor to it with concomitant continuous addition of sodium acetate as lipid inducer. Maintenance of broth pH and acetate concentration in the second reactor was performed by supplying acetic acid in cascade mode. Filled & non-filled bars on the top of graph represent dilution rates of first reactor and * depicts dilution rate of second reactor.

The chemostat operation at 0.066 h^{-1}dilution rate resulted in biomass titer of 58 g L^{-1} (Fig. 7.5) with biomass productivity of 92.7 g L^{-1} day^{-1} which was 17.5 times higher than continuous mode operation with optimized BG11 media (C1) at 0.08 h^{-1} dilution rate

(Fig. 7.3 A). However, the biomass productivity was 33% lesser than model prediction due to operation at lower dilution rate. A deviation of 7% was observed between experimental and predicted phosphate utilization profile during development of multi-nutrient mechanistic model (Section 5.3.1) which would have resulted in higher consumption of phosphate than prediction leading to phosphate starvation. The phosphate depletion activates *psr*1 (phosphorus starvation response) gene which is responsible for reduction of DNA biosynthesis, activation of stress-associated chaperones, proteases and scavenging phosphatases resulting in down regulation of growth rate (Moseley et al., 2006; Wykoff et al., 1999; Yehudai-Resheff et al., 2007). To the best of our knowledge, biomass productivity obtained in the present study is the highest amongst published literatures (Table A1 in appendix A). Previously, *Chlorella vulgaris* was demonstrated with a biomass productivity of 84.48 g L^{-1} day^{-1} under fed-batch mode of cultivation (Doucha and Lívanský, 2012). An *insilico* prediction for lipid productivity of 12.27 g L^{-1} day^{-1} was reported via dynamic model based optimization of the feed-stream and dilution rate (De la Hoz Siegler et al., 2011) which supports the strategy used in present study.

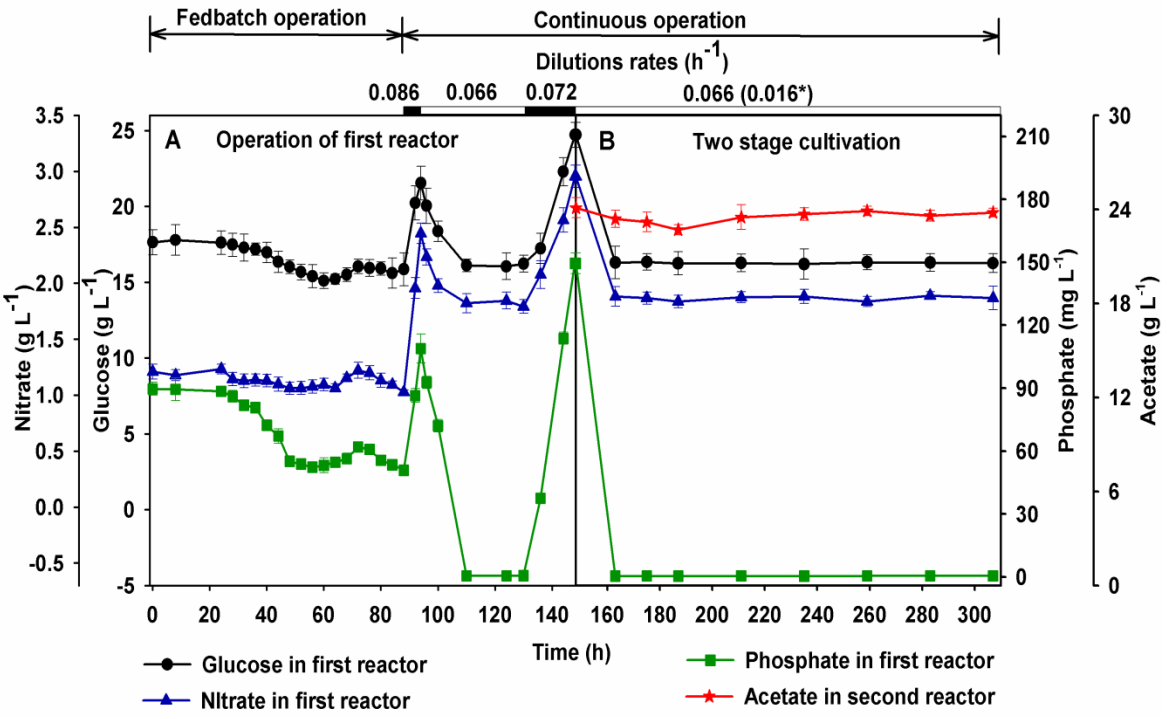

Fig. 7.6 Dynamic substrate utilization profiles of the strain FC2 grown under two stage chemostat operation for continuous production of lipid rich algal biomass with maximal productivity by connecting two reactors in series. (A) The strain was grown in the first reactor through fed-batch mode in order to achieve significantly high biomass and then shifted to continuous mode at model optimized substrate concentrations in feed stream or varied dilution rate in order to achieve steady state. After obtaining stable steady state, (B) the operation of second reactor was started by redirecting the fraction of exit stream from the first reactor to it with concomitant continuous addition of sodium acetate as lipid inducer. Maintenance of broth pH and acetate concentration in the second reactor was performed by supplying acetic acid in cascade mode. Filled & non-filled bars on the top of graph represent dilution rates of first reactor and * depicts dilution rate of second reactor.

The biomass obtained from the first reactor was subjected to lipid enrichment in the second reactor to transform the biomass into suitable feedstock for biodiesel production. The second reactor was initiated once the first reactor reached steady state and operated at dilution rate of 0.016 h^{-1} in order to provide sufficient residence time for lipid induction. This dilution rate consists of simultaneous addition of a fraction of exit stream from the first reactor, sodium acetate and acetic acid. Steady state lipid accumulation of 47.5% (w/w, DCW) with a biomass concentration of 53.5 g L^{-1} (Fig. 7.5 B) was achieved in second reactor after 87 h of operation. A marginal reduction in biomass titer in the second reactor was attributed to the dilution of the broth due to addition of acetic acid and its salt. An upregulation in intracellular lipid accumulation by 11.9 fold was observed in the second reactor as compared to the first reactor. Steady state neutral lipid productivity of 9.76 g L^{-1} day^{-1} was achieved which was significantly high in comparison with other demonstrated process for microalgal biodiesel production (Table A2 in Appendix A). The lipid productivity of 8.19 g L^{-1} day^{-1} was demonstrated in heterotrophic fed-batch cultivation of *Chlorella vulgaris* (Doucha and Lívanský, 2012). Microalga FC2 was reported to show pH rise with consumption of acetate molecules (Section 6.3.4) as H^+ ion and acetate were concurrently consumed for their metabolism (Perez-Garcia et al., 2011). Hence the addition of acetic acid via cascade mode was able to control pH at its set value ~8 and additionally maintained the acetate concentration in the media (Fig. 7.6 B).

Freshwater microalga *Chlorella sorokiniana* FC6 IITG was demonstrated with a lipid productivity of 1.27 g L^{-1} day^{-1} in a continuous mode of operation under mixotrophic condition via addition of sodium acetate and sodium chloride as inducers (Kumar et al., 2016). The acetate being two carbon moiety, is consumed easily and converted acetyl COA directly which leads to upregulation of lipid biosynthesis pathway (Qiao and Wang, 2009).

7.3.4. Evaluation of fatty acid methyl esters (FAME) composition and biodiesel properties

Analysis of FAME composition of the algal biomass collected from the second reactor revealed that 98% of the total FAME comprised of C16:0, C16:1, C18:0, C18:1 and C18:2 (Table 7.3). Therefore, majority of the carbon chain length was found to be similar to petroleum based diesel which contains alkanes in the ranges of C15 - C19 (McArthur and Spalding, 2004).

Table 7.3 Fatty acid methyl ester (FAME) compositions obtained from the strain FC2 grown in two stage chemostat operation for continuous production of lipid rich algal biomass with maximal productivity by connecting two reactors in series. First reactor was used for the generation of biomass followed by intracellular lipid enrichment in the second reactor through addition of lipid inducer.

Fatty acid name	Code	FAME composition (% of total FAME)
Lauric acid	[C12:0]	0.664
Miristic acid	[C14:0]	0.22
Palmitic acid	[C16:0]	22.9
Palmitoleic acid	[C16:1]	6.44
Stearic acid	[C18:0]	6.1
Oleic acid	[C18:1]	33.3
Linoleic acid	[C18:2]	29.15
Arachidic acid	[C20:0]	0.21
Behenic acid	[C22:0]	0.145
Total saturation (% of total FAME)		30.239
Total mono-unsaturation (% of total FAME)		39.74
Total poly-unsaturation (% of total FAME)		29.15
Other components (% of total FAME)		1.04
Total FAME (%, w/w, DCW)		50.7

According to European standards, linolenic acid (C18:3) should be lesser than 12 mol% (Chisti, 2007) and interestingly, C18:3 was not found to be present in the current study. Biodiesel properties were calculated based on empirical correlations (Francisco et al., 2010; Ramírez-Verduzco et al., 2012; Su et al., 2011) involving experimentally obtained FAME composition. The biodiesel properties were compared with ASTM international standards (ASTM D6751–15a) & European standards (EN 14214) and represented in Table 7.4.

Table 7.4 Property of biodiesel obtained from the strain FC2 grown in two stage chemostat operation for continuous production of lipid rich algal biomass with maximal productivity by connecting two reactors in series. First reactor was used for the generation of biomass followed by intracellular lipid enrichment in the second reactor through addition of lipid inducer. Biodiesel properties were calculated based on empirical correlations (Francisco et al., 2010; Ramírez-Verduzco et al., 2012; Su et al., 2011) involving experimentally obtained FAME composition

Biodiesel properties	**Units**	**Property values**	**Standards**	
			ASTM D6751–15a	**EN 14214**
Viscosity	$mm^2\ s^{-1}$	4.43	1.9 - 6	3.5 – 5
Cetane number		56.56	>47	>51
Flash point	°C	159.42	>93	>101
Cloud point	°C	4.55	ND	ND
Pour point	°C	1.48	ND	ND
Saponification value	mg KOH g^{-1}	203.43	ND	ND
Iodine value	% (g I_2 g^{-1} oil)	89.17	ND	<120
Degree of unsaturation		96.76	ND	ND
Highest Heating value	MJ kg^{-1}	39.72	ND	ND

The FAME obtained from lipid rich biomass showed kinematic viscosity (η) ~ 4.4 $mm^2\ s^{-1}$; hence operational problems like engine deposits will not appear as it lies within range of the standards (Knothe and Steidley, 2005). The presence of desirable properties like shortened ignition delay, less flammability, reduced double bonds was confirmed by

comparing cetane number, flash point and iodine value with the standards. The heating value was found to be ~40 MJ kg^{-1} which was comparable to the permissible range (40 – 45 MJ kg^{-1}) of petroleum based diesel (Xu et al., 2006). Therefore, biodiesel produced from *Chlorella* sp. FC2 IITG grown in heterotrophic multistage chemostat operation has potential in commercial applications as all the properties were found to follow the ASTM D6751–15a and EN 14,214 standards.

7.4. Conclusions

The novel strategy for high productivity of lipid rich algal biomass was demonstrated in the current study via two-stage continuous cultivation of FC2 where first reactor was used for the generation of biomass followed by intracellular lipid enrichment in the second reactor through addition of lipid inducer. In comparison with bioprocesses reported in literature for microalgal based biodiesel production, the strategy yielded highest biomass and lipid productivity of 92.7 g L^{-1} day^{-1} and 9.76 g L^{-1} day^{-1} respectively. Further, as lipid rich biomass was continuously generated with significantly high cell density (53.5 g L^{-1}); it offers additional advantages such as decrement of unproductive time, harvesting and biomass processing cost. The process strategy designed in the current study can be applied to other metabolites for their higher productivity. Further, the present strategy opens up scope for large scale production of biodiesel for commercial applications.

7.5. References

1. Chen F., Johns M.R., 1996. Heterotrophic growth of *Chlamydomonas reinhardtii* on acetate in chemostat culture. Process Biochemistry. 31, 601–604.
2. Chen F., Johns M.R., 1995. A strategy for high cell density culture of heterotrophic microalgae with inhibitory substrates. Journal of Applied Phycology. 7, 43–46.

3. Chisti Y., 2007. Biodiesel from microalgae. Biotechnology Advances. 25, 294–306.

4. De la Hoz Siegler H., Ben-Zvi A., Burrell R.E., McCaffrey W.C., 2011. The dynamics of heterotrophic algal cultures. Bioresource Technology. 102, 5764–5774.

5. Doucha J., Lívanský K., 2012. Production of high-density *Chlorella* culture grown in fermenters. Journal of Applied Phycology. 24, 35–43.

6. Francisco E.C., Neves D.B., Jacob–Lopes E., Franco T.T., 2010. Microalgae as feedstock for biodiesel production: carbon dioxide sequestration, lipid production and biofuel quality. Journal of Chemical Technology and Biotechnology. 85, 395–403.

7. Herbert D., Elsworth R., Telling R.C., 1956. The continuous culture of bacteria; a theoretical and experimental study. Microbiology. 14, 601–622.

8. Knothe G., Steidley K.R., 2005. Kinematic viscosity of biodiesel fuel components and related compounds. Influence of compound structure and comparison to petrodiesel fuel components. Fuel. 84, 1059–1065.

9. Kumar V., Muthuraj M., Palabhanvi B., Das D., 2016. Synchronized growth and neutral lipid accumulation in *Chlorella sorokiniana* FC6 IITG under continuous mode of operation. Bioresource Technology. 200, 770–779.

10. McArthur H., Spalding D., 2004. Engineering materials science: Properties, uses, degradation, remediation. Woodhead Publishing, Cambridge.

11. Moseley J.L., Chang C.-W., Grossman A.R., 2006. Genome-based approaches to understanding phosphorus deprivation responses and PSR1 control in *Chlamydomonas reinhardtii*. Eukaryotic Cell. 5, 26–44.

12. Perez-Garcia O., Escalante F.M., de-Bashan L.E., Bashan Y., 2011. Heterotrophic cultures of microalgae: metabolism and potential products. Water Research. 45, 11–36.

13. Qiao H., Wang G., 2009. Effect of carbon source on growth and lipid accumulation in *Chlorella sorokiniana* GXNN01. Chinese Journal of Oceanology and Limnology. 27, 762–768.

14. Ramírez-Verduzco L.F., Rodríguez-Rodríguez J.E., del Rayo Jaramillo-Jacob A., 2012. Predicting cetane number, kinematic viscosity, density and higher heating value of biodiesel from its fatty acid methyl ester composition. Fuel. 91, 102–111.

15. Rodolfi L., Chini Zittelli G., Bassi N., Padovani G., Biondi N., Bonini G., Tredici M.R., 2009. Microalgae for oil: Strain selection, induction of lipid synthesis and outdoor mass cultivation in a low-cost photobioreactor. Biotechnology and Bioengineering. 102, 100–112.

16. Stanbury P.F., Whitaker A., Hall S.J., 2003. Principles of fermentation technology. 2nd ed. Butterworth-Heinemann, Oxford, UK.

17. Su Y.-C., Liu Y.A., Diaz Tovar C.A., Gani R., 2011. Selection of prediction methods for thermophysical properties for process modeling and product design of biodiesel manufacturing. Industrial & Engineering Chemistry Research. 50, 6809–6836.

18. Ullrich W.R., Lazarova J., Ullrich C.I., Witt F.G., Aparicio P.J., 1998. Nitrate uptake and extracellular alkalinization by the green alga *Hydrodictyon reticulatum* in blue and red light. Journal of Experimental Botany. 49, 1157–1162.

19. Wykoff D.D., Grossman A.R., Weeks D.P., Usuda H., Shimogawara K., 1999. Psr1, a nuclear localized protein that regulates phosphorus metabolism in

Chlamydomonas. Proceedings of the National Academy of Sciences. 96, 15336–15341.

20. Xin L., Hong-Ying H., Ke G., Ying-Xue S., 2010. Effects of different nitrogen and phosphorus concentrations on the growth, nutrient uptake, and lipid accumulation of a freshwater microalga *Scenedesmus* sp. Bioresource Technology. 101, 5494–5500.

21. Xu H., Miao X., Wu Q., 2006. High quality biodiesel production from a microalga *Chlorella protothecoides* by heterotrophic growth in fermenters. Journal of Biotechnology. 126, 499–507.

22. Yehudai-Resheff S., Zimmer S.L., Komine Y., Stern D.B., 2007. Integration of chloroplast nucleic acid metabolism into the phosphate deprivation response in *Chlamydomonas reinhardtii*. The Plant Cell. 19, 1023–1038.

CHAPTER 8

Flux balance analysis to understand the lipid metabolism under different nutritional conditions

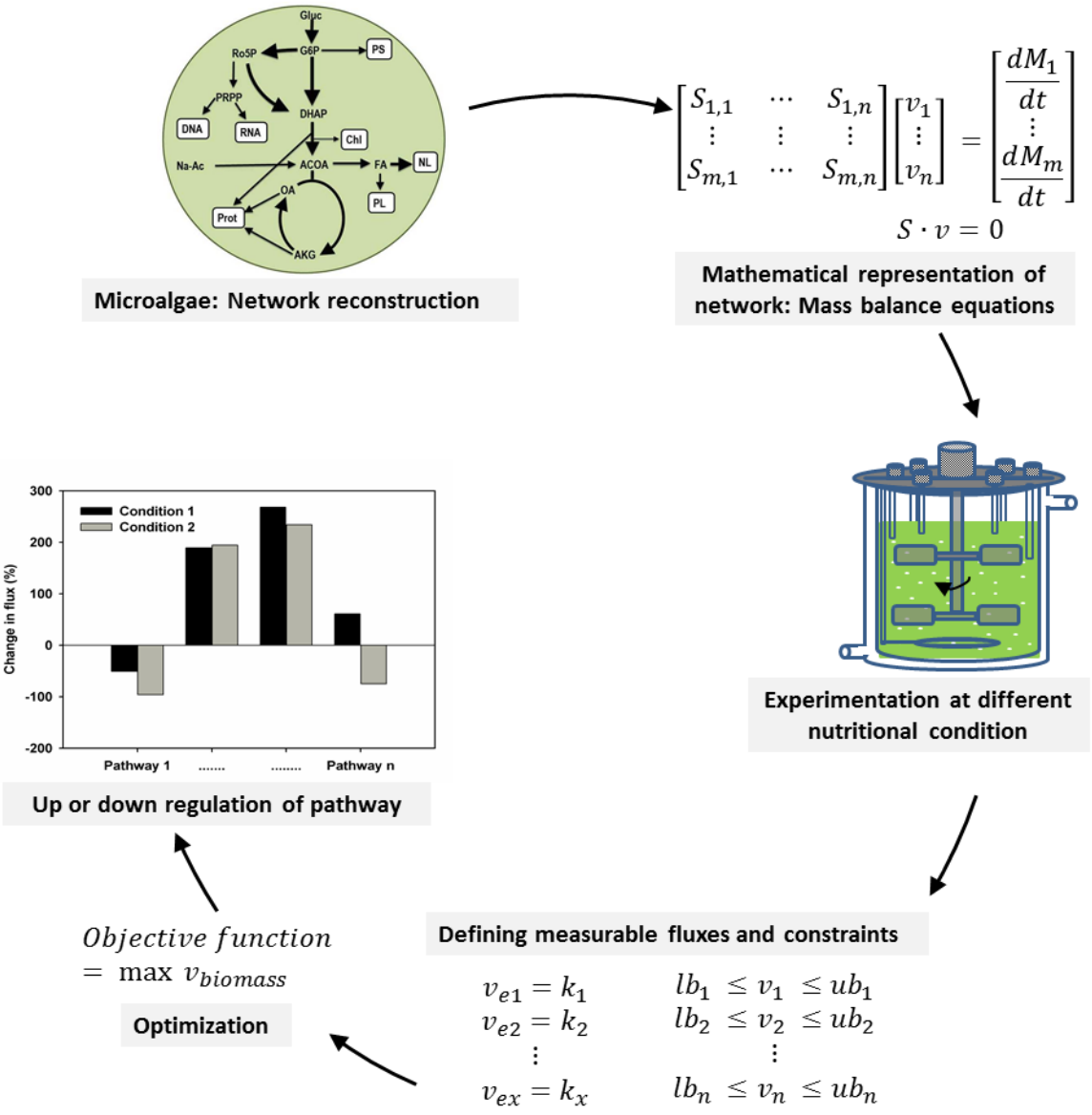

Flux balance analysis to understand the regulations of carbon partitioning and lipid metabolism of *Chlorella* sp. FC2 IITG at different nutritional condition under heterotrophic cultivation.

8.1. Background and motivation

All the biotic components are made up of several building blocks such as polysaccharides, proteins, lipids, DNA and RNA etc (Nelson and Cox, 2012). The proper composition and synthesis of these intracellular macromolecules is controlled by various genes in order to adjust and grow in exposed environment. During this process, large amount of nutrients flow through various pathways in order to synthesize building blocks and to meet energy demand (Trinh et al., 2009). This nutrient distribution map varies with the growth conditions and can be calculated by flux balance analysis (FBA) methodology. FBA can also be used to simulate the behavior of desired mutant before its development and further construction of mutant can be optimized for product of interest. For example, flux map of *Chlamydomonas reinhardtii* for autotrophic, heterotrophic and mixotrophic conditions were compared and *in-silico* mutant was developed for hyper production of hydrogen (de Oliveira Dal'Molin et al., 2011). Quantification of carbon flux distribution in the metabolic network of organisms has been found to be important to understand the complex interplay between genotypic alterations and the corresponding phenotypic response (Boyle and Morgan, 2009; Shastri and Morgan, 2005).

Microalgae are known to accumulate huge amount of intracellular lipid under various stress conditions in contrast to growth favorable condition and hence, considered as metabolically flexible microorganisms. Unfortunately, the expression and regulation of genes involved in lipid biosynthesis pathway is not yet clear in microalgae (Hu et al., 2008). The better understanding of interaction between energy metabolism, carbon fixation and assimilation pathways would result in optimal exploitation of microalgae as cell factory for biodiesel production. Many studies have been reported for comparative analysis of pathway regulation via flux balance analysis for autotrophic, heterotrophic and mixotrophic growth of microalgae (Boyle and Morgan, 2009; de Oliveira Dal'Molin et al.,

2011; Shastri and Morgan, 2005; Yang et al., 2000). However, FBA under growth and lipid induction phase is sparsely studied though it is very important towards biodiesel production. The flux distribution and energetics study may search efficient energy utilization condition (Yang et al., 2000) for enhanced growth and/or lipid induction, which can be used for process development.

In the present study, Flux Balance Analysis (FBA) was carried out for *Chlorella* sp. FC2 IITG under various lipid induction conditions and compared with growth favorable cultivation. The analysis was based on the development of stoichiometric model for the organism coupled with linear programming optimization. While extracellular nutrient uptake rates were used as the model inputs, validation of the metabolic model was performed by comparing model predicted specific growth rate with the corresponding experimental values. In the first step, a shift in intracellular flux distribution was predicted during transition from nutrient sufficient phase to nutrient starvation phase. The nutrient sufficient phase is marked with phosphate available condition in the medium. Similarly, the nutrient starvation phase corresponds to phosphate exhausted condition which is termed as starvation based lipid induction phase. In the next step, FBA was performed for sodium acetate based lipid induction phase and compared with nutrient sufficient phase. These results point towards efficient energetics of lipid biosynthesis in FC2 which could be strategic methodology for process development.

8.2. Material and methods

8.2.1. Cultivation conditions

Seed culture was prepared as the protocol mentioned in section 3.2.1. Active mid-log phase seed of 1%, v/v was used as inoculum in all the experiments. All the experiments were performed in a 3.0 L automated bioreactor (Bio Console ADI 1025, Applikon Biotechnology, Holland) at temperature of 28ºC, agitation of 400 rpm and

aeration of 1 vvm. The reactor was maintained in dark condition in order to avoid the exposure of cells to light source. Basic BG11 media (composition as mentioned in Table 3.1 in section 3.2.1) with supplementation of 15 g L^{-1} glucose was used for inoculum preparation and all the experiments.

Two different experiments were performed in order to assess flux distribution towards lipid biosynthesis and energetics under different nutritional conditions. These batches differ in terms of strategy for lipid induction in biomass. While, in the first experiment induction of neutral lipid was achieved by nutritional stress, in the second experiment the same was achieved via addition of lipid inducer. The first experiment was carried out in batch mode and hence organism was expected to enter the nutrient starvation phase (phosphate exhaustion) during the course of fermentation which triggers the lipid accumulation in cells. The second experiment was also conducted with basic BG11 medium. However, sodium acetate as lipid inducer (20 g L^{-1}) and limiting substrate phosphate were supplied to the reactor as soon as phosphate was exhausted from media. The limiting nutrient phosphate was added to reactor in order to avoid any effect in microalgal metabolism due to nutrient starvation. The dynamic profiles of biomass synthesis, intracellular macromolecular compositions and substrate utilization were determined by sampling at regular time intervals. All the experiments were conducted in triplicate and the data are expressed as mean value ± standard error.

8.2.2. Flux balance analysis

FBA was performed based on three key steps: defining the biological system via reconstruction of metabolic network, formulation of reconstructed metabolic network into a stoichiometric model and solving stoichiometric model using linear programming with a suitable objective function (Shastri and Morgan, 2005). In the present work, the metabolic network for FC2 was reconstructed from the Gene-Protein-Reaction associations for green

algae *Chlamydomonas reinhardtii* available in KEGG database (Kanehisa et al., 2008) and other relevant literatures (Boyle and Morgan, 2009; de Oliveira Dal'Molin et al., 2011; Shastri and Morgan, 2005). All the reactions (detailed list is given in Table A3 in Appendix A) were elementally balanced except for protons (Montagud et al., 2010) and water molecules. The FBA model captures cellular behavior under pseudo steady state conditions where, the metabolic model is transformed to a stoichiometric model $\boldsymbol{S}.\boldsymbol{v} = \boldsymbol{0}$. The stoichiometric matrix $\boldsymbol{S}$ contains the stoichiometric coefficients of *i* metabolites in the *j* reactions and flux vector $\boldsymbol{v}$ corresponds to the flux of the *j* reactions (Srivastava et al., 2012). Dimension of the stoichiometric matrix was 113 × 159 where, rows represent metabolites and columns represent reactions. Finally, the stoichiometric model was solved using linear programming by defining a suitable objective function.

Flux balance analysis was carried out for two phases: growth phase marked with nutrient sufficient condition and lipid induction phase. Further, lipid induction phase was achieved either by nutritional starvation or addition of lipid inducer sodium acetate. Flux distributions in these two types of lipid induction phases were compared with the nutrient sufficient phase in order to capture change in carbon flow through various pathways during phase transitions. Flux analysis was performed by employing *Maximization of biomass* as the objective function and experimentally determined uptake rates of glucose and nitrate as model inputs. Additionally sodium acetate utilization flux was used as input in case of sodium acetate based lipid induction. Growth associated (GA) and non-growth associated (NGA) maintenance energy utilizations were considered in the metabolic model which accounts for growth and survival of the organism respectively. GA maintenance energy requirement was assumed to be 38.78 mmol ATP g^{-1} DCW for heterotrophic condition which is same as that reported for *Chlamydomonas reinhardtii* (Boyle and Morgan, 2009). NGA maintenance energy was obtained during the course of metabolic

modeling. Presence of any other overflow products as potential sink for carbon assimilation was assumed to be negligible. Model was validated by comparing predicted specific growth rate and experimentally obtained specific growth rate. Flux balance analysis was performed by *fmincon* routine in MATLAB (MATHWORK, Natick, MA) which uses linear programming based optimization algorithm.

8.2.3. Biomass composition

Major macromolecular composition of the biomass such as carbohydrate, protein, neutral lipid and chlorophyll were experimentally determined. The ratio of RNA to DNA was assumed to be 28 (Boyle and Morgan, 2009) and RNA content in the biomass was assumed to be 2.8% of dry cell weight for all the analysis (Fuentes et al., 2000; Yang et al., 2000). The polar lipid content was determined as a remaining portion required to make up biomass on equating the all components to 100%. Polar lipid composition was assumed to be as follows: 50% MGDG, 20% DGDG, 10% SQDG, 10% PG, 5% PE and 5% PI (Dörmann and Benning, 2002; El-Sheekh, 1993). The composition of total lipid content of the biomass was obtained by GC analysis.

8.2.4. Estimation of biomass, its macromolecular composition & substrate consumption

Sample of fermentation broth was centrifuged at 8000 × *g* for 10 minutes at 4°C to collect the pellet for measurement of growth and macromolecular composition while supernatant was used to determine substrate utilization profiles. Biomass was measured by reading the optical density (OD) of the cells at 690 nm (A_{690}) in a UV-Visible spectrophotometer (Detailed in Section 3.2.5.1). Nitrate concentration was evaluated by salicylic acid method as described in section 3.2.5.1. The concentration of phosphate was determined by ascorbic acid method as explained in the section 3.2.5.4. Glucose concentration was estimated via dinitrosalicyclic acid (DNS) method as mentioned in

section 3.2.5.3. Intracellular neutral lipid content was quantified by Nile-red dye based fluoroscence method (Detailed in 3.2.5.5). The fatty acid composition of total lipid was evaluated by using sequential two-step direct transesterification method as explained in section 3.2.5.6. Intracellular protein concentration was estimated by Lowry's method as explained in section 5.2.2.2. The colorimetric method reported by Pruvost et al. (2011) was used to determine the intracellular chlorophyll concentration (Detailed in Section 5.2.2.3).

8.2.4.1. Estimation of intracellular carbohydrate concentration

Phenol sulfuric acid method was employed to measure the intracellular total carbohydrate concentration (Dubois et al., 1956). The pellet obtained after centrifugation was washed and re-suspended in deionized water. The sample of 0.5 mL was mixed with 0.5 mL of phenol (5%, w/v) and then 2.5 mL of concentrated sulfuric acid was added along the side of test tubes. Mixture was allowed attain equilibrium with room temperature for 10 min and then incubated at 35°C for 30 min. Absorbance was measured at 490 nm and calibration curve was developed between absorbance and concentration of total sugars as shown in Fig. 8.1 A (one absorbance A_{490nm} = 0.223 g L^{-1} total sugars).

8.2.4.2. Analysis of sodium acetate concentration of sample

Acetate concentration was determined using high pressure liquid chromatograph (Shimadzu LC-20AD Prominence HPLC, USA) equipped with photo diode array detector. The cell free supernatant was injected into a (7.8 x 300 mm, 8µm) Rezex ROA-Organic Acid column (Phenomenex, USA) with detection at λ = 210 nm. Sulfuric acid (0.005N) was used as mobile phase with flow rate of 0.5 mL min^{-1} (Kumar et al., 2013). The standard calibration curve was developed between acetate concentration and peak area (Fig. 8.1 B), where 10^4 V min area corresponds to 2.065 g L^{-1} sodium acetate.

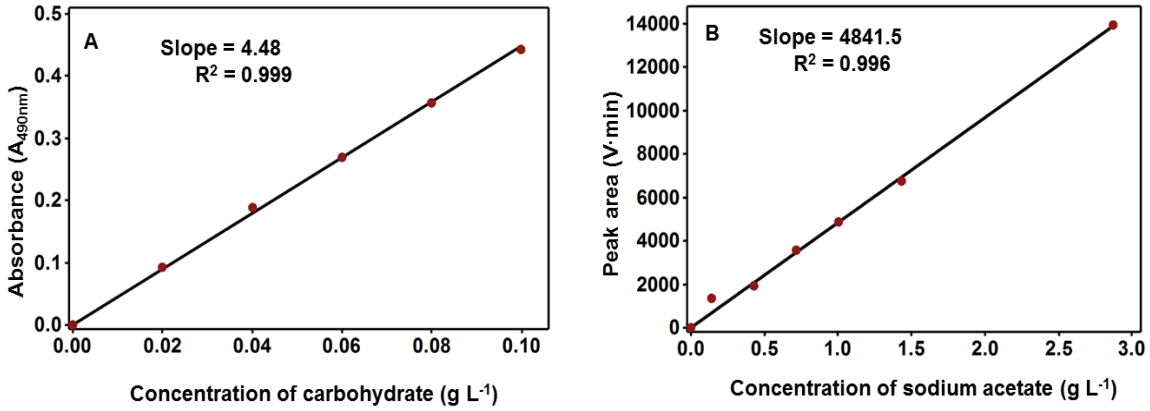

Fig. 8.1 Standard correlation graphs of (A) Carbohydrate which was developed by comparing its concentration with corresponding absorbance, and (B) Sodium acetate which was developed by comparing its concentration with corresponding peak area in HPLC.

8.3. Results and discussion

8.3.1. Flux estimation under growth supporting (nutrient sufficient) and lipid inducing (nutrient starvation or sodium acetate supplementation) phases

Organism was found to grow exponentially till 96 h of fermentation even after exhaustion of phosphate at 72 h (Fig. 8.2) under heterotrophic growth of FC2 with basic BG11 media. Typically microalgae can grow significantly under nutrient starvation by using its internal nutrient pool (Bernard, 2011). The cultivation until 72 h was considered as nutrient sufficient condition and thereafter nutrient starved condition as phosphate was exhausted from the media. In order to compare carbon flux distribution between these two phases, the time segment of 48 – 72 h and 72 – 96 h of cultivation were used for the metabolic modeling studies as representatives of nutrient sufficient and starvation conditions respectively. The transition from nutrient sufficient phase to nutrient starvation phase was found to effect macromolecular composition of biomass (Table 8.1).

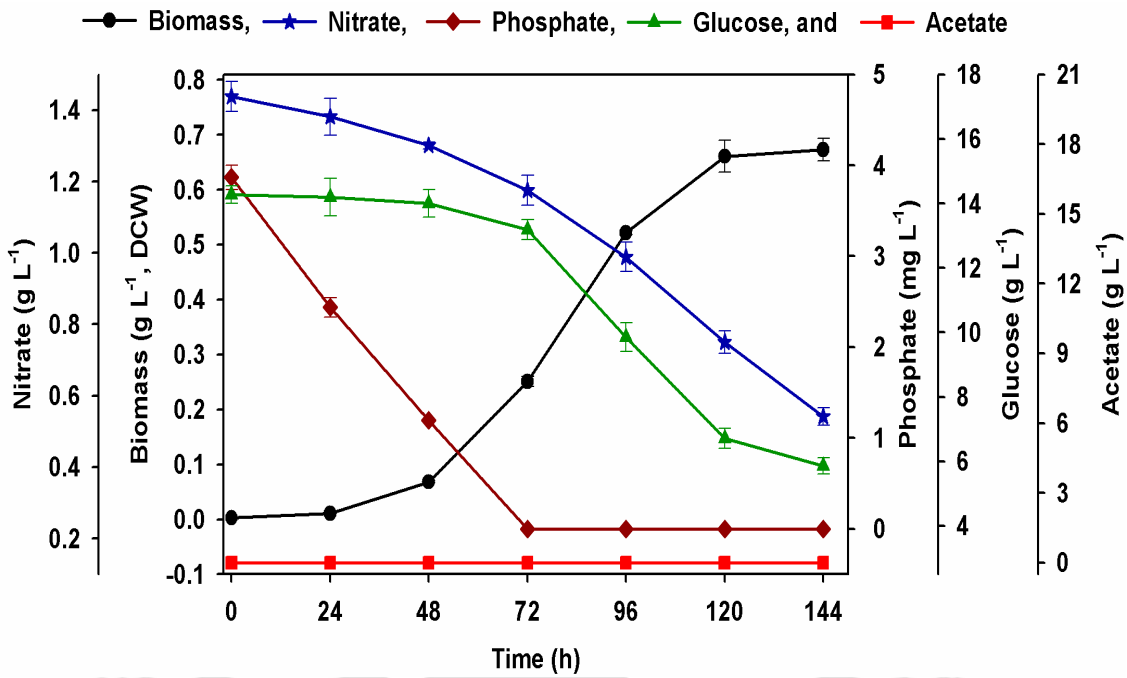

Fig. 8.2: Dynamic profiles of biomass formation and substrate utilization by strain FC2 grown heterotrophically in basic BG11 medium.

Table 8.1 Biomass composition for heterotrophically grown *Chlorella* sp. FC2 IITG under nutrient sufficient, nutrient starvation, and sodium acetate supplemented condition in basic BG11 medium. The values represent the % (w/w) of dry biomass

Metabolites	Biomass composition, % (w/w)			Reference
	Nutrient sufficient	Starvation	Sodium acetate	
Neutral lipid	12.9	29.97	31.74	Experimentally determined
Polar lipid	8.3	7.91	8.14	Determined by equating the components to 100%
Polysaccharide	42.36	29.62	24.67	Experimentally determined
Protein	32.04	28.12	31.08	Experimentally determined
DNA	0.1	0.1	0.1	Boyle and Morgan 2009
RNA	2.8	2.8	2.8	Yang et al. 2009; Fuenters et al. 2000
Chlorophyll	1.5	1.48	1.46	Experimentally determined

In the second experiment, glucose consumption by organism was significantly reduced due to supplementation of sodium acetate and addition of phosphate showed extended growth (Fig. 8.3). The macromolecular composition of biomass was also found to vary with sodium acetate supplementation (Table 8.1) which also depicts a transition

from growth phase to lipid induction phase. The carbon flux distribution map and energetics may uncover the underlying mechanism of varying composition of biomass in association with external cues.

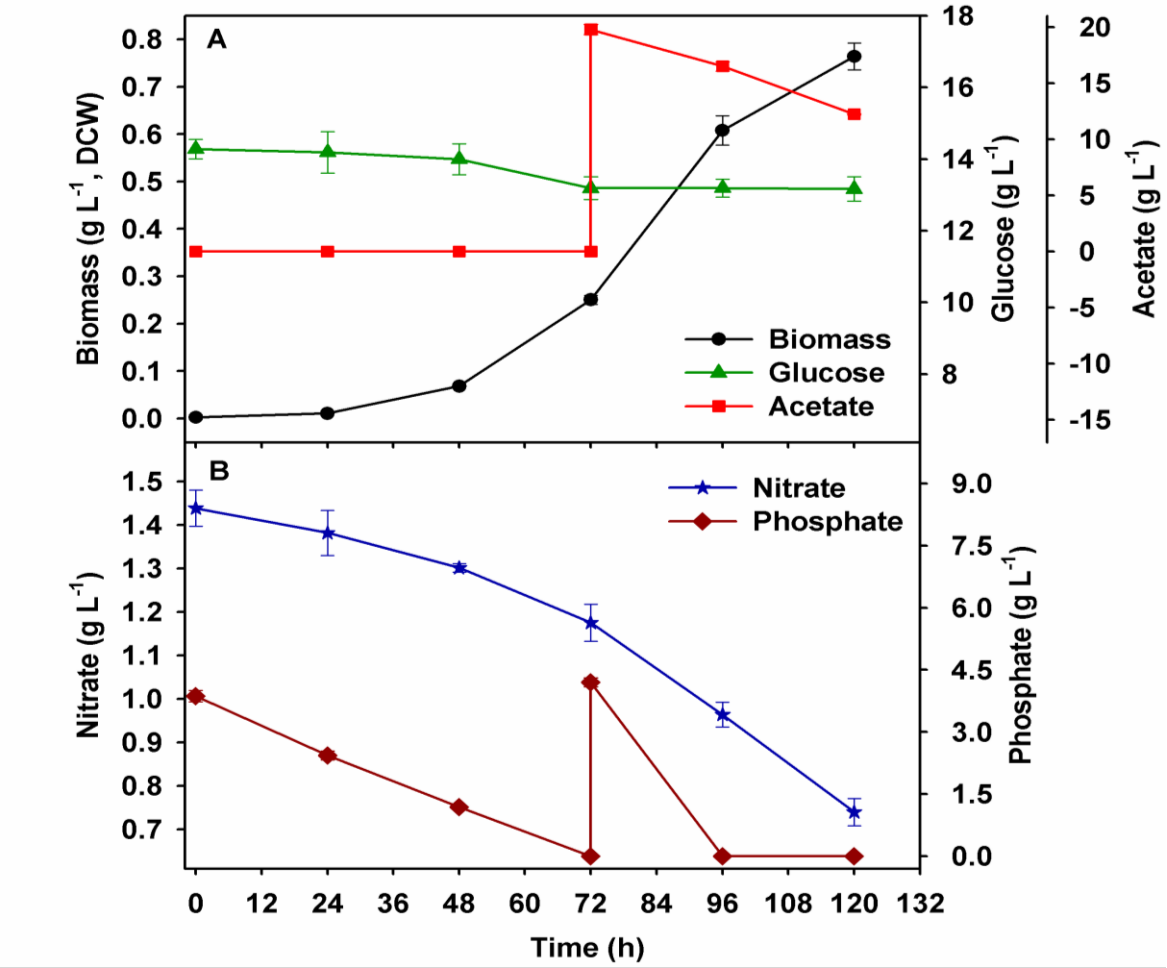

Fig. 8.3 Dynamic profiles of biomass formation and substrate utilization by strain FC2 grown heterotrophically in basic BG11 medium along with addition of sodium acetate and limiting substrate (phosphate) at 72 h of fermentation. (A) depicts the growth, glucose and sodium concentration profiles, and (B) shows the nitrate and phosphate concentration in the medium.

Heterotrophic growth was simulated using reconstructed metabolic network to calculate the intracellular carbon fluxes of FC2 at nutrient sufficient (Fig. 8.4), nutrient starvation (Fig. 8.5) and sodium acetate (Fig. 8.6) supplemented conditions (Detailed in Table A5 in Appendix A). Model predicted and experimentally determined specific growth rates exhibited better match in all the conditions (Table 8.2) and hence model can be used for flux map determination.

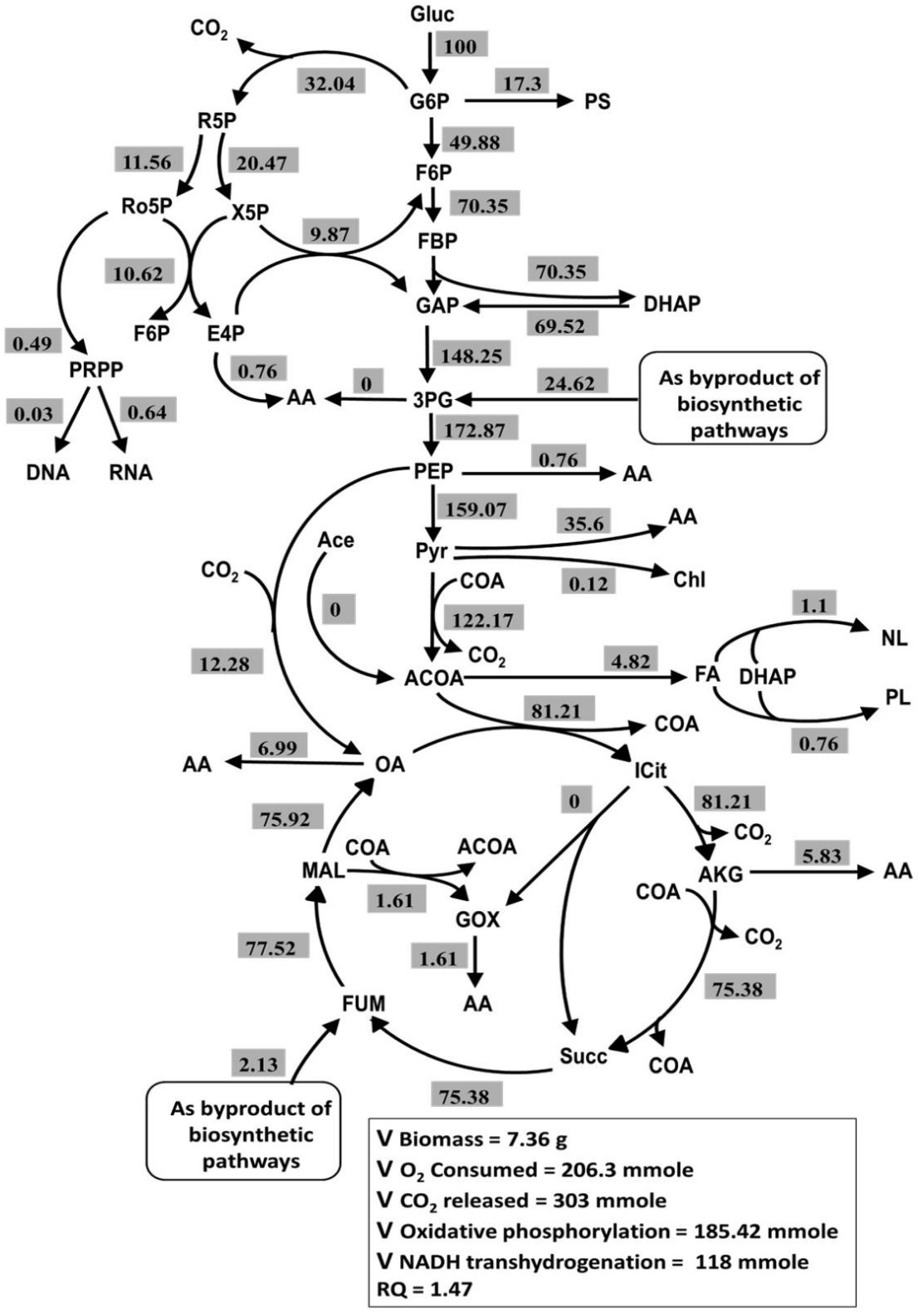

Fig. 8.4 Distribution of carbon fluxes under nutrient sufficient condition (72 h) with maximization of biomass as objective function. All the flux values are normalized to 100 mmol glucose assimilated and are measured in mmol g^{-1} DCW h^{-1}.

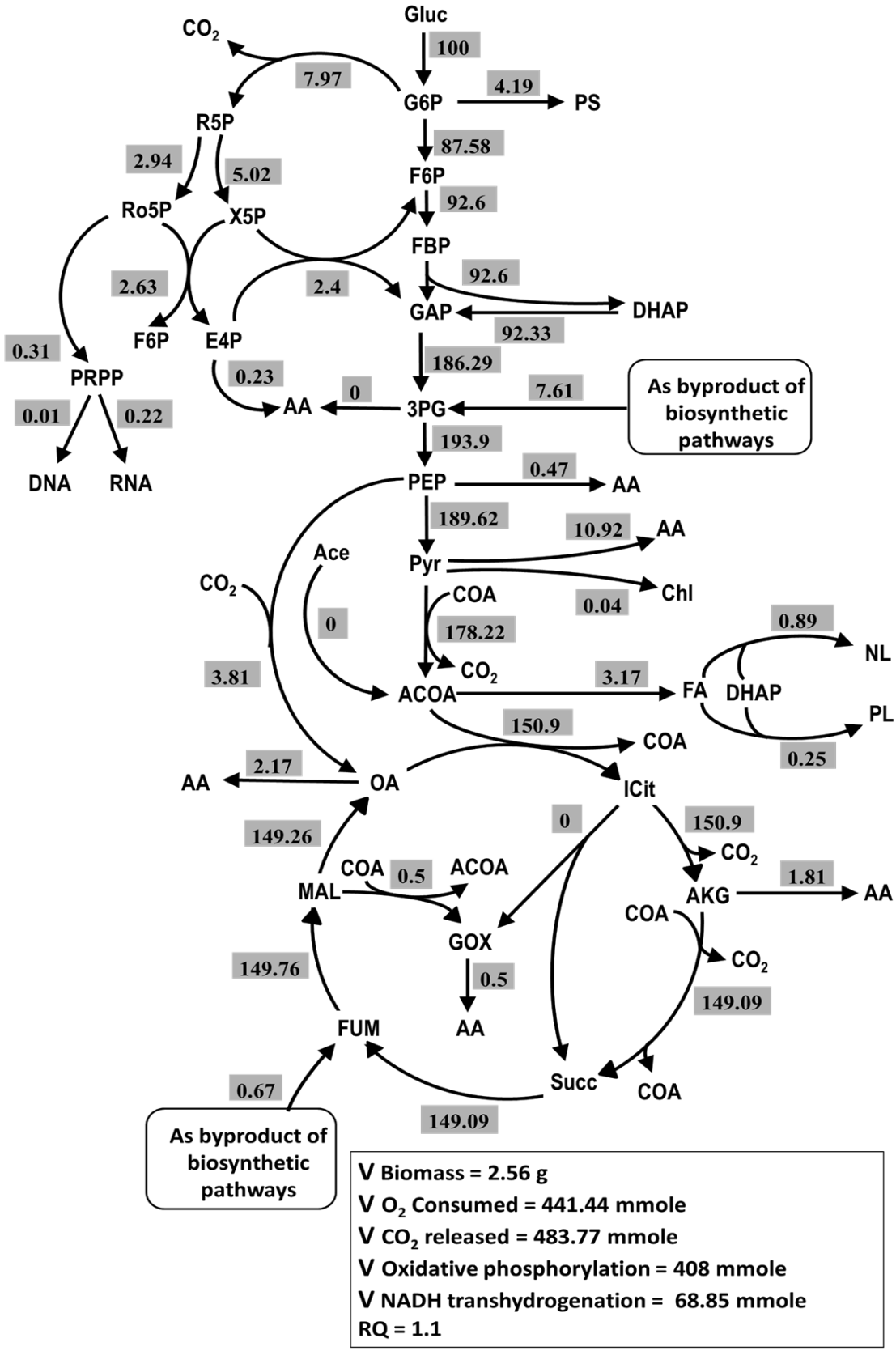

Fig. 8.5 Distribution of carbon fluxes under nutrient starvation condition (96 h) with maximization of biomass as objective function. All the flux values are normalized to 100 mmol glucose assimilated and are measured in mmol g^{-1} DCW h^{-1}.

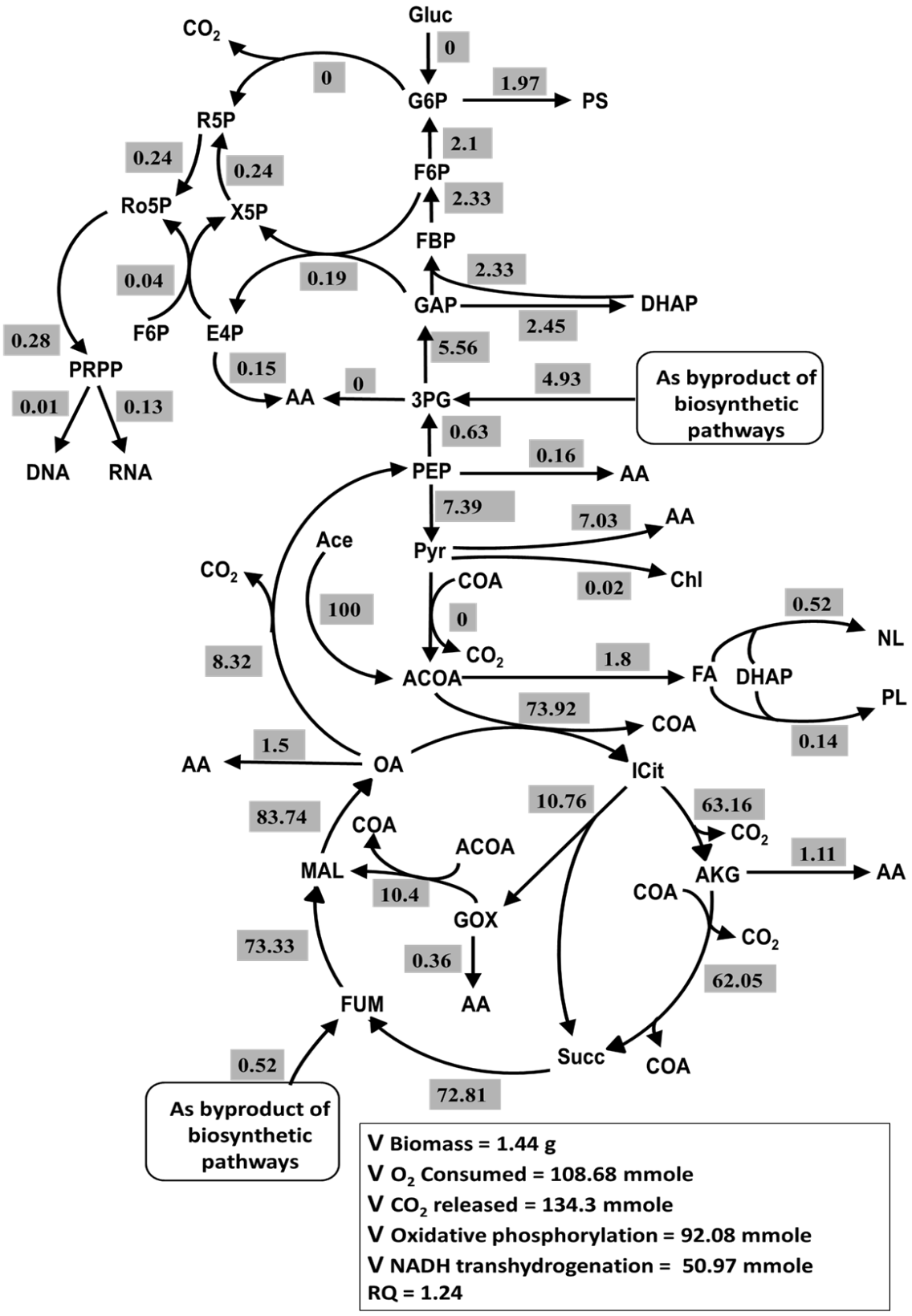

Fig. 8.6 Distribution of carbon fluxes under sodium acetate supplemented condition (96 h) with maximization of biomass as objective function. All the flux values are normalized to 100 mmol sodium acetate assimilated and are measured in mmol g^{-1} DCW h^{-1}.

Under nutrient sufficient condition, the flux distribution in central metabolic pathways started with glucose uptake and 50% of the total carbon influx was directed towards glycolysis pathway (Fig. 8.4) at glucose-6-phosphate (G6P) node. The second major fraction of the incoming carbon flux was channeled into pentose phosphate (PP) pathway (32%) followed by distribution of the remaining flux towards polysaccharide biosynthesis which was attributed towards synthesis of cell wall components and storage carbohydrates (Barsanti and Gualtieri, 2014). C^{13} based analyses in *Chlorella protothecoides* showed similar flux bifurcations at the G6P node (glycolysis - 54.4% and PP pathway - 33.3%) under heterotrophic condition (Xiong et al., 2010). The majority of this carbon flux partitioning between glycolysis and PP pathway at the G6P node provides large amount of biosynthetic precursors, chemical energy and reducing equivalent required for active cellular metabolism. Carbon flux of 27.07% and 8.19% of total carbon uptake was streamed to TCA cycle flux from Acetyl-CoA (ACOA) node and anapleurotic reaction (PEP carboxylase) respectively. Majority of amino acids are synthesized from TCA cycle intermediates and hence imbalanced cycle was replenished through oxaloacetate supply by forward reaction of PEP carboxylase (Xiong et al., 2010). However, majority of this carbon flux was lost in the form of CO_2 for energy production as reported in the literature (Shastri and Morgan, 2005).

Table 8.2 Comparison of model predicted and experimentally determined specific growth rates (h^{-1}) in nutrient sufficient, starvation and sodium acetate supplemented conditions under heterotrophic cultivation.

Nutritional Condition	**Specific growth rate μ (h^{-1})**	
	Experimental	**Predicted**
Sufficient	0.054	0.055
Starvation	0.031	0.038
Sodium acetate	0.037	0.039

Under starvation, majority of carbon flux (87.6%) was directed towards glycolysis while pentose phosphate pathway and polysaccharide biosynthesis together share only 12.2% (Fig. 8.5). Similarly the contribution of flux in all other biosynthetic pathways such as protein, chlorophyll, lipid etc. was also less due to most of the glycolytic carbon flux was utilized into energy yielding pathway, TCA cycle (52.8% of total carbon uptake). PEP carboxylase reaction was reduced by 69% in comparison to nutrient sufficient condition may be due to decreased protein synthesis in starvation.

Acetyl COA biosynthesis is the first committing step in case of acetate metabolism under sodium acetate supplementation (Fig. 8.6). Carbon flux of 73.9% was streamed to TCA cycle and remaining 26.1% was assimilated in lipid biosynthesis pathway. In this condition, 16.64% of carbon flux was redirected towards gluconeogenesis pathway through reverse reaction of PEP carboxylase in order to provide precursors for synthesis of polysaccharides, nucleic acids, pigments and amino acids. Chemical energy and reducing equivalent required for active cellular metabolism was only supplied by TCA cycle and hence non-oxidative pentose pathway was operative just to provide required carbon flux for nucleic acid biosynthesis. In correspondence with the present results, *Chlamydomonas reinhardtii* reported to show fluxes through non-oxidative pentose pathway only when it was grown in sodium acetate nutrition (de Oliveira Dal'Molin et al., 2011). Existence of active glyoxylate shunt points towards its role in replenishing malate and succinate in TCA cycle under reverse reaction of PEP carboxylase. In case of nutrient sufficient and starvation condition, glyoxylate shunt was non operative due to active forward reaction of PEP carboxylase. This depicts that TCA cycle can be replenished by forward reaction of PEP carboxylase under glucose as a carbon source and glyoxylate shunt in case of sodium acetate (de Oliveira Dal'Molin et al., 2011; Xiong et al., 2010). In a photosynthetic organism, various anabolic reactions such as biosynthesis of lipids, chlorophyll, amino

acids and deoxy sugars are catalyzed by the NADPH dependent enzymes (Kanehisa et al., 2008). In order to satisfy this requirement of NADPH, NADH transhydrogenation reaction was found to be highly active under all heterotrophic conditions.

8.3.2. Variation of flux distribution in key pathways during phase transitions

In the first experiment, after 72 h of cultivation a shift in growth environment was observed in terms of transition from nutrient sufficient phase to the nutrient starvation phase which was attributed to the exhaustion of phosphate from medium. Changes in intracellular flux distribution during this transition period were captured by comparing flux values of starvation phase (96 h) with that of nutrient sufficient phase (72 h). The nutritional phase transition was marked with induction of neutral lipid accumulation in the biomass. For instance, at starvation (96 h of growth) carbon flux towards neutral lipid biosynthesis was found to be up-regulated by 1.6-fold with respect to nutrient sufficient condition (Fig. 8.7). Under phosphate or nitrate starvation, the microalgae experiences a gradual decrease in growth rate and the newly fixed carbon and chemical energy gets diverted towards neutral lipid accumulation which can generate more energy upon oxidation than carbohydrates. Hence, the neutral lipids can serve as the best energy reserve for the cell under stress condition (Rodolfi et al., 2009).

In the second experiment, organism was subjected to a shift in growth environment by addition of sodium acetate at 72 h of cultivation. Variation in flux distribution during phase transition from growth phase to lipid induction phase (via addition of sodium acetate) was captured by estimating the flux values at 72 h and 96 h respectively. At 96 h of cultivation, operation of neutral lipid biosynthesis pathway was 1.75 times more active with respect to 72 h of cultivation (Fig. 8.7). This lipid induction was even higher by 8.8% when compared with starvation based lipid accumulation. It was attributed to availability of significant amount of precursor acetyl COA which is formed readily during sodium

acetate uptake as a carbon source (Qiao and Wang, 2009) and enhanced formation of reducing equivalents such as NADH, $FADH_2$ from highly active TCA cycle.

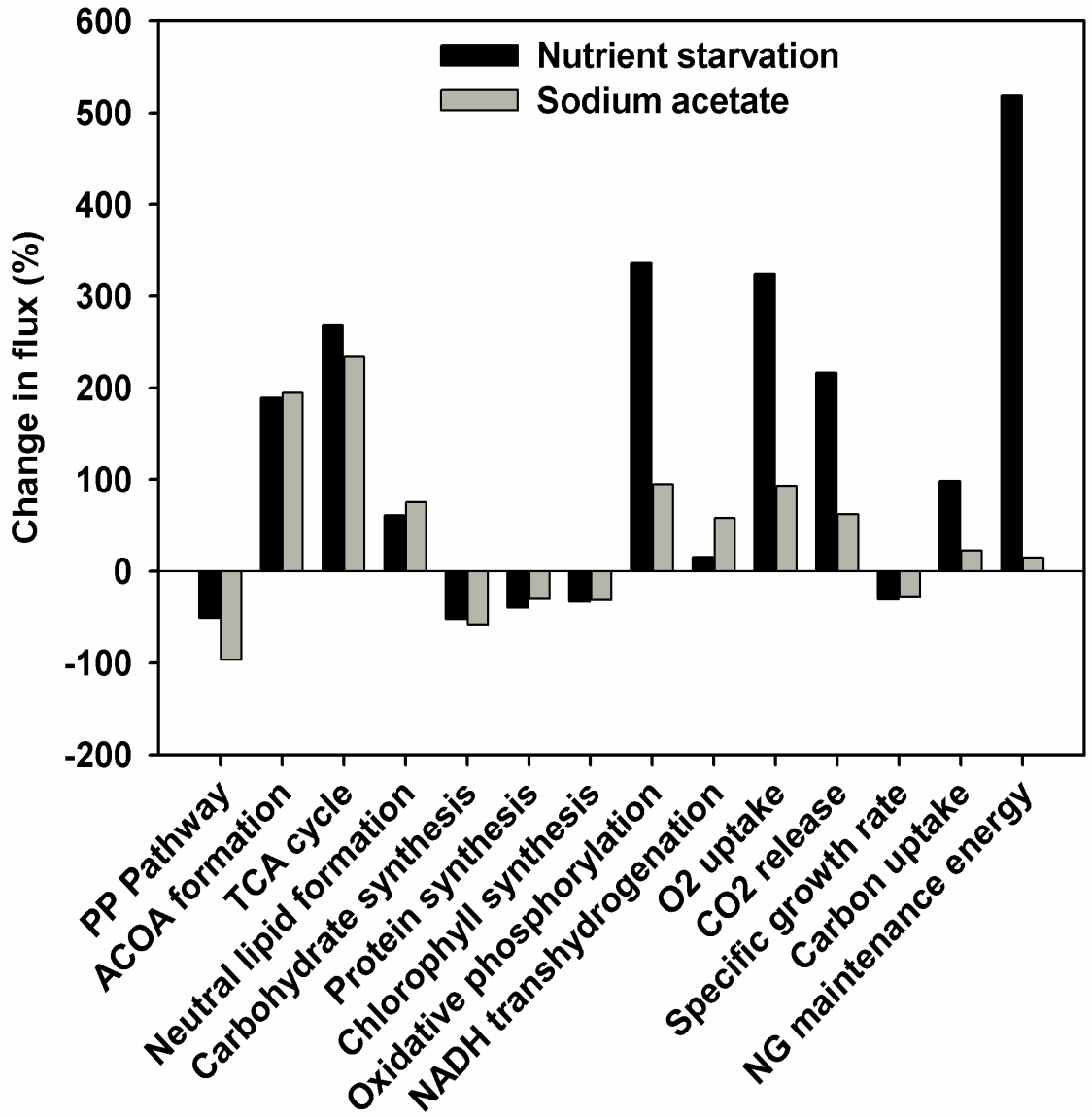

Fig. 8.7 Percentage change in absolute flux values of nutrient starvation and sodium acetate supplemented condition with respect to nutrient sufficient condition. FBA in all conditions was performed with *maximization of biomass* as an objective function.

Under the starvation, 6 fold increased NGA maintenance energy was observed as compared to nutrient sufficient condition (Fig. 8.7). This requirement of higher NGA maintenance energy in the nutritional starvation phase may be attributed to various cellular maintenance operations under nutritional stress (Boyle and Morgan, 2009). Our simulation results that the higher demand for NGA maintenance energy was satisfied by the up-

regulated generation of NADH (1.6 fold), $FADH_2$ (2 fold) and ATP (1.5 fold) through glycolysis and TCA cycle (Table 8.3).

Table 8.3 Balance for the co-factors such as NADPH, NADH, $FADH_2$ and ATP under nutrient sufficient, starvation and sodium acetate supplemented conditions

Co-factor	Pathways	[a] Nutrient sufficient condition	[a] Nutrient starvation condition	[b] Sodium acetate supplemented condition
NADPH	Pentose phosphate	64.09	15.95	0.00
	Lipid synthesis	-80.86	-53.44	-30.3
	Nitrogen assimilation	-90.31	-27.95	-18.6
	Trans hydrogenation	118.06	68.85	50.97
	Other pathways	-10.86	-3.40	-2.07
NADH	Glycolysis & Gluconeogenesis	148.25	186.29	-5.56
	ACOA & TCA cycle	354.70	627.46	208.95
	Oxidative phosphorylation	-325.82	-726.63	-140.51
	Nitrogen assimilation	-30.10	-9.32	-6.2
	Trans hydrogenation	-118.06	-68.85	-50.97
	Other pathways	-28.93	-8.96	-5.7
$FADH_2$	TCA cycle	75.38	149.09	72.82
	Oxidative Phosphorylation	-75.03	-148.98	-72.74
	Amino acid & Protein	-0.35	-0.11	-0.08
ATP	Glycolysis & Gluconeogenesis	149.25	187.12	-6.48
	ACOA & TCA cycle	75.38	149.09	62.05
	Sodium acetate uptake	—	—	-200.0
	Oxidative Phosphorylation	927.11	2040.05	460.38
	Amino acid & Protein	-87.09	-26.83	-16.69
	Maintenance energy	-709.12	-2214.72	-222.55
	Biomass	-285.38	-99.24	-55.8
	Other pathways	-70.38	-35.66	-20.22

[a] The flux (mmol g^{-1} h^{-1}) values are expressed per 100 mmol glucose consumed
[b] The flux (mmol g^{-1} h^{-1}) values are expressed per 100 mmol sodium acetate consumed

Further, an increased oxidative phosphorylation flux at starvation was also observed to generate required ATP from reducing equivalents. Interestingly, in spite of

higher glucose uptake rates, a significant fraction of this was invested to meet high requirements of NGA maintenance energy under phosphate exhausted phase of the growth and hence biomass yield was observed to be reduced by 65% which is in accordance with the previous report (Kliphuis et al., 2012).

In case of sodium acetate supplemented condition, no significant increment in NGA maintenance energy was observed when compared with nutrient sufficient condition (Fig. 8.7). This was also evident from energetics where only 42% of total ATP generated for energy was utilized for NGA maintenance (Table 8.3). However in case of starvation 93% of total ATP generated for energy was used for NGA maintenance to combat the nutrient stress. Sodium acetate was found to be a good lipid inducer without imposing any stress on organism which is the cause of higher NGA maintenance energy. In terms of energetics, it suggests that lipid induction by sodium acetate will be energy efficient than starvation based lipid enrichment. Hence sodium acetate is a better option for lipid induction in biomass towards cost effective bioprocess development for biodiesel production.

8.4. Conclusions

In this study, a metabolic modeling was carried out to study the flux map and energetics during nutrient sufficient, starvation and sodium acetate supplemented conditions. Model has shown that TCA cycle can be replenished by forward reaction of PEP carboxylase under glucose as a carbon source and glyoxylate shunt in case of sodium acetate. During nutrient starvation, an enhanced lipid accumulation in biomass was observed with concomitant 6 fold increase in non-growth associated (NGA) maintenance energy to combat stress. In case of sodium acetate supplementation, lipid induction in biomass was found to be higher than starvation with no significant increase in NGA

maintenance energy. Hence sodium acetate is a better option for lipid induction in biomass towards cost effective bioprocess development for biodiesel production.

8.5. References

1. Barsanti L., Gualtieri P., 2014. Algae: anatomy, biochemistry, and biotechnology. CRC Press, Taylor & Francis, Boca Raton, Florida.
2. Bernard O., 2011. Hurdles and challenges for modelling and control of microalgae for CO_2 mitigation and biofuel production. Journal of Process Control. 21, 1378–1389.
3. Boyle N.R., Morgan J.A., 2009. Flux balance analysis of primary metabolism in *Chlamydomonas reinhardtii*. BMC System Biology. 3, 4.
4. de Oliveira Dal'Molin C.G., Quek L.-E., Palfreyman R.W., Nielsen L.K., 2011. AlgaGEM–a genome-scale metabolic reconstruction of algae based on the *Chlamydomonas reinhardtii* genome. BMC Genomics 12, S5.
5. Dörmann P., Benning C., 2002. Galactolipids rule in seed plants. Trends in Plant Science. 7, 112–118.
6. Dubois M., Gilles K.A., Hamilton J.K., Rebers Pa., Smith F., 1956. Colorimetric method for determination of sugars and related substances. Analytical chemistry. 28, 350–356.
7. El-Sheekh M.M., 1993. Lipid and fatty acids composition of photoautotrophically and heterotrophically grown *Chlamydomonas reinhardtii*. Biologia Plantarum. 35, 435–441.
8. Fuentes M.R., Fernández G.A., Pérez J.S., Guerrero J.G., 2000. Biomass nutrient profiles of the microalga *Porphyridium cruentum*. Food Chemistry. 70, 345–353.

9. Hu Q., Sommerfeld M., Jarvis E., Ghirardi M., Posewitz M., Seibert M., Darzins A., 2008. Microalgal triacylglycerols as feedstocks for biofuel production: perspectives and advances. The Plant Journal. 54, 621–639.

10. Kanehisa M., Araki M., Goto S., Hattori M., Hirakawa M., Itoh M., Katayama T., Kawashima S., Okuda S., Tokimatsu T., 2008. KEGG for linking genomes to life and the environment. Nucleic Acids Research. 36, D480–D484.

11. Kliphuis A.M., Klok A.J., Martens D.E., Lamers P.P., Janssen M., Wijffels R.H., 2012. Metabolic modeling of *Chlamydomonas reinhardtii*: energy requirements for photoautotrophic growth and maintenance. Journal of Applied Phycology. 24, 253–266.

12. Kumar M., Gayen K., Saini S., 2013. Role of extracellular cues to trigger the metabolic phase shifting from acidogenesis to solventogenesis in *Clostridium acetobutylicum*. Bioresource Technology. 138, 55–62.

13. Montagud A., Navarro E., de Córdoba P.F., Urchueguía J.F., Patil K.R., 2010. Reconstruction and analysis of genome-scale metabolic model of a photosynthetic bacterium. BMC System Biology. 4, 156.

14. Nelson D.L., Cox M.M., 2012. Lehninger Principles of Biochemistry. 6th ed. W H Freeman and Company, New York.

15. Pruvost J., Van Vooren G., Le Gouic B., Couzinet-Mossion A., Legrand J., 2011. Systematic investigation of biomass and lipid productivity by microalgae in photobioreactors for biodiesel application. Bioresource Technology. 102, 150–158.

16. Qiao H., Wang G., 2009. Effect of carbon source on growth and lipid accumulation in *Chlorella sorokiniana* GXNN01. Chinese Journal of Oceanology and Limnology. 27, 762–768.

17. Rodolfi L., Chini Zittelli G., Bassi N., Padovani G., Biondi N., Bonini G., Tredici M.R., 2009. Microalgae for oil: Strain selection, induction of lipid synthesis and outdoor mass cultivation in a low-cost photobioreactor. Biotechnology and Bioengineering. 102, 100–112.

18. Shastri A.A., Morgan J.A., 2005. Flux balance analysis of photoautotrophic metabolism. Biotechnology Progress. 21, 1617–1626.

19. Srivastava R.K., Maiti S.K., Das D., Bapat P.M., Batta K., Bhushan M., Wangikar P.P., 2012. Metabolic flexibility of d-ribose producer strain of Bacillus pumilus under environmental perturbations. Journal of Industrial Microbiology and Biotechnology. 39, 1227–1243.

20. Trinh C.T., Wlaschin A., Srienc F., 2009. Elementary mode analysis: a useful metabolic pathway analysis tool for characterizing cellular metabolism. Applied Microbiology and Biotechnology. 81, 813–826.

21. Xiong W., Liu L., Wu C., Yang C., Wu Q., 2010. 13C-tracer and gas chromatography-mass spectrometry analyses reveal metabolic flux distribution in the oleaginous microalga *Chlorella protothecoides*. Plant Physiology. 154, 1001–1011.

22. Yang C., Hua Q., Shimizu K., 2000. Energetics and carbon metabolism during growth of microalgal cells under photoautotrophic, mixotrophic and cyclic light-autotrophic/dark-heterotrophic conditions. Biochemical Engineering Journal. 6, 87–102.

CHAPTER 9

Conclusions

The lower biomass titer, productivity, understanding of growth kinetics, metabolism and process control are some of the existing bottlenecks in commercial scale production of biodiesel from microalgae. In order to address these bottlenecks, combined bioprocess development and metabolic modeling approaches were employed to characterize the *Chlorella* sp. FC2 IITG in detail and to achieve high cell density and improve high neutral lipid productivity which are the desired characteristics while choosing a feedstock for microalgae based biodiesel production. The microalga *Chlorella* sp. FC2 IITG is a novel indigenous strain isolated in our laboratory from the North-East region of India. Characterization of the strain under different pH and temperatures revealed the robustness of the strain to grow in wide range of pH from 4 to 10 and temperatures of range 20-44°C. Enhanced growth and lipid induction was observed when glucose and sodium acetate were used as carbon sources respectively. Similarly sodium nitrate, yeast extract, glycine and peptone were found to be growth supportive nitrogen sources. Irrespective of carbon sources and nutritional condition, biodiesel obtained from the strain FC2 was found to be suitable for commercial use as its properties lie in the range of ASTM and European standards.

Initial characterization of strain in basic BG11 media showed that phosphate is the limiting substrate in medium and organism soon enters the nutrient starvation on cultivation which resulted in lowered biomass titer of 0.67 g L^{-1}. Hence, media composition for maximal growth and lipid induction was optimized separately with the use of best carbon and nitrogen sources obtained from their screening experiment. Two optimizations were performed for the growth where highest growth rate of 2.115 day^{-1} was

achieved during maximization of specific growth rate as objective function and in case of maximization biomass titer highest biomass concentration of 7.81 g L^{-1} was obtained. Optimal media components for specific growth rate can be used in operation of continuous and fed batch cultivation. Similarly media components optimized for biomass titer can be used for batch cultivation of the organism. During the media optimization for lipid, 24 g L^{-1} sodium acetate supplementation was found to be optimal with lipid induction of ~66% w/w, DCW. High cell density or productivity cultivation can be a strategy for cost effective bioprocess development which can be achieved by combining wet lab experiments and *in silico* modeling towards optimal nutrition of organism in fed-batch or continuous operation.

The multi-nutrient mechanistic model was developed based on segregation of intracellular nutrients into SFN, RUN & Non-RUN and their sequential utilization during starvation. The preferential utilization of ECN under nutrient sufficient condition and then RUN followed by Non-RUN under nutrient deplete condition for the growth of microalgae was modeled and experimentally validated. The SFN is the remaining fraction after exhaustion of both RUN and NonRUN which is required to maintain integrity of cell structure. Model exhibited improved predictability over existing models like Monod kinetics, Droop cell quota model. This multi-nutrient model was used to design the substrate feeding strategy for high cell density-lipid rich cultivation. This involves biphasic fed-batch fermentation: (i) growth phase, where high cell density was achieved through model guided substrate feeding recipe coupled with substrate (nitric acid) driven pH control and (ii) lipid enrichment phase via addition of sodium acetate. This strategy resulted in biomass titer of 90.15 g L^{-1} with biomass and lipid productivity 19.75 g L^{-1} day^{-1} and 7.7 g L^{-1} day^{-1} respectively. Similarly, two-stage chemostat cultivation was designed for continuous production of lipid rich algal biomass with improved productivity. This

involved two reactors connected in series where first reactor was operated at model optimized substrate concentration of feed-stream and dilution rate for generation of biomass with enhanced productivity while the second reactor was dedicated for intracellular lipid enrichment via addition of lipid inducer. Biomass and lipid productivity of 92.7 g L^{-1} day^{-1} and 9.76 g L^{-1} day^{-1} was observed in first and second reactors respectively. The obtained productivities are significantly higher amongst the published literatures for microalgae based biodiesel production.

The understanding of lipid biosynthesis pathway in terms of energetics and carbon flux distribution is important towards biodiesel production. A metabolic network was reconstructed and analyzed for nutrient sufficient, starvation and sodium acetate supplemented conditions. Forward reaction of PEP carboxylase was active under nutrient sufficient and starvation condition in order to replenish the TCA cycle of the organism. However in case of sodium acetate supplementation, backward reaction of PEP carboxylase was operative and hence glyoxylate shunt reaction was activated in order to satisfy TCA cycle requirements. Further, enhanced intracellular lipid accumulation was observed along with 6 fold increase in non-growth associated (NGA) maintenance energy during the starvation phase in comparison to nutrient sufficient condition. However in case of sodium acetate based lipid induction, an improved lipid accumulation was achieved without significant increase in NGA maintenance energy with respect to nutrient sufficient condition. This suggests that lipid induction by sodium acetate will be energy efficient condition than starvation based lipid enrichment. Hence sodium acetate was used as lipid inducer in current process development strategies. The biodiesel obtained from microalga FC2 grown under heterotrophic condition can be used for commercial applications as it satisfies American and European standards. Therefore the process strategy developed in

present study opens up scope for further economic feasibility analysis and scale up for commercial production.

Engineering Significance

Microalgae based fuel generation remains unachievable in terms of sustainability and economic feasibility. The present study targeted to attain sustainability and economic feasibility by employing following engineering interventions which have resulted in significant increase in the biomass and lipid productivity.

- ✓ Physicochemical understanding of the organism FC2 resulted in the identification of sodium acetate and glucose as lipid inducing and growth supporting carbon sources respectively. With this as a lead, a two stage bioprocess was developed in the present study with sequential utilization of glucose and sodium acetate for growth and lipid accumulation.
- ✓ A mechanistic model was developed in the present study incorporated with nutrient quota and different forms of intracellular nutrients available for growth during the nutrient sufficient and starvation conditions. The model captured the physiological changes of the microalgae with respect to the nutrient sufficient and starvation conditions and predicted the fate of the process and production levels accurately.
- ✓ With the mechanistic model developed, fed-batch and continuous production process for biodiesel production was developed with the maximum net lipid productivity of 9.76 g L^{-1} day^{-1} which was several folds higher than that obtained in the photoautotrophic process as reported in literatures thereby reducing the net energy ratio.
- ✓ Substrate driven pH control was also developed which avoided the toxicity of alkali and acids added for pH control.
- ✓ Metabolic flux balance analysis based modeling approach revealed the physiological significance and energy conservation with sodium acetate as lipid inducer as compared to the conventional nutrient starvation strategy.

Future Prospects

- ✓ Evaluating the strains performance in pilot scale and demonstration of a large scale bioprocess for biodiesel production under heterotrophic condition in continuous mode of operation using wild type strain *Chlorella* sp. FC2 IITG.
- ✓ Energy efficient harvesting strategy and downstream process technology for biodiesel production need to be developed to attain net sustainability.
- ✓ Further extension of metabolic engineering may be employed to determine the sensible targets of modification which can come up with new producer strains with enhanced productivity.
- ✓ Production of biodiesel from the low cost renewable substrates such as lignocellulosic wastes.
- ✓ Economic feasibility analysis and sustainability analysis for the technology developed in the present study has to be conducted.

Appendix A

1. Determination of proportionality constant $K_{V/X}$

$K_{V/X}$ is the proportionality constant which depicts the volume of TME stock required for formation of 1 g biomass. One unit of TME supports biomass formation up to 5.17 g without compromising the maximum specific growth rate (Section 4.3.2). In the fed-batch experiment, TME stock was prepared in such a way 10 mL of stock contains one unit of TME; hence 10 mL of TME stock can support 5.17 g biomass.

As per definition,

$K_{V/X}$

$= (Volume\ of\ TME\ stock\ required)\ /\ (Biomass\ formed\ by\ addition\ of\ TME)$

$K_{V/X} = 10 \cdot 10^{-3}/5.17$

$K_{V/X} = 0.001934$

Hence, $K_{V/X} = \sim 0.002$

2. Effect of 90 mM sodium chloride on organism growth

Effect of sodium chloride on the growth was assessed by cultivating FC2 in optimized BG11 medium with supplementation of 90 mM sodium chloride in the conical flask. Optimized BG11 media without sodium chloride was used as control experiment. Inoculum was prepared as explained in section 3.2.1 with optimized BG11 media. 1% (v/v) of active mid-log phase inoculum was transferred to both the experiment. The biomass concentration of 1.7 g L^{-1} was achieved under 90 mM salinity which was 70% lesser in comparison to control experiment (Fig. A1). This depicted that growth f FC2 is abruptly hindered by salinity stress as it isolated from fresh water bodies (Muthuraj et al., 2014).

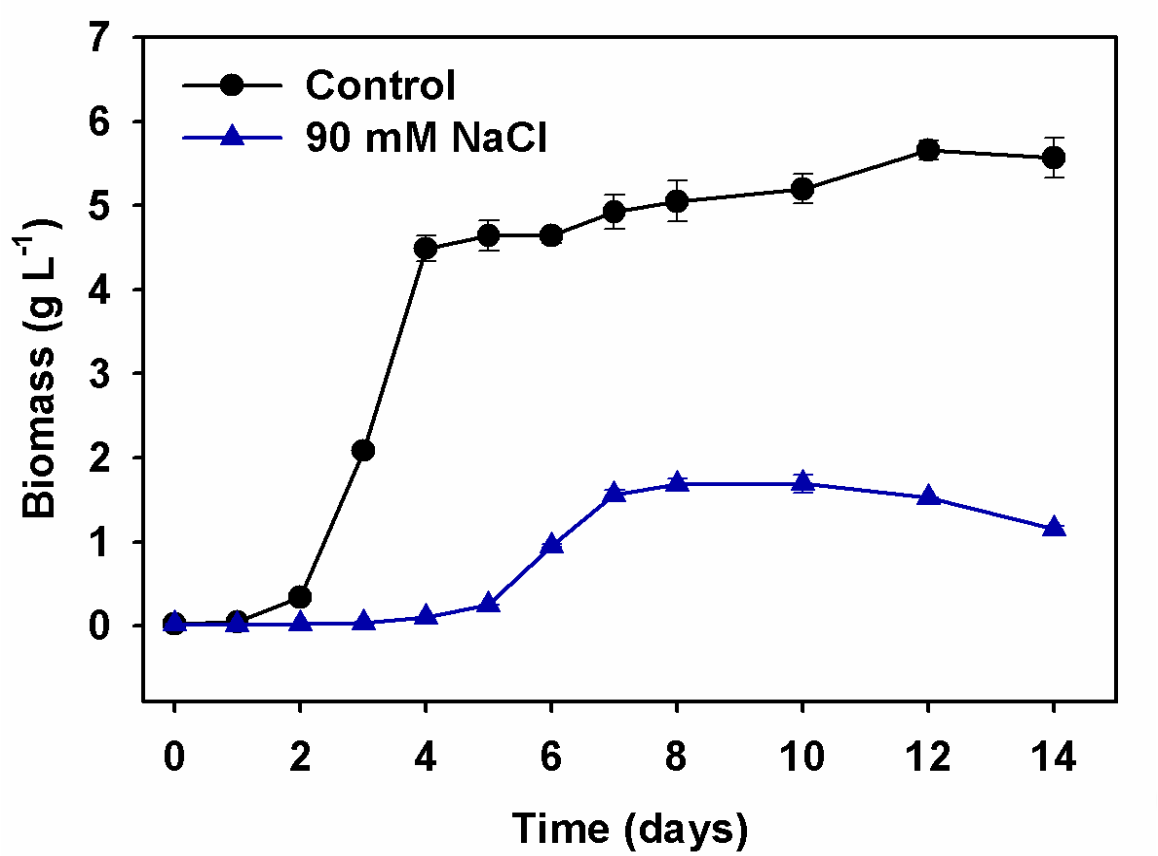

Fig. A1 Dynamic profiles of biomass of FC2 grown in conical flask containing optimized BG11 medium and optimized BG11 medium with supplementation of 90 mM sodium chloride.

3. Tabular representations

Appendix A

Table A1 Comparison of biomass titer, biomass productivity and yield coefficient for different microalgae grown under various conditions with the strain FC2 grown in a 7.5 L automated bioreactor under heterotrophic fed-batch or continuous mode of operation

SI No	Microalgae	Condition	DCW ($g\ L^{-1}$)	Biomass productivity $g\ L^{-1}\ day^{-1}$	Mode	Data	Yield ($g\ g^{-1}$)	Reference
1	***Chlorella* sp. FC2 IITG**	**Heterotrophy**	**58**	**92.75**	**C**	**Given**	**0.66**	**Present study**
2	*Chlorella vulgaris*	Heterotrophy	117.2	84.48	FB	Given	0.625	Doucha 2012
3	*Chlorella pyrenoidosa*	Heterotrophy	116.2	24.48	FB	Given	0.455	Wu 2007
4	*Chlorella sorokiniana*	Heterotrophy	103.8	24.2	FB	Given	0.47	Zheng 2013
5	***Chlorella* sp. FC2 IITG**	**Heterotrophy**	**87**	**19.75**	**FB**	**Given**	**0.735**	**Present study**
6	*Chlorella sorokiniana*	Heterotrophy	37.6	12.2	B	Given	0.5	Zheng 2013
7	*Auxenochlorella (Chlorella) protothecoides*	Photoautotrophy followed by Heterotrophy	116	12	FB	Given	~ 0.45	Rismani-Yazdi 2015
8	*Chlorella protothecoides* UTEX 25	Heterotrophy	64	9.4	FB	Given	0.33^{GO}	Cerón-García 2013
9	*Chlorella protothecoides*	Heterotrophy	48	8.9	FB	Given	0.47	Shi 2012
10	*Galdieria sulphuraria*	Heterotrophy	116	8	FB	Calc	0.5	Schmidt 2005
11	*Galdieria sulphuraria*	Heterotrophy	109	7.79	FB	Calc	0.43	Graverholt 2007
12	*Chlorella protothecoides*	Heterotrophy	51.2	7.36	FB	Given	--	Xiong 2008
13	*Chlorella protothecoides*	Heterotrophy	49.3	6.97	FB	Calc	--	Lu 2011
14	*Crypthecodinium cohnii*	Heterotrophy	109	6.54	FB	Calc	0.13^{AA}	De-Swaaf 2003
15	*Chlorella protothecoides*	Heterotrophy	45.2	5.51	FB	Given	--	Chen 2011
16	*Chlorella sorokinana* FC6 IITG	Mixotrophy	15.81	1.93	FB	Given	--	Kumar 2014
17	*Chlorella sp.* FC2 IITG	Autotrophy	13.5	0.675	FB	Given	--	Muthuraj 2015

FB – fed-batch, B – batch, Calc. – calculated from given data, GO – glycerol and AA – acetic acid.

Table A2 Comparison of lipid content and lipid productivity for different microalgae grown under various conditions with the strain FC2 grown in a 7.5 L automated bioreactor under heterotrophic fed-batch or continuous mode of operation

SI No	Microalgae	Condition	Lipid content % DCW	Lipid productivity g L^{-1} day^{-1}	Mode	Data	Reference
1	***Chlorella* sp. FC2 IITG**	**Heterotrophy**	**48**	**9.76**	**C**	**Given**	**Present study**
2	*Chlorella vulgaris*	Heterotrophy	9.7	8.19	FB	Calc.	Doucha 2012
3	***Chlorella* sp. FC2 IITG**	**Heterotrophy**	**70.2**	**7.7**	**FB**	**Given**	**Present study**
4	*Auxenochlorella (Chlorella) protothecoides*	Photoautotrophy followed by Heterotrophy	60	6.48	FB	Given	Rismani-Yazdi 2015
5	*Chlorella protothecoides* UTEX 25	Heterotrophy	49.8	4.3	SC	Given	Cerón-García 2013
6	*Chlorella sorokiniana*	Heterotrophy	38.7	4.2	FB	Given	Zheng 2013
7	*Chlorella protothecoides*	Heterotrophy	54.6	3.8	FB	Calc.	Lu 2011
8	*Chlorella protothecoides*	Heterotrophy	50.3	3.68	FB	Calc.	Xiong 2008
9	*Chlorella protothecoides*	Heterotrophy	54.4	3	FB	Calc.	Chen 2011
10	*Chlorella sorokiniana*	Heterotrophy	31.5	2.9	B	Given	Zheng 2013
11	*Chlorella protothecoides*	Heterotrophy	--	1.19	FB	Given	Li 2015
12	*Chlorella protothecoides*	Heterotrophy	~50	0.85	FB	Given	Shen 2010
13	*Chlorella sorokiniana* FC6 IITG	Mixotrophy	55	0.55	FB	Given	Kumar 2014
14	*Chlorella* sp. FC2 IITG	Autotrophy	56	0.313	FB	Given	Muthuraj 2015
15	*Desmodesmus* sp. F2	Photoautotrophy	64.13	0.263	B	Given	Ho 2014
16	*Nannochloropsis* sp. F&M-M24	Photoautotrophy	60	0.204	B	Given	Rodolfi 2009
17	*Nannochloropsis* sp.	Mixotrophy	25.3	0.148	FB	Given	Cheirsilp 2012

FB – fed-batch, B – batch, SC – semi-continuous and Calc. – calculated from given data

Appendix A

Table A3 Reconstruction of the metabolic network of *Chlorella* sp. FC2 IITG: List of reactions involved in the central metabolism and their enzyme catalysts under heterotrophic conditions

SI No.	EC No.	Enzyme	Pathway	Reactions*
1	2.7.1.1	Hexokinase	**Glycolysis**	Gluc + ATP --> G6P + ADP
2	5.3.1.9	Glucose 6 phosphate isomerase		G6P --> F6P
3	5.3.1.9	Glucose 6 phosphate isomerase		F6P --> G6P
4	2.7.1.11	6-phospho fructokinase		F6P + ATP --> FBP + ADP
5	4.1.2.13	Fructose biphosphate aldolase		FBP --> GAP + DHAP
6	4.1.2.13	Fructose biphosphate aldolase		DHAP + GAP --> FBP
7	5.3.1.1	Triose phosphate isomerase		DHAP --> GAP
8	5.3.1.1	Triose phosphate isomerase		GAP --> DHAP
9	1.2.1.12	Glyceraldehyde 3 phosphate dehydrogenase		GAP + Pi + NAD --> BPG + NADH
10	1.2.1.12	Glyceraldehyde 3 phosphate dehydrogenase		NADH + BPG --> GAP + Pi + NAD
11	2.7.2.3	Phosphoglycerate kinase		BPG + ADP --> 3PG + ATP
12	2.7.2.3	Phosphoglycerate kinase		3PG + ATP --> BPG + ADP
13	5.4.2.1, 4.2.1.11	Phosphoglycerate mutase, enolase		3PG --> PEP
14	5.4.2.1, 4.2.1.11	Phosphoglycerate mutase, enolase		PEP --> 3PG
15	2.7.1.40	Pyruvate kinase		PEP + ADP --> Pyr + ATP
16	1.2.4.1, 2.3.1.12, 1.8.1.4	E1 and E2 components of Pyruvate dehydrogenase, dihydrolipoamide dehydrogenase	**Acetyl CoA biosynthesis**	Pyr + COA + NAD --> ACOA + CO2 + NADH

17	2.3.3.1	Citrate synthase	**Tri-Carboxylic acid cycle (TCA)**	ACOA + OA --> Cit + COA
18	4.2.1.3	aconitate hydratase		Cit --> ICit
19	4.2.1.3	aconitate hydratase		ICit --> Cit
20	1.1.1.41	Isocitrate dehydrogenase		ICit + NAD --> AKG + NADH + CO2
21	1.2.4.2, 2.3.1.61, 1.8.1.4	E1 and E2 components of 2-oxoglutarate dehydrogenase, dihydrolipoamide dehydrogenase		AKG + COA + NAD --> SCOA + CO2 + NADH
22	6.2.1.4, 6.2.1.5	Succinyl CoA ligase		SCOA + Pi + ADP --> Succ + ATP + COA
23	6.2.1.4, 6.2.1.5	Succinyl CoA ligase		Succ + ATP + COA --> SCOA + Pi + ADP
24	1.3.5.1	Succinate dehydrogenase		Succ + FAD --> Fum + FADH2
25	1.3.5.1	Succinate dehydrogenase		Fum + FADH2 --> Succ + FAD
26	4.2.1.2	Fumarate hydratase		Fum --> Mal
27	4.2.1.2	Fumarate hydratase		Mal --> Fum
28	1.1.1.37	Malate dehydrogenase		Mal + NAD --> OA + NADH
29	1.1.1.37	Malate dehydrogenase		'OA + NADH --> Mal + NAD'
30	4.1.1.49	phosphoenol pyruvate carboxykinase	**Gluco-neogenesis & Anaplerotic reaction**	'OA + ATP --> PEP + ADP + CO2'
31	4.1.1.31	phosphoenol pyruvate carboxylase		'PEP + ADP + CO2 --> OA + ATP'
32	3.1.3.11	Fructose 1 6 - biphosphatase		'FBP --> F6P + Pi'
33	3.1.3.9	Glucose 6 phosphatase		'G6P --> Gluc + Pi'

34	4.1.3.1	Isocitrate lyase	**Glyoxalate cycle**	'ICit --> Succ + GOX'
35	2.3.3.9	Malate synthase		'GOX + ACOA --> Mal + COA'
36	2.3.3.9	Malate synthase		'Mal + COA --> GOX + ACOA'
37	1.1.1.49	Glucose 6 phosphate 1 dehydrogenase	**Pentose Phosphate Pathway (PPP)**	'G6P + NADP --> PGL + NADPH'
38	3.1.1.31, 1.1.1.44	6 phosphogluconolactonase, 6 phosphogluconate dehydrogenase		'PGL + NADP --> R5P + CO2 + NADPH'
39	5.3.1.6	Ribose 5 phosphote isomerase		'R5P --> Ro5P'
40	5.3.1.6	Ribose 5 phosphote isomerase		'Ro5P --> R5P'
41	5.1.3.1	Ribulose phosphate 3-epimerase		'R5P --> X5P'
42	5.1.3.1	Ribulose phosphate 3-epimerase		'X5P --> R5P'
43	2.2.1.1	Transketolase	**Pentose Phosphate Pathway (PPP)**	'Ro5P + X5P --> SH7P + GAP'
44	2.2.1.1	Transketolase		'SH7P + GAP --> Ro5P + X5P'
45	2.2.1.2	Transaldolase		'SH7P + GAP --> E4P + F6P'
46	2.2.1.2	Transaldolase		'E4P + F6P --> SH7P + GAP'
47	2.2.1.1	Transketolase		'E4P + X5P --> F6P + GAP'
48	2.2.1.1	Transketolase		'F6P + GAP --> E4P + X5P'
49	6.4.1.2, 2.3.1.39, 2.3.1.38, 2.3.1.179, 1.1.1.100, 4.2.1.58, 1.3.1.9, 1.14.19.2, 3.1.2.14	Lumped reaction	**Lipid biosynthesis**	Fatty acid(FA) synthesis (Average FA consired so it varies with culturing mode)

50	2.7.1.30, 1.1.1.72, 1.2.1.3, 2.7.1.31, 1.2.1.12, 2.7.2.3, 6.2.1.3, 2.3.1.15, 2.3.1.51, 3.1.3.4, 3.1.1.3	Lumped reaction	**Lipid biosynthesis**	'3 FA + ATP + GAP + NADPH + ADP --> NL + 2 AMP + 4 Pi + NADP'
51	2.7.7.9	UTP glucose 1 phosphate uridylyltransferase		'UTP + G1P --> UDP_gluc + 2 Pi'
52	5.1.3.2	UDP glucose 4 epimerase		'UDP_gluc --> UDP_gal'
53	2.3.1.15, 2.3.1.51, 3.1.3.4, 2.4.1.46	Lumped reaction		'DHAP + NADH + 2 FA + 2 ATP + UDP_gal --> MGDG + UDP + NAD + 2 AMP + 5 Pi'
54	2.3.1.15, 2.3.1.51, 3.1.3.4, 2.4.1.46, 2.4.1.184	Lumped reaction		'DHAP + NADH + 2 FA + 2 ATP + 2 UDP_gal --> DGDG + 2 UDP + NAD + 2 AMP + 5 Pi'
55	1.8.3.1, 3.13.1.1, 2.3.1.15, 2.3.1.51, 3.1.3.4	Lumped reaction		'SO4 + UDP_gluc + DHAP + NADH + 2 FA + 2 ATP --> SQDG + 2 AMP + UDP + NAD + 0.5 O2 + 5 Pi'
56	2.3.1.15, 2.3.1.51, 2.7.7.41, 2.7.8.5, 3.1.3.27	Lumped reaction		'2 DHAP + 2 NADH + 2 FA + 2 ATP + CTP --> PG + CMP + 2 AMP + 2 NAD + 7 Pi'
57	2.3.1.15, 2.3.1.51, 2.7.7.41, 2.7.8.8, 4.1.1.65	Lumped reaction		'DHAP + NADH + 2 FA + 2 ATP + CTP + Ser --> PE + CMP + NAD + 2 AMP + CO2 + 6 Pi'
58	5.5.1.4, 3.1.3.25, 2.3.1.15, 2.3.1.51, 2.7.7.41, 2.7.8.11	Lumped reaction		'DHAP + NADH + 2 FA + 2 ATP + CTP + G6P --> PI + CMP + NAD + 2 AMP + 7 Pi'
59		Average polar lipid		'0.5 MGDG + 0.2 DGDG + 0.1 SQDG + 0.1 PG + 0.05 PE + 0.05 PI --> PL'

60	6.3.1.2	Glutamine synthetase	**Amino acid biosynthesis**	'Glu + NH4 + ATP --> Gln + ADP + Pi'
61	1.4.1.13, 1.4.1.14	Glutamate synthase		'AKG + Gln + NADPH --> 2 Glu + NADP'
62	1.5.1.12, 1.5.1.2	1-pyrroline-5-carboxylate dehydrogenase, pyrroline-5-carboxylate reductase		Glu + 2 NADH --> Pro + 2 NAD'
63	2.6.1.1	Aspartate aminotransferase		'OA + Glu --> Asp + AKG'
64	2.6.1.1	Aspartate aminotransferase		'Asp + AKG --> OA + Glu'
65	2.3.1.1, 2.7.2.8, 1.2.1.38, 2.6.1.11, 2.3.1.35, 3.5.1.16, 2.1.3.3, 6.3.4.5, 4.3.2.1	Lumped reaction		'2 Glu + 2 ATP + NADH + CAP + Asp + ACOA --> Arg + Fum + ace + AKG + NAD + 4 Pi + ADP + AMP + COA'
66	1.5.1.12, 2.6.1.13, 2.1.3.3, 6.3.4.5, 4.3.2.1	Lumped reaction		'2 Glu + ATP + NADH + CAP + Asp --> Arg + Fum + AKG + NAD + 3 Pi + AMP'
67	1.1.1.95, 2.6.1.52, 3.1.3.3	Lumped reaction		'3PG + NAD + Glu --> Ser + NADH + AKG + Pi'
68	4.3.1.19	Threonine dehydratase		'Pyr + NH4 --> Ser'
69	4.3.1.19	Threonine dehydratase		'Ser --> Pyr + NH4'
70	2.1.2.1	Glycine hydroxymethyltransferase		'Ser + THF --> Gly + MnTHF'
71	2.1.2.1	Glycine hydroxymethyltransferase		'Gly + MnTHF --> Ser + THF'
72	2.7.7.4, 1.8.99.2, 1.8.1.2	Lumped reaction		'ATP + SO4 + FADH2 + 3 NADH --> H2S + 3 NAD + AMP + FAD + 2 Pi'
73	2.3.1.30, 2.5.1.47	Serine O-acetyltransferase, cysteine synthase		'Ser + ACOA + H2S --> Cys + ace + COA'
74	2.6.1.2	Alanine transaminase		'Pyr + Glu --> Ala + AKG'

75	2.6.1.2	Alanine transaminase	**Amino acid biosynthesis**	'Ala + AKG --> Pyr + Glu'
76	2.6.1.51	Serine-pyruvate transaminase		'Ser + Pyr --> Ala + 3HPyr'
77	2.6.1.51	Serine-pyruvate transaminase		'Ala + 3HPyr --> Ser + Pyr'
78	6.3.5.4	Asparagine synthase		'Asp + Gln + ATP --> Asn + Glu + AMP + 2 Pi'
79	2.7.2.4, 1.2.1.11, 4.2.1.52, 1.3.1.26, 2.6.1.83, 5.1.1.7, 4.1.1.20	Lumped reaction		'Asp + Pyr + NADH + Glu + ATP + NADPH --> Lys + AKG + NADP + ADP + CO2 + Pi + NAD'
80	2.7.2.4, 1.2.1.11, 1.1.1.3	Lumped reaction		'Asp + ATP + 2 NADPH --> HSer + ADP + 2 NADP + Pi'
81	2.3.1.31, 2.5.1.48, 4.4.1.8, 2.1.1.13	Lumped reaction		'HSer + ACOA + Cys + MTHF --> Met + THF + Pyr + COA + ace + NH4'
82	2.7.1.39, 4.2.3.1	Homoserine kinase, threonine synthase		'HSer + ATP --> Thr + ADP + Pi'
83	4.3.1.19, 2.2.1.6, 1.1.1.86, 4.2.1.9, 2.6.1.42	Lumped reaction		'Pyr + Thr + NADPH + Glu --> Ile + AKG + NADP + NH4 + CO2'
84	2.2.1.6, 1.1.1.86, 4.2.1.9, 2.6.1.42	Lumped reaction		'2 Pyr + Glu + NADPH --> Val + AKG + NADP + CO2'
85	2.2.1.6, 1.1.1.86, 4.2.1.9, 2.3.3.13, 4.2.1.33, 1.1.1.85, 2.6.1.42	Lumped reaction		'2 Pyr + ACOA + Glu + NADPH + NAD --> Leu + AKG + NADP + NADH + COA + 2 CO2'
86	2.5.1.54, 4.2.3.4, 4.2.1.10, 1.1.1.25, 2.7.1.71, 2.5.1.19, 4.2.3.5	Lumped reaction		'2 PEP + E4P + NADPH + ATP --> Chr + NADP + ADP + 4 Pi'
87	4.1.3.27, 2.4.2.18,	Lumped reaction		'Chr + Gln + PRPP + Ser --> Trp + Glu + GAP + Pyr + CO2 + 2

	5.3.1.24, 4.1.1.48, 4.2.1.20		**Amino acid biosynthesis**	Pi'
88	5.4.99.5, 2.6.1.78, 1.3.1.78	Lumped reaction		'Chr + NADP + Asp --> Tyr + OA + NADPH + CO2'
89	5.4.99.5, 2.6.1.78, 4.2.1.51, 4.2.1.91	Lumped reaction		'Chr + Asp --> Phe + OA + CO2'
90	2.4.2.17, 3.6.1.31, 3.5.4.19, 5.3.1.16, 2.4.2.-	Lumped reaction		'PRPP + ATP + Gln --> IGo3P + AICAR + Glu + 4 Pi'
91	4.2.1.19, 2.6.1.9, 3.1.3.15, 1.1.1.23	Lumped reaction		'IGo3P + Glu + 2 NAD --> His + 2 NADH + AKG + Pi'
92	2.7.6.1	Ribose-phosphate pyrophosphokinase		'Ro5P + ATP --> PRPP + AMP'
93	6.3.4.16	Carbamoyl-phosphate synthase		'CO2 + 2 ATP + Gln --> CAP + 2 ADP + Pi + Glu'
94	6.2.1.1	Acetyl-CoA synthetase		'ace + ATP + COA --> ACOA + AMP + 2 Pi'
95	6.2.1.1	Acetyl-CoA synthetase		'ACOA + AMP + 2 Pi --> ace + ATP + COA'
96	2.6.1.44	Alanine-glyoxylate transaminase		'Ala + GOX --> Pyr + Gly'
97	2.6.1.44	Alanine-glyoxylate transaminase		'Pyr + Gly --> Ala + GOX'
98	2.6.1.45	Serine-glyoxylate transaminase		'Ser + GOX --> 3HPyr + Gly'
99	2.6.1.45	Serine-glyoxylate transaminase		'3HPyr + Gly --> Ser + GOX'
100	2.6.1.4, 2.6.1.44	Glutamate--glyoxylate aminotransferase		'Gly + AKG --> Glu + GOX'
101	2.6.1.4, 2.6.1.44	Glutamate--glyoxylate aminotransferase		'Glu + GOX --> Gly + AKG'
102	1.1.2.29, 2.7.1.31	Hydroxypyruvate reductase, glycerate 3-kinase		'3HPyr + NADH + ATP --> 3PG + ADP + NAD'

103	1.5.1.3	Dihydrofolate reductase		'THF + NADP --> DHF + NADPH'
104	1.5.1.3	Dihydrofolate reductase		'DHF + NADPH --> THF + NADP'
105	1.5.1.20	Methylenetetrahydrofolate reductase		'MnTHF + NADPH --> MTHF + NADP'
106	1.6.5.3, 1.6.99.3, 1.10.2.2, 1.9.3.1, 3.6.3.6, 3.6.3.14	Lumped reaction	**Oxidative phosphorylation**	'2 NADH + 5 ADP + 5 Pi + O2 --> 2 NAD + 5 ATP'
107	1.3.5.1, 1.10.2.2, 1.9.3.1, 3.6.3.6, 3.6.3.14	Lumped reaction		'2 FADH2 + 3 ADP + 3 Pi + O2 --> 2 FAD + 3 ATP'
108	2.4.2.14, 6.3.4.13, 2.1.2.2, 6.3.5.3, 6.3.3.1, 4.1.1.21, 6.3.2.6, 4.3.2.2	Lumped reaction	**Nucleotide biosynthesis**	'PRPP + 2 Gln + Gly + 5 ATP + Pyr + COA + CO2 + Asp --> AICAR + Fum + 2 Glu + ACOA + 5 ADP + 7 Pi'
109	2.1.2.3, 6.3.4.4, 4.3.2.2	Lumped reaction		AICAR + Pyr + COA + Asp + 2 ATP --> AMP + 2 ADP + Fum + ACOA + 2 Pi'
110	2.1.2.3, 1.1.1.205, 6.3.5.2	Lumped reaction		'AICAR + Pyr + COA + NAD + Gln + 2 ATP --> GMP + AMP + Glu + 3 Pi + NADH + ACOA + ADP'
111	6.3.5.5, 2.1.3.2, 3.5.2.3, 1.3.5.2, 1.6.5.10, 2.4.2.10, 4.1.1.23	Lumped reaction		'Asp + CAP + NADP + PRPP --> UMP + CO2 + NADPH + 3 Pi'
112	6.3.4.2	CTP synthase		'UTP + ATP + Gln --> CTP + ADP + Glu + Pi'
113	2.7.4.3	Adenylate kinase		'ATP + AMP --> 2 ADP'
114	2.7.4.3	Adenylate kinase		'2 ADP --> ATP + AMP'
115	2.7.4.8, 2.7.4.6	Guanylate kinase, nucleoside-diphosphate kinase		'GMP + 2 ATP --> GTP + 2 ADP'
116	2.7.4.8, 2.7.4.6	Guanylate kinase, nucleoside-		'GTP + 2 ADP --> GMP + 2 ATP'

		diphosphate kinase	**Nucleotide biosynthesis**	
117	2.7.4.14, 2.7.4.22	UMP-CMP kinase, uridylate kinase		'UMP + ATP --> UDP + ADP'
118	2.7.4.14, 2.7.4.22	UMP-CMP kinase, uridylate kinase		'UDP + ADP --> UMP + ATP'
119	2.7.4.6	Nucleoside-diphosphate kinase		'UDP + ATP --> UTP + ADP'
120	2.7.4.6	Nucleoside-diphosphate kinase		'UTP + ADP --> UDP + ATP'
121	2.7.4.6	Nucleoside-diphosphate kinase		'CTP + ADP --> CDP + ATP'
122	2.7.4.6	Nucleoside-diphosphate kinase		'CDP + ATP --> CTP + ADP'
123	2.7.4.14	UMP-CMP kinase		'CDP + ADP --> CMP + ATP'
124	2.7.4.14	UMP-CMP kinase		'CMP + ATP --> CDP + ADP'
125	3.6.1.5	Apyrase		'CTP --> CDP + Pi'
126	2.7.4.3, 1.17.4.1, 2.7.4.6	Lumped reaction		'AMP + 2 ATP + NADPH --> dATP + 2 ADP + NADP'
127	2.7.4.8, 1.17.4.1, 2.7.4.6	Lumped reaction		'GMP + 2 ATP + NADPH --> dGTP + 2 ADP + NADP'
128	1.17.4.1, 1.8.1.9	Ribonucleoside-diphosphate reductase, thioredoxin reductase		'CDP + NADPH --> dCDP + NADP'
129	2.7.4.6	Nucleoside-diphosphate kinase		'dCDP + ATP --> dCTP + ADP'
130	2.7.4.14	UMP-CMP kinase	**Nucleotide biosynthesis**	dCDP + ADP --> dCMP + ATP'
131	3.5.4.12, 2.1.1.45	dCMP deaminase, thymidylate synthase		'dCMP + MnTHF --> dTMP + DHF + NH4'
132	2.7.4.9, 2.7.4.6	dTMP kinase, nucleoside-diphosphate kinase		'dTMP + 2 ATP --> dTTP + 2 ADP'
133	6.1.1.17, 1.2.1.70, 5.4.3.8, 4.2.1.24,	Lumped reaction	**Chlorophyll biosynthesis**	'8 Glu + 9 ATP + 7 O2 + SAM + 13 NADPH + PPP --> Chl + 19 Pi + 13 NADP + SAHC + ADP + 4 NH4 + 8 AMP + 6 CO2

	2.5.1.61, 4.2.1.75, 4.1.1.37, 1.3.3.3, 1.3.99.22, 1.3.3.4, 6.6.1.1, 2.1.1.11, 1.14.13.81, 1.3.1.75, 1.3.7.7, 1.3.1.33, 2.5.1.62		**Chlorophyll biosynthesis**	+ 3 H2O2'
134	2.5.1.6	S-adenosylmethionine synthetase		'Met + ATP --> SAM + 3 Pi'
135	3.3.1.1, 2.1.1.13	Adenosylhomocysteinase, 5-methyltetrahydrofolate--homocysteine methyltransferase		'SAHC + MTHF --> Met + ade + THF'
136	2.7.1.20	Adenosine kinase		'ade + ATP --> AMP + ADP'
137	2.2.1.7, 1.1.1.267, 2.7.7.60, 2.7.1.148, 4.6.1.12, 1.17.7.1, 1.17.1.2, 5.3.3.2, 2.5.1.1, 2.5.1.10, 2.5.1.29, 1.3.1.83	Lumped reaction		'4 GAP + 4 Pyr + 11 NADPH + 8 NADH + 8 ATP --> PPP + 11 NADP + 14 Pi + 4 CO2 + 4 ADP + 4 AMP + 8 NAD'
138	1.11.1.6	Catalase		'2 H2O2 --> O2'
139	5.4.2.2	Phosphoglucomutase	**Polysaccharide biosynthesis**	'G6P --> G1P'
140	5.4.2.2	Phosphoglucomutase		'G1P --> G6P'
141	2.7.7.27, 2.4.1.21, 2.4.1.18	Lumped reaction		'G1P + ATP --> PS + ADP + 2 Pi'
142	2.4.1.1	Starch phosphorylase		'PS + Pi --> G1P'

143	Ribosomes and RNAs	Lumped reaction	**Protein biosynthesis**	Protein synthesis (Average protein consired varies with culturing mode)
144	2.7.7.7, DNA replication mechanism	DNA polymerase	**DNA biosynthesis**	'0.19 dATP + 0.19 dTTP + 0.31 dGTP + 0.31 dCTP + 0.25 ATP --> DNA + 0.25 ADP + 2.25 Pi'
145	2.7.7.6, transcription mechanisms	RNA polymerase	**RNA biosynthesis**	'0.19 ATP + 0.19 UTP + 0.31 GTP + 0.31 CTP --> RNA + 2 Pi'
146	1.7.1.1, 1.7.7.1	Nitrate reductase, nitrite reductase	**Nitrate assimilation**	'NO3 + NADH + 3 NADPH --> NH4 + NAD + 3 NADP'
147	2.7.1.23	NAD+ kinase	**Transhydro-genation**	'NAD + ATP --> NADP + ADP'
148	1.6.1.2	NAD(P) transhydrogenase		'NADH + NADP --> NAD + NADPH'
149	1.6.1.2	NAD(P) transhydrogenase		'NADPH + NAD --> NADH + NADP'
150	Kinases	Lumped reaction	**Maintenance energy**	'ATP --> ADP + Pi'
151	Cellular mechanism	Lumped reaction	**Biomass synthesis**	Macromolecular composition in biomass varies with culturing age and mode)
152			**Transport reactions**	# --> Pi'
153				'# --> Gluc'
154				'# --> NO3'
155				'# --> O2'
156				'# --> SO4'
157				'CO2 --> #'
158				'BM --> #'
159				'# --> ace'

*- Abbreviations of the metabolites involved in the reactions are listed in table A4

Table A4 Abbreviations and notations used in the reactions and in model development

Abbreviations and meaning	
3HPyr	3 hydroxy pyruvate
3PG	3-phospho glycerate
ace	Acetate
ACOA	Acetyl coenzyme A
ade	Adenosine
ADP	Adenosine diphosphate
AICAR	5 Aminoimidazole 4 carboxamide ribonucleotide
AKG	α keto glutarate
Ala	Alanine
AMP	Adenosine monophosphate
Arg	Arginine
Asn	Aspargine
Asp	Asparate
ATP	Adenosine triphosphate
BM	Biomass
BPG	1,3 biphospho glycerate
CAP	Carbamoyl phosphate
CDP	Guanosine diphosphate
Chl	Chlorophyll
Chr	Chorismate
Cit	Citric acid
CMP	Cytidine diphosphate
CO2	Carbon dioxide
COA	Coenzyme A
CTP	Cytidine triphosphate
Cys	Cysteine
dATP	Deoxy adenosine triphosphate
dCDP	Deoxy cytidine diphosphate
dCMP	Deoxy cytidine 5' monophosphate
dCTP	Deoxy cytidine triphosphate
DGDG	Digalactosyldiacylglycerol
dGTP	Deoxy guanosine triphosphate
DHAP	Dihydroxy acetone phosphate
DHF	Dihydro folate
DNA	Deoxy ribose nucleic acid
dTMP	Deoxy thymidine 5' monophosphate
dTTP	Deoxy thymidine triphosphate
E4P	Erythrose 4 phosphate
F6P	Fructose 6 phosphate
FA	Fatty acid
FAD	Flavin adenine dinucleotide (Oxidized form)

FADH2	Flavin adenine dinucleotide (reduced form)
FBP	Fructose 1,6 biphosphate
Fum	Fumarate
G1P	Glucose 1 phosphate
G6P	Glucose 6 phosphate
GAP	Glyceraldehyde 3 phosphate
Gln	Glutamine
Glu	Glutamate
Gluc	Glucose
Gly	Glycine
GMP	Guanosine 5' monophosphate
GOX	Glyoxalate
GTP	Guanosine triphosphate
H2O2	Hydrogen peroxide
H2S	Hydrogen sulfide
His	Histidine
HSer	Homo serine
ICit	Isocitrate
IGo3P	Imidazole glycerol 3 phosphate
Ile	Isoleucine
Leu	Leucine
Lys	Lysine
Mal	Malate
Met	Methionine
MGDG	Monogalactosyldiacylglycerol
MnTHF	N5,N10 Methylene tetra hydrofolate
MTHF	N5 Methyl tetrahydrofolate
NAD	Nicotinamide adenine dinucleotide (oxidized form)
NADH	Nicotinamide adenine dinucleotide (reduced form)
NADP	Nicotinamide adenine dinucleotide phosphate (oxidized form)
NADPH	Nicotinamide adenine dinucleotide phosphate (reduced form)
NH4	Ammonium
NL	Neutral lipid
NO3	Nitrate
O2	Oxygen
OA	Oxaloacetate
PE	Phosphatidylethanolamine
PEP	Phosphoenol pyruvate
PG	Phosphatidylglycerol
PGL	6 phospho glucono δ-lactone
Phe	Phenyl alanine
Pi	Inorganic phosphate
PI	Phosphatidylinositol
PL	Polar lipid

PPP	Phytyl pyrophosphate
Pro	Proline
PRPP	5 phosphoribosyl 1 pyrophosphate
Prt	Protein
PS	Polysaccharide
Pyr	Pyruvate
R5P	Ribulose 5 phosphate
RNA	Ribose nucleic acid
Ro5P	Ribose 5 phosphate
SAHC	S- Adenosyl homocysteine
SAM	S Adenosyl methionine
SCOA	Succinyl coenzyme A
Ser	Serine
SH7P	Sedoheptulose 7 phosphate
SO4	Sulfate
SQDG	Sulfoquinovosyldiacylglycerol
Succ	Succinate
THF	Tetra hydrofolate
Thr	Threonine
Trp	Tryptophan
Tyr	Tyrosine
UDP	Uridine diphosphate
UDP_gal	UDP-galactose
UDP_gluc	UDP-glucose
UMP	uridine 5' monophosphate
UTP	Uridine triphosphate
Val	Valine
X5P	Xylulose 5 phosphate

Table A5 Flux distribution in metabolic network of *Chlorella* sp. FC2 IITG grown in nutrient sufficient, starvation and sodium acetate supplemented heterotrophic conditions.

SN	Absolute fluxes at		
	Nutrient sufficient condition	**Nutrient starved condition**	**Sodium acetate supplemented condition**
1	0.7474	1.481	0
2	0.3728	1.297	0
3	0	0	0.05744999
4	0.5258	1.3714	0
5	0.5258	1.3714	0
6	0	0	0.06385918
7	0.5196	1.3674	0
8	0	0	0.06725256

9	1.108	2.759	0
10	0	0	0.15234569
11	1.108	2.759	0
12	0	0	0.15234008
13	1.292	2.8716	0
14	0	0	0.01729147
15	1.1889	2.8083	0.2026581
16	0.9131	2.6394	0
17	0.607	2.2348	2.02623705
18	0.607	2.2348	2.02624556
19	0	0	0
20	0.607	2.2348	1.73123661
21	0.5635	2.208	1.70083038
22	0.5634	2.208	1.70083364
23	0	0	0
24	0.5634	2.208	1.99585743
25	0	0	0
26	0.5794	2.2179	2.01007082
27	0	0	0
28	0.5674	2.2105	2.29521802
29	0	0	0
30	0	0	0.2279406
31	0.0918	0.0564	0
32	0	0	0.06387221
33	0	0	1.0215E-07
34	0	0	0.29501746
35	0	0	0.28514142
36	0.012	0.0074	0
37	0.2395	0.1181	0
38	0.2395	0.1181	0
39	0.0864	0.0436	0.00647217
40	0	0	0
41	0.153	0.0744	0
42	0	0	0.00646132
43	0.0794	0.039	0
44	0	0	0.0012381
45	0.0794	0.039	0
46	0	0	0.0012229
47	0.0738	0.0356	0
48	0	0	0.00521236
49	0.036	0.047	0.04929021
50	0.0082	0.0132	0.01435758
51	0.0057	0.0037	0.00338094

52	0.0051	0.0033	0.00308522
53	0.0028	0.0019	0.00179045
54	0.0011	0.0007	0.00063012
55	0.0006	0.0004	0.00026119
56	0.0006	0.0004	0.00026644
57	0.0003	0.0002	0.00011127
58	0.0003	0.0002	7.3975E-05
59	0.0057	0.0037	0.00382311
60	0.0412	0.0258	0.0348277
61	0	0	0
62	0.0055	0.0033	0.00387581
63	0.0572	0.035	0.04451688
64	0	0	0
65	0	0	0
66	0.0112	0.0068	0.00792736
67	0	0	0
68	0.1928	0.1178	0.14167909
69	0	0	0
70	0.0022	0.0014	0.00183724
71	0	0	0
72	0.0026	0.0016	0.00218561
73	0.0026	0.0016	0.0021896
74	0	0	0
75	0.0648	0.0398	0.04812733
76	0.0952	0.0582	0.06935301
77	0	0	0
78	0.0077	0.0047	0.00543317
79	0.0023	0.0014	0.00167449
80	0.0161	0.0098	0.01166392
81	0.0013	0.0008	0.00125367
82	0.0148	0.009	0.0103853
83	0.0039	0.0024	0.0027557
84	0.0067	0.004	0.00468574
85	0.0096	0.0058	0.00671103
86	0.0057	0.0034	0.00399814
87	0.0007	0.0004	0.00054696
88	0.0007	0.0004	0.00051947
89	0.0042	0.0025	0.00295217
90	0.0013	0.0008	0.00104879
91	0.0013	0.0008	0.00099761
92	0.007	0.0046	0.00772113
93	0.0137	0.0085	0.01062395
94	0.004	0.0024	2.74444906

95	0	0	0
96	0	0	0
97	0.0062	0.0036	0.00425287
98	0.089	0.0544	0.06568638
99	0	0	0
100	0.0708	0.0434	0.05155529
101	0	0	0
102	0.1841	0.1126	0.13504337
103	0	0	0
104	0	0	0.00013078
105	0.0022	0.0014	0.00170556
106	1.2176	5.3807	1.92571992
107	0.2804	1.1032	0.99683604
108	0.0025	0.0017	0.00347221
109	0.0023	0.0014	0.00280802
110	0.0015	0.0011	0.00159975
111	0.0025	0.0017	0.00266475
112	0.0016	0.0011	0.00177989
113	0.221	0.1522	2.91562812
114	0	0	0
115	0.0014	0.001	0.00124006
116	0	0	0
117	0.0024	0.0018	0.00261647
118	0	0	0
119	0.0082	0.0054	0.00588041
120	0	0	0
121	0	0	0.00015199
122	0.001	0.0006	0
123	0	0	0
124	0.0012	0.0008	0.0003712
125	0	0	0
126	0	0	0.00018709
127	0.0001	0	0.00021536
128	0.0001	0.0001	0.00044307
129	0.0001	0	0.00015158
130	0	0	0.00021225
131	0	0	0.00013259
132	0	0	8.8393E-05
133	0.0009	0.0006	0.00061771
134	0.0009	0.0006	0.00077795
135	0.0009	0.0006	0.0004537
136	0.0009	0.0006	0.00030921
137	0.0009	0.0006	0.00055057
138	0.0014	0.0009	0.00092656

139	0.135	0.0658	0.05738894
140	0	0	0
141	0.1293	0.0621	0.05402103
142	0	0	0
143	0.1452	0.0879	0.10140005
144	0.0002	0.0001	0.00023425
145	0.0048	0.0033	0.00353692
146	0.225	0.138	0.16992692
147	0	0	5.4425E-06
148	0.8824	1.0196	1.39712362
149	0	0	0
150	5.3	32.8	6.1
151	0.055	0.0379	0.03944118
152	0.0061	0.0042	0.00794827
153	0.7474	1.481	0
154	0.225	0.138	0.17
155	1.5416	6.5378	2.97897733
156	0.0032	0.002	0.0024468
157	2.2647	7.1647	3.68115257
158	0.055	0.0379	0.03944118
159	0	0	2.741

Table A6 Composition of optimized BG11 media for maximal specific growth rate of FC2

Group name	Compounds	Composition
Glucose (g L^{-1})	$C_6H_{12}O_6$	17.73
Nitrogen (g L^{-1})	$NaNO_3$	1.2
Phosphorous (g L^{-1})	K_2HPO_4	0.107
Trace elements (g L^{-1})	$MgSO_4.7H_2O$	0.075
	$CaCl_2.2H_2O$	0.036
	Na_2CO_3	0.02
	Citric acid	0.006
	Ferric ammonium citrate	0.006
	EDTA	0.001
Micro elements (mg L^{-1})	H_3BO_3	2.86
	$MnCl_2.H_2O$	1.81
	$ZnSO_4.7H_2O$	0.222
	$CuSO_4.5H_2O$	0.079
	$Na_2MoO_4.2H_2O$	0.390
	$Co(NO_3)_2.6H_2O$	0.049

Table A7 Composition of optimized BG11 media for maximal biomass titer of FC2

Group name	Compounds	Composition
Glucose (g L^{-1})	$C_6H_{12}O_6$	26.21
Nitrogen (g L^{-1})	$NaNO_3$	1.37
Phosphorous (g L^{-1})	K_2HPO_4	0.149
Trace elements (g L^{-1})	$MgSO_4.7H_2O$	0.075
	$CaCl_2.2H_2O$	0.036
	Na_2CO_3	0.02
	Citric acid	0.006
	Ferric ammonium citrate	0.006
	EDTA	0.001
Micro elements (mg L^{-1})	H_3BO_3	2.86
	$MnCl_2.H_2O$	1.81
	$ZnSO_4.7H_2O$	0.222
	$CuSO_4.5H_2O$	0.079
	$Na_2MoO_4.2H_2O$	0.390
	$Co(NO_3)_2.6H_2O$	0.049

4. References

1. Cerón-García M.C., Macías-Sánchez M.D., Sánchez-Mirón A., García-Camacho F., Molina-Grima E., 2013. A process for biodiesel production involving the heterotrophic fermentation of *Chlorella protothecoides* with glycerol as the carbon source. Applied Energy. 103, 341–349.
2. Cheirsilp B., Torpee S., 2012. Enhanced growth and lipid production of microalgae under mixotrophic culture condition: effect of light intensity, glucose concentration and fed-batch cultivation. Bioresource Technology. 110, 510–516.
3. Chen Y.-H., Walker T.H., 2011. Biomass and lipid production of heterotrophic microalgae *Chlorella protothecoides* by using biodiesel-derived crude glycerol. Biotechnology Letters. 33, 1973–1983.
4. De Swaaf M.E., Sijtsma L., Pronk J.T., 2003. High-cell-density fed-batch cultivation of the docosahexaenoic acid producing marine alga *Crypthecodinium cohnii*. Biotechnology and Bioengineering. 81, 666–672.

5. Doucha J., Lívanský K., 2012. Production of high-density *Chlorella* culture grown in fermenters, Journal of Applied Phycology. 24, 35–43.

6. Graverholt O.S., Eriksen N.T., 2007. Heterotrophic high-cell-density fed-batch and continuous-flow cultures of *Galdieria sulphuraria* and production of phycocyanin. Applied Microbiology and Biotechnology. 77, 69–75.

7. Ho S.-H., Chang J.-S., Lai Y.-Y., Chen C.-N.N., 2014. Achieving high lipid productivity of a thermotolerant microalga *Desmodesmus* sp. F2 by optimizing environmental factors and nutrient conditions. Bioresource Technology. 156, 108–116.

8. Kumar V., Muthuraj M., Palabhanvi B., Ghoshal A.K., Das D., 2014. High cell density lipid rich cultivation of a novel microalgal isolate *Chlorella sorokiniana* FC6 IITG in a single-stage fed-batch mode under mixotrophic condition. Bioresource Technology. 170, 115–124.

9. Li T., Zheng Y., Yu L., Chen S., 2013. High productivity cultivation of a heat-resistant microalga *Chlorella sorokiniana* for biofuel production. Bioresource Technology. 131, 60–67.

10. Lu Y., Ding Y., Wu Q., 2011. Simultaneous saccharification of cassava starch and fermentation of algae for biodiesel production. Journal of Applied Phycology. 23, 115–121.

11. Mu J., Li S., Chen D., Xu H., Han F., Feng B., et al., 2015. Enhanced biomass and oil production from sugarcane bagasse hydrolysate (SBH) by heterotrophic oleaginous microalga *Chlorella protothecoides.* Bioresource Technology. 185, 99–105.

12. Muthuraj M., Chandra N., Palabhanvi B., Kumar V., Das D., 2014. Process Engineering for High-Cell-Density Cultivation of Lipid Rich Microalgal Biomass of *Chlorella* sp. FC2 IITG. BioEnergy Research. 8, 726–739.

13. Rismani-Yazdi H., Hampel K.H., Lane C.D., Kessler B.A., White N.M., Moats K.M., et al., 2015. High-productivity lipid production using mixed trophic state cultivation of *Auxenochlorella* (*Chlorella*) *protothecoides.* Bioprocess and Biosystems Engineering. 38, 639–650.

14. Rodolfi L., Chini Zittelli G., Bassi N., Padovani G., Biondi N., Bonini G., et al., 2009. Microalgae for oil: Strain selection, induction of lipid synthesis and outdoor mass cultivation in a low-cost photobioreactor. Biotechnology and Bioengineering. 102, 100–112.

15. Schmidt R.A., Wiebe M.G., Eriksen N.T., 2005. Heterotrophic high cell-density fed-batch cultures of the phycocyanin-producing red alga *Galdieria sulphuraria.* Biotechnology and Bioengineering. 90, 77–84.

16. Shen Y., Yuan W., Pei Z., Mao E., 2010. Heterotrophic culture of *Chlorella protothecoides* in various nitrogen sources for lipid production. Applied Biochemistry and Biotechnology. 160, 1674–1684.

17. Shi X.-M., Chen F., 2002. High-Yield Production of Lutein by the Green Microalga *Chlorella protothecoides* in Heterotrophic Fed-Batch Culture. Biotechnology Progress. 18, 723–727.

18. Wu Z., Shi X., 2007. Optimization for high-density cultivation of heterotrophic *Chlorella* based on a hybrid neural network model. Letters in Applied Microbiology. 44, 13–18.

19. Xiong W., Li X., Xiang J., Wu Q., 2008. High-density fermentation of microalga *Chlorella protothecoides* in bioreactor for microbio-diesel production. Applied Microbiology and Biotechnology. 78, 29–36.

20. Zheng Y., Li T., Yu X., Bates P.D., Dong T., Chen S., 2013. High-density fed-batch culture of a thermotolerant microalga *Chlorella sorokiniana* for biofuel production. Applied Energy. 108, 281–287.

List of Publications

Published Manuscripts

1. **Basavaraj Palabhanvi**, Muthusivaramapandian Muthuraj, Mayurketan Mukherjee, Vikram Kumar, Debasish Das*. (2016) "Process engineering strategy for high cell density-lipid rich cultivation of *Chlorella* sp. FC2 IITG via model guided feeding recipe and substrate driven pH control". Algal Research, 16:317-329.

2. **Basavaraj Palabhanvi**, Vikram Kumar, Muthusivaramapandian Muthuraj, Debasish Das*. (2014) "Preferential utilization of intracellular nutrients supports microalgal growth under nutrient starvation: multi-nutrient mechanistic model and experimental validation". Bioresource Technology, 173: 245–255.

3. Vikram Kumar[+], Muthusivaramapandian Muthuraj[+], **Basavaraj Palabhanvi**[+], Aloke Kumar Ghoshal, Debasish Das* (2014) "Evaluation and optimization of two stage sequential *in situ* transesterification process for fatty acid methyl ester quantification from microalgae". Renewable Energy, 68: 560-569.

4. Muthusivaramapandian Muthuraj[+], **Basavaraj Palabhanvi**[+], Shamik Misra, Vikram Kumar, Kumaran SV, Debasish Das*. (2013) "Flux balance analysis of *Chlorella* sp. FC2 IITG under photoautotrophic and heterotrophic growth conditions". Photosynthesis Research, 118: 167-179.

Manuscripts under preparation

1. **Basavaraj Palabhanvi**, Muthusivaramapandian Muthuraj, Mayurketan Mukherjee, Vikram Kumar, Debasish Das*. "Continuous cultivation of lipid rich microalga *Chlorella* sp. FC2 IITG for improved biodiesel productivity via control parameter optimization and substrate driven pH control".

Manuscripts from collaborative work

1. Vikram Kumar, Muthusivaramapandian Muthuraj, **Basavaraj Palabhanvi**, Debasish Das* (2016) "Synchronized growth and neutral lipid accumulation in *Chlorella sorokiniana* FC6 IITG under continuous mode of operation". Bioresource Technology, 200: 770–779.
2. Muthusivaramapandian Muthuraj, Niharika Chandra, **Basavaraj Palabhanvi**, Vikram Kumar, Debasish Das* (2015) "Process engineering for high-cell-density cultivation of lipid rich microalgal biomass of *Chlorella* sp. FC2 IITG" Bioenergy Research, 8: 726-739.
3. Muthusivaramapandian Muthuraj, Vikram Kumar, **Basavaraj Palabhanvi**, Debasish Das* (2014) "Evaluation of indigenous microalgal isolate *Chlorella* sp. FC2 IITG as a cell factory for biodiesel production and scale up in outdoor conditions." Journal of Industrial Microbiology & Biotechnology, 41: 499–511.
4. Vikram Kumar, Muthusivaramapandian Muthuraj, **Basavaraj Palabhanvi**, Aloke Kumar Ghoshal, Debasish Das* (2014) "High cell density lipid rich cultivation of a novel microalgal isolate *Chlorella sorokiniana* FC6 IITG in a single-stage fed-batch mode under mixotrophic condition." Bioresource Technology, 170: 115–124.

+ represents equal authorship
** represents corresponding author*

List of Conferences/Workshops/ Symposia

1. **Basavaraj Palabhanvi**, Muthusivaramapandian Muthuraj, Vikram Kumar and Debasish Das (2015). Development of multi-nutrient mechanistic model and its usage in feeding strategy of fed-batch cultivation for high cell density cultivation. International workshop on 'Advances in algal biotechnology', held at Indian Institute of Technology Bombay, Mumbai.

2. **Basavaraj Palabhanvi**, Muthusivaramapandian Muthuraj, Vikram Kumar and Debasish Das (2015). Screening and optimization of lipid inducers towards biodiesel production. Workshop on 'Frontier energy research with industry academia partnership', held at Indian Institute of Technology Guwahati.

3. Muthusivaramapandian Muthuraj, **Basavaraj Palabhanvi**, Vikram Kumar and Debasish Das (2015). Improvement of lipid content in *Chlorella* sp. FC2 IITG via conventional mutagenesis using Ultra-violet radiations. Workshop on 'Frontier energy research with industry academia partnership', held at Indian Institute of Technology Guwahati.

4. **Basavaraj Palabhanvi**, Muthusivaramapandian Muthuraj, Vikram Kumar, Baskar Selvaraj and Debasish Das (2014). Process optimization for high cell density cultivation of novel microalga *Chlorella* sp. FC2 IITG towards biodiesel production. International Conference on 'New dimension in chemistry & chemical

technologies applications in pharma industry', held at Jawaharlal Nehru Technological University Hyderabad.

5. Vikram Kumar, Muthusivaramapandian Muthuraj, **Basavaraj Palabhanvi**, Basker Selvaraj, Aloke Kumar Ghoshal, Debasish Das (2014). Evaluation of new isolate *Chlorella sorokiniana* FC6 IITG: feed stock for biodiesel production. International Conference on 'New dimension in chemistry & chemical technologies-applications in pharma industry', held at Jawaharlal Nehru Technological University Hyderabad.

6. **Basavaraj Palabhanvi** (2014). National conference on 'Recent advances in cancer biology and therapeutics', held at Indian Institute of Technology Guwahati.

7. **Basavaraj Palabhanvi**, Muthusivaramapandian Muthuraj, Kumaran Sivalingavasu, Debasish Das (2012). Metabolic flux analysis of *Chlorella* sp. FC2 IITG under photoautotrophic and heterotrophic growth conditions. International Conference on 'Indo - US workshop Cyanobacteria: Molecular Networks to Biofuels', held at Lonavala, India.

8. **Basavaraj Palabhanvi**, Muthusivaramapandian Muthuraj, Debasish Das (2012). Characterization of a novel freshwater isolate *Navicula* sp. FD1 IITG under nutritional stress conditions: strategy for enhanced lipid productivity. International Conference on 'Indo - US workshop Cyanobacteria: Molecular Networks to Biofuels', held at Lonavala, India.

9. Vikram Kumar, Muthusivaramapandian Muthuraj, **Basavaraj Palabhanvi**, Aloke Kumar Ghoshal, Debasish Das (2012). Optimization of two step sequential direct transesterification for biodiesel production from *Chlorella* sp. FC2 IITG.

International Conference on 'Indo - US workshop Cyanobacteria: Molecular Networks to Biofuels', held at Lonavala, India.

10. **Basavaraj Palabhanvi** (2012). SERC School on 'Introduction to systems and synthetic biology for scientists and engineers', held at Indian Institute of Technology Bombay, Mumbai.

11. Bikash C Maharaj, Minakshi Bhattacharjee, Saumya Ahlawat, Muthusivaramapandian Muthuraj, **Basavaraj Palabhanvi**, Debasish Das (2013). *Streptococcus* sp. W3: A new isolate as a cell factory for hyaluronic acid production. International Conference on 'Advances in Biotechnology and Patenting', held at Bharathidasan University, Tamil Nadu, India.

12. Naveen Bedi, Saumya Ahlawat, Mehak Kaushal, **Basavaraj Palabhanvi**, Vikram Kumar, Muthusivaramapandian Muthuraj, Debasish Das (2014). Development of an intermittent in situ butanol recovery strategy to overcome product toxicity and improve productivity. National conference on 'Bioprocessing India', held at Institute of Chemical Technology, Mumbai.

13. Saumya Ahlawat, Mehak Kaushal, **Basavaraj palabhanvi**, Vikram Kumar, Muthusivaramapandian Muthuraj, Debasish Das (2014). Screening and characterization of 12 *Clostridium* strains for butanol production: Effect of glucose and organic nitrate source. National conference on 'Bioprocessing India', held at Institute of Chemical Technology, Mumbai.

14. Sumanth Govathati, **Basavaraj Palabhanvi**, Vikram Kumar, Muthusivaramapandian Muthuraj, Debasish Das (2014). Screening and optimization of lipid inducer for single stage lipid rich cultivation of *Chlorella* sp.

FC2 IITG targeted towards biodiesel production. National conference on 'Bioprocessing India', held at Institute of Chemical Technology, Mumbai.

15. Mayurketan Mukherjee, Saumya Ahlawat, **Basavaraj Palabhanvi**, Anwesha Purakayastha, Mehak Kaushal, Debasish Das (2016). System biology approach to understand the regulation in metabolic shift from acidogenesis to solventogenesis in *Clostridium acetobutylicum* ATCC 824. International conference on 'Indo-US Workshop on Cell Factories', held at Indian Institute Of Technology Bombay, Mumbai.

16. Saumya Ahlawat, Mehak Kaushal, Mayurketan Mukherjee, Muthusivaramapandian Muthuraj, **Basavaraj Palabhanvi**, Debasish Das (2016). Alleviation of end product toxicity by strain level improvement in *Clostridium acetobutylicum* via combinatorial strategy of mutagenesis and serial adaptation. International conference on 'Indo-US Workshop on Cell Factories', held at Indian Institute Of Technology Bombay, Mumbai.

Underline represents presenting author

Vitae

The author was born on June 1st 1987 in Belagali, Karnataka, India. He passed the Secondary School Examination conducted by the Karnataka Secondary Education Examination Board, Bangalore, in 2003. He qualified the Higher Secondary School Examination conducted by Department of Pre University Education, Bangalore, Karnataka, in 2005. He completed Bachelor of Engineering in Biotechnology from Visvesvaraya Technological University, Belgaum, Karnataka, in 2009. He did his Master of Technology in Industrial Biotechnology from National Institute of Technology Karnataka, Surathkal, in 2011.

Basavaraj Palabhanvi joined his Ph.D. Programme in July 2011 at Department of Biosciences and Bioengineering, Indian Institute of Technology Guwahati, Assam, India. He received Junior and Senior research fellowships under the scheme run by the Ministry of Human Resource and Development (MHRD), India. He successfully completed the course work with 9.5/10 Cumulative Point Index (CPI). He gave the Open (PhD Synopsis) Seminar on January 1st 2016 and presented his thesis work before the Doctoral Committee and his performance was satisfactory. He presented his final viva voce seminar on 9th September 2016.